

# **Enzymatic synthesis of polyesters and their application in protein-polymer conjugation and networks formation**

## **Kumulative Dissertation**

zur Erlangung des akademischen Grades

**Doctor rerum naturalium (Dr. rer. nat.)**

der Naturwissenschaftlichen Fakultät I

- Biowissenschaften -

der Martin-Luther-Universität Halle-Wittenberg

vorgelegt von

**Frau Razan Alaneed**

geboren am 22.11.1987 in Damaskus, Syrien

### **Gutachter:**

1. Prof. Dr. Jörg Kreßler
2. Prof. Dr. Markus Pietzsch
3. Prof. Dr. Jörg C. Tiller

Tag der Verteidigung: 27.10.2022

*„Der Mensch kann in seinem kurzen und gefahrenreichen Leben einen Sinn nur finden, wenn er sich dem Dienst an der Gesellschaft widmet.“*

**Albert Einstein, deutsch-amerikanischer Physiker**

14. März 1879 - 18. April 1955

# Table of Contents

<b>1</b>	<b>Introduction .....</b>	<b>1</b>
1.1	Enzymatic polyester synthesis .....	1
1.1.1	Enzymes for polyester synthesis .....	3
1.1.2	Biocatalysis using lipases .....	4
1.1.3	Enzymatic polymerization by lipases .....	11
1.1.4	Synthesis and applications of graft copolymers .....	13
1.2	Protein-polymer conjugation .....	16
1.2.1	Synthesis of protein-polymer conjugates .....	19
1.2.2	Transglutaminases .....	20
1.2.2.1	Microbial transglutaminases .....	20
1.2.2.2	Applications of microbial transglutaminases .....	23
1.3	Polymer networks and hydrogels .....	25
1.3.1	Classification of hydrogels .....	27
1.3.2	Synthesis of chemically cross-linked hydrogels .....	28
<b>2</b>	<b>Aim and objectives .....</b>	<b>33</b>
<b>3</b>	<b>Results.....</b>	<b>36</b>
3.1	Paper I: Conjugation of amine-functionalized polyesters with dimethyl-casein using microbial transglutaminase .....	37
3.2	Paper II: Microbial transglutaminase-mediated formation of erythropoietin-polyester conjugates .....	49
3.3	Paper III: Network formation by aza-Michael addition of primary amines to vinyl end groups of enzymatically synthesized poly(glycerol adipate).....	71
<b>4</b>	<b>Summary and outlook.....</b>	<b>88</b>
	<b>Bibliography</b>	<b>92</b>
	<b>Erklärung</b>	<b>109</b>
	<b>Acknowledgments</b>	<b>110</b>
	<b>List of publications</b>	<b>113</b>
	<b>Curriculum vitae</b>	<b>114</b>

## List of abbreviations and symbols

$^{13}\text{C}$ NMR	Carbon-13 nuclear magnetic resonance spectroscopy
$^{13}\text{C}$ SP MAS NMR	Carbon-13 single-pulse magic-angle spinning nuclear magnetic resonance spectroscopy
3D	Three-dimensional
6-(Fmoc-Ahx)	6-(fluorenylmethyloxycarbonyl-amino)hexanoic acid
$^1\text{H}$ NMR	Proton nuclear magnetic resonance spectroscopy
$^1\text{H}$ DQ NMR	Proton double-quantum nuclear magnetic resonance spectroscopy
ABC	Accelerated blood clearance
Ac-L-Cys ME	<i>N</i> -acetyl-L-cysteine methyl ester
ADCs	Antibody-drug conjugates
AIBN	2-2'-azobisisobutyronitrile
AP	Alkaline phosphatase
apoMb	Apomyoglobin
APS	Ammonium persulfate
ARTP	Atmospheric and room temperature plasma
Asp	Aspartic acid
ATP	Adenosine triphosphate
ATRP	Atom transfer radical polymerization
BSA	Bovine serum albumin
C	Carbon atom
CAL-B	<i>Candida antarctica</i> Lipase B
CuAAC	Copper-catalyzed azide-alkyne cycloaddition
Cys	Cysteine
Cyt <i>c</i>	Cytochrome <i>c</i>
Da	Dalton
DA	Diels-Alder
DDS	Drug delivery system
DMA	Dimethyl adipate
DMAP	4-(dimethylamino)pyridine
DMC	Dimethylcasein
DMSO	Dimethyl sulfoxide
DNA	Deoxyribonucleic acid
DVA	Divinyl adipate
EPO	Erythropoietin
epPCR	Error-prone polymerase chain reaction
ES	Enzyme substrate
FDA	Food and Drug Administration
FGE	Formylglycine generating enzyme
Fmoc	Fluorenylmethyloxycarbonyl
FTIR	Fourier-transform infrared spectroscopy
GCSF	Granulocyte colony-stimulating factor
GFP	Green fluorescent protein
Gln	Glutamine
GMA	Glycerol monomethacrylate
GPC	Gel permeation chromatography
h	Hour

HA	Hyaluronic acid
HES	Hydroxyethyl starch
hGH	Human growth factor
His	Histidine
HIV	Human immunodeficiency virus
HR MALDI-TOF	High-resolution matrix-assisted laser desorption ionization time-of-flight mass spectrometry
IFN	Interferon
IgG	Immunoglobulin G
ILs	Ionic liquids
IPN(s)	Interpenetrating network(s)
IRs	Infusion reactions
kDa	Kilodalton
$K_i$	Inhibition constant
$K_m$	Michaelis constant
KPS	Potassium persulfate
LC-ESI-LIT MS	Liquid chromatography-electrospray-linear ion trap-tandem mass spectrometry
Lipase MM	<i>Mucor miehei</i> lipase
Lipase PC	<i>Pseudomonas cepacia</i> lipase
Lipase PF	<i>Pseudomonas fluorescens</i> lipase
Lipase PPL	<i>Porcine pancreas</i> lipase
Lys	Lysine
MDC	Monodansyl cadaverine
MHUTP	Methyl 3-((11-hydroxyundecyl)thio)propanoate
$M_n$	Number average molar mass
mPEG	Methoxy poly(ethylene glycol)
mPEO-N <sub>3</sub>	Azide-terminal poly(ethylene oxide) monomethylether
MPs	Microparticles
mTGase(s)	Microbial transglutaminase(s)
NanoDSF	Nano differential scanning fluorimetry
NMP	Nitroxide-mediated radical polymerization
NPs	Nanoparticles
NSAIDs	Non-steroidal anti-inflammatory drugs
PAMAM	Polyamidoamine
PBS	Poly(butylene succinate)
PBSI	Poly(butylene succinate- <i>co</i> -itaconate)
PC	Polycondensation
PCL	Poly( $\epsilon$ -caprolactone)
PDB	Protein data bank
PDSA	Poly(D-sorbitol adipate)
PDSA- <i>g</i> -NH <sub>2</sub>	Poly(D-sorbitol adipate)- <i>graft</i> -6-aminohexanoate
PEG	Poly(ethylene glycol)
PEI	Polyethyleneimine
PEO	Poly(ethylene oxide)
PEOZ	Poly(2-ethyl 2-oxazoline)
PGA	Poly(glycerol adipate)
PGA- <i>co</i> -PDL	Poly(glycerol adipate- <i>co</i> - $\omega$ -pentadecalactone)
PGA- <i>g</i> -PCL	Poly(glycerol adipate)- <i>graft</i> -poly( $\epsilon$ -caprolactone)
PGA- <i>g</i> -(PCL- <i>b</i> -PEO)	Poly(glycerol adipate)- <i>graft</i> -(poly( $\epsilon$ -caprolactone)- <i>block</i> -poly(ethylene oxide))

PGA(M)	Poly(glycerol adipate)(M), where the symbol (M) refers to the PGA synthesis using dimethyl adipate as a monomer
PGA(M)- <i>g</i> -NH <sub>2</sub>	Poly(glycerol adipate)(M)- <i>graft</i> -6-aminohexanoate
PGA(M)- <i>g</i> -NH <sub>2</sub> - <i>g</i> -mPEG12	Poly(glycerol adipate)(M)- <i>graft</i> -6-aminohexanoate- <i>graft</i> -methoxy poly(ethylene glycol)12, where 12 is related to the number of repeating units of PEG chains
PGOS	Poly(glycerol-1,8-octanediol-sebacate)
PGS	Poly(glycerol sebacate)
PHA	Polyhydroxyalkanoate
Phe	Phenylalanine
PHEMA	Poly(2-hydroxyethyl methacrylate)
PLA	Poly(lactic acid)
PLGA	Poly(lactic- <i>co</i> -glycolic acid)
PLLA	Poly(lactide)
PMMA- <i>co</i> -BMA	Poly(methyl methacrylate- <i>co</i> -butyl methacrylate)
PNGase F	Peptide- <i>N</i> -glycosidase F
Poly(OEGMA)	Poly(oligo(ethylene glycol) methyl ether methacrylate)
PSAs	Polysialic acids
PVA	Poly(vinyl alcohol)
PVP	Poly(vinylpyrrolidone)
PXA	Poly(xylitol adipate)
RAFT	Reversible addition fragmentation chain transfer polymerization
RBCs	Red blood cells
rHuEPO	Recombinant human erythropoietin
ROMP	Ring-opening metathesis polymerization
ROP	Ring-opening polymerization
sCT	Salmon calcitonin
SDS-PAGE	Sodium dodecyl sulphate-polyacrylamide gel electrophoresis
Ser	Serine
SPAAC	Strain-promoted azide-alkyne cycloaddition
<i>t</i> <sub>1/2</sub>	Half-life
TGase(s)	Transglutaminase(s)
Thr	Threonine
<i>T</i> <sub><i>m</i></sub>	Transition temperature
UV	Ultraviolet
<i>V</i> <sub>max</sub>	Maximum reaction rate

# 1 | Introduction

## 1.1 Enzymatic polyester synthesis

In recent years, various polymers have been investigated for a wide range of pharmaceutical and biomedical applications [1-4]. Among synthetic polymers, aliphatic polyesters have advanced significantly due to their promising biodegradability and biocompatibility making them desirable candidates for biomedical uses [5-7]. Indeed, biodegradability and biocompatibility are highly preferable in the biomedical field since polyesters can undergo an enzymatic degradation *in vivo* as the ester bonds are susceptible to cleavage by a range of enzymes into non-toxic biocompatible monomers without eliciting any adverse effects [8-10]. For this, various biodegradable polyesters such as poly(lactic acid) (PLA) and poly(lactic-co-glycolic acid) (PLGA) have been broadly used as biodegradable drug delivery system (DDS) owing to their tailored properties [11-13]. Despite great success, PLA- and PLGA-based drug carriers exhibit a relatively low capacity for drug loading and commonly an undesirable initial burst release of the drug [14-17]. Furthermore, aggregation and instability of therapeutics caused by a pH drop inside the DDS after polymer degradation resulted in undesirable immunogenic response [18, 19]. Thus, there was a need for the development of novel systems with tunable degradation behaviors by introducing various functional groups along the polymer backbones. Examples include biodegradable polyesters containing biocompatible components such as, tartaric acid, 1,8-octanediol, and non-steroidal anti-inflammatory drugs (NSAIDs) like ibuprofen or naproxen as pendant groups [20, 21] or salicylic acid containing polymers that undergo hydrolytic degradation to release salicylic acid and the biocompatible linker, adipic acid [22]. With these polymers, controlled drug release was achieved without initial burst effect. Alternatively, linear biocompatible and biodegradable polyesters were synthesized *via* enzymatic methods. For instance, poly(glycerol adipate) (PGA) (Figure 1(A)) is an enzymatically synthesized biodegradable polyester with promising properties for nanoparticulate drug carrier systems [23]. One of its advantages over PLA/PLGA is the presence of free pendant hydroxyl (OH-) groups along its backbone, which allow further functionalization in order to alter the physicochemical properties of the polymer for specific applications [24]. Beside PGA, poly(D-sorbitol adipate) (PDSA) (Figure 1 (B)), an enzymatically synthesized sugar-based polyester, was subsequently designed with high

tendency to form well-arranged nanoparticles [25] as well as polymer networks with potential application as drug carriers [26]. Most recently, PGA and PDSA were successfully applied in the field of protein-polymer conjugation [27, 28].

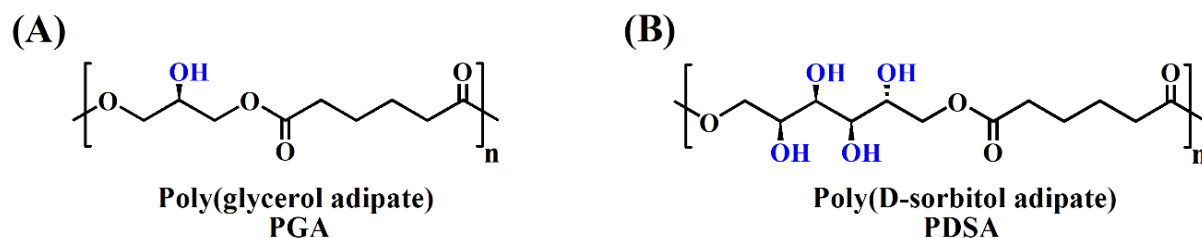


**Figure 1.** Chemical structures of (A) the poly(glycerol adipate) backbone and (B) the poly(D-sorbitol adipate) backbone.

In general, polyesters can be synthesized *via* two pathways: (1) step-growth polycondensation of diols/polyalcohols and diacid/diesters or polycondensation of hydroxyacids/hydroxyesters, and (2) ring-opening polymerization (ROP) of cyclic monomers such as lactones and other cyclic diesters [29, 30]. Each of these methods exhibits some advantages and disadvantages. For instance, polycondensation reaction has the advantage of using a variety of monomers derived from renewable resources with low costs. Nevertheless, this process operates under severe conditions as high temperature (above 150 °C) and vacuum for the continuous removal of by-products and thus, shifting the reaction equilibrium in the forward direction. As a result, undesirable side reactions, i.e. dehydration of diols or  $\beta$ -scissions of polyesters to form acid and alkene terminal groups, resulting in anhydride and acetaldehyde, often occur especially when thermally or chemically unstable monomers such as, epoxy and vinyl moieties are used [31]. On the contrary, polyester synthesis *via* ROP does not require any by-products removal and accordingly, high molar mass polymers products can be produced under relatively mild reaction conditions. However, these traditional pathways for the synthesis of polyesters are catalyzed by a broad range of catalysts, such as tin, zinc, calcium, cobalt, acetates of manganese, and many other metal-based catalysts [31, 32]. Residual metals in these catalysts are difficult to remove and therefore, have an adverse impact on the environment [31]. As a consequence, the resulting polyesters with metal traces are not suitable for pharmaceutical application due to their toxicity. Other than these concerns, most metal-based catalysts lack selectivity, leading to uncontrolled branching of polyesters. Owing to these issues, *in vitro* enzyme-catalyzed polyester synthesis has been investigated as an environmentally benign process which promotes the synthesis of linear polyesters under mild reaction conditions [33-37]. Enzymatic synthesis of polyesters has significant advantages compared to conventional chemical pathways including (a) high ability

to catalyze polycondensation or ROP without multiple protection/deprotection steps, however, protection/deprotection are considered as critical steps for enzymatic polymerization while using some highly polar monomers such as L-tartaric acid [38], (b) high ability to control enantio-, regio-, and chemoselectivity, (c) tunable catalytic activity under mild reaction conditions with few by-products, (d) low toxicity and recyclability of biocatalysts especially, in their immobilized form, which in turn reduces the production cost, (e) renewable materials, (f) ability to work in organic solvents as well as in bulk conditions, and (g) ability to degrade the synthesized polymers by changing the conditions [39-42]. On the other hand, however, the use of enzymes has some drawbacks such as (a) limited thermostability, (b) narrow specificity, (c) low conversion yields, (d) high amount of catalyst is required, and (e) sometimes impure biocatalysts are obtained mainly, when whole cells are used [31, 43].

### 1.1.1 Enzymes for polyester synthesis

Enzymes are proteins that catalyze all biochemical reactions in living organisms as well as in industrial processes [44]. Enzymes are able to accelerate the rate of chemical reactions as they lower the energy of activation through the formation of an enzyme-substrate complex [45]. They adapt to different substrates *via* a conformational change according to the lock-and-key model, also known as induced fit hypothesis, proposed by Emil Fischer in 1894 [46]. Enzymes are classified into six categories based on the type of chemical reactions they catalyze [47]:

- 1) Oxidoreductases (EC1) catalyze oxidation-reduction reactions through the transfer of electrons from one substrate to another. Examples include peroxidases, reductases, dehydrogenases, oxygenases, and laccase.
- 2) Transferases (EC2) catalyze functional group transfer reactions from one substrate (act as a donor) to another (act as an acceptor). The functional groups include methyl, glycosyl, acyl, carboxyl, amino, and phosphate. An example of transferases is transglutaminase (TGase, protein-glutamine  $\gamma$ -glutamyltransferase, EC 2.3.2.13) [48].
- 3) Hydrolases (EC3) catalyze hydrolytic reactions, i.e. they promote the cleavage of C—O, C—N, C—S, and O—P bonds in proteins, carbohydrates, and fats during the digestion process by addition of water molecules. An example of hydrolases is lipases or triacylglycerol acylhydrolases (EC 3.1.1.3) [49].
- 4) Lyases (EC4) catalyze either the formation of new double bonds or rings by removing functional groups from the substrate (e.g., dehydratases) or the addition of functional groups to double bonds (e.g., carboxylase).

- 5) Isomerases (EC5) catalyze structural changes or rearrangements within one molecule. Examples include racemases and epimerases.
- 6) Ligases (EC6) such as, DNA ligases which catalyze ligation or joining of two molecules using an energy source usually through the hydrolysis of a diphosphate bond in adenosine triphosphate (ATP) or other triphosphates. Another important group of enzymes that catalyze the movement of atoms or molecules across the membrane or their separation within membranes through the hydrolysis of ATP, has been classified under a new class of translocases (EC7).

Different enzyme classes have been used as biocatalysts for *in vitro* enzymatic polymerization. This includes oxidoreductases (e.g., peroxidase and laccase), transferases (e.g., PHA synthase), hydrolases (e.g., lipase and cellulase), and ligases (e.g., cyanophycin synthetase) [50]. Some examples of enzymatically synthesized polymers are polyesters [51], polyamides [52], vinyl polymers [53], and polysaccharides [54]. To date, polyesters are amongst the most intensively studied polymers in the enzymatic polymerization field and lipases are the most efficient biocatalysts for polyester synthesis by virtue of their high catalytic reactivity, selectivity, and thermal stability [50].

### 1.1.2 Biocatalysis using lipases

In general, lipases (triacylglycerol lipase, triacylglycerol acylhydrolase, EC 3.1.1.3) belong to the hydrolase class of enzymes that catalyzes the hydrolysis of the ester bonds of triacylglycerol to yield di- and monoglycerides, glycerol, and fatty acids *in vivo* as well as the synthesis of esters *in vitro* under anhydrous conditions [49]. They are widespread distributed in nature and can be found in plants, animals, and microorganisms (e.g., bacteria, fungi, and yeast), in order to metabolize lipids [55]. These enzymes can be extracted from animal sources as well as from several microorganisms and then applied as biocatalysts for *in vitro* synthesis of polyesters [33, 56]. Among different lipases, microbial lipases exhibit high stability, selectivity, and substrate specificity. In addition, ease and lower production cost of microbial lipases make them favorable for commercial use [57]. In 1984, Okumura et al. first studied the synthesis of ester oligomers from various dicarboxylic acids and polyols catalyzed by lipase from *Aspergillus niger* [58]. Afterwards, many different lipases have been utilized for *in vitro* polyester synthesis [59]. However, lipase B derived from *Candida antarctica* (CAL-B) has shown the best catalytic efficiency for this purpose due to its high chemo-, regio- and stereoselectivity, catalytic reactivity, and thermal stability especially, in its immobilized form [60, 61]. By definition,

chemoselectivity refers to the enzyme remarkable selectivity to a specific functional group in the presence of other functional groups. For example, CAL-B was found to exhibit a greater selectivity for alcohols than for thiol acyl acceptors in a transacylation reaction [62]. Regioselectivity is the preference of lipases towards a specific ester bond, primary or secondary, in the glycerol backbone. For example, CAL-B was found to show higher selectivity towards primary OH-groups compared to the secondary ones in the enzymatic synthesis of poly(glycerol adipate) (PGA) [63]. Stereoselectivity refers to an enzyme selectivity to a particular stereoisomer in the presence of other isomers in the same reaction. For example, the enzymatic stereoselectivity of lipase towards the  $\alpha$ -anomer in the deacylation reaction of  $\alpha,\beta$ -D-ribofuranosides [64].

*Candida antarctica* lipase B (CAL-B) is a globular protein that is composed of 317 amino acid residues with a molar mass of 33 kDa. It belongs to the  $\alpha/\beta$  hydrolase fold that consists of eight parallel  $\beta$ -sheets flanked by a number of  $\alpha$ -helices on both sides. The structure of CAL-B was determined by Uppenberg et al. in 1994 (Figure 2) [65].

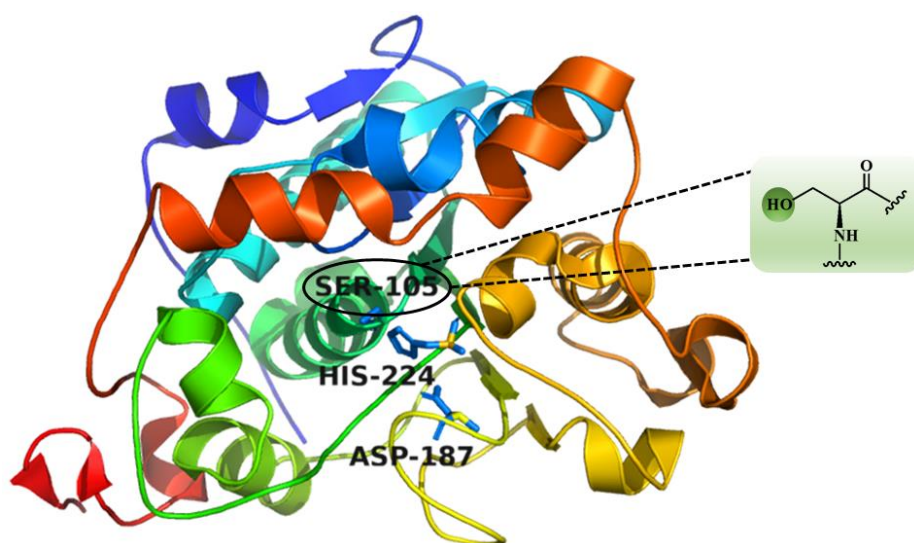
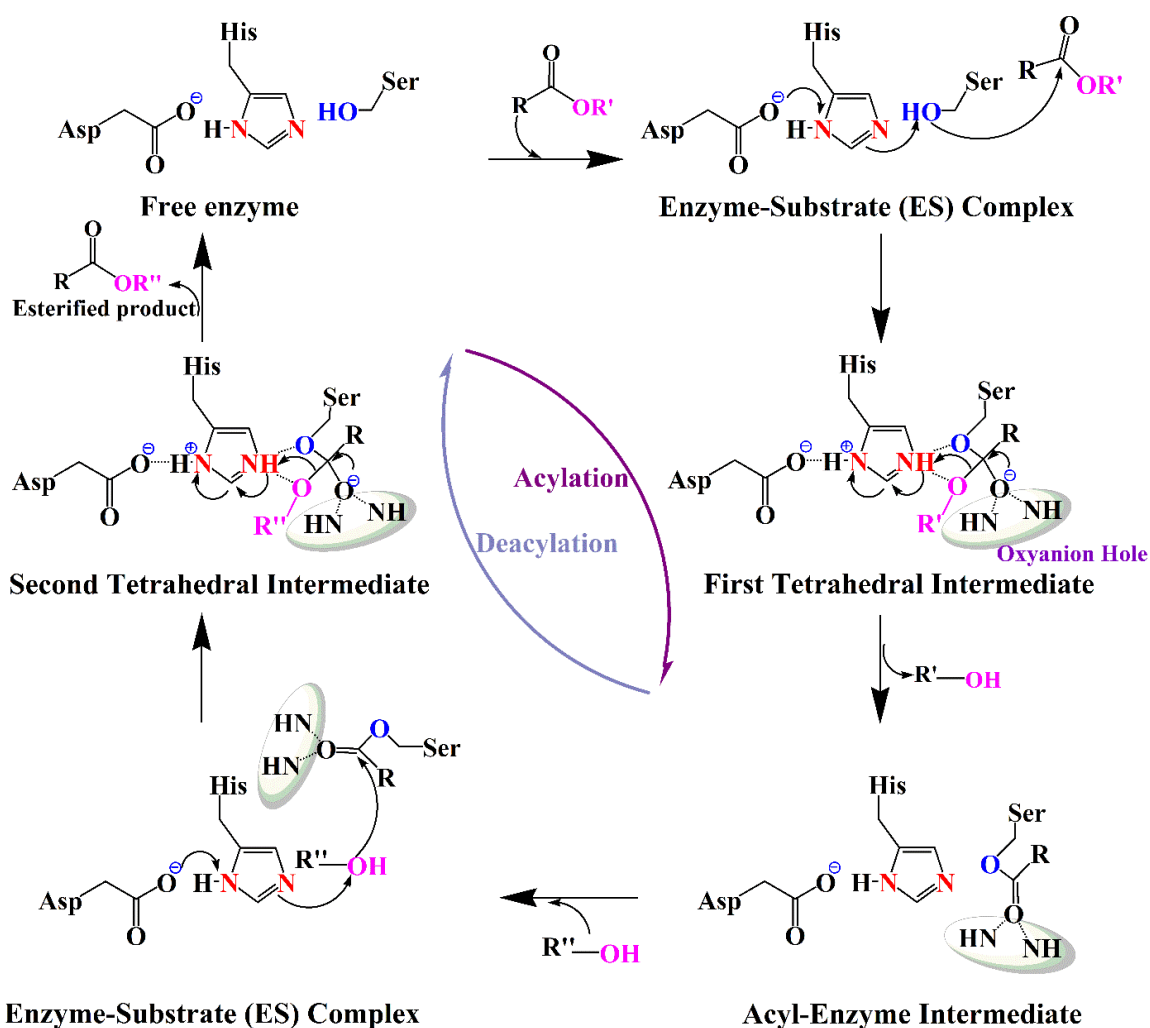


**Figure 2.** 3D structure of lipase B derived from *Candida antarctica* (PDB code 4K5Q) [66]. The structure is drawn using PyMOL (The PyMOL Molecular Graphics System, Schrödinger, LLC). Ser105, His224, and Asp187 residues represent the catalytic triad of CAL-B. The structure given in the green box belongs to serine which is considered as an essential residue for the lipase catalytic activity.

As shown in Figure 2, the active site of CAL-B contains a catalytic triad which is made up of three amino acids, a serine (Ser105) as nucleophile, a histidine (His224), and aspartic acid (Asp187). The active site of CAL-B possesses an oxyanion hole (Thr40 and Gln106) which stabilizes the oxyanion formed in the tetrahedral intermediate [67]. Additionally, this catalytic center is covered by a highly mobile and lipophilic  $\alpha$ -helical domain called lid which regulates

the access of substrates to the active site of lipase, i.e. the lid opens at the lipid-water interface to yield an active enzyme conformation with a catalytic center accessible to substrates [68].

A generally accepted catalytic mechanism of lipase-catalyzed acylation and deacylation is shown in Scheme 1. In the acylation step, the imidazole group of the His residue serves as a general base catalyst for deprotonation of the OH-group of the catalytic serine (-CH<sub>2</sub>OH). As a result, nucleophilicity of the catalytic serine increases in order to attack the carbonyl group of the susceptible substrate. The first product (R-OH) leaves the active site and the first tetrahedral intermediate is formed with a negative charge on the oxygen of the carbonyl group.



**Scheme 1.** Catalytic mechanism of lipases, adapted from [67, 69].

This intermediate is stabilized by the oxyanion hole (Gln106, Thr40) through three hydrogen bonds. In the deacylation step, a nucleophile (either water in case of hydrolysis or an alcohol in case of alcoholysis) further attacks the carbonyl carbon of the acyl-enzyme intermediate, releasing an esterified product and regenerating the enzyme in its native form [67].

The catalytic activity and stability of the enzyme is highly dependent on a number of parameters including enzyme immobilization, enzyme type and concentration, water content, reaction temperature and time, solvent nature, and chain length/feed ratio of monomers used.

***Effect of enzyme immobilization:*** The use of soluble enzymes as catalysts in biocatalytic processes is limited by their poor stability under certain reaction conditions as well as their high production cost and a lack of recycling and reusing [70]. To overcome these shortcomings, enzyme immobilization on a solid support has been established. Enzyme immobilization can be defined as the attachment of the enzyme molecules to the surface of a solid support, maintaining their catalytic activities. There are three major methods for enzyme immobilization: 1) binding to a solid support *via* adsorption, ionic immobilization, or covalent binding, 2) cross-linking (e.g., by glutaraldehyde), and 3) inclusion or entrapment in gels or in membrane reactors [71]. Basically, the most commonly employed method is the covalent immobilization since the enzymes are covalently bonded to the functional groups present on the support. The formation of covalent bonds usually depends on the functional groups present on the surface of the enzyme as well as on the support. The reactive  $\epsilon$ -amino group of lysine (Lys) is frequently used for the covalent interactions with the support as it is mainly located on the enzyme surface. On the other hand, a number of supports having reactive groups like epoxy rings and activated carbonyl groups are usually chosen [72]. Enzyme immobilization on a solid support can result in enhanced enzymes stability and activity by increasing their tolerance at high temperatures and in organic solvents as well as recyclability of the enzymes. For example, Mahapatro et al. reported the solvent-free polycondensation of adipic acid and 1,8-octanediol using immobilized CAL-B to obtain higher molar mass polyesters compared to those obtained when free CAL-B was utilized [73]. The most widely used commercial biocatalyst is Novozym 435, where the lipase B is immobilized on a hydrophobic macroporous carrier resin, poly(methyl methacrylate-*co*-butyl methacrylate) (PMMA-*co* BMA). Novozym 435 has shown a significant stability and recyclability under different reaction conditions [74]. Despite many merits of enzyme immobilization, it also has some potential drawbacks including substrate diffusional limitations and blocking of the support pores by products [71, 72].

***Effect of enzyme type and concentration:*** Other important parameters that can influence the enzyme's catalytic activity are the enzyme type and concentration. For example, Uyama et al. [75] investigated the polymerization of sebacic acid with 1,4-butanediol at 60 °C under solvent-free conditions in the presence of five commercially available lipases of different origin, i.e. lipases derived from *Candida antarctica* (CAL-B), *Mucor miehei* (lipase MM), *Pseudomonas*

*cepacia* (lipase PC), *Pseudomonas fluorescens* (lipase PF), and *Porcine pancreas* (lipase PPL). The results showed that the polyester was obtained only in the presence of CAL-B. This fact is supported by its high catalytic activity and selectivity for polyester synthesis. Mahapatro et al. [73] studied the effect of enzyme concentration on the CAL-B-catalyzed polymerization of 1,8-octanediol and adipic acid. They found that an increase of the catalyst concentration from 0.1 to 10 wt% resulted in higher molar mass polymers. In contrast, increasing the CAL-B concentration from 10% to 20% for the polymerization reaction of 1,12-dodecanedioic acid and 1,8-octanediol has shown a positive impact on obtaining polymers with higher yield with no significant effect on the molar mass. This is, probably, due to a sterical hindrance and restriction of enzyme activity when long chain substrates are used [76]. Most recently, Perin et al. [77] studied the influence of CAL-B amount on the degree of branching of poly(glycerol sebacate) (PGS). A relatively high degree of branching (41%) with a number of dendritic units along the PGS chains was achieved, when using a CAL-B amount of 13.6 wt % at 40 °C under dry reaction conditions.

***Effect of water content:*** Apart from the influence of enzyme type and concentration, the water content can also affect the catalytic activity of CAL-B. As previously reported, a trace amount of water within the enzyme active site, known as “surface bound water”, plays an essential role in maintaining the enzyme activity and conformational flexibility [78]. Nevertheless, any increase in the water content of the reaction can result in polymers with low molar mass as the number of propagating chains increases [33].

***Effect of reaction temperature and time:*** In addition to the water content, temperature and reaction time greatly affect enzyme reactivity and selectivity. For instance, lipases exhibit remarkable stability and catalytic activity at elevated temperatures up to 95 °C. Nevertheless, any further increase in the temperature results in enzyme inactivation and, therefore, polymers with low molar mass can be produced [79, 80]. Azim et al. [80] stated the CAL-B-catalyzed synthesis of poly(butylene succinate) (PBS) at different temperatures (60, 70, 80, and 90 °C) in bulk as well as in diphenyl ether. PBS precipitates were obtained at 80 °C after 5-10 h reaction time, resulting in low molar mass polymer. In order to maintain a homogeneous reaction mixture, temperature was elevated from 80 to 95 °C after 21 h reaction time. As a result, a considerable increase in the number average molar mass ( $M_n$ ) of PBS was observed. The authors also noticed that there was no significant increase in  $M_n$  after a reaction time of 72 h. Wu et al. [81] reported the synthesis of renewable semicrystalline poly( $\beta$ -thioether ester) *via* CAL-B-catalyzed polycondensation of methyl 3-((11-hydroxyundecyl)thio)propanoate (MHUTP)

derived from castor oil applying different polymerization conditions like reaction temperature (50, 70 and 90 °C) and time (2, 6, 10, 24, 48 and 72 h). It was found that the highest  $M_n$  was achieved at 90 °C after 72 h reaction time. On the other side, many reports explained the temperature effects on enzyme selectivity. For example, Taresco et al. [82] synthesized PGA *via* CAL-B-catalyzed polycondensation reaction of glycerol and divinyl adipate (DVA) at different temperatures. They found that the molar mass of PGA was considerably reduced upon increasing the reaction temperature from 50 to 70 °C along with an increase in the degree of branching (5-30%), i.e. the selectivity of CAL-B towards primary OH-groups decreased at higher reaction temperature, resulting in polymers with higher degree of branching.

***Effect of solvent nature:*** Beside the mentioned parameters, the solvent used for enzymatic polymerization plays a crucial role in enzyme stability and activity. The use of hydrophilic solvents results in hydrogen bond formation between water molecules and the active center of the enzyme, which in turn is distorting its catalytic conformation and thus, reducing its activity [83]. Conversely, the use of hydrophobic solvents with low polarity (log  $P$  value between 1.9 and 4.5) such as n-hexane, diphenyl ether, and toluene preserves the enzyme catalytic activity by leaving a water layer on its surface as a protective sheath [30, 84]. Additionally, it is important to consider the solubility of all monomers in the solvent used as well as other solvent properties like its boiling point and its reactivity under specific reaction conditions [84]. Such solvents like diphenyl ether having a relatively high boiling point were found to be preferred solvents for enzymatic polymerization. For example, Linko et al. [85] reported the enzymatic synthesis of poly(1,4-butyl sebacate) with a molar mass of 42,000 g mol<sup>-1</sup> when diphenyl ether was used. Likewise, poly(butylene succinate-*co*-itaconate) (PBSI) with high  $M_n$  value was obtained in diphenyl ether. These results suggest that CAL-B has more accessibility in this solvent, which in turn leads to a greater growth of polymer chains [86]. As green alternative solvents, ionic liquids (ILs) have been used for enzymatic polymerization. Yoshizawa-Fujita et al. [87] demonstrated the lipase-catalyzed ROP of lactide in four different ILs. The data revealed that the monomer conversions and the  $M_n$  values of poly(lactide) (PLLA) obtained from ILs were higher than those of bulk and solution polymerization, while the polymer yields were comparatively lower than those obtained from bulk polymerization due to the high solubility of PLLA in ILs.

It is worth noting that the enzymatic polymerization can be conducted under solvent-free conditions (bulk) as well. Uyama et al. reported the lipase-catalyzed regioselective polymerization of activated ester, divinyl sebacate, and triols in bulk [88]. The use of activated

ester affords irreversible process as the by-product, vinyl alcohol, tautomerizes to acetaldehyde which can be evaporated at the reaction temperature. Another recent study reported by Lang et al. described the synthesis of PGS analogues in bulk using CAL-B as a catalyst and 1,8-octanediol, glycerol, and sebacic acid as monomers to produce poly(glycerol-1,8-octanediol-sebacate) (PGOS) with enhanced physicochemical properties for various biomedical applications [89]. Under these conditions, the enzyme is dispersed within the reactants mixture, resulting in highly efficient polymerization reaction [90].

***Effect of chain length and feed ratio of monomers:*** Other critical parameters that can affect the enzyme's catalytic activity are the chain length and feed ratio of monomers applied. Uyama and Kobayashi have polymerized DVA with different glycols using lipase derived from *Pseudomonas fluorescens* in isopropyl ether for 48 h [91]. Results showed that an increase in the diol chain length from ethylene glycol to 1,6-hexanediol resulted in polyesters with higher molar mass. Nevertheless, a further increase in diol chain length from C6 to C10 has greatly decreased the  $M_n$  values. In another study, an increase in the polymer molar mass obtained from the enzymatic polymerization of 1,8-octanediol with dicarboxylic acids was observed. However, a further increase of the diacid chain length from C10 to C14 resulted in polymers with lower  $M_n$  value [76]. Mahapatro et al. [92] showed that the systems with longer chain length diacids (sebacic acid and adipic acid) as well as diols (1,8-octanediol and 1,6-hexanediol) exhibit higher reactivity than those with shorter chain length (succinic acid and glutaric acid/1,4-butanediol). Accordingly, the use of diacids/its derivatives and diols having medium chain length is preferred to achieve polymers with an optimum molar mass.

In the line of monomers ratio, it has been shown that an increase in the acid derivative concentration e.g., vinyl esters, led to a higher transesterification rate and conversion. While, increasing the alcohol concentration has been found to reduce the reaction rates due to a dead-end inhibition complex formation by alcohol with the enzyme active site [93-95]. For instance, enzyme kinetic constants such as, maximum reaction rate ( $V_{max}$ ), substrate concentration at which the reaction rate is half  $V_{max}$  (Michaelis constant,  $K_m$ ), and inhibition constant ( $K_i$ ) were determined and the data showed that the lipase-catalyzed esterification reaction follows the ping-pong bi-bi kinetic model.

Further, the CAL-B-catalyzed polymerization of glycerol and oleic acid applying different molar ratios was reported. Authors observed that the formation of the highest molar mass polymer with low branching degree was achieved after 24 h reaction when equimolar

monomers ratio was applied [96]. In a recent research, the influence of monomers feed ratio on the polymer structure and molar mass was described. For instance, PGS with the highest molar mass was obtained when equimolar feed ratio of sebacic acid/glycerol was applied. The data also revealed that any deviation from equimolarity between the monomers led to a change in the polymer structure like, the use of higher glycerol feed resulted in the formation of more linear polymers with fewer dendritic units while, an increase in the sebacic acid feed yielded polymers with high degree of branching and less glyceride end groups [77].

To sum up, any change in the monomers feed ratio would be an efficient approach toward the control of the polymer structure by changing the polymer molar mass, end group functionality, and degree of branching.

### **1.1.3 Enzymatic polymerization by lipases**

#### ***Lipase-catalyzed polycondensation (PC)***

Lipase-catalyzed polycondensation is defined as the lipase-catalyzed esterification and transesterification between diacids or their activated esters with diols/polyalcohols or self-polycondensation of hydroxyacids/hydroxyesters under anhydrous conditions. It has significantly developed as a method for polyester synthesis, especially, polyesters having pendant functionalities at the polymer backbone, also known as functional polyesters [97]. Polycondensation reactions are commonly reversible as they are accompanied by the release of low molar mass by-products, thus, an efficient removal of these by-products is critical in order to shift the equilibrium towards products [98]. In general, monomers derived from plant oils (triglycerides) of varying fatty acid compositions are used for enzymatic synthesis of functional polyesters [99, 100]. The presence of fatty acid chains at the polymer backbone has shown to enhance some of its physical properties. Glycerol is obtained from biodiesel production and emerged as a cheap easily available, non-toxic, and biocompatible monomer for the synthesis of functional polyesters [63, 101]. Besides, other multihydroxy alcohols (polyols) derived from the hydrogenation of sugar molecules, e.g., xylitol and galactitol, were also used for this purpose [102]. Nevertheless, these polyols are soluble in highly polar solvents which negatively affect the enzyme activity. On the other hand, many diacids with different chain lengths have been subjected to enzymatic polymerization such as, malonic acid, succinic acid, glutaric acid, adipic acid, and sebacic acid. However, these traditional diacids often exhibit less reactivity, resulting in low molar mass products. Hence, many approaches have been established to overcome this concern. As previously mentioned, the use of activated esters such as, vinyl esters

as acyl donors has gained a great attention as they result in an easily removable by-products (vinyl alcohols) which rapidly tautomerize to give the corresponding aldehydes, making the reaction irreversible [103]. As a consequence, it is not necessary to apply certain conditions such as, vacuum or high temperatures for by-product removal, which in turn allows to maintain the regioselectivity of lipase and to produce linear polyesters [88]. Kline et al. [63] first reported the enzymatic synthesis of PGA using glycerol and DVA as monomers and Novozym 435 as a catalyst. During the polymerization process, most vinyl groups undergo enzyme bounded water-induced hydrolysis side reaction resulting in the formation of polyesters terminated with carboxylic acid end groups [90]. In some cases, some of these vinyl end groups are remaining at the end of the reaction and are able to react with different functional groups *via* Michael addition reaction. In order to overcome this reaction, polyester synthesis using dimethyl esters such as, dimethyl adipate (DMA), which is considerably cheaper than DVA and more suitable for large-scale production of polyesters, has been reported. In this regard, Naolou et al. [104] used glycerol and DMA as monomers for the enzymatic synthesis of PGA. Results showed that the  $M_n$  values obtained from the reaction of DMA are lower than that of DVA within a longer reaction time. This is due to the liberated by-product, methanol, which cannot be easily removed. To shift the reaction equilibrium towards the polymer synthesis, a continuous removal of methanol is required using a specific experimental set up with molecular sieves packed into a Soxhlet apparatus on top of the reaction vessel.

### ***Lipase-catalyzed ring-opening polymerization (ROP)***

Enzymatic ROP of lactones and other cyclic diesters with different ring sizes has been extensively studied for biomedical applications [105]. By comparison with polycondensation reaction, enzymatic ROP is not accompanied with by-products (water or alcohol) affording functional polyesters with favorable molar mass in good yields [37]. The first report of a lipase-catalyzed ROP of 6-membered ring  $\delta$ -valerolactone and 7-membered ring  $\epsilon$ -caprolactone was reported by two research groups, in 1993 [106-108]. Subsequently, enzymatic synthesis of different polymers *via* ROP and copolymerization of substituted and unsubstituted lactones with various ring sizes along with lactides, macrolides, cyclic carbonates, and cyclic depsipeptides has been extensively investigated as an efficient alternative to organometallic-based catalytic polymerization [84, 109]. In particular, the use of CAL-B has proven to be the most effective catalyst for the ROP of  $\epsilon$ -caprolactone and other lactones having different ring sizes. In addition, the effect of ring size on the enzymatic ROP reactivity has been explored, i.e.

larger ring-sized monomers having lower ring strain exhibit higher reactivity for enzymatic ROP than small and medium ring-sized in contrast to non-enzymatic processes [110].

### ***Combination of lipase-catalyzed ring-opening polymerization (ROP) and polycondensation (PC)***

Combination of lipase-catalyzed ROP and PC for developing novel polymeric structures with unique properties has been established. For example, Namekawa et al. [111] reported the enzymatic synthesis of complex polyesters from lactones, divinyl esters, and glycols using lipase as catalyst through combination of ROP and PC.

#### **1.1.4 Synthesis and applications of graft copolymers**

Graft copolymer consists of a linear polymer backbone and randomly distributed side chains (branches) of a different composition along the backbone. For instance, the polymer backbone and the branched side chains are two different homopolymers as well as the branched chains might be homopolymers or copolymers. Three main strategies have been developed for the synthesis of graft copolymers; (1) “grafting onto” strategy, (2) “grafting from” strategy, and (3) “grafting through” strategy [112].

The “grafting from” method is carried out by the preparation of a macromolecular backbone with distributed initiation sites (macroinitiators) capable of initiating the polymerization of a second monomer, resulting in graft copolymers. These initiation sites can be introduced onto the polymer backbone before polymerization or after the first step of polymerization. Well-defined graft copolymers with high grafting density are prepared by this method, especially, when controlled radical polymerization such as, atom transfer radical polymerization (ATRP) or ring-opening metathesis polymerization (ROMP) being applied for grafting reactions. In this approach, there is no unreacted macroinitiator and thus, purification of the final graft copolymer is not required in contrast to the “grafting onto” and “grafting through” routes. However, these grafting reactions are performed in diluted systems and require several steps of protection and deprotection which result in long reaction times as well as loss of monomers. The “grafting onto” method involves a coupling reaction between end-functionalized graft chains with randomly distributed functional groups along the polymer backbone. Such techniques are applied to synthesize these graft copolymers including free radical polymerization, anionic polymerization, ATRP, and living polymerization. Despite presenting some drawbacks such as limited grafting density and the need for additional purification steps to remove unreacted side chains, this technique has the advantage of preparing well-defined graft copolymers since

precise characterization of the polymer branches can be achieved before being grafted. The “grafting through” or macromonomer method is performed in two steps including the synthesis of macromonomers with polymerizable terminal groups and their copolymerization with comonomers to obtain the brush structure. This approach has the advantage of preparing graft copolymers with controlled grafting density (a defined number of side chains per repeating unit) by controlling the molar ratio of monomers to macromonomers during the polymerization process. Due to the low reactivity of macromonomers and high steric hindrance of the propagating chain end, the complete conversion of macromonomers is not achievable. Therefore, a tedious purification step is necessary for the removal of unreacted macromonomers. It is worth noting that the synthesis of graft copolymers can be achieved by one of these mentioned methods or by a combination of “grafting from” and “grafting onto” strategies [113].

The presence of functional pendant groups in the polymer backbone offers the potential for further conjugation with side chains having a variety of functional groups, which in turn tailor the physicochemical properties of polyesters [114]. Therefore, they have been used for many advanced applications. Parrish et al. [115] prepared aliphatic polyesters having pendant acetylene groups by controlled ROP and then grafted with poly(ethylene glycol) (PEG)-azide side chains as well as with various oligopeptides by “click” chemistry to produce amphiphilic graft polyesters that might be applied for a range of biomaterial applications such as tissue engineering and drug delivery. In another study, Lenoir et al. [116] prepared  $\alpha$ -chloro- $\epsilon$ -caprolactone and then copolymerized this monomer with  $\epsilon$ -caprolactone to obtain chloro-functionalized caprolactone. These pendant activated chlorides of the copolymer were used to initiate the “grafting from” of poly(methyl methacrylate) and poly(butenyl benzoate) by ATRP. Later on, they used the same copolymer and substituted all pendant chlorides by azides to further react with alkyne functionalized chains having ester, amine, and ammonium groups. In addition, alkyne-functionalized PEG was grafted to poly( $\epsilon$ -caprolactone) (PCL) resulting in amphiphilic copolymers [117]. Naolou et al. [118] prepared aliphatic polyesters with pendant azide groups *via* CAL-B-catalyzed polycondensation of 2-(azidomethyl)-2-methylpropane-1,3-diol and DVA and then grafted with alkyne-PEG side chains *via* “click” reaction resulting in well-defined water soluble graft copolymers.

Many reports have described the synthesis of graft copolymers based on PGA. PGA is a glycerol-based polyester with one pendant secondary free OH-group per repeating unit which renders the polyester hydrophilic. These free OH-groups along the PGA backbone have been

used for further modifications with a variety of molecules, such as fatty acids, amino acids, and many therapeutics. Kalinteri et al. [23] stated the esterification reaction of various amounts of different fatty acyl substituents with the pendant OH-groups along the polyester backbones to form amphiphilic comb-like polyesters able to self-assemble into well-defined nanoparticles with a very low toxicity for beneficial use in the field of nanoparticulate drug delivery system. Another study carried out from the same research group described the synthesis of functionalized PGA with different fatty acids as well as with the amino acid, tryptophan, for optimized preparation of nanoparticles based on surface energy determinations [119]. Likewise, our group has reported the modification of the PGA backbone with fatty acids of various lengths at different substitution degrees, in order to obtain comb-like polymers that can undergo nanophase separation between the side chains and the polymer backbone. Based on the degree of substitution, nanoparticles with various morphologies (lamellar and polygonal nanoparticles) were obtained. Owing to their biodegradability and non-toxicity, they were applied in the field of drug delivery [120, 121]. Afterwards, the relationship between the structure of amphiphilic comb-like fatty acid modified-PGA and its molecular arrangement at the air/water interface was investigated [122]. In another study, the synthesis of biodegradable graft copolymer, poly(glycerol adipate)-*graft*-(poly( $\epsilon$ -caprolactone)-*block*-poly(ethylene oxide)) (PGA-*g*-(PCL-*b*-PEO)) was reported. Initially, poly(glycerol adipate)-*graft*-poly( $\epsilon$ -caprolactone) (PGA-*g*-PCL) was prepared by ROP of  $\epsilon$ -caprolactone using the OH-groups of PGA as initiators. Then, PGA-*g*-(PCL-*b*-PEO) was synthesized by grafting of azide-terminal PEO monomethylether (mPEO-N<sub>3</sub>) onto PCL blocks by copper-catalyzed azide-alkyne cycloaddition (“click” reaction) [123]. Authors also studied the crystallization and melting behavior of PGA-*g*-(PCL-*b*-PEO) in addition to its phase behavior at the air/water interface [124, 125]. Saleem and co-workers reported the synthesis of biodegradable PGA-based copolymer, poly(glycerol adipate-*co*- $\omega$ -pentadecalactone) (PGA-*co*-PDL), *via* CAL-B-catalyzed ring-opening copolymerization reaction of DVA, glycerol, and lactone monomers with tunable thermal properties and amphiphilicity. PGA-*co*-PDL before and after modification with PEG has been formulated into nanoparticles (NPs) or microparticles (MPs). These biodegradable NPs and MPs were further used for drug delivery [126-128]. Jbeily et al. [129] studied the modification of hydroxyl pendant groups of the PGA backbone with ATRP macroinitiators, followed by the subsequent grafting-from ATRP of glycerol monomethacrylate (GMA) to produce well-defined amphiphilic graft copolymers able to self-assemble in aqueous solutions. In a recent study, PGA was grafted with different amounts of hydrophobic fatty acid side chains and hydrophilic PEG side chains to form grafted polyesters able to self-assemble into NPs for delivery of hydrophilic

and lipophilic drugs as well as to sterically stabilize cubosomes *via* controlling the degree of grafting of hydrophilic and hydrophobic moieties [130].

Due to the tunable properties of PGA such as biodegradability and biocompatibility, it has been also used for the conjugation with a variety of drug molecules. The conjugation of PGA-*co*-PDL to ibuprofen was reported and the results showed that the ester linkages formed between the polymer and ibuprofen were highly stable, thus, the rate of drug release was slower compared with the unconjugated drug form [131]. Wersig et al. stated the grafting of PGA with the anti-inflammatory drug indomethacin in order to develop promising prodrugs for sustained drug release [132]. Suksiriworapong et al. [133] reported the first polymer-anticancer drug methotrexate conjugate with PGA. These conjugates showed promising properties in terms of biocompatibility, stability, and enzymatic degradability. Subsequently, authors studied comprehensively the enzymatic degradation of PGA [10]. They found that the enzymatic degradation rate of PGA depends to a highly extent on the enzyme type and polymer modifications with various side chains. Beside PGA, sugar-based polyesters, namely PDSA and poly(xylitol adipate) (PXA) were successfully grafted with stearic acid side chains at different degrees of substitutions to produce amphiphilic polymers able to self-assemble into NPs [25]. In recent research studies, PGA and PDSA were subjected to protein conjugation using microbial transglutaminase (mTGase) as a catalyst [27, 28].

## 1.2 Protein-polymer conjugation

Therapeutic proteins are an important class of drugs that often exhibit low toxicity, high potency and selectivity as well as have shown to be effective in the treatment of a wide range of diseases such as, diabetes, anemia, multiple sclerosis, human immunodeficiency virus (HIV), cancer and other diseases [134, 135]. However, these therapeutics in their native form have some limitations for instance, short circulating half-life ( $t_{1/2}$ ), susceptibility to enzymatic degradation and rapid renal clearance, and immunogenicity [136]. Many therapeutic proteins exhibit short half-lives in plasma and therefore, daily administration of these therapeutics is required. For example, erythropoietin (EPO), a glycoprotein hormone that mainly regulates the generation and maintenance of red blood cells (RBCs) and has been widely used as a therapeutic agent to treat anemia, exhibits a fairly short  $t_{1/2}$  *in vivo* [137-139]. Many attempts, therefore, have been made to improve the bioavailability of proteins through introducing additional glycosylation sites into proteins [140], amino acids substitutions [141], generation of fusion protein *via* recombinant DNA technology [141], covalent lipid modifications of proteins [142], and

especially the covalent attachment of synthetic polymers to therapeutic proteins (Figure 3) that results in improved pharmacokinetic properties of the native proteins [143].

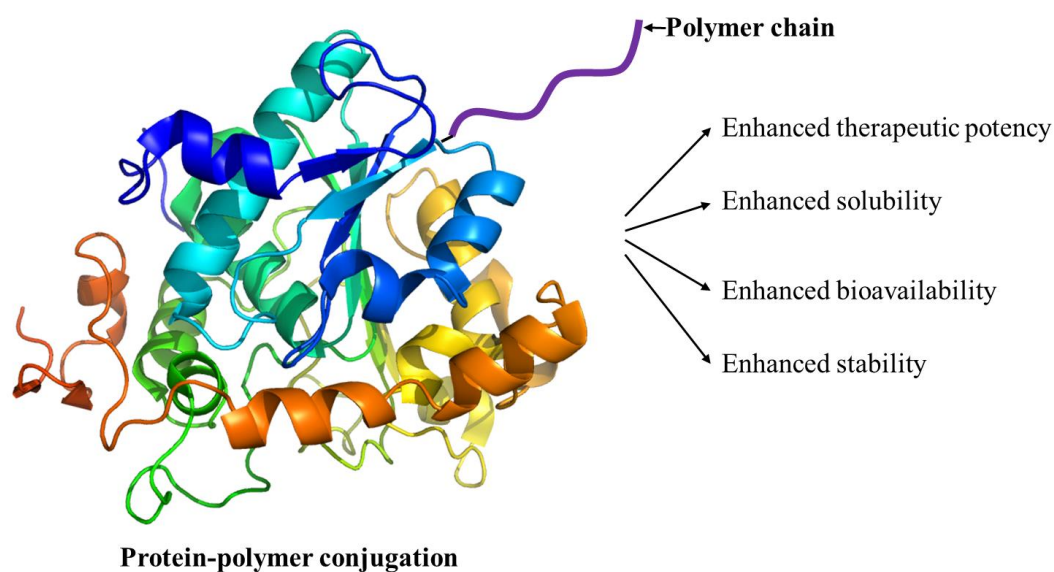


**Figure 3.** Protein-polymer conjugation influence on many pharmacokinetic properties of the native proteins.

Protein-polymer conjugates comprise a class of hybrid molecules that have been widely applied in therapeutic fields due to the unique combination of the stability and multifunctionality of synthetic polymers with the biological activity of proteins. The first covalent attachment of PEG, also known as PEGylation, to bovine serum albumin (BSA) and bovine liver catalase using cyanuric chloride as a coupling agent was reported by Abuchowski et al. [144, 145]. The data revealed that PEGylation of proteins resulted in conjugates with enhanced *in vivo*  $t_{1/2}$  and lower immunogenicity in comparison with the native proteins. Subsequently, many research studies have been performed applying different proteins. For instance, granulocyte colony-stimulating factor (GCSF) displays a short circulating  $t_{1/2}$ , around 24 h and hence, Do et al. [146] studied the effect of polymer conjugation on the activity and plasma circulation of GCSF. The conjugation of hydrophilic PEG (20 kDa) to the amine terminus of GCSF resulted in bioconjugates with similar biological activity of native GCSF. Interestingly, this study showed increased plasma  $t_{1/2}$  of GCSF from 24 h to 72 h upon PEGylation. Similarly, plasma  $t_{1/2}$  of PEGylated erythropoietin has shown to be remarkably prolonged compared with that of native protein [147, 148]. Other authors stated that the effects of polymer conjugation on the protein activity and pharmacokinetics are mainly dependent on the conjugation site and the polymer molar mass. Kim and co-workers investigated the covalent attachment of methoxy poly(ethylene glycol) (mPEG) (750 and 2000 Da) chains to the amino groups of N-terminal phenylalanine B1 (PheB1) or lysine B29 (LysB29) residues of human insulin [149]. The *in vivo*

activity of insulin was observed to increase by 4 and 12% for mPEG750 conjugated at PheB1 and LysB29, respectively. However, the conjugation of mPEG2000 at PheB1 and LysB29 led to a decrease in its bioactivity by approximately 15%. The data also showed that mPEG750 conjugated at PheB1 and LysB29 exhibited an increase in the  $t_{1/2}$  of human insulin from 12 h to 18.4 and 4.3 days, respectively. While, mPEG2000 conjugated at PheB1 and LysB29 displayed half-lives of 20.7 and 8.6 days, respectively.

According to the literature reviewed, it is evident that PEG is widely used as a gold standard in the field of protein conjugation since several PEGylated proteins are already approved by the Food and Drug Administration (FDA) and used clinically as therapeutics e.g., PEG-L-asparaginase (Oncaspar) used to treat acute lymphoblastic leukaemia, PEG-GCSF (Neulasta) used to prevent neutropaenia associated with cancer chemotherapy, PEG-adenosine deaminase used for severe combined immunodeficiency, PEG-interferon (IFN) $\alpha$ 2a (PEG-asys) and PEG-IFN $\alpha$ 2b (PEG-Intron) used for the treatment of Hepatitis C [134]. Despite its great achievements in the field of protein/drug conjugation, there have been some concerns about PEG safety which limit its use in this field. Although PEG is considered safe, it has been reported that chronic use of PEGylated therapeutics can cause vacuoles accumulation in organs like, kidney, liver, and spleen due to its non-biodegradability [150, 151]. Furthermore, the repetitive administration of PEGylated therapeutics as well as PEGylated liposomes, PEGylated nanoparticles, and PEGylated micelles has been shown to cause immunogenic response known as accelerated blood clearance (ABC) phenomenon resulting in high clearance and loss of therapeutic efficacy. In this respect, clinical studies of PEGylated uricase (Pegloticase) have shown that formation of anti-PEG antibodies is associated with increased Pegloticase clearance, reduced therapeutic efficacy, and increased risk of infusion reactions (IRs) [152-154]. Alternatives to PEG have been investigated for protein conjugation such as poly(vinylpyrrolidone) (PVP), dextran, polysialic acids (PSAs), hyaluronic acid (HA), dextrin, hydroxyethyl starch (HES), poly(2-ethyl 2-oxazoline) (PEOZ), polyolefins carrying N-hydroxypropyl, sulfonate, oligo ethylene glycol, PGA, and PDSA. Along with that, the modification of protein with synthetic polypeptides, also known as poly( $\alpha$ -amino acid)s or PEPylation was investigated as a promising approach to obtain therapeutic conjugates with longer circulation  $t_{1/2}$  and lower immunogenicity [27, 28, 155].

Beside therapeutic proteins, many enzymes e.g., cellulase, lipase, xylanase are used in industrial processes. Hence, polymer conjugation with these proteins can potentially impact their activity and stability. Ge et al. [156] reported the conjugation of lipase with hyperbranched aromatic

polyamides which resulted in enhanced lipase activity and stability compared to the native lipase. This work showed also that conjugated lipase exhibited a significant activity and stability in organic solvents or at elevated temperatures.

### 1.2.1 Synthesis of protein-polymer conjugates

The conjugation of proteins to small molecules or synthetic polymers is usually achieved *via* one of three synthetic strategies: grafting to, grafting from and grafting through. Indeed, these conventional chemical procedures are not sufficiently selective resulting in heterogeneous mixtures of protein conjugates. In particular, the conjugation reactions with the abundantly present  $\epsilon$ -amine groups of Lys residues on the protein surface led to a heterogeneous conjugate mixture with reduced protein bioactivity [157, 158]. Therefore, the development of site-specific protein-polymer conjugation was widely explored. Since cysteine (Cys) residues having free thiol groups are rarely present in protein sequences, genetic incorporation of Cys residues at a specific site of protein is applied as an effective approach to achieve site-specific conjugation. In this sense, protein modification can be carried out *via* either exchange reaction with disulfide-containing reagents or alkylation with electrophiles containing compounds and Michael acceptors, especially maleimides [159]. Besides, aromatic residues, such as tyrosine, were used for protein conjugation *via* Mannich-type reaction [160]. Additionally, N-terminal amine can be used for the site-specific attachment of different molecules or polymers [161]. Such techniques have been utilized for the development of well-defined bioconjugate including, ATRP, nitroxide-mediated radical polymerization (NMP), reversible addition fragmentation chain transfer polymerization (RAFT), ROMP, and “click” chemistry. Basically, they use either amino acids present within the protein structure or non-natural amino acids/different functional groups that can be introduced into proteins [162]. For example, Gao et al. [163, 164] reported the *in situ* ATRP growth of a PEG-like polymer, poly(oligo(ethylene glycol) methyl ether methacrylate) [poly(OEGMA)], with low polydispersity and high yield from the N-terminus of myoglobin or C-terminus of green fluorescent protein (GFP). This resulted in significantly improved pharmacological properties of proteins.

Apart from these approaches, enzyme-catalyzed bioconjugation provides a viable alternative to achieve a site-specific protein conjugation under mild reaction conditions. This includes the use of phosphopantetheinyltransferase [165], formylglycine generating enzyme (FGE) [166], sortase [167], farnesyltransferase [168], biotin ligase [169], lipoic acid ligase [170], *N*-myristoyl transferase [171], and mTGase. In particular, mTGase from *Streptomyces*

*mobarraensis* have been considered one of the most favored candidates for this purpose [172-174].

### 1.2.2 Transglutaminases

Transglutaminases (TGases, protein-glutamine  $\gamma$ -glutamyltransferases, EC 2.3.2.13) belong to the transferase class of enzymes that cross-link proteins by catalyzing an acyl transfer reaction between  $\gamma$ -carboxamide groups of peptide or protein-bound glutamine (Gln) residues, which act as acyl donors, and a variety of free primary amine groups including the  $\epsilon$ -amino group of Lys residues, which act as acyl acceptors. This reaction results in the formation of isopeptide bonds between proteins accompanied with the consequent loss of ammonia (Figure 4). In the absence of free primary amine groups, TGase catalyzes the deamination reaction of Gln residues, where water or alcohol molecules act as acyl acceptors [48, 175].

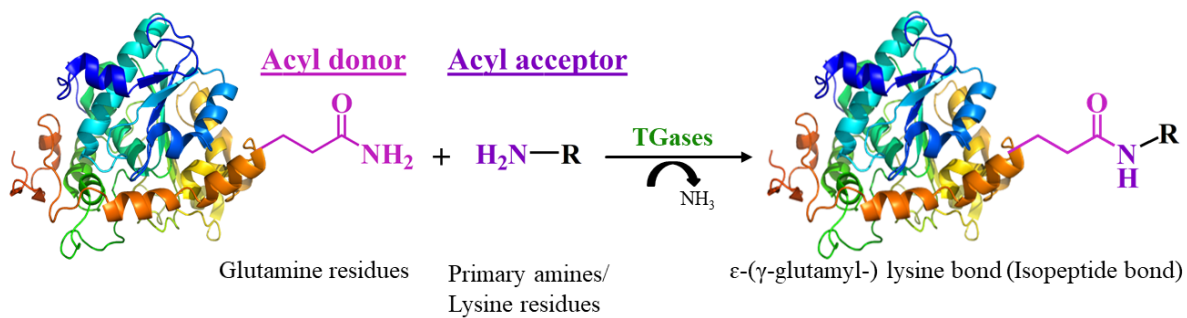


**Figure 4.** TGase-mediated cross-linking reactions between protein-bound Gln and Lys residues which result in the formation of isopeptide bonds.

So far, TGases have been isolated from animal and plant tissues as well as from microorganisms. Indeed, tissue TGase isolated and purified from guinea-pig liver was the first and only commercially available TGase until the late 1980s. However, tissue TGase is calcium ( $\text{Ca}^{2+}$ )-dependent which leads to protein destabilization in some food proteins. In addition, the rare source and complex purification process to produce tissue TGases resulted in very high cost of the enzymes that in turn limited their applications on a large industrial scale. Consequently, research efforts have been made to obtain TGases from microbial sources, which are generally cost-effective and easy to produce in high quantities and purity [176].

#### 1.2.2.1 Microbial transglutaminases

Compared to eukaryotic TGase, mTGase is a monomeric simple protein with a relatively low molar mass,  $\text{Ca}^{2+}$ -independent, and significantly stable over a wide range of pH-values and

temperatures [176]. In 1989, Ando et al. [177] reported the first mTGase from a strain of *Streptomyces mobaraensis*. mTGase is a monomeric enzyme consisting of a 331 amino acid single polypeptide chain with a molar mass of 37.9 kDa. It possesses an  $\alpha/\beta$  folding class that consists of eight  $\beta$ -strands surrounded by 11  $\alpha$ -helices forming a disk-like structure (Figure 5) [178]. The enzyme active site has a catalytic triad comprised of cysteine (Cys64), histidine (His274), and aspartic acid (Asp255) residues. The thiol group of the Cys64 residue plays an essential role in the catalytic activity of mTGase.

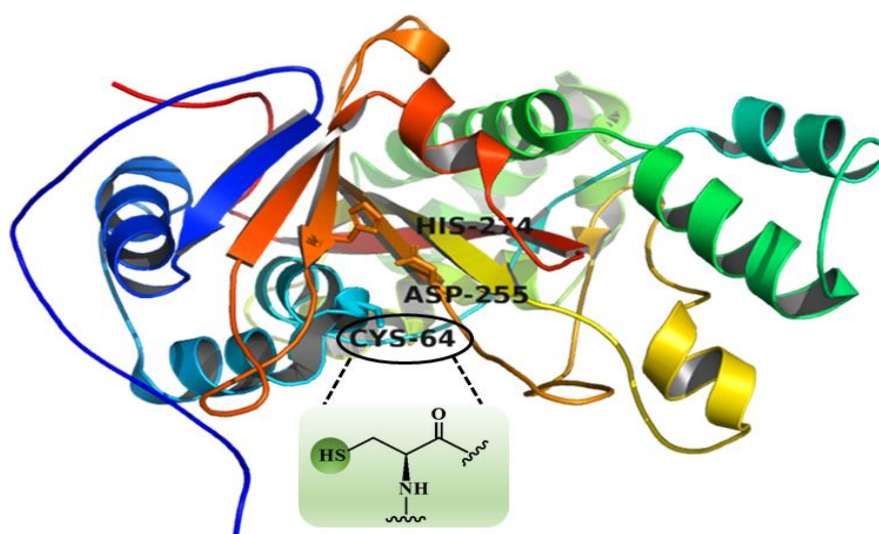
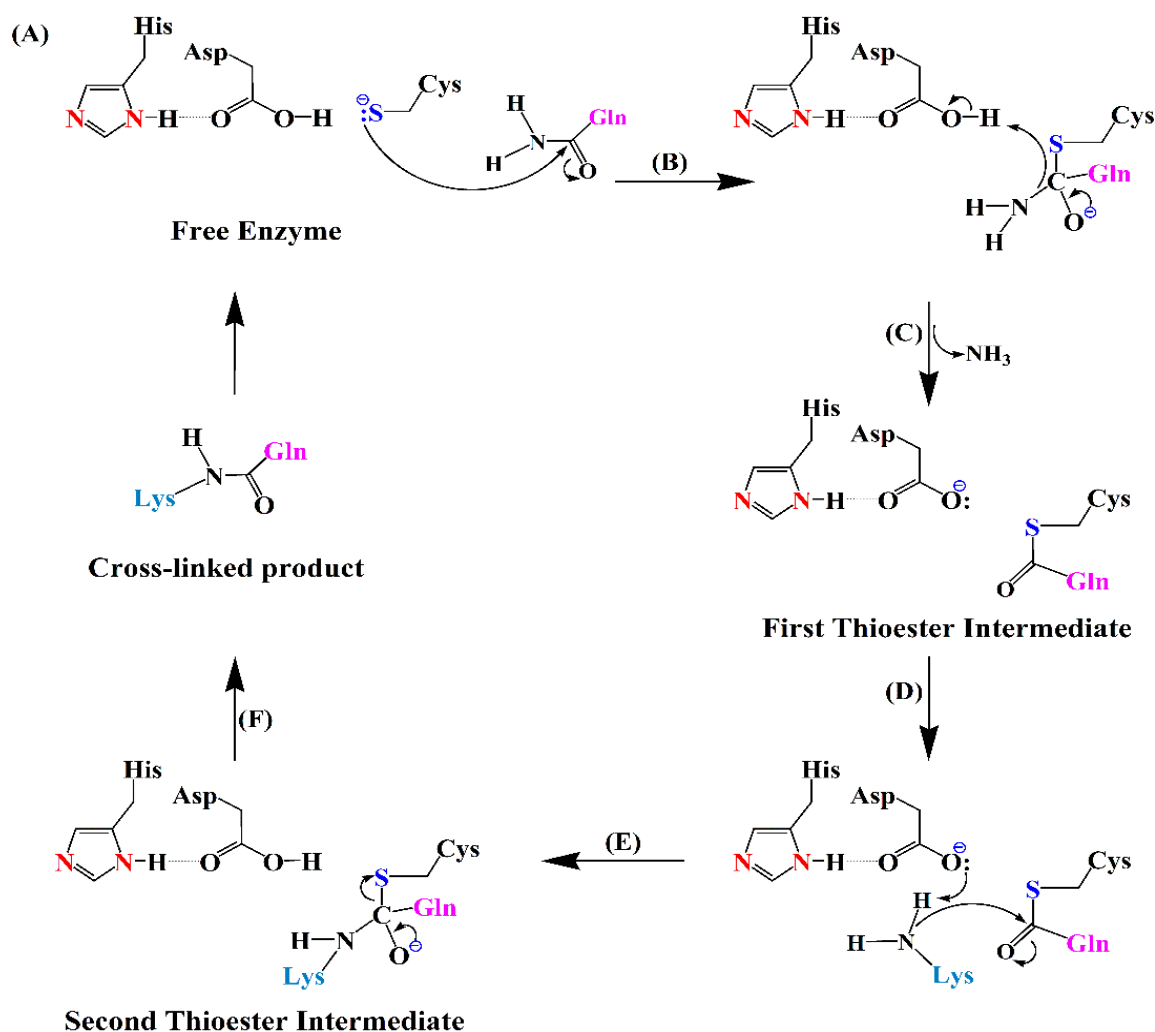


**Figure 5.** 3D structure of mTGase (PDB code 1IU4) [178]. The structure is drawn using PyMOL (The PyMOL Molecular Graphics System, Schrödinger, LLC). Cys64, His274, and Asp255 residues represent the catalytic triad of mTGase. The structure given in the green box belongs to Cys which is considered as an essential residue for the mTGase catalytic activity.

The proposed mechanism by which TGase catalyzes isopeptide bond formation between proteins is illustrated in Scheme 2. The catalytic mechanism of mTGase proceeds *via* a nucleophilic attack by the enzyme's catalytic Cys64 at the susceptible Gln residue (acyl donor) of a protein (step (A)). In step (B), Asp255 donates a proton, which results in the formation of a first thioester intermediate along with a consequent release of ammonia as a by-product (step (C)). Subsequent nucleophilic attacks by an amine substrate (acyl acceptor) at the carbonyl group of the intermediate and by Asp255 at a proton of the acyl acceptor lead to the formation of a second thioester intermediate (step (D)). In steps (E) and (F), the cross-linked product is released from the intermediate and the free enzyme is regenerated [178].



**Scheme 2.** Catalytic mechanism of mTGase, adapted from [178].

In general, the optimal temperature for mTGase activity ranges between 45–55 °C and varies among different species. For instance, mTGase from *Streptomyces mobaraensis* exhibits maximum activity at 55 °C, while the optimum temperature of mTGase derived from *Streptomyces cinnamoneum* and *Streptomyces griseocarneum* is 45 °C. The optimum pH for mTGase activity ranges between 5 and 8 and some activity was reported at pH 4 or 9. The activity of mTGases can be affected by the presence of  $Zn^{2+}$ ,  $Cu^{2+}$ ,  $Hg^{2+}$  and  $Pb^{2+}$  ions which bind to the thiol group of Cys in the catalytic center, resulting in loss of activity [176]. The selectivity and catalytic efficiency of mTGase is based on the amino acid sequence adjacent to the Gln and Lys residues. In this regard, Malešević et al. [179] investigated the effect of flanking amino acids of donor Gln residue and acceptor Lys residue for the recombinant *Streptomyces mobaraensis* mTGase catalytic efficiency. It was found that hydrophobic and basic residues especially, arginine, tyrosine, and leucine have a significant preference at Gln+1 and Gln-1 while, the presence of negatively charged amino acids at Gln-1 inhibits the TGase activity. They

also found that proline residue is accepted by mTGase at Gln-1 but not at Gln+1. Furthermore, no peptide with Lys residues at Gln+1 or Gln-1 was recognized by mTGase which is explained by their inter- or intramolecular cross-linking with other reactive groups. Regarding the acyl acceptor substrates, it was stated that peptides with aromatic amino acids adjacent to the Lys residue as well as peptides containing two Lys residues show the highest mTGase activity. While, peptides having negatively charged amino acids at Lys+1 or Lys-1 are not accepted by mTGase. In addition, the selectivity of mTGase is based on the conformational features of the substrates since the Gln and Lys residues recognized by TGases as acyl donor and acceptor substrates, respectively, are located in highly flexible and unfolded regions of a protein [180]. Spolaore et al. [180] studied the site-specific derivatization of avidin using mTGase. The results showed that avidin was modified at the level of Lys127 which is located in the flexible/unfolded C-terminal region of the protein. Another study carried out from the same research group reported the site-specific mTGase-catalyzed conjugation of IFN $\alpha$ 2b at Gln101 and Lys164 residues which are embedded at the level of flexible protein regions [181].

### **1.2.2.2 Applications of microbial transglutaminases**

Regarding its applications, mTGase is widely used in the food industry to modify the appearance and texture of the protein-rich food like meat and fish and to enhance the gel strength of cheese and yogurt [182, 183]. Apart from that, it is used to increase the tensile strength of wool and leather [182, 184] and to produce biodegradable protein films [185]. Another field of application is the site-specific modification of therapeutic proteins, which is considered as a powerful technique to improve their pharmacokinetic properties. Sato et al. [186] reported a method for site-specific modification of recombinant human interleukin-2 to PEG using mTGase. Subsequently, the PEGylation of recombinant GCSF, human growth factor (hGH), apomyoglobin (apoMb), salmon calcitonin (sCT), and cytochrome *c* (cyt *c*) as well as the HESylation (i.e. conjugation with HES) of a model protein, dimethylcasein (DMC), catalyzed by mTGase were reported [187-191]. Besides, PGA was used for the mTGase-mediated conjugation reaction with DMC under mild reaction conditions [27]. The successful formation of PGA-DMC conjugates was promising to expand the research scope to use therapeutic proteins that may contribute to the biomedical field. Thus, PDSA was successfully conjugated with a therapeutic protein, recombinant human erythropoietin (rHuEPO), at its transition temperature  $T_m$  in the presence of a thermostable variant mTGase-TG<sup>16</sup>. The data showed that only rHuEPO-PDSA conjugates with high molar mass were obtained because of multi-site conjugation [28]. Furthermore, the site-specific conjugation of polyacrylamide

grafted with multiple mTGase-recognizable substrates to functional proteins with a Lys tag by mTGase for immunological biosensing applications and the mTGase-mediated conjugation of DNA aptamer with enhanced GFP were stated [192, 193]. mTGase has also been utilized in the field of antibody-drug conjugates (ADCs), which are considered as promising agents for the treatment of tumors. For example, Strop et al. [194] developed an enzymatic method for site-specific antibody-drug conjugation using mTGase and lately, the successful site specific conjugation of drug-linker constructs to a fully glycosylated immunoglobulin G (IgG)-type antibodies using mTGase was reported [195]. In addition, mTGase has other applications concerning protein immobilization e.g., the successful mTGase-mediated site-specific immobilization of functional proteins such as *Escherichia coli* alkaline phosphatase (AP) on solid surfaces and magnetic particles, providing an efficient approach to generate a variety of protein-based solid formulations for biotechnological applications [196, 197].

It is worth noting that some cross-linking reactions catalyzed by mTGase require high temperatures with retained mTGase activity. Therefore, many attempts have been made to produce mTGase variants with higher activity and thermostability. Marx et al. [198] established, for the first time, a screening method applied to a randomly mutated pro-transglutaminase resulting in thermostable and heat-sensitive variants of mTGase. It was stated that seven mutants (S2P, S23 L, Y24 N, G257S, K269E, H289Y, and L294 M) engineered by error-prone polymerase chain reaction (epPCR) exhibit a remarkably improved thermostability at 60 °C, especially, S2P with single amino acid substitutions, i.e. the exchange of Ser close to the N-terminus against proline, showed 270% increased  $t_{1/2}$  at 60 °C as well as higher specific activity at 37 °C. Afterwards, saturation-site mutagenesis of these seven “hot spots” along with DNA-shuffling was conducted in order to further improve the thermal stability of mTGase. As a result, the most thermostable mutant, the triple mutant S23V-Y24N-K294L showed a 12-fold improved  $t_{1/2}$  at 60 °C and a 10-fold higher  $t_{1/2}$  at 50 °C compared to the wild-type mTGase [199]. In another study, a novel mTGase mutant with enhanced activity and thermostability was obtained *via* direct evolution strategy, i.e. it exhibits a 1.95-fold specific activity and a 1.66-fold higher  $t_{1/2}$  at 50 °C compared to the wild-type mTGase [200]. Jiang et al. [201] applied the atmospheric and room temperature plasma (ARTP) mutagenesis to enhance the fermentation production of TGase from *Streptomyces mobaraensis* for various applications in the food industry. Ohtake et al. [202] utilized genetic code expansion to enhance the thermostability of mTGase from *Streptomyces mobaraensis*. By introducing 3-chlorotyrosines at positions 20, 62, and 171, variant mTGase with a 5.1-fold longer  $t_{1/2}$  than that of the wild-type enzyme at 60 °C

was obtained. Recently, Böhme et al. [203] represented a novel thermoresistant recombinant variant TG<sup>16</sup> of mTGase using *E. coli* BL21Gold (DE3) cells for the production of recombinant proteins. Their study based on a combination of previously determined amino acid substitutions, i.e. S2P, S23Y-Y24 N, H289Y, and K294L, resulted in a mTGase-TG<sup>16</sup> variant with a 19-fold improved  $t_{1/2} = 38$  min at 60 °C compared to the wild-type mTGase. On the other hand, and for mTGase applications in food processing, it is preferable to carry out the cross-linking reactions under low temperature conditions. Thus, heat-sensitive mTGase variants with high activity at low reaction temperatures are favorable [198]. These strategies explain the structure-activity relationship of mTGase which in turn provides preliminary information on its tailored catalytic activity to fit real industrial requirements by protein engineering.

To sum up, mTGase has emerged as a versatile tool for enzymatic bioconjugation due to its high selectivity and catalytic activity under mild conditions. Apart from its widespread applications in the food industry, mTGase has proved its potential in biomedical research.

### **1.3 Polymer networks and hydrogels**

Polymer networks are three-dimensional (3D) cross-linked macromolecules with a wide range of biomedical and industrial applications. In general, polymer networks can be formed by chemical cross-linking of polymer chains through stable covalent interactions, reversible physical gelation *via* noncovalent interactions, or by a combination of both. These networks exhibit some specific mechanical properties like high porosity, elasticity, and swelling ability that can be tuned towards the desired properties for their intended application [204]. Hydrophilic polymer networks with a tunable capacity to retain a massive amount of water or biological fluids, known as hydrogels, display great biocompatibility as their mechanical properties can be modulated in order to match those of biological tissues and cells [205, 206]. Their affinity to absorb water is mainly attributed to the presence of hydrophilic functional moieties like sulphate, carboxylic acid, hydroxyl, amine, and amide groups.

In the 1960s, poly(2-hydroxyethyl methacrylate) (PHEMA) hydrogels were first applied as soft contact lenses [207]. In the following decades, hydrogels have been investigated for various biotechnological and biomedical applications due to their tunable properties like flexibility, hydrophilicity, and biocompatibility. Such applications include, cosmetics and hygiene products, microfluidics, wound dressings, scaffolds for soft tissue engineering, and drug delivery systems [208]. Due to their porous structure, hydrogels have been used for the localized and sustained release of biologically active agents in which the therapeutics sustained release

can be controlled by modifying polymer molar mass and composition. The use of controlled release hydrogel formulations is regarded as a vital approach to allow less frequent administration of therapeutics as well as to protect them from enzymatic degradation [206]. For example, the hydrogel contact lenses have been utilized as ocular drug carriers in order to enhance the bioavailability of many ophthalmic therapeutics [209].

Generally, the therapeutics release can be achieved by various mechanisms controlled by diffusion, swelling, chemical, and environmentally-based stimuli (e.g., temperature, pH-value, light, etc.) [208, 210]. Diffusion-controlled drug release is the most frequently used mechanism for releasing drugs from hydrogels. This system is represented by two main types, reservoir and matrix devices. In a reservoir delivery system, the drug core is covered by a hydrogel membrane which can be capsule, cylinder, or slab. Here, the drug can be sustainably released from the center of the system. Whereas in a matrix system, the drug is dispersed throughout a hydrogel and its release is proceeded by the network's meshes or pores. In swelling-controlled drug release, the drug is dispersed in glassy polymers and the swelling starts when the polymeric network is in contact with biological fluids, allowing the diffusion of drugs. Chemically-controlled drug release is based on a chemical reaction that occurs within a delivery system to initiate the drug release from hydrogels. This includes reversible or irreversible reactions between the polymeric network and releasable drug as well as polymer chains cleavage through hydrolysis or enzymatic degradation.

PEG-based hydrogels have been widely explored as controlled drug carriers and as anti-adhesive biomaterials owing to the excellent properties of PEG such as, biocompatibility and hydrophilicity. Graham et al. [211, 212] reported the sustained release of prostaglandin E2 and morphine from PEG hydrogels through diffusion controlled release. Although PEG is non-biodegradable, it still remains one of the mostly investigated systems, especially, upon copolymerization with biodegradable polyesters such as, PLGA and PLA in order to obtain biodegradable hydrogels [213, 214]. The preparation of hydrogels based on biodegradable polymers has shown to offer unique advantage in the field of drug delivery as they offer a controlled release of various therapeutic agents over a long period of time, which in turn improve the bioavailability of these therapeutics. In this regard, many biodegradable and naturally occurring biopolymers, synthetic polymers, or blends of synthetic and natural polymers (hybrid) have been extensively investigated. Natural biodegradable hydrogels such as, alginate and sodium alginate/collagen have shown to provide a sustained drug release [215, 216]. Despite the fact that natural polymers have excellent biocompatibility, they exhibit low

stability and poor mechanical properties and thus, they have been blended with synthetic polymers having well-defined structures that can be modified to promote desirable properties [217]. For instance, early research reported on cross-linked blends of biodegradable poly(vinyl alcohol) (PVA) and collagen or hyaluronic acid for the release of recombinant human growth hormone [218]. More recently, hydrogels based on PVA were applied as controlled drug delivery in cancer treatment through swelling-controlled release, i.e. the drug is released upon exposure to biological fluids [219].

Furthermore, aliphatic polyesters, especially, PLA has been extensively studied in the preparation of networks for biomedical applications. Nevertheless, the hydrophobicity and the high glass transition temperature of PLA together with the lack of pendant functionality limit its application in the biomedical field. Therefore, PLA were cross-linked with hydrophilic synthetic polymers or polysaccharides to form hydrogels with tunable properties [220]. Alternatively, our group described the synthesis of polymeric networks based on enzymatically synthesized functional polyester PDSA. Authors further introduced some PEG side chains to the PDSA backbone which results in hydrophilic networks with higher swelling ability that may serve as promising materials for drug delivery system [26]. Moreover, the synthesis of hydrogels based on enzymatically synthesized functional polyester PGA was stated [221]. These biodegradable hydrogels can be used further for potential pharmaceutical applications such as, sustained-release carriers of various hydrophilic drugs.

### **1.3.1 Classification of hydrogels**

In general, hydrogels can be categorized into three main classes as homopolymer, copolymer, interpenetrating network (IPN), and semi-IPN based on their preparation method. For instance, homopolymers consist of one type of monomers while, copolymers composed of more than one type of monomers with at least one hydrophilic component. In contrast, IPNs or multipolymer hydrogels consist of different types of cross-linked polymer chains and semi-IPNs comprise of cross-linked and linear polymers. Besides, hydrogels can be further classified based on their charge into nonionic, anionic, cationic, ampholytic, or zwitterionic as well as on their physical structure into amorphous with random structure, and semi-crystalline. An important hydrogel classification is based on the type of cross-linking interactions between polymer chains, which can be either chemical or physical [222]. Physical hydrogels are formed when the cross-linking between polymer chains is caused by non-covalent forces such as, ionic/electrostatic forces, hydrogen bonding, stereo-complex formation, and hydrophobic interactions. These hydrogels are reversible, i.e. they are mechanically weak and fragile upon exposure to environmental

changes (e.g., temperature or pH-value). While, chemically cross-linked hydrogels are prepared by covalent cross-linking between polymer chains and hence, they do not possess a reversible response to external stimuli. Compared to physical hydrogels, covalent cross-linked polymers have an improved swelling behavior, controlled biodegradability, and mechanical strength, which make them more suitable for pharmaceutical applications [223].

### 1.3.2 Synthesis of chemically cross-linked hydrogels

To achieve chemically cross-linked hydrogels, several approaches have been established, for example, classical esterification reaction of carboxylic acids and alcohols, free radical polymerization, high energy radiation, enzyme-induced cross-linking, and “click” chemistry including copper-catalyzed azide-alkyne cycloaddition (CuAAC), strain-promoted azide-alkyne cycloaddition (SPAAC), Diels-Alder (DA) reactions, Schiff base/oxime formation, and Michael addition reactions [223, 224].

For instance, a simple and convenient method for hydrogels preparation is the Steglich esterification reaction of carboxylic acids and alcohols with the help of carbodiimides as coupling agents and 4-dimethylaminopyridine (DMAP) as a catalyst [26]. Besides, free radical polymerization of low molar mass monomers in the presence of cross-linking agents has been considered as a versatile technique for the preparation of hydrogels. Initially, the reactions are started by a sequential addition of free radical initiators such as, ammonium persulfate (APS), potassium persulfate (KPS), and 2-2'-azobisisobutyronitrile (AIBN) or by applying UV-, gamma- or electron beam-radiation. In this method, vinyl monomers like acrylic acid, acrylamide, and vinyl chloride radically polymerize in the presence of cross-linking agents to produce chemically cross-linked hydrogels. Chemically cross-linked hydrogels can be further prepared through high energy radiation. It is mainly dependent on the presence of light-sensitive functional groups. For example, chitosan-based hydrogels have been synthesized by incorporating azide and lactose as light-sensitive groups. After exposure to UV light, azide groups were converted into nitrene and then bound to amine groups of chitosan to form a hydrogel in a very short time [225]. This approach offers simple and relatively fast formation of hydrogels as well as lower cost production compared to the chemical strategies. Another potential route for hydrogel synthesis is the enzyme-induced cross-linking of macromolecules under physiological conditions. In this regard, Sperinde et al. [226] reported the formation of a hydrogel network by cross-linking reaction of glutaminamide-functionalized PEG with a Lys-containing polypeptide using TGase. As previously mentioned, TGase is a cross-linker enzyme that can form isopeptide bonds between substrates. Besides, other enzymes like peroxidases,

tyrosinase, phosphopantetheinyl transferase, lysyl oxidase, and phosphatases were investigated in this respect [223, 224]. Further, utilization of “click” chemistry for the synthesis of chemically cross-linked hydrogels developed rapidly since it benefits from high selectivity, high product yields under mild reaction conditions, and fewer side reactions [224, 227]. Figure 6 highlights a summary of main “click” chemistry strategies that have been used to produce hydrogels.

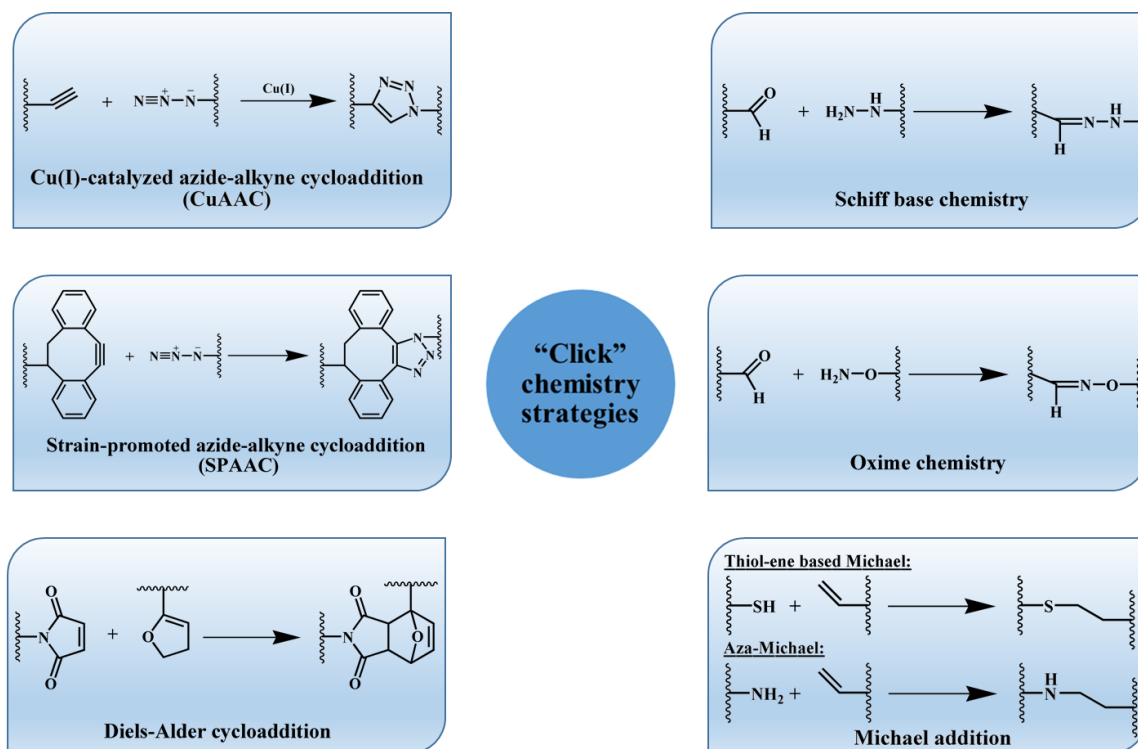


**Figure 6.** Summary of “click” chemistry strategies which have been used in the synthesis of hydrogels, adapted from [227].

**Cross-linking through copper-catalyzed azide-alkyne cycloaddition (CuAAC):** It is a highly selective cycloaddition between terminal alkynes and azides to form 1,4-disubstituted 1,2,3-triazoles. Hydrogels utilizing CuAAC chemistry benefit from fast reaction rates and high yields. However, it requires the use of a copper (I) catalyst, which may result in many adverse effects in the biomedical field. Hence, the use of copper-free strategies has been developed and is listed below.

**Cross-linking through strain-promoted azide-alkyne cycloaddition (SPAAC):** It is a metal-free alternative to CuAAC. This reaction is based on the increased reactivity of inherent ring strain of cyclooctyne groups to achieve efficient cross-linking under catalysts-free conditions.

**Cross-linking through Diels-Alder (DA) reaction:** DA is a highly specific cycloaddition between a diene (furan or its derivatives) and maleimide groups to form stable hydrogels.

Interestingly, this reaction is free from by-products and can be employed in the absence of catalysts, initiators, or coupling agents.

***Cross-linking through Schiff base formation:*** It is usually occurred by the reaction between amino/ hydrazide and aldehyde groups to result in hydrogels *via* forming an imine bond under mild conditions. This method is preferred for biomedical applications since unbound aldehyde groups can adhere to living tissues or organs while preserving the cross-linked hydrogels.

***Cross-linking through oxime formation:*** It is usually occurred by the reaction between an aminoxy/hydroxylamine group and an aldehyde or ketone to generate hydrogels *via* a highly stable oxime bond under physiological conditions.

***Cross-linking through Michael addition:*** The Michael addition reaction, also termed as conjugate addition, is a versatile synthetic approach for the addition of nucleophiles, referred as Michael donors, to electron-deficient  $\alpha,\beta$ -unsaturated carbonyl, e.g., vinyl esters, vinyl ketones, vinyl sulfones, vinyl phosphonates, acrylamides, and maleimides which act as Michael acceptors to produce a new single bond. For this reaction, various nucleophiles bearing heteroatoms beside carbon nucleophiles have been utilized. Examples include, nitrogen (aza-Michael), sulfur (thiol-ene based Michael), alcohol (oxa-Michael), and phosphorous (phospha-Michael) to create C–N, C–S, C–O and C–P single bonds, respectively. The major advantages of Michael addition reactions involve high selectivity under ambient conditions and desirable reaction rates [228], thereby, their applications are diverse, especially, for the synthesis of different polymer architectures including linear, hyperbranched, dendritic, and polymeric networks such as, hydrogels [229]. Hubbell and co-workers were the first to report the synthesis of PEG-based hydrogels through a cross-linking of vinyl sulfone-terminated PEG macromers and oligopeptides containing Cys (thiol-reactive amino acid) *via* thiol-ene based Michael addition reaction [230]. Subsequently, this approach has become a popular strategy for the synthesis of hydrogels. To avoid the badly smelling thiol containing precursors as well as the side reaction products (disulfide bond formation), other efficient approaches like aza-Michael addition reactions have been developed.

Aza-Michael addition has drawn a great interest towards modern organic synthesis for C-N bonds formation to generate important compounds such as  $\beta$ -aminocarbonyls and N-containing heterocycles that are found in many antibiotics and other bioactive molecules. This method was described in 1874 [231], which includes the addition of amine groups (Michael donors) to electron deficient alkenes (Michael acceptors). Previously, these reactions were performed in the presence of strong acid, base, or metal-based catalysts which have undesirable effects on

the environment. As a result, the use of several heterogeneous catalysts has been developed such as Amberlyst-15, silica-supported sulphuric acid, silica-supported aluminum chloride, basic aluminum oxide, graphene oxide, metal organic frameworks, and polymer-supported catalysts (polystyrene-supported aluminum chloride). Furthermore, the aza-Michael additions of amines to methyl acrylates catalyzed by microwave-assisted irradiation and ultra-sound irradiations have been reported [232]. It is worth noting that many efforts have been made to shift towards environmentally benign and facile method for the aza-Michael reaction. For example, the aza-Michael addition of amines using acidic alumina under solvent-free conditions and the aza-Michael addition of amines catalyzed by lipases [232, 233]. Moreover, no catalyst is needed in some cases as amine groups can act as nucleophiles and bases.

Aza-Michael addition of amines to alkenes has been widely used to prepare polymers that act as degradable pro-drug conjugates or as carriers for protein delivery to generate thermosets and silicon-based macromolecules and to produce functional biomaterials [234]. The utility of aza-Michael addition chemistry for the synthesis of chemically cross-linked hydrogels has also been established, especially, for biotechnological and biomedical applications. In a previous study by Southan et al. [235], the aza-Michael addition of amino-functionalized polymers to acrylate and acrylamide cross-linkers for the synthesis of hydrogels was stated. They studied the influence of the reaction conditions (e.g., pH-value) on the cross-linking and degradation rate of the formed gels. In another study, well-defined hydrogels based on PEG were synthesized *via* aza-Michael addition of amine functional groups to acrylate [236]. Hoffmann et al. [237] reported the preparation of hydrogel through a nucleophilic addition of multiple amine groups, present along the polyethyleneimine (PEI) backbone, to an activated carbon-carbon double bond present on PEG-based polyesters. Retailleau et al. [238] described the synthesis of polymeric networks *via* a combination of aza-Michael addition of diamines to diacrylates and radical photopolymerization. A novel type of polyamidoamine (PAMAM) dendrimer hydrogel was successfully developed based on aza-Michael addition chemistry under catalyst-free conditions. These hydrogels are biocompatible and, therefore, can be used for drug delivery and tissue engineering [239]. Most recently, the aza-Michael addition of primary amines to vinyl end groups of enzymatically synthesized PGA under catalyst-free conditions to generate hydrogels based on biodegradable and biocompatible polyester was reported [221]. These hydrogels with tunable properties prepared by aza-Michael addition reaction can serve as a new platform for pharmaceutical applications such as carriers for sustained release of hydrophilic drugs and biodegradable implants for controlled drug delivery.

Overall, through the efforts of researchers, it is believed that copper-free click reactions display many significant benefits including, high reaction rates, selectivity, excellent biocompatibility, versatility, less by-products, and high product yields making them promising approaches for the synthesis of hydrogels with a great potential within the field of tissue engineering and therapeutic delivery.

## 2 | Aim and objectives

Polyester syntheses *via* enzymatic polymerizations of bio-based monomers provide an opportunity for achieving green polymer chemistry. A part of research in green chemistry focuses on the use of highly regioselective CAL-B to produce biocompatible and biodegradable polyesters with numerous functionalities. These functionalities along the polyester backbone provide an access to versatile pathways for further modification with a variety of fatty acids, amino acids, and drugs to afford grafted polymers with tunable physicochemical properties for pharmaceutical applications. The first aim of the present work is to generate functional polyesters by enzymatic transesterification between either DVA or DMA and glycerol as well as between DVA and D-sorbitol using CAL-B, resulting in PGA, poly(glycerol adipate)(M) (PGA(M)), and PDSA, respectively. These functional polyester backbones are then grafted with side chains terminated with primary amine groups through simple Steglich esterification reaction to obtain new biodegradable amine-grafted polyesters that are suitable for being utilized in different applications like protein-polymer conjugation and hydrogel formation.

Over recent years, many proteins produced by recombinant DNA technologies have become powerful therapeutics for treating various diseases such as, anemia, cancer, diabetes, and many others. Despite this success, therapeutic proteins often suffer from poor stability, short bioavailability, and immunogenicity. Thus, a number of valuable techniques have been explored to enhance their pharmacokinetics whilst maintaining biological activity. One approach that is gaining considerable attention to address these challenges is the covalent attachment of polymer chains to proteins. The resulting conjugates exhibit a unique combination of properties which can be tuned to prompt a desired effect. For this purpose, various chemical methods have been routinely utilized. However, many of them can have deteriorating effects on the protein molecules. Hence, the second objective of this work is to apply the synthesized amine-modified polyesters for the covalent attachment with different proteins using enzymatic approach as a green and mild alternative to the conventional chemical procedures. To achieve this, amine-modified PGA(M) is synthesized, characterized by <sup>1</sup>H NMR spectroscopy, Fourier-transform infrared (FTIR) spectroscopy, and gel permeation chromatography (GPC). Then, amine-modified PGA(M) is applied for the conjugation reaction with a model protein, DMC, using a highly thermoresistant variant mTGase-S2P. DMC is chosen for this work as it can act only as an acyl donor for mTGase whereas all Lys residues

are blocked by methylation, thus, it is an appropriate substrate to test the conjugation with acyl acceptors without undergoing any self-cross-linking within the protein molecules. Furthermore, some positive and negative control experiments are performed to further confirm our results. Here, the main investigation centers on the use of sodium dodecyl sulphate-polyacrylamide gel electrophoresis (SDS-PAGE) as a direct proof technique to detect the resulting protein-polymer conjugates.

Another objective is to further expand the application of this enzymatic approach using therapeutic proteins-based conjugation that can improve their biological performance. In order to accomplish this, amine-modified PDSA is prepared, well characterized by  $^1\text{H}$  NMR spectroscopy and GPC, and subsequently subjected for the conjugation reaction with rHuEPO using another thermoresistant variant mTGase-TG<sup>16</sup> in the presence of N- and O-glycans as well as after treatment with peptide-N-glycosidase F (PNGase F). Since the sites of mTGase modification are mainly located in flexible-unfolded chain segments of the protein, the enzymatic protein-polymer conjugation is carried out at the  $T_m$  of rHuEPO, where half of the protein is in the unfolded state. As a proof of principle study, the well-known substrate for mTGase, i.e. monodansyl cadaverine (MDC), is used for the enzymatic conjugation with rHuEPO along with many different control experiments in order to support our findings. To analyze the formed conjugates, SDS-PAGE, matrix-assisted laser desorption ionization time-of-flight (MALDI-TOF) mass spectrometry, and liquid chromatography-electrospray-linear ion trap-tandem mass spectrometry (LC-ESI-LIT MS) are conducted.

The final aim of this work is to design polymeric networks based on a biodegradable and biocompatible PGA using aza-Michael chemistry. This approach is a good choice for this purpose as it benefits from being facile, mild, and a catalyst-free method to produce polymeric networks with great potential for various pharmaceutical applications, especially, in drug delivery system. For this, enzymatic polymerization of glycerol and DVA results in linear PGA terminated with some electron-deficient carbonyl groups (vinyl end groups) serving as aza-Michael acceptors. By acylation, PGA is grafted with side chains bearing free amine groups which form aza-Michael donors able to undergo aza-Michael addition to the vinyl end groups of PGA to finally result in the synthesis of hydrophilic PGA-based networks (hydrogels) under catalyst-free conditions. The bulk properties of the PGA backbone and amine-modified PGA are investigated by GPC, high-resolution (HR) MALDI-TOF mass spectrometry,  $^1\text{H}$  NMR,  $^{13}\text{C}$  NMR, and FTIR spectroscopy. To analyze the network structure, FTIR and solid state  $^{13}\text{C}$  single-pulse (SP) magic-angle spinning (MAS) NMR spectroscopy are conducted while to

investigate the network defects and dynamics,  $^1\text{H}$  double-quantum (DQ) NMR experiments are performed.

### 3 | Results

The published results are presented in this chapter. The research aims to introduce an environmentally benign approach for the synthesis of biocompatible and biodegradable polyesters using highly regioselective CAL-B as well as to apply these polyesters in the field of mTGase-mediated protein-polymer conjugation and polymeric networks formation *via* aza-Michael addition chemistry. The investigated polyesters for protein-polymer conjugation purpose are synthesized by enzymatic polytransesterification reaction of glycerol with DMA and D-sorbitol with DVA using CAL-B to obtain PGA(M) and PDSA, respectively. By direct grafting of OH-groups along the PGA(M) backbone with side chains bearing primary amine groups along with hydrophilic PEG side chains, water soluble amine-modified PGA(M) is designed to act as an acyl acceptor substrate for mTGase and then applied for the conjugation reaction with DMC beside a series of control experiments using a variant thermostable mTGase-S2P. The published results of amine-modified PGA(M) synthesis and its conjugation with DMC catalyzed by mTGase-S2P are presented in chapter 3.1. This enzymatic approach can also be used for the conjugation of fully biodegradable polyesters with therapeutic proteins which may have a positive impact on their biological efficacy. Therefore, PDSA is further investigated for the conjugation reaction with rHuEPO using a variant mTGase-TG<sup>16</sup> which exhibits higher thermostability than mTGase-S2P. By direct modification of OH-groups along the PDSA backbone with side chains having primary amine groups, amine-modified PDSA is prepared to serve as an acyl acceptor substrate for mTGase and subsequently subjected for the mTGase-TG<sup>16</sup>-mediated conjugation with rHuEPO at its transition temperature  $T_m$  in addition to a series of control experiments. The published results of amine-modified PDSA synthesis and its conjugation with rHuEPO mediated by mTGase-TG<sup>16</sup> are presented in chapter 3.2. The investigated polyester for polymeric network formation purpose is synthesized by enzymatic polytransesterification reaction of glycerol with DVA using CAL-B to achieve PGA having some vinyl end groups. Upon direct grafting of OH-groups along the PGA backbone with amine-terminated side chains, aza-Michael addition of these amine groups to vinyl end groups of PGA and the formation of hydrophilic PGA-based networks under catalyst-free conditions are explored and discussed in the published results presented in chapter 3.3.

### 3.1 Paper I:

#### **Conjugation of amine-functionalized polyesters with dimethylcasein using microbial transglutaminase<sup>1</sup>**

The conjugation of polymer chains to proteins has been widely employed for many industrial and biomedical applications. Although proteins have numerous advantages as therapeutic drugs, some shortcomings when used in their native form, such as short *in vivo* circulation time, poor stability, low solubility, and immunogenicity limit their clinical applications. Many attempts, therefore, have been made to covalently attach water soluble polymers to these proteins which can improve their solubility and bioavailability as well as their therapeutic potency. For this purpose, various chemical and enzymatic approaches were investigated to prepare protein-polymer conjugates especially, the mTGase-mediated conjugation reactions under mild conditions have gained a significant attention in the field of protein-polymer conjugation.

To this aim, the feasibility of using the mTGase-mediated reaction to conjugate DMC with a biodegradable and water soluble polyester is investigated. In the following publication, PGA (M) was synthesized by enzymatic transesterification between glycerol and DMA, chemically modified with side chains having free primary amine groups as well as with hydrophilic mPEG12 side chains, thoroughly characterized by <sup>1</sup>H NMR spectroscopy, FTIR spectroscopy, and GPC, and then applied for the variant mTGase-S2P-catalyzed conjugation reaction with DMC. DMC-PGA(M) conjugates generated by this approach were detected by SDS-PAGE technique. This enzymatic procedure is promising for a mild conjugation of various therapeutic proteins with biodegradable and highly water soluble polyesters that may potentially enhance their pharmacokinetics and therapeutic performance.

The author contributions of the following article are: R. Alaneed, M. Pietzsch, and J. Kressler designed research. R. Alaneed performed all experiments with characterizations. T. Hauenschild performed the FTIR measurements. K. Mäder supervised and complemented the writing. R. Alaneed wrote the first draft of the paper. R. Alaneed wrote the paper in the final form with revisions by M. Pietzsch and J. Kressler.

---

<sup>1</sup>The following article is adapted with permission from (Conjugation of amine-functionalized polyesters with dimethylcasein using microbial transglutaminase; Razan Alaneed, Till Hauenschild, Karsten Mäder, Markus Pietzsch, and Jörg Kressler. *J. Pharm. Sci.*, **109**, 981-991 (2020) DOI: 10.1016/j.xphs.2019.10.052). Copyright (2020) American Pharmacists Association. Published by Elsevier Inc. All rights reserved. The link to the article on the publisher's website is: <https://doi.org/10.1016/j.xphs.2019.10.052>. No changes were made.



## Pharmaceutical Biotechnology

# Conjugation of Amine-Functionalized Polyesters With Dimethylcasein Using Microbial Transglutaminase



Razan Alaneed<sup>1,2</sup>, Till Hauenschild<sup>1</sup>, Karsten Mäder<sup>2</sup>, Markus Pietzsch<sup>2,\*</sup>, Jörg Kressler<sup>1,\*</sup>

<sup>1</sup> Department of Physical Chemistry, Institute of Chemistry, Martin Luther University Halle-Wittenberg, D-06099 Halle/Saale, Germany

<sup>2</sup> Department of Pharmaceutical Technology and Biopharmacy, Institute of Pharmacy, Martin Luther University Halle-Wittenberg, Wolfgang-Langenbeck-Str. 4, D-06120 Halle/Saale, Germany

## ARTICLE INFO

## Article history:

Received 9 August 2019

Revised 28 October 2019

Accepted 28 October 2019

Available online 2 November 2019

## Keywords:

poly(glycerol adipate) (M)  
enzymatic polymerization  
CAL-B  
amine-functionalized polyester  
microbial transglutaminase (mTGase)  
protein-polymer conjugate

## ABSTRACT

Protein-polymer conjugates have been used as therapeutics because they exhibit frequently higher stability, prolonged *in vivo* half-life, and lower immunogenicity compared with native proteins. The first part of this report describes the enzymatic synthesis of poly(glycerol adipate) (PGA(M)) by transesterification between glycerol and dimethyl adipate using lipase B from *Candida antarctica*. PGA(M) is a hydrophilic, biodegradable but water insoluble polyester. By acylation, PGA(M) is modified with 6-(Fmoc-amino)hexanoic acid and with hydrophilic poly(ethylene glycol) side chains (mPEG12) rendering the polymer highly water soluble. This is followed by the removal of protecting groups, fluorenylmethyloxycarbonyl, to generate polyester with primary amine groups, namely PGA(M)-g-NH<sub>2</sub>-g-mPEG12. <sup>1</sup>H NMR spectroscopy, FTIR spectroscopy, and gel permeation chromatography have been used to determine the chemical structure and polydispersity index of PGA(M) before and after modification. In the second part, we discuss the microbial transglutaminase-mediated conjugation of the model protein dimethylcasein with PGA(M)-g-NH<sub>2</sub>-g-mPEG12 under mild reaction conditions. SDS-PAGE proves the protein-polyester conjugation.

© 2020 American Pharmacists Association®. Published by Elsevier Inc. All rights reserved.

## Introduction

Conjugation of functional polymer side chains to proteins has been extensively studied during the last few decades for various industrial and biomedical applications.<sup>1</sup> The advantages of proteins as therapeutic agents include low toxicity, high selectivity and specific activity, as well as they have contributed significantly toward the successful treatment of many diseases such as cancer, diabetes, anemia, multiple sclerosis, and others.<sup>2</sup> Nevertheless, therapeutic proteins have some drawbacks when used in their native form, for example, their short circulation half-life, susceptibility to proteolytic degradation, and immunogenicity, which have limited their clinical use.<sup>3</sup> The covalent attachment of synthetic polymers, as, for example, poly(ethylene glycol) (PEG) to these native proteins, results in better water solubility and

improved the therapeutic potency of proteins.<sup>4</sup> For this purpose, Abuchowski et al.<sup>5</sup> have introduced the first covalent attachment of PEG to bovine serum albumin (BSA). Subsequently, they have reported that PEGylation improved many pharmacological properties of proteins, that is, increased circulation half-life and reduced immunogenicity.<sup>6</sup> As a result, several FDA-approved protein-PEG conjugates are currently available in market for clinical use, for example, PEG-adenosine deaminase, PEG-L-asparaginase, PEG-interferon- $\alpha$ -2b, PEG-interferon- $\alpha$ -2a, PEG-urate oxidase, PEG-granulocyte colony-stimulating factor, PEG-growth hormone receptor antagonist, and PEG-erythropoietin.<sup>7</sup> PEG has achieved great success in protein conjugation because of its hydrophilicity and biocompatibility. Although PEG has been regarded long time as nonimmunogenic, recent findings clearly show evidence that PEG antibodies can be formed and impact the pharmacokinetics and pharmacological performance.<sup>8–10</sup> Therefore, the search for PEG alternatives has increased within the last years. Examples include poly(vinyl alcohol), dextran, poly(N-vinyl pyrrolidone), poly(maleic acid),<sup>11</sup> N-(2-hydroxypropyl) methacrylamide,<sup>12</sup> poly(2-ethyl-2-oxazoline),<sup>13</sup> and hydroxyethyl starch (HES). Among these polymers, HES conjugation was extensively studied. Besheer et al. have

\* Correspondence to: Jörg Kressler (Telephone: +49-345-55-25-800) and Markus Pietzsch (Telephone: +49-345-55-25-949).

E-mail addresses: [markus.pietzsch@pharmazie.uni-halle.de](mailto:markus.pietzsch@pharmazie.uni-halle.de) (M. Pietzsch), [joerg.kressler@chemie.uni-halle.de](mailto:joerg.kressler@chemie.uni-halle.de) (J. Kressler).

reported the use of HES in nanoparticle (NP) stabilization<sup>14</sup> and in protein conjugation using microbial transglutaminase (mTGase) as biocatalyst.<sup>15</sup>

Generally, various chemical strategies have been developed over the past years to prepare protein-polymer conjugates. However, some of these traditional pathways are not selective, which resulted in a heterogeneous mixture of protein conjugates with reduced bioactivity. Hence, an alternative approach to produce these conjugates through enzymatic procedures has been extensively developed because of high catalytic activity and high selectivity of the enzymes under mild reaction conditions as compared with other chemical catalysts. mTGase-mediated conjugation is one of the most promising enzymatic procedures for selective protein cross-linking.<sup>16,17</sup>

mTGases (protein-glutamine  $\gamma$ -glutamyltransferase) are enzymes that crosslink proteins by catalyzing an acyl transfer reaction between  $\gamma$ -carboxamide groups of peptides or protein-bound glutamine residues (which act as an acyl donor) and different free primary amine groups, for example, the  $\epsilon$ -amino group of lysine residues (which act as an acyl acceptor), with the consecutive loss of ammonia as by-product. This reaction results in the formation of highly protease-resistant isopeptide bonds between proteins.<sup>18</sup> mTGase was first isolated from *Streptomyces mobaraensis* and reported by Ando et al. in 1989.<sup>19</sup>

mTGase is widely used in the food industry.<sup>20</sup> Another field of application is the site-specific modification of therapeutic proteins, for example, Sato et al.<sup>21</sup> have reported a site-specific modification of recombinant human interleukin-2 with PEG using mTGase. Subsequently, the PEGylation of recombinant granulocyte colony-stimulating factor,<sup>22</sup> and human growth factor catalyzed by mTGase were reported.<sup>23</sup> Afterward, Strop et al.<sup>24</sup> developed an enzymatic method for site-specific antibody-drug conjugation using mTGase. Recently, Spolaore et al.<sup>25</sup> studied the reactivity of human IFN $\alpha$ -2b toward mTGase.

This article is divided into 2 main parts, which explain in detail the synthetic pathway for the preparation of protein-polyester conjugate. First, we describe the full syntheses of amine-functionalized polyester starting from poly(glycerol adipate) (PGA(M)) backbone, where the symbol (M) refers to the PGA synthesis using dimethyl adipate (DMA) as a monomer instead of using divinyl adipate (DVA). PGA(M) is then modified with 6-(Fmoc-amino)hexanoic acid [6-(Fmoc-Ahx)] side chains followed by the removal of protecting groups to produce the amine-functionalized polyester (PGA(M)-g-NH<sub>2</sub>-g-mPEG12), where 12 is related to the number of repeating units of PEG chains. Second, we describe the conjugation between dimethylcasein (DMC) and amine-functionalized PGA(M) using mTGase (S2P), a variant possessing a single amino acid exchange resulting in higher thermostability and higher specific activity compared with the wild type<sup>26</sup> under mild reaction conditions.

## Experimental

### Materials

Lipase B derived from *Candida antarctica* immobilized on an acrylic resin (Sigma-Aldrich, St. Louis, MO), commercially known as Novozyme (N435), was dried over phosphorus pentoxide (P<sub>2</sub>O<sub>5</sub>) at 4°C for 24 h before use. P<sub>2</sub>O<sub>5</sub> ( $\geq 99\%$ ), 4-(dimethylamino)pyridine (DMAP), 1-ethyl-3-(3-dimethylaminopropyl)carbodiimide hydrochloride (EDC·HCl), silica gel (SiO<sub>2</sub>, 0.03-0.2 mm), dialysis membranes (having a cut-off molar mass of 1000 g mol<sup>-1</sup>), and deuterated chloroform (CDCl<sub>3</sub>, 99.8%) were purchased from Carl Roth (Karlsruhe, Germany). 6-(Fmoc-Ahx) 98% was purchased from Alfa Aesar (Kandel, Germany). Glycerol ( $\geq 99.5\%$ ), DMA ( $\geq 99\%$ ), PEG

monomethyl ether (mPEG) 550 g mol<sup>-1</sup> (mPEG550 g mol<sup>-1</sup>; denominated as "mPEG12"), succinic anhydride ( $\geq 99\%$ ), N,N-DMC, monodansylcadaverine (MDC),  $\beta$ -casein, dimethyl sulfoxide (DMSO, anhydrous), and magnesium sulfate (MgSO<sub>4</sub>, anhydrous,  $\geq 99.5\%$ ) were obtained from Sigma-Aldrich (Steinheim, Germany). Dichloromethane (DCM, anhydrous, 99.9%) was obtained from Acros Organics (Schwerte, Germany). All chemicals were used as received without further purification. All HPLC-grade solvents such as tetrahydrofuran (THF), ethyl acetate, *tert*-butylmethylether, chloroform, and acetone were purchased from Carl Roth (Karlsruhe, Germany).

### Preparation of Recombinant (mTGase-S2P) and Purification

The recombinant enzyme was produced following the same procedure used by Sommer et al.<sup>27</sup> A typical procedure to obtain mTGase (S2P) was as follows: the inactive pro-enzyme (pro-mTGase S2P) was activated by cleaving with proteinase K, and then, the activated enzyme was purified by immobilized metal affinity chromatography. Aliquots were stored at -80°C. In advance of the cross-linking experiment, the specific activity of mTGase-S2P was determined by hydroxamate-based colorimetric assay.

### Methods

#### NMR Spectroscopy

<sup>1</sup>H NMR spectra were recorded on a VNMRs spectrometer 400 MHz (Agilent Technologies) at 27°C using tetramethylsilane as an internal calibration reference. Approximately 30-40 mg of polymer was dissolved in 0.8 mL of deuterated solvent (CDCl<sub>3</sub>). Later, NMR spectral data were interpreted using MestRec (v.4.9.9.6) software (Mestrelab Research, Santiago de Compostela, Spain).

#### Gel Permeation Chromatography

Gel permeation chromatography (GPC) measurements (number-average molar mass ( $M_n$ ), weight-average molar mass ( $M_w$ ), and polydispersity index (PDI) ( $M_w/M_n$ ) for PGA(M), PGA(M)-g-6-(Fmoc-Ahx), PGA(M)-g-6-(Fmoc-Ahx)-g-mPEG12, and PGA(M)-g-NH<sub>2</sub>-g-mPEG12 were performed on a Viscotek GPC max VE 2002 using HHRH Guard-17360 and GMHH-N-18055 columns and refractive index detector (VE 3580 RI detector, Viscotek). DMF + 0.01 M LiBr was used as mobile phase in a column kept at 25°C and calibrated with poly(methyl methacrylate) standards. For all samples, the concentration was 3 mg mL<sup>-1</sup>, and the flow rate was 1 mL min<sup>-1</sup>. The data were analyzed using Origin 8 software.

#### FTIR Spectroscopy

The IR spectra were recorded at 25°C and 256 scans with a Bruker Vector 22 FT-IR spectrometer. For the production of 13 mm KBr pellets, a hydraulic press was used and an associated pressing tool of Perkin-Elmer. During the measurements, the KBr pellets were permanently flushed with a stream of dry air, to counteract an air moisture influence that could interfere with the measurements. Exclusively dry KBr was used for sample preparation. The KBr pellets were pressed using a sample concentration of ~1.5 mg sample per 150 mg KBr. The FTIR spectra were interpreted using OMNIC Spectra Software.

#### SDS-PAGE

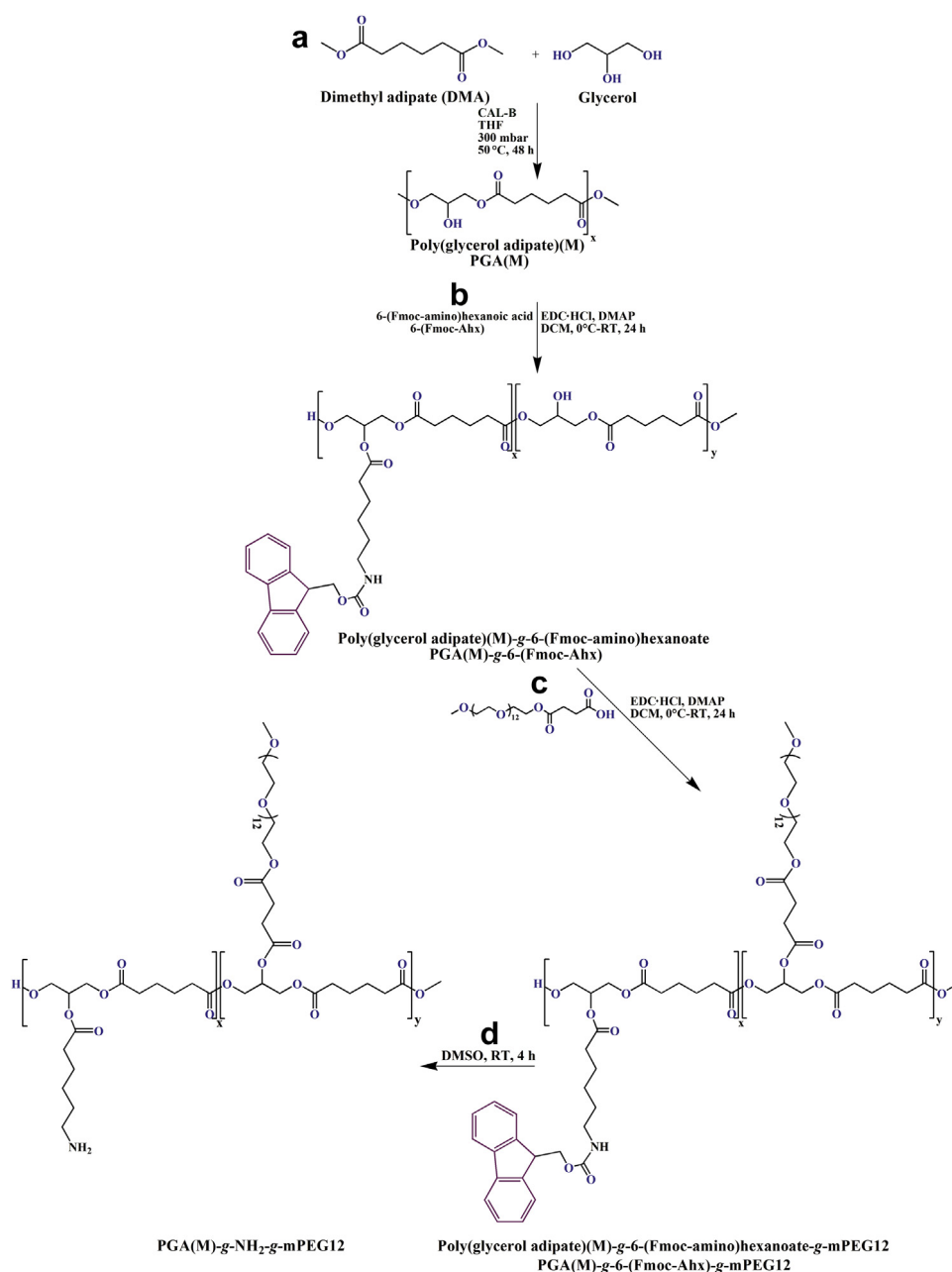
SDS-PAGE was performed according to the method reported by Laemmli.<sup>28</sup> This technique is based on separation of protein-containing samples depending on their size. All samples were

resolved using 12.5% separation gel (resolving gel) and 4.5% stacking gel. After the conjugation experiments, all samples were mixed with SDS sample buffer (1:1 ratio), heated for 3 min at 95°C, and then cooled down to room temperature. After that, 5  $\mu$ L of protein ladder and 10  $\mu$ L of each sample were loaded into the wells. Here, the protein ladder used is a protein molar mass marker (Fermentas Life Sciences, St. Leon-Rot, Germany). The electrophoresis was carried out in a 2-step mode. The first run was at 300 V, 80 mA, for 6 min. This was followed by the second run at 300 V, 60 mA, for 40 min (for 2 gels). For band visualization, both gels were stained with Coomassie Brilliant Blue G-250 overnight. Then, both gels were incubated with destaining solution to remove the unbound dyes from the gels until the desired contrast between the bands and the gel background was achieved (around 3 h).

## Synthesis

### Synthesis of Poly(Glycerol Adipate) (M)

PGA(M) was obtained by polytransesterification reaction between glycerol and DMA following the procedure used by Naolou et al.,<sup>29</sup> as shown in Scheme 1a. A mixture of glycerol (11 g, 120 mmol), an equimolar amount of DMA (23.8 g, 120 mmol), and 13 mL anhydrous THF were charged in a 250 mL 2-neck round-bottom flask equipped with a Soxhlet extractor (150 mL), which was connected to a reflux condenser. The Soxhlet extractor was filled with molecular sieve (5Å, 105 g) and 100 mL anhydrous THF. The reaction mixture was stirred using a magnetic stirrer for 30 min at 50°C. Then, the reaction was started by the addition of Novozyme (N435) (0.72 g, 2 wt% of the total mass of the monomers). To remove the by-product, methanol, the pressure was reduced gradually to 300



**Scheme 1.** Synthetic route to (a) poly(glycerol adipate) (M) (PGA(M)), (b) PGA(M)-g-6-(Fmoc-Ahx), (c) PGA(M)-g-6-(Fmoc-Ahx)-g-mPEG12, and (d) PGA(M)-g-NH<sub>2</sub>-g-mPEG12.

mbar. As a result, the mixture of THF and methanol was collected in the Soxhlet extractor and methanol was captured by the molecular sieve. The resulting mixture was stirred for 48 h at 50°C. At the end of the reaction, 50 mL of THF was added, and the product was passed through Whatman filter paper to remove the enzyme beads, and THF was evaporated by rotary evaporation at 60°C under reduced pressure. In the last step, the crude product was dried overnight under vacuum at 35°C to remove the residual THF. The  $^1\text{H}$  NMR spectrum of PGA(M) is shown in Figure 1.  $^1\text{H}$  NMR (400 MHz,  $\text{CDCl}_3$ )  $\delta$  [ppm]: 5.28 (m, 1H), 5.10 (m, 1H), 4.36–3.99 (m, 6H), 3.65 (s, 3H), 3.58 (dd,  $J = 11.5, 6.1$  Hz, 2H), 2.48–2.20 (m, 4H), 1.75–1.53 (m, 4H). IR (KBr)  $\nu(\text{cm}^{-1})$ : 3470 ( $\nu(-\text{OH})$ ), 2953 ( $\nu_{\text{as}}(\text{C}-\text{H})$ ), 2875 ( $\nu_{\text{s}}(\text{C}-\text{H})$ ), 1726 ( $\nu(\text{C}=\text{O})$ ), 1463 ( $\delta_{\text{s}}(\text{C}-\text{H})$ ), 1392–1280 ( $\text{C}-\text{H}$  ( $\omega, \tau$ )), 1264–1180 ( $\nu_{\text{as}}(\text{C}-\text{O}-\text{C})$ ), 1144–1080 ( $\nu_{\text{s}}(\text{C}-\text{O}-\text{C})$ ) and ( $\text{C}-\text{H}$  ( $\rho$ )), 1075–1055 ( $\delta(-\text{OH})$ ), 982–733 ( $\text{C}-\text{H}$  ( $\rho$ )).

#### Synthesis of Poly(Glycerol Adipate) (M)-g-6-(Fmoc-Amino) Hexanoate

PGA(M) with a molar mass  $M_n$  of  $2600 \text{ g mol}^{-1}$  was modified further with 6-(Fmoc-Ahx) via Steglich esterification reaction<sup>30</sup> in the presence of EDC·HCl, which was used as an esterification promoting agent catalyzed by 4-(dimethylamino)-pyridine (DMAP) to yield PGA(M)-g-6-(Fmoc-Ahx) as shown in Scheme 1b.

In a 100 mL 3-neck round-bottom flask, PGA(M) (1.5 g, 7.42 mmol) was dissolved in 20 mL anhydrous DCM and cooled with an ice bath for 20 min. This was followed by the addition of 6-(Fmoc-Ahx) (intended conversion of 20 mol% of all OH-groups, 0.52 g, 1.47 mmol). Afterward, DMAP (50 mg, 0.4 mmol) and EDC·HCl (0.84 g, 4.4 mmol) were dissolved in 10 mL of DCM and added dropwise to the polymer solution over 20 min. The mixture was stirred at room temperature for 24 h to yield a yellowish solution. The solution was then filtered, and the most of DCM was removed by rotary evaporator at 30°C under reduced pressure. The grafted polymer was eluted with HPLC grade ethyl acetate through a silica gel column to remove the excess of 6-(Fmoc-Ahx). Further separation was also performed by column chromatography using HPLC-grade acetone

as an eluent. The eluent containing the product was concentrated on rotary evaporator under reduced pressure, and the crude product was further purified by precipitation into cold diethyl ether 2 times followed by drying to yield highly viscous, yellowish product. The total yield was 70 wt%. The molar mass of PGA(M)-g-6-(Fmoc-Ahx) was calculated on the basis of mol% degree of grafting from  $^1\text{H}$  NMR spectrum (Fig. 2a). PDI was determined by GPC in DMF + 0.01 M LiBr as PDI = 1.8.

$^1\text{H}$  NMR (400 MHz,  $\text{CDCl}_3$ )  $\delta$  [ppm]: 7.75 (d,  $J = 7.5$  Hz, 2H), 7.58 (d,  $J = 7.4$  Hz, 2H), 7.38 (t,  $J = 7.5$  Hz, 2H), 7.29 (t,  $J = 7.4$  Hz, 2H), 5.25 (d,  $J = 66.1$  Hz, 1H), 5.09 (m, 1H), 4.38–3.56 (m, 9H), 3.66 (s, 4H), 3.16 (s, 2H), 2.36 (m, 6H), 1.65 (m, 6H), 1.51 (s, 2H), 1.38–1.24 (m, 2H). IR (KBr)  $\nu(\text{cm}^{-1})$ : 3470 ( $\nu(-\text{OH})$ ), 3455 ( $\nu(-\text{NH})$ ), 2953 ( $\nu_{\text{as}}(\text{C}-\text{H})$ ), 2875 ( $\nu_{\text{s}}(\text{C}-\text{H})$ ), 1726 ( $\nu(\text{C}=\text{O})$ ), 1535 ( $\delta(\text{R}-\text{NHC}=\text{O})$ ), 1452 ( $\delta_{\text{s}}(\text{C}-\text{H})$ ), 1384–1280 ( $\text{C}-\text{H}$  ( $\omega, \tau$ )), 1260–1180 ( $\nu_{\text{as}}(\text{C}-\text{O}-\text{C})$ ), 1144–1075 ( $\nu_{\text{s}}(\text{C}-\text{O}-\text{C})$ ) and ( $\text{C}-\text{H}$  ( $\rho$ )), 1075–1055 ( $\delta(-\text{OH})$ ), 753, 760 ( $=\text{CH}$  ( $\gamma$ )).

#### Synthesis of Succinylated mPEG12

Carboxylic acid-terminated mPEG12 was synthesized to convert the hydroxyl (OH) groups into carboxylic acid (COOH) groups to couple these chains to polymer repeating units via Steglich esterification reaction. Succinylated mPEG was synthesized according to the procedure reported by Lu et al.,<sup>31</sup> with slight modifications. The synthesis was carried out by the reaction of mPEG12, with a molar mass  $M_n$  of  $550 \text{ g mol}^{-1}$ , with succinic anhydride in the presence of DMAP as a catalyst to produce succinylated mPEG12 with a molar mass of  $650 \text{ g mol}^{-1}$ . The number 12 corresponds to the number of repeating units in PEG chains. In a 250 mL 3-neck round-bottom flask equipped with reflux condenser with a  $\text{CaCl}_2$  drying tube, mPEG12 (10 g, 18 mmol) was mixed with an excess of succinic anhydride (3.6 g, 36 mmol) in 100 mL chloroform. This was followed by the addition of DMAP (0.122 g, 1 mmol). The reaction mixture was stirred for 24 h at 30°C. The resulting solution was washed 3 times with brine solution and the organic layer was released into a 250 mL beaker, dried over

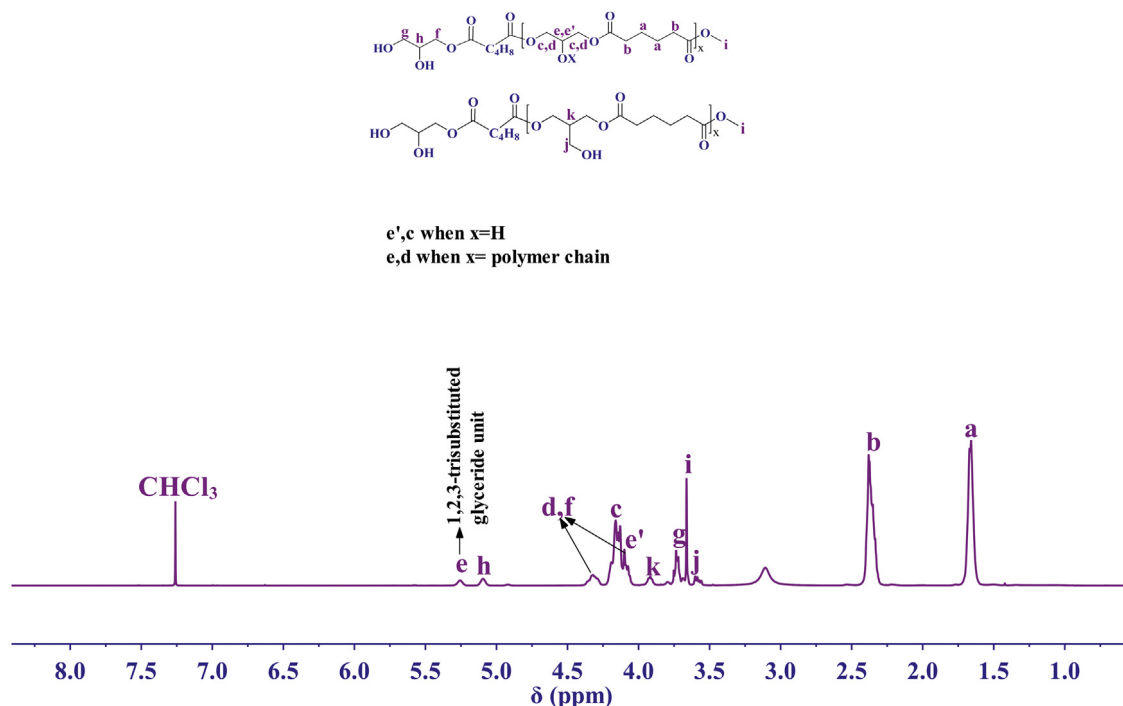
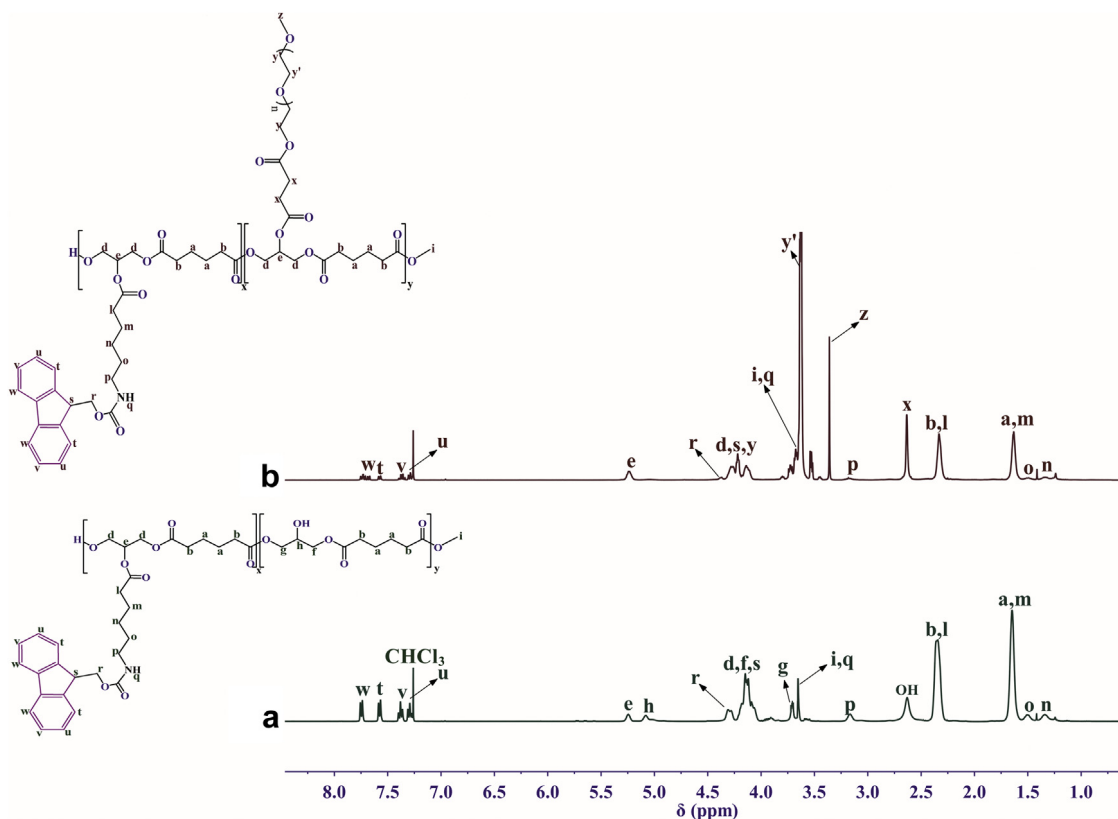


Figure 1.  $^1\text{H}$  NMR spectrum of PGA(M) in  $\text{CDCl}_3$  at 27°C.



**Figure 2.**  $^1\text{H}$  NMR spectra of (a) PGA(M)-g-6-(Fmoc-Ahx), and (b) PGA(M)-g-6-(Fmoc-Ahx)-g-mPEG12 in  $\text{CDCl}_3$  at  $27^\circ\text{C}$ .

magnesium sulfate ( $\text{MgSO}_4$ ), and stirred for 15 min. The inorganic salts were filtered over a funnel through Whatman filter paper, and the filtrate was collected in a 250 mL round bottom flask and concentrated to a small volume by rotary evaporator at  $30^\circ\text{C}$  under reduced pressure. Then, the crude product was purified by recrystallization in ethyl acetate and dried overnight under vacuum at  $35^\circ\text{C}$ .  $^1\text{H}$  NMR (400 MHz,  $\text{CDCl}_3$ )  $\delta$  [ppm]: 4.26-4.20 (m, 2H), 3.71-3.52 (m, 44H), 3.37 (s, 3H), 2.68-2.56 (m, 4H).

#### Synthesis of Poly(Glycerol Adipate) (M)-g-6-(Fmoc-Amino) Hexanoate-g-mPEG12

PGA(M)-g-6-(Fmoc-amino)hexanoate was modified further with succinylated mPEG12 via Steglich esterification (see Scheme 1c) according to the same procedure described previously to yield PGA(M)-g-6-(Fmoc-Ahx). The amounts used for this reaction were as follows: PGA(M)-g-6-(Fmoc-Ahx) (1 g, 4.9 mmol), succinylated mPEG12 (intended conversion of 80 mol% of all OH-groups, 2.5 g, 3.8 mmol), DMAP (0.14 g, 1.15 mmol), and EDC·HCl (1.8 g, 9.4 mmol). This modification was performed to afford the water solubility of the polymer. The purification steps were performed by dialysis against distilled water using regenerated cellulose membrane having a cut-off molar mass of  $1000\text{ g mol}^{-1}$  for 2 days to yield water-soluble, yellowish product. Total product yield was 70 wt%. The molar mass of PGA(M)-g-6-(Fmoc-Ahx)-g-mPEG12 was calculated on the basis of mol% degree of grafting from  $^1\text{H}$  NMR spectrum (Fig. 2b). PDI was determined by GPC in DMF +0.01 M LiBr as PDI = 1.7.  $^1\text{H}$  NMR (400 MHz,  $\text{CDCl}_3$ )  $\delta$  [ppm]: 7.75 (m, 2H), 7.58 (d,  $J = 7.5$  Hz, 2H), 7.38 (t,  $J = 7.5$  Hz, 2H), 7.29 (t,  $J = 7.4$  Hz, 2H), 5.25 (q,  $J = 5.2$  Hz, 1H), 4.38-3.56 (m, 11H), 3.71-3.52 (m, 44H), 3.6 (s, 4H), 3.37 (s, 3H), 3.18 (s, 2H), 2.68-2.56 (m, 4H), 2.36 (m, 6H), 1.65 (m, 6H), 1.51 (s, 2H), 1.38-1.24 (m, 2H).

#### Deprotection of Fluorenylmethyloxycarbonyl (Fmoc) Groups

Deprotection of Fmoc protecting groups was carried out following the procedure used by Höck et al.,<sup>32</sup> with a slight modification. PGA(M)-g-6-(Fmoc-Ahx)-g-mPEG12 with a molar mass  $M_n$  of  $11,500\text{ g mol}^{-1}$ , ~ 1 g was dissolved in anhydrous DMSO (8 mL), and the resulting solution was stirred at room temperature. After 4 h, the reaction was quenched by precipitation twice into an excess cold *tert*-butylmethylether to remove the by-product (dibenzofulvene) and most of DMSO. After drying under nitrogen flow for 1 h, PGA(M)-g-NH<sub>2</sub>-g-mPEG12 was obtained as shown in Scheme 1d.  $^1\text{H}$  NMR (400 MHz,  $\text{CDCl}_3$ )  $\delta$  [ppm]: 5.25 (d,  $J = 10.5$  Hz, 1H), 4.38-3.56 (m, 6H), 3.71-3.52 (m, 44H), 3.6 (s, 3H), 3.20 (d, 2H), 3.37 (s, 5H), 2.68-2.56 (m, 4H), 2.36 (m, 6H), 1.65 (m, 6H), 1.51 (s, 2H), 1.38-1.24 (m, 2H). IR (KBr)  $\nu(\text{cm}^{-1}) = 3470$  ( $\nu(-\text{OH})$ ), 3387 ( $\nu(-\text{NH}_2)$ ), 2953 ( $\nu_{\text{as}}(\text{C}-\text{H})$ ), 2875 ( $\nu_{\text{s}}(\text{C}-\text{H})$ ), 1726 ( $\nu(\text{C}=\text{O})$ ), 1651 ( $\delta_{\text{s}}(-\text{NH}_2)$ ), 1452 ( $\delta_{\text{s}}(\text{C}-\text{H})$ ), 1384-1280 (C-H ( $\omega, \tau$ )), 1260-1180 ( $\nu_{\text{as}}(\text{C}-\text{O}-\text{C})$ ), 1144-1075 ( $\nu_{\text{s}}(\text{C}-\text{O}-\text{C})$ ) and (C-H ( $\rho$ )), 1075-1055 ( $\delta(-\text{OH})$ ), 982-733 (C-H ( $\rho$ )), 700 ( $-\text{NH}_2$  ( $\omega$ )).

#### Reaction of PGA(M)-g-NH<sub>2</sub>-g-mPEG12 With DMC

DMC was modified with the synthesized polymer, amine-functionalized PGA(M) using mTGase (S2P). One hundred microliter of PGA(M)-g-NH<sub>2</sub>-g-mPEG12 (with a concentration of 60 mg/mL) was added to 100  $\mu\text{L}$  of DMC (with a concentration of 5 mg/mL) and dissolved in 50 mM phosphate buffer, pH 8. One sample was taken and boiled with SDS buffer at  $95^\circ\text{C}$  for 3 min. Afterward, 100  $\mu\text{L}$  of 15 U/mL mTGase-S2P was added to start the reaction. Then the reaction mixture was incubated at  $37^\circ\text{C}$  for 120 min. Samples were taken after 15, 30, 60, and 120 min and boiled with SDS buffer for 3 min. Finally, all samples were analyzed by SDS-PAGE and

stained with Coomassie blue. As controls, (1) 100  $\mu\text{L}$  of DMC was added to 100  $\mu\text{L}$  of MDC followed by the addition of mTGase-S2P, as MDC is a well-known substrate for mTGase. Then the gel was exposed to UV light (excitation filter 365 nm, emission filter 520 nm) and (2) a negative control, DMC and mTGase-S2P, was used to prove that no self-cross-linking of DMC could happen because its amine groups are methylated, (3) as a positive control,  $\beta$ -casein and mTGase-S2P, was used to investigate the ability of mTGase to cross-link  $\beta$ -casein.

## Results and Discussion

### PGA(M) Characterization

Amine-functionalized polyester, PGA(M)-g-NH<sub>2</sub>-g-mPEG12, was successfully synthesized from PGA(M) backbone in several steps via the above described methods. PGA(M) is biodegradable polyester, that is, it undergoes an enzymatic degradation into nontoxic monomers, glycerol and adipic acid, as the ester bonds are susceptible to cleavage by a range of enzymes. Swainson et al.<sup>33</sup> have reported that the enzymatic degradation of poly(glycerol adipate) mainly depends on the enzyme and various modifications of polymer backbone. In the case of polymer modifications, the susceptibility of enzymatic degradation will be affected because the polymer becomes more stable after introducing side chains along its backbone as well as the increased steric hindrance, for example, the enzymatic degradation of PGA-PEG occurs at a slower rate than in the case of unmodified PGA. The reason for this is that PEG is hindering sterically the enzyme access to the polymer backbone that can slow the release *in vivo*.<sup>34</sup> Furthermore, Meng et al.<sup>35</sup> have reported PGA NP uptake and metabolism by DAOY cells and the results showed that the intracellular degradation of NPs is faster than in cell culture medium *in vitro*. In addition, Suksiriworapong et al.<sup>36</sup> have discussed the degradation of methotrexate-poly(glycerol adipate) analogs once internalized in the cells. Weiss et al.<sup>37</sup> have investigated the use of NPs based on stearic acid-modified poly(glycerol adipate) as biodegradable drug carriers *in vivo*. Initially, the enzymatic synthesis of PGA(M) was carried out by transesterification reaction between glycerol and DMA in equimolar ratio. Although, use of DVA in the synthesis of PGA is more efficient as higher molar mass polymers are produced, here DMA is used because the synthesized PGA from DVA has some vinyl end groups that are able to undergo cross-linking reaction with the primary amine groups according to Aza-Michael addition

reaction.<sup>38</sup> Because lipase B derived from *Candida antarctica* reacts more preferably with the primary hydroxyl groups than secondary hydroxyl groups,<sup>39</sup> linear PGA(M) with pendant OH-groups should be obtained. Synthesis of aliphatic functional polyesters using enzymatic catalysts as biocatalysts can be considered as an environmentally benign synthesis process that provides a good direction to achieve "green polymer chemistry."<sup>40</sup> This avoids typical esterification catalysts based on tin, which are toxic and not good for the environment.<sup>41</sup> Enzymatic polycondensation pathway, especially lipase/esterase-catalyzed polymerization in organic medium has many advantages,<sup>42,43</sup> such as (1) they are stable in organic media and can catalyze the reverse reactions in nonaqueous media, resulting in transesterification reactions, (2) they operate at mild temperature where the chemical polycondensation does not work at this temperature and does not yield a linear polymer, (3) due to their high enantioselectivity and regioselectivity in organic media, protection-deprotection steps are not required, (4) simple enzyme immobilization which increases its stability in organic media.

The polymer structure is investigated by <sup>1</sup>H NMR spectroscopy given in Figure 1. It shows the resonances of the methylene and methine protons of the glycerol part as well as the 2 methylene resonances of the adipic acid part. The presence of peaks at 5.28 and 5.10 ppm corresponding to the methine protons of 1,2,3-trisubstituted and 1,2-disubstituted glyceride units, respectively, indicates some lack of enzyme regioselectivity during polymerization reaction toward primary hydroxyl groups.<sup>44,45</sup> The peak at 3.65 ppm belongs to the methyl end group of methyl adipate. The molar mass and PDI are determined by GPC in DMF + 0.01 M LiBr. The number average molar mass is  $M_n = 2600 \text{ g mol}^{-1}$  with a degree of polymerization of 13 and a PDI of 1.8. The low number average molar mass ( $M_n$ ) obtained from the reaction of DMA instead of DVA is due to the resulting by-product, methanol, which shifts the equilibrium direction toward the monomers.

### Modification of PGA(M) With 6-(Fmoc-Amino)Hexanoic Acid

In the second synthesis step, 6-(Fmoc-Ahx) was reacted with the OH-groups of the PGA(M) backbone via Steglich esterification reaction in the presence of DMAP and EDC·HCl as catalysts. The grafting of 6-(Fmoc-Ahx) to the polymer backbone is successfully achieved and confirmed in the <sup>1</sup>H NMR spectrum by the appearance of signals corresponding to the methylene protons of the 6-(Fmoc-Ahx) side chains in addition to the resonance of the Fmoc

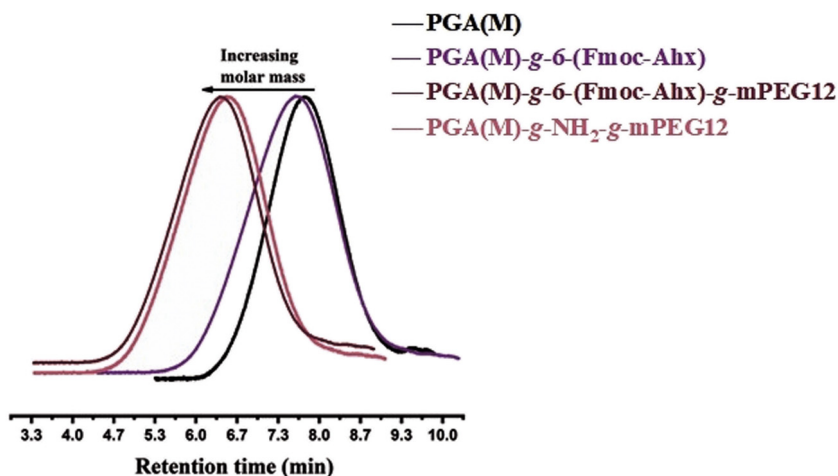


Figure 3. GPC traces of PGA(M) before and after modification with primary amine groups and mPEG side chains in DMF + 0.01 M LiBr at RT.

**Table 1**  
Molar Masses and PDI of PGA(M) Before and After Modification

Polymer	$M_n$ (g mol <sup>-1</sup> )	PDI
PGA(M)	2600 <sup>a</sup> (DP = 13)	1.8 <sup>a</sup>
PGA(M)-g-6-(Fmoc-Ahx)	3400 <sup>b</sup>	1.8 <sup>a</sup>
PGA(M)-g-6-(Fmoc-Ahx)-g-mPEG12	11,500 <sup>b</sup>	1.7 <sup>a</sup>
PGA(M)-g-NH <sub>2</sub> -g-mPEG12	10,000 <sup>b</sup>	1.7 <sup>a</sup>

<sup>a</sup>  $M_n$  of PGA(M) backbone and polydispersity index (PDI) are obtained from GPC using DMF+ 0.01 M LiBr as eluent.

<sup>b</sup>  $M_n$  is calculated on the basis of mol% degree of grafting from <sup>1</sup>H NMR spectra.

(RNHC=O) proton at 3.66 ppm and the resonances of the aromatic rings labeled with (t, u, v, w, and s). The peak labeled with (r) reflects the methylene protons of fluorenylmethyloxycarbonyl protecting groups (see Fig. 2a). The degree of grafting is calculated quantitatively from the integral value of peak (e) represented in the <sup>1</sup>H NMR spectrum of unmodified PGA(M) (Fig. 1), and the integral values of peaks (e) and OH-groups represented in the <sup>1</sup>H NMR spectrum (Fig. 2a) using the following equation:

$$\% \text{ degree of grafting} = \frac{f_e(\text{modified PGA}) - f_e(1,2,3\text{-trisubstituted part(unmodified PGA)})}{f_e(\text{modified PGA}) - [f_e(1,2,3\text{-trisubstituted part(unmodified PGA)})] + f_{\text{OH}}}$$

Analysis of the <sup>1</sup>H NMR spectrum for the grafted polymer shows that the degree of grafting is 16 mol% (~2 amine residues per polymer chain) (in which a theoretical value of 20 mol% grafting with respect to OH-groups was applied). Although the polymer is modified with 2 amine groups per chain, it is still water insoluble. The GPC traces of PGA(M)-g-6-(Fmoc-Ahx) in Figure 3 also show a slight shift of the peak to shorter retention time indicating a slight increase in the polymer molar mass after grafting. The molar masses and polydispersities are given in Table 1.

The grafting is further investigated with FTIR spectroscopy. In Figure 4, the FTIR spectra of PGA(M) before and after grafting with 6-(Fmoc-Ahx) side chains are given. After modification, 3 characteristic bands appear indicating the successful formation of PGA(M)-g-6-(Fmoc-Ahx), that is, the appearance of the Fmoc (RNHC=O) stretching and bending vibration at 3455 and 1535 cm<sup>-1</sup>, respectively, in addition to the bending vibration of Fmoc aromatic rings at around 753 and 760 cm<sup>-1</sup>.

#### Modification of PGA(M)-g-6-(Fmoc-Ahx) With Succinylated mPEG12

Because PGA(M)-g-6-(Fmoc-Ahx) is water insoluble, some hydrophilic side chains were introduced to the polymer backbone as

depicted in the Scheme 1c, to afford the desired water solubility. For this purpose, mPEG12 with a molar mass of 550 g mol<sup>-1</sup> was used. Initially, mPEG12 was reacted with succinic anhydride in the presence of DMAP as a catalyst to modify the polymer with these side chains via Steglich esterification reaction and yield PGA(M)-g-6-(Fmoc-Ahx)-g-mPEG12, while 12 corresponds to the number of repeating units. In the light of pharmaceutical application and by taking into account that the use of high molar mass PEGs can cause kidney clearance problems,<sup>46</sup> low molar mass PEG having 550 g mol<sup>-1</sup> (12 repeating units) was used.

<sup>1</sup>H NMR spectroscopy measurements prove the successful grafting reaction. The <sup>1</sup>H NMR spectrum of PGA(M)-g-6-(Fmoc-Ahx)-g-mPEG12 with the peak assignments is shown in Figure 2b. The multiplet signal (x) in the range of 2.68-2.56 ppm is assigned to the succinyl protons, multiplet signal (y') in the range of 3.71-3.52 ppm is assigned to the methylene protons of the repeating units, and the singlet signal (z) at 3.37 ppm corresponds to the methyl protons. The high intensity of the peaks belonging to the mPEG12 side chains indicates very high degree of grafting (excess was applied, ~80 mol%). The PDI is obtained from GPC measurements. Analysis of the GPC traces in Figure 3 indicates that the grafting is accomplished with the absence of unreacted mPEG12 chains as a unimodal distribution of the GPC trace occurs. GPC analysis also shows that after modification, the peak shifts to smaller retention times related to an increase of the molar mass and a decrease of the PDI. Table 1 summarizes the molar masses and PDI of the grafted polymers.

#### Deprotection of Fmoc Protecting Groups and Formation of PGA(M)-g-NH<sub>2</sub>-g-mPEG12

The removal of the protective groups, fluorenylmethyloxycarbonyl (Fmoc), was achieved via a facile method under mild reaction conditions (see Scheme 1d), to yield functional polyester with side chains terminated with primary amine groups acting as mTGase substrate for protein conjugation. Deprotection of Fmoc groups is confirmed by the disappearance of Fmoc aromatic protons between 7 and 8 ppm as given in Figure 5. The chemical structure of PGA(M)-g-NH<sub>2</sub>-g-mPEG12 is confirmed by the shifting of the methylene protons (p) connected to the amine group downfield. Moreover and from the integration values, it is noticed that the Fmoc (RNHC=O) protons (q) disappear and the primary amine protons appear at 3.37 ppm, labeled with (q').

FTIR spectroscopy is also used to verify the structure of the formed polymer. Figure 6 shows the disappearance of the Fmoc group's vibration at 753 and 760 cm<sup>-1</sup> assuming the complete

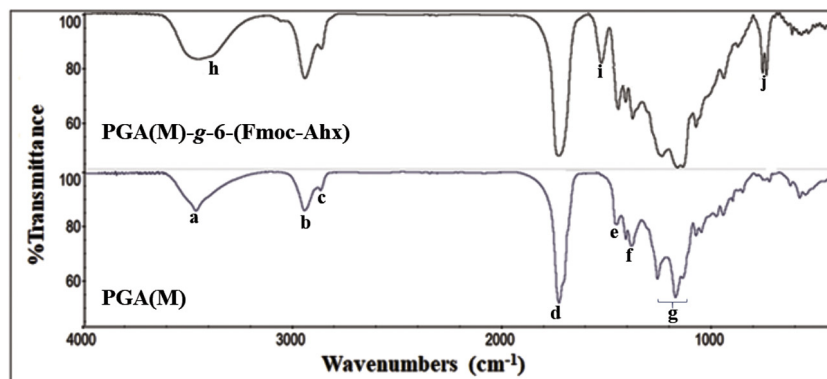


**Figure 4.** FTIR spectra of PGA(M) and PGA(M)-g-6-(Fmoc-Ahx) at RT in the spectral range between 4000 and 400 cm<sup>-1</sup>. Bands arise from the following vibrations: (a) OH stretching,  $\nu(\text{-OH})$ , (b) C-H asymmetric stretching,  $\nu_{\text{as}}(\text{C-H})$ , (c) C-H symmetric stretching,  $\nu_{\text{s}}(\text{C-H})$ , (d) C=O stretching,  $\nu(\text{C=O})$ , (e) C-H scissoring bending,  $\delta_{\text{s}}(\text{C-H})$ , (f) C-H wagging and twisting, C-H ( $\omega, \tau$ ), (g) C-O-C asymmetric and symmetric stretching,  $\nu_{\text{as,s}}(\text{C-O-C})$ , (h) -NH stretching,  $\nu(\text{-NH})$ , (i) R-NHC=O bending,  $\delta(\text{R-NHC=O})$ , and (j) R-CH=CH<sub>2</sub> out of plane bending, =CH ( $\gamma$ ).

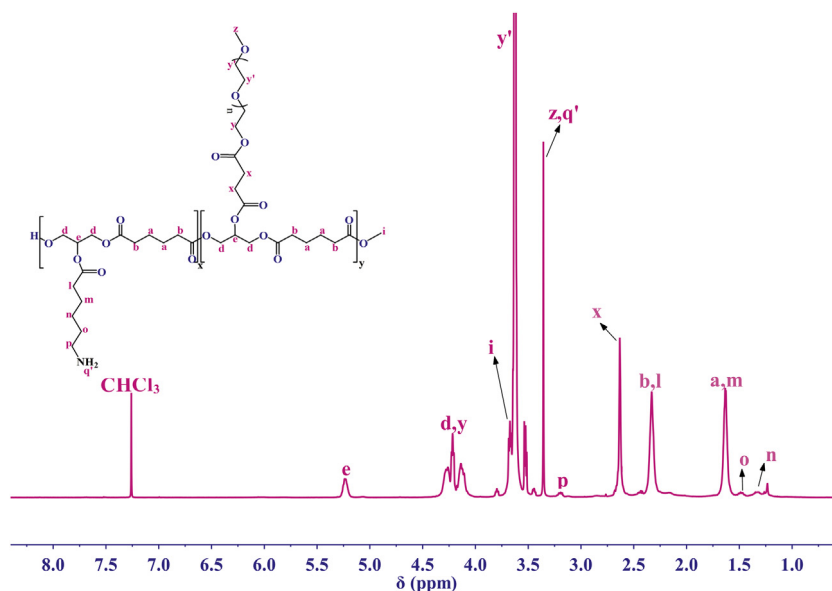


**Figure 5.**  $^1\text{H}$  NMR spectrum of PGA(M)-g-NH<sub>2</sub>-g-mPEG12 in CDCl<sub>3</sub> at 27°C.

removal of the protective groups and formation of primary amine ( $-\text{NH}_2$ ) groups. Furthermore, it reveals the disappearance of the Fmoc (RNHC=O) vibration and appearance of the primary amine stretching and bending vibrations at 3387 (overlapped with OH groups) and 1651  $\text{cm}^{-1}$ , respectively.

The GPC traces presented in Figure 3 prove the deprotection as the peak shifts slightly to a longer retention time (reduction of the molar mass from 11,500 to 10,000  $\text{g mol}^{-1}$ ) because of the removal of Fmoc groups. GPC results are given in Table 1.

#### Polymer-Protein Conjugation

PGA(M)-g-NH<sub>2</sub>-g-mPEG12 was subsequently conjugated to DMC via the reaction between the glutamine residues of DMC and the primary amine groups along the polymer backbone using the cross-linker enzyme mTGase. As previously reported and according to the results obtained by Ohtsuka et al.,<sup>18</sup> the use of aliphatic amines with more than 4 carbon atoms as spacers is desirable as they can be identified as substrates by mTGase. Therefore, the polymer was modified with *n*-alkyl side chains containing 6 carbon atoms that are terminated with primary

amine groups to provide a good substrate for mTGase (acyl acceptor).

For this experiment, DMC was used as a model protein which is well-known to act as an acyl donor only because all amine groups of lysine residues are protected by methylation.<sup>15</sup> Therefore, it is beneficial to investigate the conjugation of DMC to the amine-functionalized polyester to prevent any possibility for self-cross-linking of DMC in the presence of mTGase. In the case of therapeutic proteins containing free primary amine groups, mTGase catalyzes the formation of protein oligomers (dimer, trimer, or higher molar mass oligomers) in the absence of amine-functionalized polymer because of the cross-linking between the lysine (Lys) residues of one protein molecule and the glutamine (Gln) residues of another protein molecule. Although, using an excess of amine-functionalized polymer results in the formation of protein conjugates (monoderivatives) as main products. Therefore, the production of protein oligomers as by-products will be reduced accordingly.<sup>23,25</sup> The formed conjugates are analyzed by SDS-PAGE for a direct proof as shown in Figure 7.

It reveals the appearance of the conjugate on the SDS gel as higher molar mass band at the interface between the stacking and

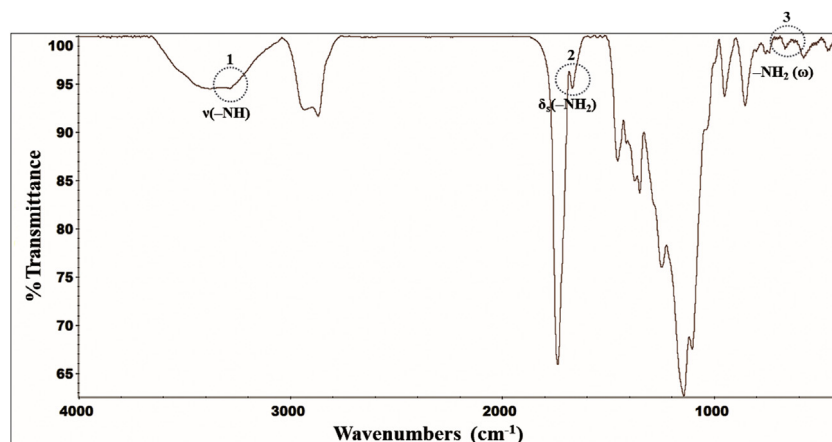


**Figure 6.** FTIR spectrum of PGA(M)-g-NH<sub>2</sub>-g-mPEG12 at RT in the spectral range between 4000 and 400  $\text{cm}^{-1}$ . Three characteristic bands for primary amine groups appeared as (1)  $-\text{NH}_2$  stretching,  $\nu(-\text{NH})$ , (2)  $-\text{NH}_2$  scissoring bending,  $\delta_s(-\text{NH}_2)$ , and (3)  $-\text{NH}_2$  wagging,  $-\text{NH}_2(\omega)$ .

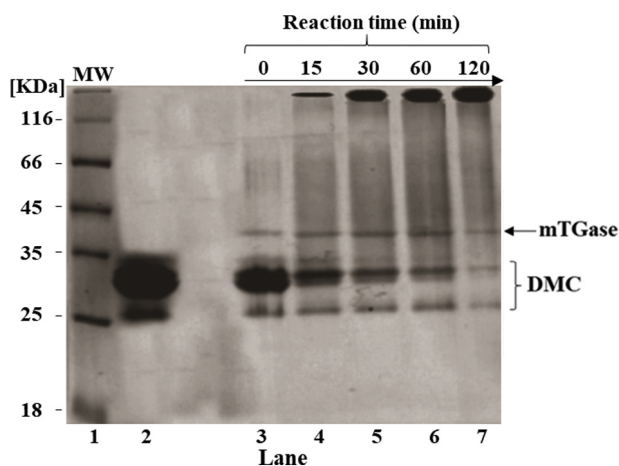


**Figure 7.** Image of SDS-PAGE gel for the coupling of PGA(M)-g-NH<sub>2</sub>-g-mPEG12 with DMC using mTGase-S2P. Lane 1: molecular weight marker; Lane 2: PGA(M)-g-NH<sub>2</sub>-g-mPEG12 and DMC (without mTGase-S2P); Lanes 3-7: PGA(M)-g-NH<sub>2</sub>-g-mPEG12 and DMC in the presence of mTGase-S2P after 0, 15, 30, 60, and 120 min, respectively. Lanes 4-7 show the conjugate product (polymer and DMC) at the interface between the stacking and separation gels (the product intensity increased with the time and pure DMC is disappeared after 120 min).

separation gels after a period of 15 min (lane 4). By increasing the reaction time, the same bands with higher intensity appears (lanes 5, 6, 7), whereas the band of unreacted DMC almost completely disappears after a period of 2 h (lane 7), indicating that the polymer is successfully conjugated to DMC in the presence of the mTGase. Because DMC has 65 glutamine residues and the polymer has 2 amine groups per chain, only conjugates with large molar masses and high molar mass distribution are formed. Further analyzing the SDS gel in Figure 7, it can be noted that the formed bands exhibit some smearing effect on the gel. This might arise from the presence of PEG side chains along the polymer backbone, which can interact with the SDS gel and form long tailing bands.<sup>47</sup> The high degree of grafting with hydrophilic PEG side chains (~80 mol% grafting with respect to OH-groups) affirms the high water solubility of the obtained protein-polymer conjugate, which was represented as a clear solution in phosphate buffer at pH 8.

For further investigations, some control experiments were carried out. Figure 8 shows the results of SDS-PAGE for the 3 controls

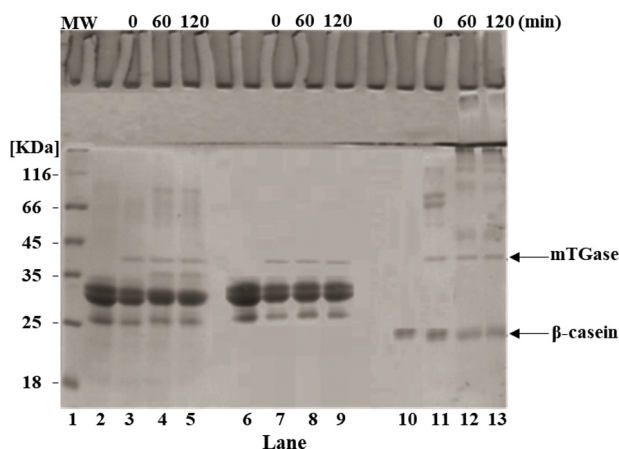


**Figure 8.** Image of the SDS-PAGE gel for controls used in the experiment. Lane 1: molecular weight marker; Lane 2: MDC and DMC (without mTGase-S2P); Lanes 3-5: MDC and DMC in the presence of mTGase-S2P after 0, 60, and 120 min, respectively. Lane 6: only DMC; Lanes 7-9: DMC and mTGase-S2P as a negative control after 0, 60, and 120 min, respectively. Lane 10:  $\beta$ -casein only; Lane 11-13:  $\beta$ -casein and mTGase as a positive control after 0, 60, and 120 min, respectively.

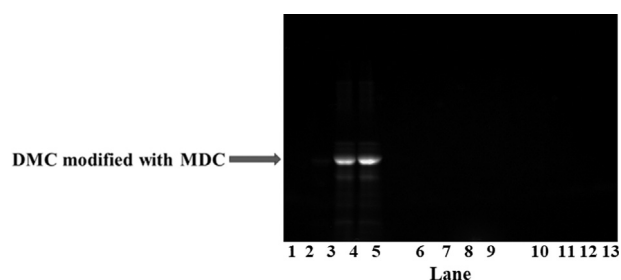


**Figure 9.** Fluorescence image of the SDS-PAGE gel for the used controls. Lane 1: MW marker; Lane 2: MDC with DMC without mTGase-S2P; Lanes 3-5: MDC with DMC in the presence of mTGase-S2P after 0, 60, and 120 min, respectively. The arrow indicates 2 fluorescence bands which confirm that DMC was coupled with MDC after 60 and 120 min. Lane 6: only DMC; Lanes 7-9: DMC and mTGase-S2P as a negative control after 0, 60, and 120 min, respectively. Lane 10:  $\beta$ -casein only; Lanes 11-13:  $\beta$ -casein and mTGase as a positive control after 0, 60, and 120 min, respectively.

used. In the first control experiment, MDC, a fluorescent dye, was incubated with DMC in the presence of mTGase. MDC is a well-known substrate for mTGase, which carries an alkyl side chain with one primary amine group to act as an acyl acceptor. Therefore, it is used widely to prove whether the glutamine residues of the protein are accessible to the catalyst mTGase.<sup>48</sup> Lanes 3, 4, and 5 in Figure 8 correspond to the reaction of MDC with DMC in the presence of mTGase. After exposing the SDS gel to UV light, high molar mass fluorescence bands appear after a period of 60 and 120 min (lanes 4 and 5 in Fig. 9), indicating the successful conjugation between MDC and DMC.

As a negative control, DMC was incubated with mTGase (lanes 7, 8, 9 in Fig. 8). The absence of higher molar mass bands confirms that no self-cross-linking of DMC appears. As a positive control,  $\beta$ -casein was incubated with mTGase (lanes 11, 12, 13 in Fig. 8). The results reveal the appearance of high molar mass bands at the interface between the stacking and separation gels (lanes 12 and 13), and on the top of the stacking gel (lane 12) that confirms the formation of cross-linked aggregates with large molar masses, that is, self-cross-linking of  $\beta$ -casein *via* lysine and glutamine residues in the presence of mTGase occurs.

As an outlook, the biodegradability of poly(glycerol adipate) has a potential advantage over PEG or also over modified methacrylamides. Etrych et al.<sup>49</sup> have, for example, reported a new strategy to couple water-soluble and drug-loaded methacrylamides with protein as a new type of antibody-drug conjugate that opens a new approach for the application of targeted drug delivery. In accordance with our findings, further experiments on different therapeutic proteins to investigate their conjugation with the amine-functionalized polymer *via* mTGase are in progress. The use of this enzymatic procedure for the conjugation of therapeutic proteins to a biodegradable and water-soluble polymer can improve the effectiveness of therapeutic proteins by increasing protein solubility and stability and by reducing protein immunogenicity. Moreover, by reducing kidney clearance of small proteins, protein-polymer conjugates can be used to prolong plasma half-life of therapeutic proteins.<sup>50</sup>

## Conclusions

PGA(M), a biodegradable polyester, was modified with PEG side chains for water solubility and side chains terminated with primary amine groups to give PGA(M)-g-NH<sub>2</sub>-g-mPEG12 with approximately 2 amine groups per polymer chain. We showed that the amine-functionalized polyester, PGA(M)-g-NH<sub>2</sub>-g-mPEG12, acted efficiently as an acyl acceptor for the reaction with DMC catalyzed

by mTGase under mild reaction conditions. Overall, the results provided evidence that the conjugation was successful by the appearance of high molar mass conjugates with increasing time intervals and the disappearance of pure DMC after a period of 2 h. This enzymatic approach for protein conjugation with biodegradable and highly water soluble polymers could be promising by further expanding the scope of research to therapeutic protein-based conjugation that can improve their pharmacokinetic and therapeutic performance. This procedure can also be used for the formation of protein-polymer conjugates using well-defined NPs,<sup>51,52</sup> or cubosomes based on hydrophobically modified PGA.<sup>53</sup> In conclusion, this study proves that the modification of PGA(M) with side chains carrying primary amine groups succeeded in developing a new substrate for mTGase.

## Acknowledgments

The present work of RA was financially supported by Deutscher Akademischer Austauschdienst (DAAD). This project was financially supported in the frame of High Performance Center Chemical and Biosystems Technology Halle/Leipzig by the European Fond for Regional Development under the support code ZS/2016/06/79645.

The authors dedicate this work to John Carpenter's and Ted Randolph's contributions to the field of pharmaceutical biotechnology.

## References

- Duncan R. The dawning era of polymer therapeutics. *Nat Rev Drug Discov*. 2003;2:347-360.
- Leader B, Baca QJ, Golan DE. Protein therapeutics: a summary and pharmacological classification. *Nat Rev Drug Discov*. 2008;7:21-39.
- Zhao W, Liu F, Chen Y, Bai J, Gao W. Synthesis of well-defined protein-polymer conjugates for biomedicine. *Polymer*. 2015;66:A1-A10.
- Thordarson P, Le Droumaguet B, Velonia K. Well-defined protein-polymer conjugates-synthesis and potential applications. *Appl Microbiol Biotechnol*. 2006;73:243-254.
- Abuchowski A, van Es T, Palczuk NC, Davis FF. Alteration of immunological properties of bovine serum albumin by covalent attachment of polyethylene glycol. *J Biol Chem*. 1977;252:3578-3581.
- Abuchowski A, McCoy JR, Palczuk NC, van Es T, Davis FF. Effect of covalent attachment of polyethylene glycol on immunogenicity and circulating life of bovine liver catalase. *J Biol Chem*. 1977;252:3582-3586.
- Veronese FM, Pasut G. PEGylation, successful approach to drug delivery. *Drug Discov Today*. 2005;10:1451-1458.
- Liu Y, Smith CA, Panetta JC, et al. Antibodies predict pegaspargase allergic reactions and failure of rechallenge. *J Clin Oncol*. 2019;37:2051-2061.
- Moreno A, Pitoc GA, Ganson NJ, et al. Anti-PEG antibodies inhibit the anticoagulant activity of PEGylated aptamers. *Cell Chem Biol*. 2019;26:634-644.e3.
- Mohamed M, Abu Lila AS, Shimizu T, et al. PEGylated liposomes: immunological responses. *Sci Technol Adv Mater*. 2019;20:710-724.
- Karte NV. The conjugation of proteins with polyethylene glycol and other polymers: altering properties of proteins to enhance their therapeutic potential. *Adv Drug Deliv Rev*. 1993;10:91-114.
- Satchi-Fainaro R, Hailu H, Davies JW, Summerford C, Duncan R. PDEPT: polymer-directed enzyme prodrug therapy. 2. HPMA copolymer-β-lactamase and HPMA copolymer-C-dox as a model combination. *Bioconjug Chem*. 2003;14:797-804.
- Mero A, Fang Z, Pasut G, Veronese FM, Viegas TX. Selective conjugation of poly(2-ethyl 2-oxazoline) to granulocyte colony stimulating factor. *J Control Release*. 2012;159:353-361.
- Besheer A, Hause G, Kressler J, Mäder K. Hydrophobically modified hydroxyethyl starch: synthesis, characterization, and aqueous self-assembly into nano-sized polymeric micelles and vesicles. *Biomacromolecules*. 2007;8:359-367.
- Besheer A, Hertel TC, Kressler J, Mäder K, Pietzsch M. Enzymatically catalyzed HES conjugation using microbial transglutaminase: proof of feasibility. *J Pharm Sci*. 2009;98:4420-4428.
- Sato H. Enzymatic procedure for site-specific pegylation of proteins. *Adv Drug Deliv Rev*. 2002;54:487-504.
- Strop P. Versatility of microbial transglutaminase. *Bioconjug Chem*. 2014;25:855-862.
- Ohtsuka T, Sawa A, Kawabata R, Nio N, Motoki M. Substrate specificities of microbial transglutaminase for primary amines. *J Agric Food Chem*. 2000;48:6230-6233.
- Ando H, Adachi M, Umeda K, et al. Purification and characteristics of a novel transglutaminase derived from Microorganisms. *Agric Biol Chem*. 1989;53:2613-2617.
- De Jong GAH, Koppelman SJ. Transglutaminase catalyzed reactions: impact on food applications. *J Food Sci*. 2002;67:2798-2806.
- Sato H, Hayashi E, Yamada N, Yatagai M, Takahara Y. Further studies on the site-specific protein modification by microbial transglutaminase. *Bioconjug Chem*. 2001;12:701-710.
- Maullu C, Raimondo D, Caboi F, et al. Site-directed enzymatic PEGylation of the human granulocyte colony-stimulating factor. *FEBS J*. 2009;276:6741-6750.
- Mero A, Spolaore B, Veronese FM, Fontana A. Transglutaminase-mediated PEGylation of proteins: direct identification of the sites of protein modification by mass spectrometry using a novel monodisperse PEG. *Bioconjug Chem*. 2009;20:384-389.
- Strop P, Liu SH, Dorywalska M, et al. Location matters: site of conjugation modulates stability and pharmacokinetics of antibody drug conjugates. *Chem Biol*. 2013;20:161-167.
- Spolaore B, Raboni S, Satwekar AA, et al. Site-specific transglutaminase-mediated conjugation of interferon α-2b at glutamine or lysine residues. *Bioconjug Chem*. 2016;27:2695-2706.
- Marx CK, Hertel TC, Pietzsch M. Random mutagenesis of a recombinant microbial transglutaminase for the generation of thermostable and heat sensitive variants. *J Biotechnol*. 2008;136:156-162.
- Sommer C, Volk N, Pietzsch M. Model based optimization of the fed-batch production of a highly active transglutaminase variant in *Escherichia coli*. *Protein Expr Purif*. 2011;77:9-19.
- Laemmli UK. Cleavage of structural proteins during the assembly of the head of bacteriophage T4. *Nature*. 1970;227:680-685.
- Naolou T, Weiss VM, Conrad D, Busse K, Mäder K, Kressler J. Fatty acid modified poly(glycerol adipate) - polymeric analogues of glycerides. In: Scholz C, Kressler J, eds. *Tailored Polymer Architectures for Pharmaceutical and Biomedical Applications*. Washington, DC: American Chemical Society; 2013:39-52. ACS Symposium Series.
- Neises B, Steglich W. Simple method for the esterification of carboxylic acids. *Angew Chem Int Ed Engl*. 1978;17:522-524.
- Lu C, Zhong W. Synthesis of propargyl-terminated heterobifunctional poly(ethylene glycol). *Polymers (Basel)*. 2010;2:407-417.
- Höck S, Marti R, Riedl R, Simeunovic M. Thermal cleavage of the Fmoc protection group. *Chimia*. 2010;64:200-202.
- Swainson SME, Styliari ID, Taresco V, Garnett MC. Poly(glycerol adipate) (PGA), an enzymatically synthesized functionalizable polyester and versatile drug delivery carrier: a literature update. *Polymers*. 2019;11:1561.
- Suk JS, Xu Q, Kim N, Hanes J, Ensign LM. PEGylation as a strategy for improving nanoparticle-based drug and gene delivery. *Adv Drug Deliv Rev*. 2016;99:28-51.
- Meng W, Parker TL, Kallinteri P, et al. Uptake and metabolism of novel biodegradable poly(glycerol-adipate) nanoparticles in DAOY monolayer. *J Control Release*. 2006;116:314-321.
- Suksiriworapong J, Taresco V, Ivanov DP, et al. Synthesis and properties of a biodegradable polymer-drug conjugate: methotrexate-poly(glycerol adipate). *Colloids Surf B Biointerfaces*. 2018;167:115-125.
- Weiss VM, Lucas H, Mueller T, et al. Intended and unintended targeting of polymeric nanocarriers: the case of modified poly(glycerol adipate) nanoparticles. *Macromol Biosci*. 2018;18:1700240.
- Rulev AY. Aza-Michael reaction: achievements and prospects. *Russ Chem Rev*. 2011;80:197-218.
- Uyama H, Klegraf E, Wada S, Kobayashi S. Regioselective polymerization of Sorbitol and divinyl sebacate using lipase catalyst. *Chem Lett*. 2000;29:800-801.
- Kobayashi S, Uyama H, Kimura S. Enzymatic polymerization. *Chem Rev*. 2001;101:3793-3818.
- Naolou T, Meister A, Schöps R, Pietzsch M, Kressler J. Synthesis and characterization of graft copolymers able to form polymersomes and worm-like aggregates. *Soft Matter*. 2013;9:10364-10372.
- Gross RA, Ganesh M, Lu W. Enzyme-catalysis breathes new life into polyester condensat-ion polymerizations. *Trends Biotechnol*. 2010;28:435-443.
- Yu Y, Wu D, Liu C, Zhao Z, Yang Y, Li Q. Lipase/esterase-catalyzed synthesis of aliphatic polyesters via polycondensation: a review. *Process Biochem*. 2012;47:1027-1036.
- Uyama H, Inada K, Kobayashi S. Regioselective polymerization of divinyl sebacate and triols using lipase catalyst. *Macromol Rapid Commun*. 1999;20:171-174.
- Taresco V, Suksiriworapong J, Creasey R, et al. Properties of acyl modified poly(glycerol-adipate) comb-like polymers and their self-assembly into nanoparticles. *J Polym Sci A Polym Chem*. 2016;54:3267-3278.
- Knop K, Hoogenboom R, Fischer D, Schubert US. Poly(ethylene glycol) in drug delivery: pros and cons as well as potential alternatives. *Angew Chem Int Ed Engl*. 2010;49:6288-6308.
- Zheng CY, Ma G, Su Z. Native PAGE eliminates the problem of PEG-SDS interaction in SDS-PAGE and provides an alternative to HPLC in characterization of protein PEGylation. *Electrophoresis*. 2007;28:2801-2807.
- Bechtold U, Otterbach JT, Pasternack R, Fuchsbauer HL. Enzymic preparation of protein G-peroxidase conjugates catalysed by transglutaminase. *J Biochem*. 2000;127:239-245.
- Etrych T, Strohal J, Kovár L, Kabešová M, Říhová B, Ulbrich K. HPMA copolymer conjugates with reduced anti-CD20 antibody for cell-specific drug targeting. I. Synthesis and in vitro evaluation of binding efficacy and cytostatic activity. *J Control Release*. 2009;140:18-26.

50. Pasut G, Veronese FM. PEGylation of proteins as tailored chemistry for optimized bio-conjugates. *Adv Polym Sci.* 2006;192:95-134.
51. Weiss VM, Naolou T, Hause G, Kuntsche J, Kressler J, Mäder K. Poly(glycerol adipate)-fatty acid esters as versatile nanocarriers: from nanocubes over ellipsoids to nanospheres. *J Control Release.* 2012;158:156-164.
52. Swainson SME, Taresco V, Pearce AK, et al. Exploring the enzymatic degradation of poly(glycerol adipate). *Eur J Pharm Biopharm.* 2019;142:377-386.
53. Bilal MH, Hussain H, Prehm M, et al. Synthesis of poly(glycerol adipate)-g-oleate and its ternary phase diagram with glycerol monooleate and water. *Eur Polym J.* 2017;91:162-175.

### 3.2 Paper II:

#### **Microbial transglutaminase-mediated formation of erythropoietin-polyester conjugates<sup>2</sup>**

Therapeutic proteins have contributed significantly to the treatment of many diseases. Among these therapeutics, EPO has been applied to treat anemia associated with renal failure and cancer chemotherapy. Despite its therapeutic uses, EPO exhibits a fairly short  $t_{1/2}$  *in vivo* and thus, the development of new EPO derivatives *via* peptide addition or through a covalent conjugation with water soluble polymers have been studied. In this regard, the accessibility of rHuEPO towards mTGase with the aim of obtaining novel rHuEPO conjugates based on a biodegradable and water soluble polyester is investigated.

In the following publication, a mTGase-recognizable substrate having primary amine groups was synthesized based on PDSA. Initially, PDSA was enzymatically synthesized in the presence of CAL-B, chemically modified with side chains terminated with primary amine groups, thoroughly characterized by <sup>1</sup>H NMR spectroscopy and GPC, and then applied for the variant mTGase-TG<sup>16</sup>-catalyzed conjugation reaction with rHuEPO at its  $T_m = 54.3$  °C. SDS-PAGE was used to confirm the formation of rHuEPO-PDSA conjugates in order to prove that the amine-modified PDSA is accepted as a substrate for mTGase-TG<sup>16</sup>. To further support our results, amine-modified PDSA was partially labelled with UV-detectable fluorescent dye, rhodamine B-isothiocyanate, to detect high molar mass fluorescent bands on SDS-PAGE. This enzymatic approach resulted in rHuEPO conjugates that may potentially contribute to improve its *in vivo* efficacy.

The author contributions of the following article are: R. Alaneed conceptualized the work, performed the experiments, wrote the original draft including the figures/scheme, and made the final version. M. Naumann carried out the MS analysis and wrote the MS part. M. Pietzsch conceptualized the work, supervised and complemented the writing, editing and finalization of manuscript. J. Kressler conceptualized the work, supervised and complemented the writing, editing and finalization of manuscript.

---

<sup>2</sup>The following article is adapted with permission from (Microbial transglutaminase-mediated formation of erythropoietin-polyester conjugates; Razan Alaneed, Marcel Naumann, Markus Pietzsch, and Jörg Kressler. *J. Biotechnol.*, **346**, 1-10 (2022) DOI: 10.1016/j.jbiotec.2022.01.001). Copyright (2022) Elsevier B.V. All rights reserved. The link to the article on the publisher's website is: <https://doi.org/10.1016/j.jbiotec.2022.01.001>. No changes were made.



# Microbial transglutaminase-mediated formation of erythropoietin-polyester conjugates

Razan Alaneed<sup>a,b</sup>, Marcel Naumann<sup>c</sup>, Markus Pietzsch<sup>b,\*</sup>, Jörg Kressler<sup>a,\*</sup>

<sup>a</sup> Department of Chemistry, Martin Luther University Halle-Wittenberg, Von-Danckelmann-Platz 4, Halle/Saale D-06099, Germany

<sup>b</sup> Department of Pharmacy, Martin Luther University Halle-Wittenberg, Weinbergweg 22, Halle/Saale D-06120, Germany

<sup>c</sup> Fraunhofer Institute for Cell Therapy and Immunology, Department of Drug Design and Target Validation, Biozentrum, Weinbergweg 22, Halle/Saale D-06120, Germany

## ARTICLE INFO

### Keywords:

Erythropoietin (EPO)  
rHuEPO conjugates  
Thermoresistant microbial transglutaminase  
Amine-grafted poly(D-sorbitol adipate) (PDSA-NH<sub>2</sub>)  
Biodegradability

## ABSTRACT

Erythropoietin (EPO) is a glycoprotein hormone that has been used to treat anemia in patients with chronic kidney disease and in cancer patients who are receiving chemotherapy. Here, we investigated the accessibility of the glutamine (Gln, Q) residues of recombinant human erythropoietin (rHuEPO) towards a thermoresistant variant microbial transglutaminase (mTGase), TG<sup>16</sup> with the aim of developing novel rHuEPO conjugates that may potentially enhance its biological efficacy. As a model bioconjugation, we studied the reactivity of rHuEPO towards TG<sup>16</sup> with a low molar mass amine group containing substrate, monodansyl cadaverine (MDC). The reactions were carried out at a  $T_m$  of 54.3 °C, the transition temperature of rHuEPO. Characterization by SDS-PAGE and mass spectrometry confirmed the conjugates formation. Then, we examined the conjugation of rHuEPO with a biodegradable and biocompatible polyester, poly(D-sorbitol adipate) (PDSA). To achieve this, PDSA was enzymatically synthesized using lipase B from *Candida antarctica* (CAL-B), chemically modified with side chains having free primary amine (NH<sub>2</sub>) groups that can be acyl acceptor substrate of TG<sup>16</sup>, thoroughly characterized by <sup>1</sup>H NMR spectroscopy, and then applied for the TG<sup>16</sup>-mediated conjugation reaction with rHuEPO. rHuEPO conjugates generated by this approach were identified by SDS-PAGE proving that the amine-grafted PDSA is accepted as a substrate for TG<sup>16</sup>. The successful conjugation was further verified by the detection of high molar mass fluorescent bands after labelling of amine-grafted PDSA with rhodamine B-isothiocyanate. Overall, this enzymatic procedure is considered as an effective approach to prepare biodegradable rHuEPO-polymer conjugates even in the presence of N- and O-glycans.

## 1. Introduction

Erythropoietin (EPO), a glycoprotein hormone produced mainly by peritubular cells in the kidney as well as by the liver during fetal life, is the main regulator of red blood cells (RBCs) production and maintenance (Suresh et al., 2020; Graber and Krantz, 1978; Jacobs et al., 1985). In 1985 (Jacobs et al., 1985; Lin et al., 1985), DNA technology has been used for the large-scale production of recombinant human erythropoietin (rHuEPO) through the cloning of the EPO gene and expression in Chinese hamster ovary cells (CHO). The primary structure of rHuEPO consists of a 165 amino acid single polypeptide chain stabilized with two intra-chain disulfide bridges. It is a heavily glycosylated protein since 40% of the total mass is composed of carbohydrates covalently attached at three N-linked glycosylation sites and one O-linked glycosylation site

(Lai et al., 1986; Skibeli et al., 2001; Jelkmann, 2013). In the last decade, rHuEPO has been used as a therapeutic agent to treat anemia associated with renal failure (Eschbach et al., 1987; Cody and Hodson, 2016), cancer chemotherapy (Glaspy, 2014; Madeddu et al., 2018), HIV infection (Henry et al., 1992; Guan et al., 2020), neurological diseases (Rey et al., 2019; Sun et al., 2019), and recently COVID-19 (Ehrenreich et al., 2020). Although, such formulations under the brand names EPOGEN® and PROCIT® have been proven to be effective for the treatment of anemia, these protein therapeutics exhibit a fairly short half-life in vivo and therefore, many studies have been made to prolong the therapeutic residence time in vivo and delay the renal clearance. Elliot et al., 2004 and Su et al., 2010 have introduced an additional glycosylation site in rHuEPO to obtain EPO analogs with higher bioactivity and prolonged plasma half-life. Lee et al., 2006 have developed

\* Corresponding authors.

E-mail addresses: [markus.pietzsch@pharmazie.uni-halle.de](mailto:markus.pietzsch@pharmazie.uni-halle.de) (M. Pietzsch), [joerg.kressler@chemie.uni-halle.de](mailto:joerg.kressler@chemie.uni-halle.de) (J. Kressler).

<https://doi.org/10.1016/j.jbiotec.2022.01.001>

Received 7 July 2021; Received in revised form 12 January 2022; Accepted 13 January 2022

Available online 15 January 2022

0168-1656/© 2022 Elsevier B.V. All rights reserved.

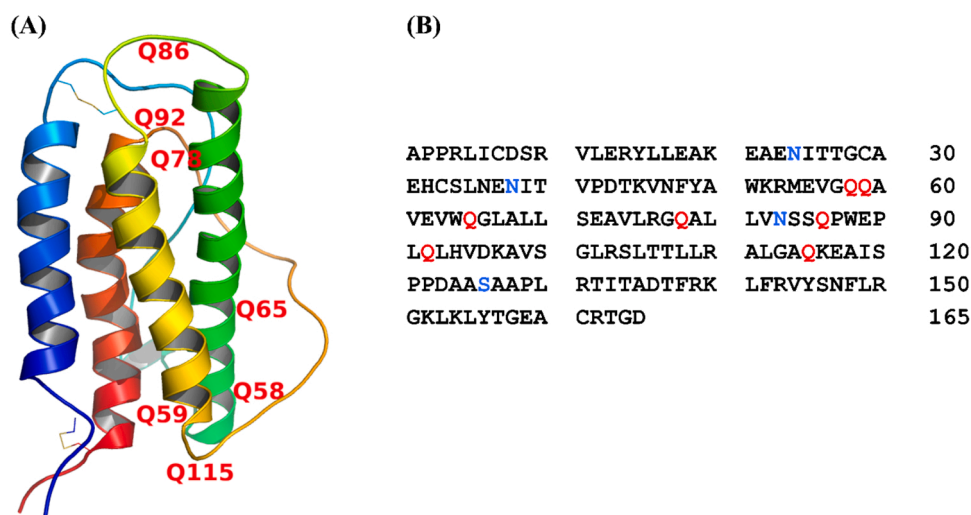


**Fig. 1.** (A) 3D structure of EPO (PDB code 1BUY) (Cheetham et al., 1998). The structure is drawn using PyMOL (The PyMOL Molecular Graphics System, Schrödinger, LLC). (B) Amino acid sequence of rHuEPO (Jelkmann, 1992). The glutamine (Gln, Q) residues potential sites of modification are shown in red. Three N-linked glycosylation sites (Asn24, Asn38, and Asn83) and one O-linked glycan (Ser126) are shown in blue.

new EPO derivatives via peptide addition at the carboxy terminus of human EPO with an enhanced circulation half-life. In recent years, PASylation of rHuEPO, i.e. the addition of repetitive blocks of the amino acids proline, alanine, and serine (PAS) at the C-terminus, has contributed to improve its *in vivo* bioactivity (Hedayati et al., 2017). Furthermore, poly(ethylene glycol) (PEG) has been widely used for the covalent modification of recombinant EPO, referred as PEGylation, in order to improve its pharmacokinetics (Hoffmann et al., 2016). Despite the significant success of PEG, some drawbacks such as its non-biodegradability and immunogenicity have limited its clinical use (Hoang Thi et al., 2020; Moreno et al., 2019). Beside PEG, biodegradable polymers have been investigated for EPO conjugation. For example, the conjugation of a novel erythropoietin mimetic peptide (EMP) to biodegradable hydroxyethyl starch (HES) with enhanced biological efficacy has been developed (Greindl et al., 2010; Kessler et al., 2012). In the field of protein conjugation, most of the approaches exclusively rely on chemical procedures which require harsh conditions, hence, a mild enzymatic approach using microbial transglutaminase (mTGase) has been established (Sato, 2002). For example, the US patent, US0116322 A1, discloses the formation of EPO conjugates with a non-antigenic hydrophilic polymer wherein a mTGase was employed as a catalyst (Pool, 2006). Besheer et al., 2009 have reported the enzymatic bioconjugation of HES to a model protein, dimethylcasein (DMC) using mTGase. Also, we recently reported a variant microbial transglutaminase (mTGase-S2P)-mediated conjugation of amine-modified poly(glycerol adipate) to DMC (Alaneed et al., 2020). Microbial transglutaminase (mTGase; protein-glutamine  $\gamma$ -glutamyltransferase, EC 2.3.2.13) is an enzyme that catalyzes the formation of protease-resistant isopeptide bonds between the  $\gamma$ -carboxamide groups of glutamine (Q) residues ( $-\text{CONH}_2$ , acyl donors) and primary amine groups as well as the  $\epsilon$ -amine group of lysine (K) residues ( $-\text{NH}_2$ , acyl acceptors), with the loss of ammonia ( $\text{NH}_3$ ) as a by-product (Strop, 2014). mTGase is intensively used in food industry (Santhi et al., 2017) as well as in biomedical field (Deweid et al., 2019; Chan and Lim, 2019). mTGase was optimized by directed evolution techniques for increased thermostability allowing reactions at elevated temperatures (Marx et al., 2008; Buettner et al., 2012; Böhme et al., 2020).

In this work, we investigated the reactivity of Q residues of rHuEPO towards the variant mTGase, TG<sup>16</sup>, with the aim to obtain novel rHuEPO conjugates at elevated temperatures. The rHuEPO polypeptide sequence contains seven Q residues (Fig. 1) that could be potential sites for modification using TG<sup>16</sup>. As a proof of principle study, we utilized

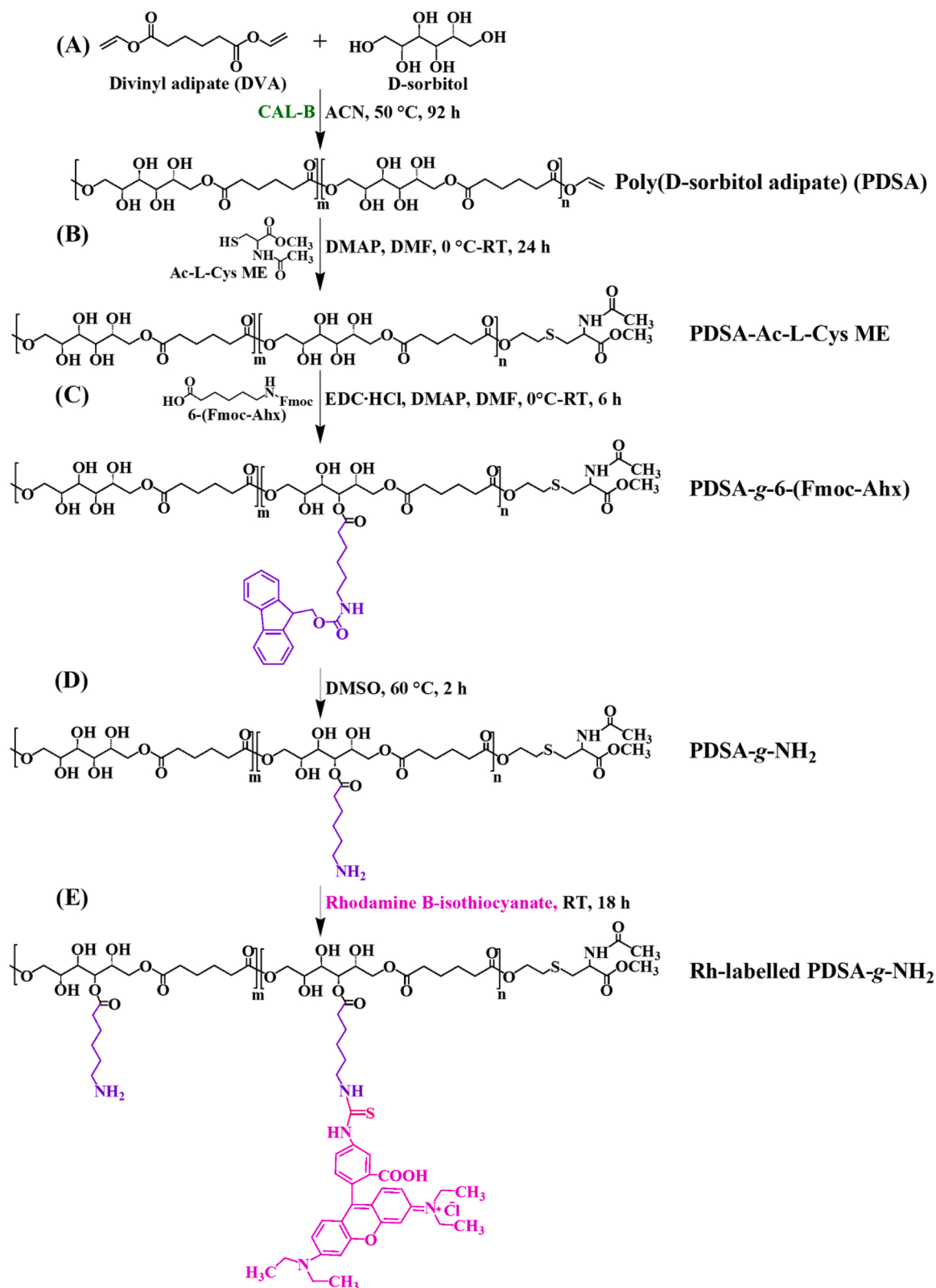
monodansyl cadaverine (MDC), a well-known fluorescent substrate for transglutaminases for the conjugation with rHuEPO. The formed conjugates were analysed by SDS-PAGE as well as by mass spectrometry (MS) after proteolytic digestion of the modified rHuEPO. After successful investigation, rHuEPO was conjugated with a water soluble, biocompatible, and biodegradable polyester, i.e. amine-grafted poly(D-sorbitol adipate) (PDSA-g-NH<sub>2</sub>). PDSA is a sugar-based polyester with four pendant free hydroxyl (OH) groups per repeating unit. Due to its biodegradability, our group has reported a modified PDSA with different fatty acids to produce amphiphilic PDSA for the formation of biodegradable nanoparticles (Bilal et al., 2016).

In the first part of our research efforts, we focused on the modification of PDSA with side chains bearing primary amine group that can be accepted as TG<sup>16</sup> substrate. After modification with primary amine groups, PDSA-g-NH<sub>2</sub> was partially labelled with a fluorescent dye, rhodamine B-isothiocyanate, to produce Rh-labelled PDSA-g-NH<sub>2</sub>. PDSA before and after modification was thoroughly characterized by <sup>1</sup>H NMR spectroscopy and GPC. In the second part, we investigated the conjugation of rHuEPO with MDC, PDSA-g-NH<sub>2</sub>, and Rh-labelled PDSA-g-NH<sub>2</sub> using TG<sup>16</sup>, a thermostable transglutaminase resulted from a combination of previously determined amino acid substitutions (Böhme et al., 2020). The formed conjugates were analysed by SDS-PAGE.

## 2. Methods

### 2.1. Synthesis of PDSA-g-NH<sub>2</sub>

The synthesis of PDSA-g-NH<sub>2</sub> was carried out in several steps starting from the polymer backbone, PDSA. Initially, PDSA was enzymatically synthesized according to the procedure described by (Bilal et al., 2016) as shown in Scheme 1 (A). The full synthetic procedure for PDSA can be found in the SI. The molar mass of PDSA was obtained by GPC as  $M_n = 12,000 \text{ g mol}^{-1}$  with PDI = 1.6. PDSA has different end groups and among them, vinyl end groups appearing as three signals in the <sup>1</sup>H NMR spectrum (see Fig. 2 (A)). In order to avoid any cross-linking possibility between vinyl groups and primary NH<sub>2</sub> groups in the last synthesis step, these end groups were removed with Ac-L-Cys ME by thiol-ene “click” reaction, using 4-(dimethylamino)pyridine (DMAP) as a catalyst (Lowe, 2014; Konuray et al., 2018). A weighed amount of PDSA (5 g, 17.12 mmol) and Ac-L-Cys ME (3 g, 16.9 mmol) was dissolved in 120 mL dry DMF in a 250 mL round-bottom flask equipped with a magnetic stirrer. Then, a catalytic amount of DMAP (0.6 g, 4.92 mmol)



**Scheme 1.** Synthetic pathways for (A) PDSA, (B) PDSA-Ac-L-Cys ME, (C) PDSA-g-6-(Fmoc-Ahx), (D) PDSA-g-NH<sub>2</sub>, (E) Rh-labelled PDSA-g-NH<sub>2</sub>.

was added at 0 °C. After 24 h, the reaction solution was dialyzed against water to remove DMAP and unreacted Ac-L-Cys ME, using a membrane with a cut-off molar mass of 1000 g mol<sup>-1</sup>. <sup>1</sup>H NMR (400 MHz, DMF-d<sub>7</sub>) δ (ppm): 8.36 (d, *J* = 8 Hz) and 8.18–8.13 (m, 1 H), 4.98–4.62 (m, 2 H), 4.66–4.47 (t, *J* = 8, 3 H), 4.53–4.29 (m, 2 H), 4.27–3.84 (m, 3 H), 3.70

(s, 3 H), 3.68 (d, *J* = 49 Hz, 2 H), 3.58–3.32 (m, 2 H), 3.22 (dd, *J* = 13.7, 8.1 Hz, 2 H), 2.65 (t, *J* = 6.8, 2 H), 2.37–2.17 (m, 4 H), 1.94 (s, 3 H), 1.63–1.41 (m, 4 H).

In the next synthesis step, PDSA was grafted with 6-(Fmoc-Ahx) side chains, by Steglich esterification (Neises and Steglich, 1978). A typical

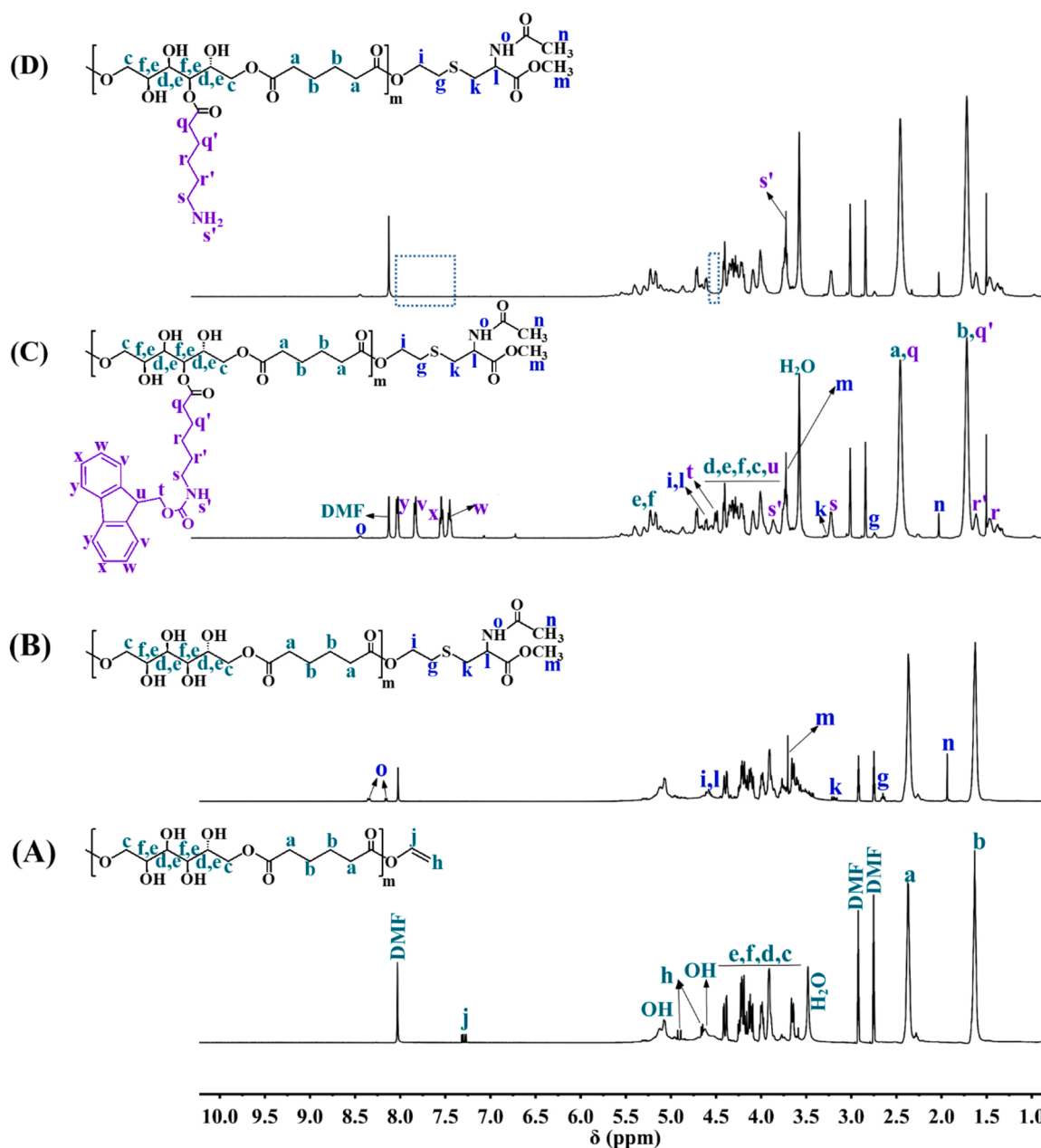


Fig. 2.  $^1\text{H}$  NMR spectra of (A) PDSA, (B) PDSA-Ac-L-Cys ME, (C) PDSA-g-6-(Fmoc-Ahx), and (D) PDSA-g-NH<sub>2</sub> where the dashed boxes indicate the disappearance of all Fmoc signals. All spectra were recorded at 27 °C, 400 MHz, using DMF-d<sub>7</sub> as solvent.

procedure for 20 mol% intended degree of grafting is as follows, PDSA (4 g, 13.7 mmol) was dissolved in 80 mL anhydrous DMF in a 250 mL two-neck round-bottom flask equipped with a magnetic stirrer. After addition of 6-(Fmoc-Ahx) (3.8 g, 10.7 mmol), DMAP (0.4 g, 3.27 mmol), and the esterification promoting agent, 1-ethyl-3-(3-dimethylaminopropyl)-carbodiimide hydrochloride (EDC·HCl) (3 g, 15.6 mmol) at 0 °C, the reaction was allowed to proceed for 6 h. The reaction was quenched by removing most of DMF by rotary evaporator under reduced pressure and the crude product was dialyzed first against water to remove the catalysts and then against tetrahydrofuran (THF) to remove the unreacted 6-(Fmoc-Ahx), using a membrane with a cut-off molar mass of 1000 g mol<sup>-1</sup>. The molar mass of PDSA-g-6-(Fmoc-Ahx) was calculated on the basis of mol% degree of grafting from the  $^1\text{H}$  NMR spectrum (Fig. 2 (C)). The PDI was determined by GPC as 1.7.  $^1\text{H}$  NMR (400 MHz, DMF-d<sub>7</sub>)  $\delta$  (ppm): 8.36 (d,  $J$  = 8 Hz) and 8.18–8.13 (m, 1H), 7.94 (d,  $J$  = 7.5 Hz, 2H), 7.73 (d,  $J$  = 7.5 Hz, 2H), 7.44 (t,  $J$  = 7.6 Hz,

2H), 7.35 (t,  $J$  = 7.5 Hz, 2H), 5.61–4.7 (m, 1H), 5.09 (m, 1H), 4.66–4.47 (t,  $J$  = 8, 3H), 4.34–3.61 (m, 9H), 3.75 (s, 1H), 3.70 (s, 3H), 3.22 (dd,  $J$  = 13.7, 8.1 Hz, 2H), 3.13 (q,  $J$  = 6.6 Hz, 2H), 2.65 (t,  $J$  = 6.8, 2H), 2.37–2.17 (m, 6H), 1.94 (s, 3H), 1.63–1.41 (m, 6H), 1.53 (s, 2H), 1.42–1.21 (m, 2H). In the final synthesis step, Fmoc groups were removed using the procedure described by (Höck et al., 2010). PDSA-g-6-(Fmoc-Ahx) (1 g, 1.6 mmol) was dissolved in 10 mL anhydrous dimethyl sulfoxide (DMSO) and the solution was stirred at 60 °C for 2 h. The reaction was stopped by precipitation of the solution twice in cold *tert*-butylmethylether (TBME) in order to remove DMSO and the by-product, dibenzofulvene, to yield PDSA-g-NH<sub>2</sub>.  $^1\text{H}$  NMR (400 MHz, DMF-d<sub>7</sub>)  $\delta$  (ppm): 8.36 (d,  $J$  = 8 Hz) and 8.18–8.13 (m, 1H), 5.25 (d,  $J$  = 66.1 Hz, 1H), 5.09 (m, 1H), 4.66–4.47 (t,  $J$  = 8, 3H), 4.34–3.61 (m, 8H), 3.64 (tdd,  $J$  = 10.8, 7.2, 3.2 Hz, 5H), 3.22 (dd,  $J$  = 13.7, 8.1 Hz, 2H), 3.13 (q,  $J$  = 6.6 Hz, 2H), 2.65 (t,  $J$  = 6.8, 2H), 2.37–2.17 (m, 6H), 1.94 (s, 3H), 1.63–1.41 (m, 6H), 1.53 (s, 2H), 1.42–1.21 (m, 2H). The full  $^1\text{H}$

NMR spectrum is given in Fig. 2 (D). GPC traces of PDSA before after modification are shown in Fig. S2.

## 2.2. Labelling of PDSA-g-NH<sub>2</sub> with rhodamine B-isothiocyanate

PDSA-g-NH<sub>2</sub> was partially labelled with the fluorescent dye, rhodamine B-isothiocyanate, in the same synthetic procedure described by (Paolini et al., 2018), with slight modification. Initially, PDSA-g-NH<sub>2</sub> and the dye were separately dissolved in anhydrous DMSO (total volume of 10 mL). Then, the dye solution was slowly added to the polymer solution under continuous stirring at RT. After 18 h, the reaction solution was dialyzed against water using a membrane with a cut-off molar mass of 1000 g mol<sup>-1</sup> and then, water was removed by lyophilisation to yield Rh-labelled PDSA-g-NH<sub>2</sub> as illustrated in Scheme 1 (E).

## 2.3. Preparation of recombinant TG<sup>16</sup>

The thermoresistant recombinant variant TG<sup>16</sup> of mTGase from *Streptomyces mobaraensis* was obtained according to the procedure of (Böhme et al., 2020). The combination of previously determined amino acid substitutions i.e. S2P, S23Y-Y24 N, H289Y, and K294L (Buettner et al., 2012) resulted in a TG<sup>16</sup> variant with a 19-fold improved half-life at 60 °C compared to the wild-type mTGase. The enzyme specific activity was measured in duplicate by a colorimetric hydroxamate procedure (Folk and Cole, 1966) prior to the conjugation reaction. The detailed procedure is included in the SI.

## 2.4. Conjugation of MDC to rHuEPO using TG<sup>16</sup>

For the conjugation of rHuEPO to the fluorescent dye, MDC, the protein concentration was adjusted to 500 µg/mL in 50 mM Tris buffer and 300 mM NaCl at pH 8 (the same rHuEPO concentration used in nanoDSF experiment).

32.5 µL of MDC solution (20 mM) was added to 45 µL of rHuEPO solution and the enzymatic reaction was initiated by the addition of 32.5 µL of TG<sup>16</sup> stock solution (60 U/mL). The reaction mixture was incubated at 54 °C for 90 min. After 60 min, an additional amount of TG<sup>16</sup> was added. Aliquots of the reaction mixture were then taken at various time points ending at 90 min, boiled with SDS buffer at 95 °C for 5 min, and subjected to SDS-PAGE for analysis. Prior to staining, the gel was exposed to UV light with excitation filter 365 nm and emission filter 520 nm. After fluorescence detection, the gel was stained with silver nitrate. Besides, different control experiments were carried out as follows; rHuEPO was incubated with TG<sup>16</sup> under the same conditions to investigate the ability for self-cross-linking of rHuEPO. MDC was incubated with TG<sup>16</sup> as a negative control. Additionally, rHuEPO was incubated with MDC without TG<sup>16</sup> to exclude any adsorption possibility of MDC on rHuEPO in the absence of TG<sup>16</sup>.

## 2.5. Conjugation of PDSA-g-NH<sub>2</sub> to rHuEPO using TG<sup>16</sup>

The conjugation reaction was performed at a protein concentration of 500 µg/mL and TG<sup>16</sup> concentration of 60 U/mL under the same conditions applied for rHuEPO-MDC conjugation. A 10-fold molar excess of amine-grafted polymer with respect to the Q residues of rHuEPO was used. The reaction mixture was prepared by dissolving PDSA-g-NH<sub>2</sub> in 32.5 µL of 50 mM Tris buffer, pH 8, to achieve a concentration of 7 mg/total reaction volume. Then, the polymer solution was added to 45 µL of rHuEPO solution and an aliquot of the reaction mixture was taken before the addition of TG<sup>16</sup>. 32.5 µL of TG<sup>16</sup> stock solution was added and the reaction was allowed to proceed at 54 °C for 90 min. After 60 min, an additional amount of TG<sup>16</sup> was freshly added. Aliquots of the reaction mixture at different time points were taken and then analysed by SDS-PAGE.

## 2.6. Conjugation of Rh-labelled PDSA-g-NH<sub>2</sub> to rHuEPO using TG<sup>16</sup>

After labelling PDSA-g-NH<sub>2</sub> with the dye, rhodamine B-isothiocyanate, the enzymatic conjugation with rHuEPO was carried out following the same procedure described above. At the end of the reaction, all samples were subjected to SDS-PAGE separation. All fluorescent bands were detected under UV light before being stained with silver nitrate. As a negative control, Rh-labelled PDSA-g-NH<sub>2</sub> was incubated with TG<sup>16</sup> at 54 °C for 60 min

## 2.7. Enzymatic N-deglycosylation of rHuEPO and rHuEPO conjugates

In order to confirm the conjugation of MDC and PDSA-g-NH<sub>2</sub> to rHuEPO and not to the glycan, the removal of N-linked glycan was required. The N-deglycosylation experiment was performed by treatment intact rHuEPO and rHuEPO conjugates with PNGase F as stated by the manufacturer's protocol. In brief, a mixture of 9 µL glycoprotein and 1 µL glycoprotein denaturing buffer was incubated at 100 °C for 10 min. Then, 2 µL of glycol buffer, 2 µL of 10% Nonidet P-40 (NP-40), H<sub>2</sub>O and 1 µL of PNGase F (total volume is 20 µL) were added. The samples were incubated at 37 °C for 1 h. After incubation, the samples were analysed by SDS-PAGE and the bands were visualized by silver staining.

## 3. Results and discussion

### 3.1. Preparation of PDSA-g-NH<sub>2</sub>

To produce TG<sup>16</sup>-recognizable substrate based on PDSA, primary amine groups were introduced to PDSA by esterification reaction between pendant secondary OH groups of the PDSA backbone and carboxylic acid (COOH) groups of 6-(fluorenylmethoxycarbonyl-amino) hexanoic acid (6-(Fmoc-Ahx)) side chains. Here, 6-(Fmoc-Ahx) was chosen as the amine group is linked to an alkyl chain with more than four carbon atoms making it an effective substrate for transglutaminases (Ohtsuka et al., 2000). The synthesis of PDSA-g-NH<sub>2</sub> was achieved by several steps as shown in Scheme 1. Initially, PDSA having pendant OH groups (Scheme 1 (A)), was enzymatically synthesized based on previous studies (Bilal et al., 2016) by polycondensation reaction of D-sorbitol and divinyl adipate using lipase B from *Candida antartica* (CAL-B). The reaction temperature was chosen to be 50 °C in order to produce a linear polyester while branching could happen at higher temperatures (Taresco et al., 2016). Number-average molar mass ( $M_n$ ) and polydispersity index (PDI) of PDSA are determined by gel permeation chromatography (GPC) in *N,N*-dimethylformamide (DMF) + 0.01 M lithium bromide (LiBr) as  $M_n = 12,000$  g mol<sup>-1</sup> and PDI = 1.6. GPC traces of PDSA are given in the Supplementary Information (SI, Fig. S2). The chemical structure of PDSA is confirmed by <sup>1</sup>H NMR spectroscopy (Fig. 2 (A)). From the <sup>1</sup>H NMR spectrum, vinyl end groups appearing as three signals at 7.32, 4.92, and 4.64 ppm along with OH and COOH groups are present. Since these vinyl end groups form suitable aza-Michael acceptors that can be involved in a nucleophilic addition reaction with free primary NH<sub>2</sub> groups in the last synthesis step resulting in hydrophilic polymer networks (Alaneed et al., 2021), the thiol-ene "click" reaction with *N*-acetyl-L-cysteine methyl ester (Ac-L-Cys ME) (see Scheme 1 (B)) was considered as a key step in this study.

The comparison between <sup>1</sup>H NMR spectra (A) and (B) in Fig. 2 shows the complete disappearance of the peaks related to vinyl end groups and the appearance of signals related to the new molecule which indicates a successful thiol-ene "click" reaction. In the next step, PDSA was modified with 6-(Fmoc-Ahx) side chains to produce PDSA-g-6-(Fmoc-Ahx) as shown in Scheme 1 (C). The peaks in the corresponding <sup>1</sup>H NMR spectrum in Fig. 2 (C) are assigned to the polymer structure by the presence of the methylene protons of the side chains in addition to the resonance of the Fmoc aromatic rings (7–8 ppm).

From the spectrum, the degree of grafting is determined quantitatively using the integrals of peaks (b) which represents the methylene

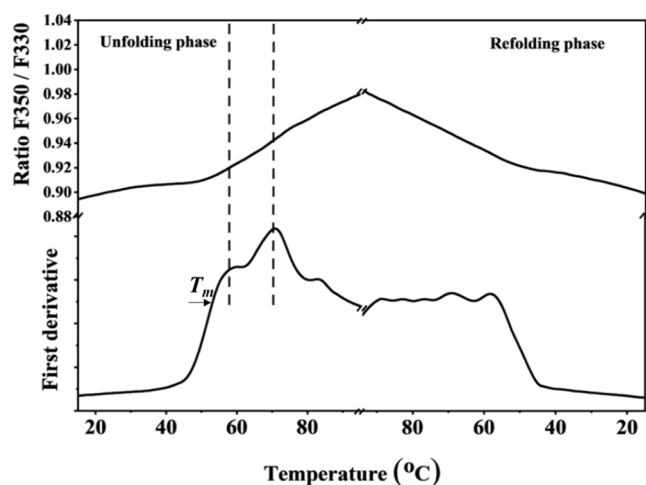


**Fig. 3.** Analysis of thermal stability (unfolding and refolding phases) of rHuEPO by nanoDSF. Changes in the F350/F330 fluorescence signal vs. temperature (top) and the corresponding first derivative are shown. Two-state unfolding transitions at 57.8 and 70.3 °C are observed (dashed lines) with increasing temperature. After cooling down, rHuEPO returned back to the native folded state. The midpoint of the transition curve,  $T_m$ , is calculated as 54.3 °C. Temperature scans were performed at a protein concentration of 500  $\mu\text{g}/\text{mL}$  with a heating rate of 1 °C  $\text{min}^{-1}$ . Scans were recorded in duplicate.

protons in the polymer backbone and ( $r'$ ) which represents the methylene protons in the side chain. The degree of grafting is calculated as  $\sim 13$  mol% per polymer chain with respect to all OH groups of the polymer backbone, considering that a theoretical value of 20 mol% grafting was applied in the feed composition. This results in nearly five OH groups per polymer chain which are modified with 6-(Fmoc-Ahx) side chains. The molar mass of PDSA-g-6-(Fmoc-Ahx) is calculated according to the degree of grafting as 13,600  $\text{g mol}^{-1}$ . In the final synthesis step, the Fmoc protecting groups were removed and the successful deprotection is verified by the disappearance of all Fmoc aromatic signals between 7 and 8 ppm in the  $^1\text{H}$  NMR spectrum as shown in Fig. 2 (D). In agreement with the calculated degree of grafting, approximately five primary  $\text{NH}_2$  groups per polymer chain could be potential sites for protein conjugation. The GPC traces presented in Fig. S2 prove the deprotection step as the peak shifts slightly to longer retention times caused by the removal of Fmoc groups.

### 3.2. Labelling of PDSA-g- $\text{NH}_2$ with rhodamine B-isothiocyanate

Labelling of PDSA-g- $\text{NH}_2$  was achieved by a facile method under mild reaction conditions. One primary  $\text{NH}_2$  group per polymer chain was labelled with the fluorescent dye. The successful labelling is proved by  $^1\text{H}$  NMR spectroscopy (given in the SI as Fig. S1) where in addition to the signals of amine-grafted polymer, signals corresponding to rhodamine B were observed specifically, the signals related to the methyl group at 1.17 ppm and the aromatic signals between 6 and 8 ppm.

### 3.3. $\text{TG}^{16}$ -mediated formation of rHuEPO conjugates

In a previous study, it was demonstrated that the Q residues recognized by transglutaminases as acyl donor substrates are located in highly flexible and unfolded regions of the protein (Spolaore et al., 2016). Hence and because attempts to modify rHuEPO with another (less) thermoresistant mTGase variant (S2P) at 37 °C failed (results not shown), thermal stability analysis of rHuEPO was performed using nano differential scanning fluorimetry (nanoDSF), which measures the intrinsic changes in the fluorescence emission of tryptophan and/or tyrosine residues between emission wavelengths  $\lambda$  330 and 350 nm as a function of temperature (Alexander et al., 2014; Magnusson et al.,

2019).

The thermal transition curve in Fig. 3 (top) and the corresponding first derivative show two-state unfolding transitions with increasing temperature indicating further unfolding of rHuEPO. Nevertheless, a reversible unfolding transition state after cooling down to 15 °C is observed.

The transition temperature  $T_m$  of rHuEPO, where 50% of the protein is unfolded (Gao et al., 2020), was determined from the peak of the first derivative of the relative fluorescence signal as 54.3 °C. A reasonable agreement was observed on comparing the  $T_m$  value of rHuEPO measured previously by far UV circular dichroism (CD) spectroscopy (Arakawa et al., 2001). Consequently, all  $\text{TG}^{16}$ -catalyzed conjugation reactions were carried out at this temperature. Due to the fact that the wild-type mTGase shows an irreversible denaturation at 60 °C and a half-life  $t_{1/2}$  of 2 min (Böhme et al., 2020), a highly thermoresistant variant  $\text{TG}^{16}$  with a  $t_{1/2}$  of 38 min at 60 °C was used.

Firstly, we tested the reactivity of Q residues of rHuEPO towards  $\text{TG}^{16}$  using a fluorescent primary amine group containing substrate, MDC. We carried out the experiment using glycosylated rHuEPO as the solubility is influenced by the presence of glycan moieties. rHuEPO was incubated with 10 molar excess of MDC at 54 °C in the presence of  $\text{TG}^{16}$  for 90 min. Aliquots of the reaction mixture were collected at different time points and analysed by SDS-PAGE (see Fig. 4 (A)). The fluorescent SDS-PAGE image shows a fluorescent band at the molar mass of rHuEPO after 30 min of reaction (lane 3) with an increase in the fluorescent intensity after 60 min of reaction (lane 4). As we mentioned previously that  $\text{TG}^{16}$  has a  $t_{1/2}$  of 38 min at 60 °C, a certain amount of fresh  $\text{TG}^{16}$  was added after 1 h. After 90 min reaction time an intensive fluorescent band (lane 5) was detected, indicating that the formation of rHuEPO-MDC conjugates was successful. Besides, an additional band above the rHuEPO band at about 66 kDa is observed indicating the presence of rHuEPO dimers which are resistant to the reduction by  $\beta$ -mercaptoethanol even after heating at 95 °C for 5 min prior gel electrophoresis. This can be explained by the intermolecular disulfide cross-linking at alkaline pH upon entering the SDS-PAGE. Additionally, this observation becomes more significant when high protein concentration is used as well as when a more sensitive silver staining is applied for protein detection (Suresh Kumar et al., 1993; Manning and Colón, 2004). However, rHuEPO dimers were reported to exhibit enhanced biological activity compared to the rHuEPO monomers (Dalle et al., 2001).

To verify that the conjugation was not due to primary  $\text{NH}_2$  group condensation reaction with the aldehyde group of the glycan moieties, the conjugates were treated with peptide-N-glycosidase F (PNGase F) to release the N-linked glycan. After N-deglycosylation, rHuEPO exhibits an increase in mobility owing to the reduction of its molar mass to  $\sim 18.4$  kDa as shown in Fig. 4 (A) (lanes 7–10). Fluorescent bands at the molar mass of N-deglycosylated rHuEPO appear which confirm the successful conjugation with MDC. According to these findings, rHuEPO-MDC conjugates were further analysed by MALDI-TOF/TOF and LC-ESI-LIT mass spectrometry. In order to investigate the basic applicability of mass spectrometry for the detection of MDC modifications in proteins, a synthetic model peptide (H-LLGDFFRKSKEKIGKEFKRIVQRIKDFLRNLPRTES-OH) was analysed as a preliminary experiment. The amino acid sequence of the model peptide was derived from the antimicrobial peptide Cathelicidin (LL-37). The respective modification site -VQR- has been reported to be a good substrate for microbial transglutaminase (Malešević et al., 2015). The MALDI-TOF mass spectrum (see Fig. S3) for modified LL-37-MDC shows two molecular ion signals for intact LL-37: one for the unmodified at  $m/z$  4491.426 and one for the modified form with MDC at  $m/z$  4809.558. The corresponding mass shift of + 318.13 Da coincides well with the theoretic value of + 318.14 Da which corresponds to the molar mass of MDC. The intensity of both mass signals allowed the estimation of the molar ratio of unmodified to modified LL-37 in the sample. The ratio was determined to be approximately 33:1, which is equal to a yield of  $\text{TG}^{16}$ -catalyzed conjugation reaction of 3.0%. Thereafter, rHuEPO-MDC conjugates were analysed.

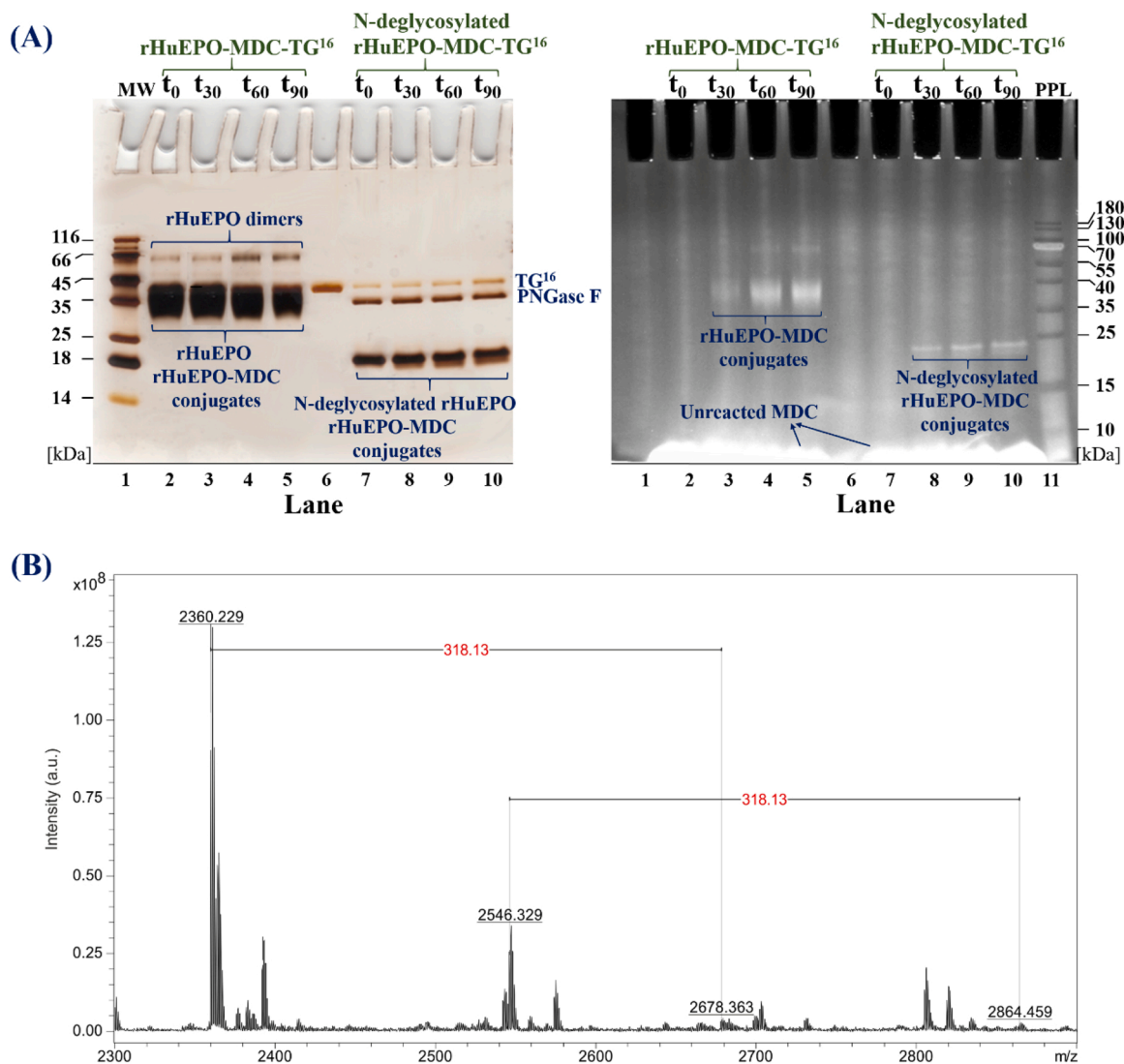


**Fig. 4.** (A) SDS-PAGE image showing silver staining (left panel) and fluorescence under UV light (right panel) for rHuEPO-MDC conjugation at 54 °C. Lane 1: MW marker, Lane 2–5: rHuEPO + MDC + TG<sup>16</sup> (t<sub>0</sub>), (t<sub>30</sub>), (t<sub>60</sub>), and (t<sub>90</sub>), respectively, Lane 6: TG<sup>16</sup> (with higher concentration than in the reaction mixture), Lane 7–10: rHuEPO + MDC + TG<sup>16</sup> (t<sub>0</sub>), (t<sub>30</sub>), (t<sub>60</sub>), and (t<sub>90</sub>), respectively, after treatment with PNGase F, Lane 11: prestained (PPL) protein marker. It is obviously noticed that the band intensity of rHuEPO dimers is increased with increasing reaction time. After N-deglycosylation, the rHuEPO dimers band disappeared as the concentration is less after treatment with PNGase F, (B) MALDI-TOF mass spectrum with mass signals for tryptic peptides of rHuEPO-MDC conjugates. The corresponding mass shift of + 318.13 Da belongs to the molar mass of MDC subtracted by the molar mass of ammonia.

The tryptic digest of rHuEPO-MDC conjugates was divided into two parts of which one was analysed on a LC-ESI-LIT and the other one on a MALDI-TOF/TOF system (see Fig. S4–S7). The results of both analyses were combined yielding a sequence coverage of 68.1% (see Fig. S8). Due to the low abundance of the MDC modification (only about 3% of the substrate sequences were modified), no fragment spectra of modified proteolytic peptides could be acquired. Inspection of the MALDI-TOF spectrum (Fig. 4 (B)) with the molecular ions of the proteolytic peptides revealed a mass shift of + 318.13 Da for the peptides H-MEVGQ-QAVEVWQGLALLSEAVLR-OH ( $m/z$  2546.329  $\rightarrow$   $m/z$  2864.459) and H-GQALLVNSSQPWEPLQLHVVDK-OH ( $m/z$  2360.229  $\rightarrow$   $m/z$  2678.363). Both peptides contain TG<sup>16</sup> substrate sequences and hence, the observed mass shift is at least indicative for the presence of an MDC modification. In particular, the respective modification site -WQG- and -LQL- have been found to be good substrates for microbial transglutaminase (Malešević et al., 2015). Due to the low signal intensity of the two mutual MDC-modified tryptic peptides, the acquisition of fragment spectra was not possible and hence, the exact position of the MDC modification could not be determined. Based on the signal intensity of

unmodified and mutual MDC-modified H-GQALLVNSSQPWEPLQLHVVDK-OH, the molar ratio was determined to be approximately 31:1. This is equal to a reaction yield of 3.3%, which coincides well with the yield that was observed in the preliminary experiment with LL-37.

At the same time, three control experiments were conducted. For the first control (Fig. S9), rHuEPO was incubated with TG<sup>16</sup> without MDC under the same reaction conditions and the results reveal that no high molar mass bands formed which conclude that rHuEPO is working as a Q substrate but obviously has no accessible K residues. For the second control (Fig. S10), TG<sup>16</sup> was incubated with MDC and the SDS-PAGE fluorescent image shows very weak fluorescent bands at the TG<sup>16</sup> molar mass after 30, 60, and 90 min indicating that MDC could modify TG<sup>16</sup> under these conditions. For the third control (Fig. S11), we incubated rHuEPO with MDC without the addition of TG<sup>16</sup>. The SDS-PAGE fluorescent image shows no high molar mass fluorescent bands, therefore, we conclude that no adsorption of MDC onto rHuEPO took place in the absence of TG<sup>16</sup>. The SDS-PAGE image with silver staining of native rHuEPO and rHuEPO after treatment with PNGase F is given in Fig. S12 of the SI. The native rHuEPO band, shown in lane 2 of Fig. S12, appears

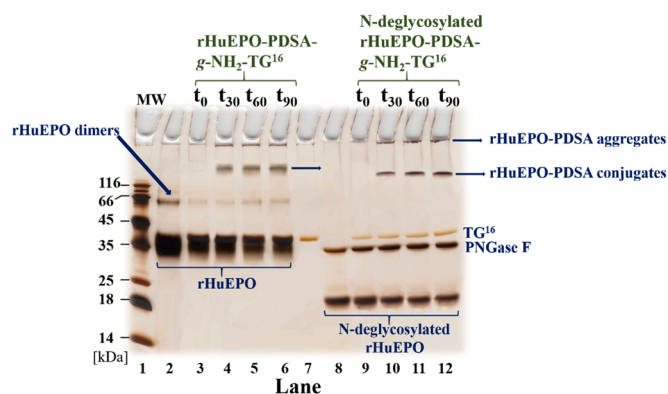


**Fig. 5.** Silver stained SDS-PAGE image for rHuEPO-PDSA-g-NH<sub>2</sub> conjugation at 54 °C. Lane 1: MW marker, Lane 2: rHuEPO + PDSA-g-NH<sub>2</sub>, Lane 3–6: rHuEPO + PDSA-g-NH<sub>2</sub> + TG<sup>16</sup> (t<sub>0</sub>), (t<sub>30</sub>), (t<sub>60</sub>), and (t<sub>90</sub>), respectively, Lane 7: TG<sup>16</sup> (with higher concentration than in the reaction mixture), Lane 8: rHuEPO + PDSA-g-NH<sub>2</sub> after treatment with PNGase F, Lane 9–12: rHuEPO + PDSA-g-NH<sub>2</sub> + TG<sup>16</sup> (t<sub>0</sub>), (t<sub>30</sub>), (t<sub>60</sub>), and (t<sub>90</sub>), respectively, after PNGase F reaction. It is obviously noticed that the band intensity of rHuEPO dimers before incubation is high due to oxidation reaction upon storage. After N-deglycosylation, the rHuEPO dimers band disappeared as the concentration is less after treatment with PNGase F.

as a broad band which is explained by the heterogeneity of the glycan moiety (Santoso et al., 2013). After enzymatic removal of the N-linked glycan moiety of rHuEPO, we observe a band with a molar mass of about 18.4 kDa which corresponds to the molar mass of the polypeptide backbone (Fig. S12, lane 3) indicating that the most prominent heterogeneity results from N-linked glycan chains.

In order to investigate further applications of this enzymatic conjugation method, PDSA-g-NH<sub>2</sub> was tested under the same reaction

conditions. A mixture of PDSA-g-NH<sub>2</sub> and rHuEPO in the ratio of 10:1, with respect to the number of NH<sub>2</sub> groups of the polymer and the Q residues of rHuEPO was applied. The conjugation of rHuEPO to PDSA-g-NH<sub>2</sub> was successful as evidenced by the presence of a new band at a significant shift to higher molar masses above 116 kDa on SDS-PAGE (see Fig. 5, lanes 4, 5, and 6). This indicates that the reaction started after 30 min incubation at 54 °C as no conjugation was observed at time 0 (see lane 3 of Fig. 5).

Before N-deglycosylation, the formed band shows a smear effect due to the glycan moieties of rHuEPO. With increasing reaction time, the band intensity of rHuEPO-PDSA conjugates is observed to increase while the band of pure rHuEPO is decreased demonstrating that rHuEPO was consumed with the time. In addition, the presence of high molar mass aggregates which cannot enter the stacking gel is noticed, as expected, due to the fact that PDSA-g-NH<sub>2</sub> has nearly five primary amine groups per polymer chain and rHuEPO has many potential Q residues. As a control, PDSA-g-NH<sub>2</sub> was incubated with rHuEPO (lane 2) and the results show that no reaction occurred in the absence of TG<sup>16</sup>. After treatment with PNGase F, the conjugates appear as more defined bands (lanes 10, 11, and 12) and exhibit a very slight increase in the mobility of the conjugates as the molar mass is decreased. Also, no conjugation was observed at time 0 (see lane 9 of Fig. 5). To further support our results, PDSA-g-NH<sub>2</sub> was partially labelled with UV-detectable fluorescent dye, rhodamine B-isothiocyanate, and the conjugation was determined by SDS-PAGE. Fig. 6 represents the SDS-PAGE analysis of the enzymatic conjugation of rHuEPO to Rh-labelled PDSA-g-NH<sub>2</sub>.

Before N-deglycosylation (Fig. 6 (A)), high molar mass conjugates with smear effect as well as aggregates along with the decrease of the rHuEPO band (lanes 4, 5, and 6) are revealed and confirmed by fluorescence under UV light. Moreover, no conjugation was observed at time 0 (see lane 3 of Fig. 6 (A)). The fluorescent image shows also a subsequent reduction of the Rh-labelled PDSA-g-NH<sub>2</sub> band with time (lanes 4, 5, and 6). After N-deglycosylation, more defined bands appear just

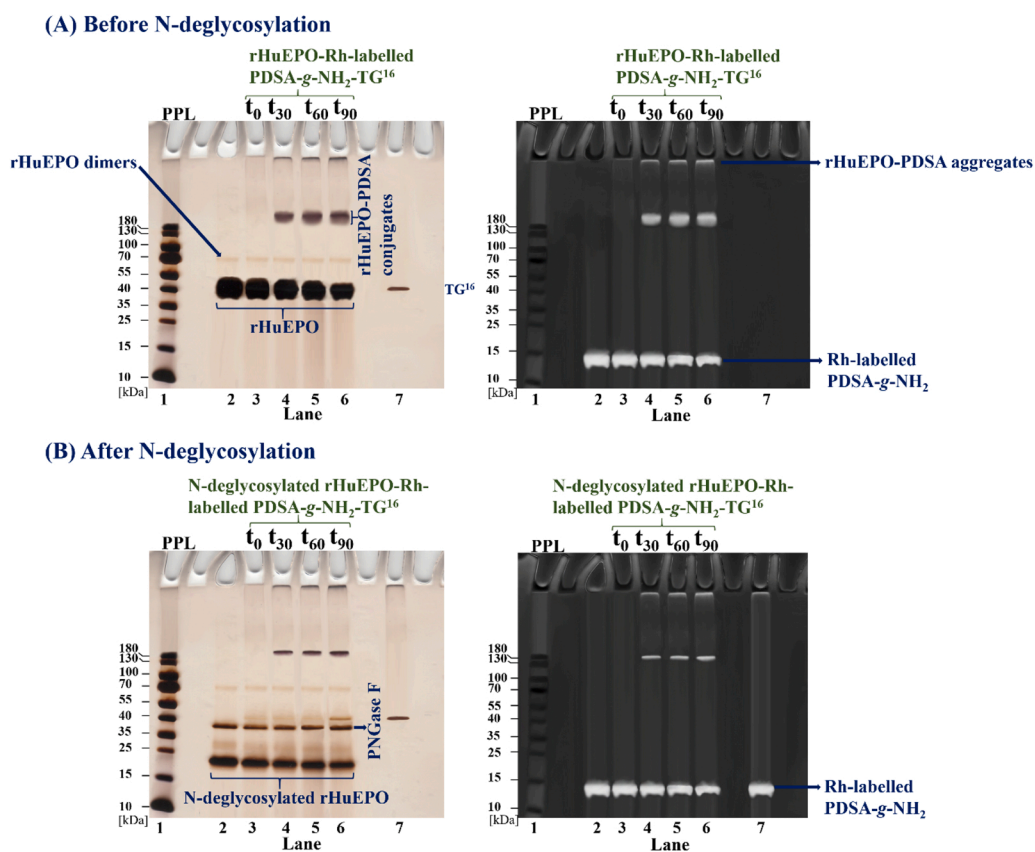


**Fig. 6.** SDS-PAGE images showing silver staining (left panel) and fluorescence under UV light (right panel) for (A) rHuEPO-Rh-labelled PDSA-g-NH<sub>2</sub> conjugation at 54 °C, before N-deglycosylation reaction, Lane 1: prestained marker, Lane 2: rHuEPO + Rh-labelled PDSA-g-NH<sub>2</sub>, Lane 3–6: rHuEPO + Rh-labelled PDSA-g-NH<sub>2</sub> + TG<sup>16</sup> (t<sub>0</sub>), (t<sub>30</sub>), (t<sub>60</sub>), and (t<sub>90</sub>), respectively, Lane 7: TG<sup>16</sup> (with higher concentration than in the reaction mixture) and (B) rHuEPO-Rh-labelled PDSA-g-NH<sub>2</sub> conjugation after treatment with PNGase F, Lane 1: prestained marker, Lane 2: rHuEPO + Rh-labelled PDSA-g-NH<sub>2</sub>, Lane 3–6: rHuEPO + Rh-labelled PDSA-g-NH<sub>2</sub> + TG<sup>16</sup> (t<sub>0</sub>), (t<sub>30</sub>), (t<sub>60</sub>), and (t<sub>90</sub>), respectively, Lane 7: Rh-labelled PDSA-g-NH<sub>2</sub> + TG<sup>16</sup> incubated for 60 min.

above 180 kDa also confirmed by the fluorescent image (lanes 4, 5, and 6, Fig. 6 (B)) and no conjugation was observed at time 0 (see lane 3 of Fig. 6 (B)). The molar mass of rHuEPO-Rh-labelled PDSA-g-NH<sub>2</sub> conjugates was determined using the SDS-PAGE image (Fig. S13 (A)). The molar masses of the protein marker PPL was plotted against their relative mobility (Fig. S13 (B)). After curve fitting with exponential function, a molar mass of ~ 184 kDa is calculated for the investigated conjugates.

Additional control experiment (Rh-labelled PDSA-g-NH<sub>2</sub> + TG<sup>16</sup>) was performed as shown in Fig. 6 (B), lane 7, which implies the formation of PDSA-TG<sup>16</sup> aggregates on the top of the stacking gel. This indicates further that the aggregates formed from the conjugation of rHuEPO with Rh-labelled PDSA-g-NH<sub>2</sub> could be a mixture of rHuEPO-PDSA and PDSA-TG<sup>16</sup> aggregates.

Overall, we were able to demonstrate the successful formation of rHuEPO conjugates with MDC and PDSA as a biodegradable polyester at the transition temperature  $T_m$  of rHuEPO, where half of the protein is in the unfolded state. Noticeably, this modification reaction was possible in the presence of N- and O-linked glycans. The rHuEPO-polymer conjugates mainly migrate at high molar mass species as a result of multi-site conjugation.

#### 4. Conclusion

In this paper, we described the enzymatic preparation of different rHuEPO conjugates using the transglutaminase TG<sup>16</sup>. Initially as a proof of principle study, rHuEPO was successfully modified with a well-known fluorescent substrate for mTGase, MDC and the SDS-PAGE results were confirmed by the presence of fluorescent bands at the molar mass of glycosylated (~ 35 kDa) and N-deglycosylated rHuEPO (~ 18.4 kDa). Although the conversion was considerably low according to the MS analysis, future studies on the optimization of transglutaminase-mediated formation of rHuEPO conjugates by replacing the glycan moieties with polymers should improve the conversion efficacy. Consequently, TG<sup>16</sup> recognizable substrate with primary NH<sub>2</sub> groups was designed based on PDSA. Thus, the conjugation of rHuEPO with the amine-grafted PDSA was achieved as confirmed by the appearance of new high molar mass bands with subsequent decrease of the pure rHuEPO band in SDS-PAGE. It was observed that two types of products were obtained, rHuEPO-polymer conjugates and cross-linked aggregates of high molar mass. In order to further confirm the conjugation, we partially labelled the polymer with a fluorescent dye to detect the conjugates as fluorescent bands after gel electrophoresis. Finally, we conclude that rHuEPO was modified with different acyl acceptor substrates at its transition temperature  $T_m$  where most Q residues are accessible for TG<sup>16</sup>. It is worth mentioning here that no conjugation took place below  $T_m$  of rHuEPO (results not shown). This enzymatic method described here can be regarded as a simple and efficient approach to prepare rHuEPO conjugates based on biodegradable and water soluble polymers that may have beneficial effects on rHuEPO in vivo potency.

#### CRedit authorship contribution statement

**Razan Alaneed:** Conceptualized the work, performed the experiments, wrote the original draft including the figures/scheme and made the final version. **Marcel Naumann:** Carried out the MS analysis and wrote the MS part. **Markus Pietzsch:** Conceptualized the work, supervised and complemented the writing, editing and finalization of manuscript. **Jörg Kressler:** Conceptualized the work, supervised and complemented the writing, editing and finalization of manuscript.

#### Declaration of Competing Interest

The authors declare that they have no known competing financial interests or personal relationships that could have appeared to influence the work reported in this paper.

#### Acknowledgments

This work was supported by Deutscher Akademischer Austauschdienst (DAAD) under a Research Grant - Doctoral Programs in Germany, 2017/18 (57299294). The authors thank Mr. Zaid Alhajaj for assistance in planning the enzymatic deglycosylation experiments of rHuEPO.

#### Appendix A. Supporting information

Supplementary data associated with this article can be found in the online version at doi:10.1016/j.jbiotec.2022.01.001.

#### References

- Alaneed, R., Hauenschild, T., Mäder, K., Pietzsch, M., Kressler, J., 2020. Conjugation of amine-functionalized polyesters with dimethylcasein using microbial transglutaminase. *J. Pharm. Sci.* 109, 981–991.
- Alaneed, R., Golitsyn, Y., Hauenschild, T., Pietzsch, M., Reichert, D., Kressler, J., 2021. Network formation by aza-Michael addition of primary amines to vinyl end groups of enzymatically synthesized poly(glycerol adipate). *Polym. Int.* 70, 135–144.
- Alexander, C.G., Wanner, R., Johnson, C.M., Breitsprecher, D., Winter, G., Duhr, S., Baaske, P., Ferguson, N., 2014. Novel microscale approaches for easy, rapid determination of protein stability in academic and commercial settings. *Biochim. Biophys. Acta* 1844, 2241–2250.
- Arakawa, T., Philo, J.S., Kita, Y., 2001. Kinetic and thermodynamic analysis of thermal unfolding of recombinant erythropoietin. *Biosci. Biotechnol. Biochem.* 65, 1321–1327.
- Besheer, A., Hertel, T.C., Kressler, J., Mäder, K., Pietzsch, M., 2009. Enzymatically catalyzed HES conjugation using microbial transglutaminase: proof of feasibility. *J. Pharm. Sci.* 98, 4420–4428.
- Bilal, M.H., Prehm, M., Njau, A.E., Samiullah, M.H., Meister, A., Kressler, J., 2016. Enzymatic synthesis and characterization of hydrophilic sugar based polyesters and their modification with stearic acid. *Polymers* 8, 80.
- Böhme, B., Moritz, B., Wendler, J., Hertel, T.C., Ihling, C., Brandt, W., Pietzsch, M., 2020. Enzymatic activity and thermostability of improved microbial transglutaminase variants. *Amino Acids* 52, 313–326.
- Buettner, K., Hertel, T.C., Pietzsch, M., 2012. Increased thermostability of microbial transglutaminase by combination of several hot spots evolved by random and saturation mutagenesis. *Amino Acids* 42, 987–996.
- Chan, S.K., Lim, T.S., 2019. Bioengineering of microbial transglutaminase for biomedical applications. *Appl. Microbiol. Biotechnol.* 103, 2973–2984.
- Cheetham, J.C., Smith, D.M., Aoki, K.H., Stevenson, J.L., Hoeffel, T.J., Syed, R.S., Egrie, J., Harvey, T.S., 1998. NMR structure of human erythropoietin and a comparison with its receptor bound conformation. *Nat. Struct. Biol.* 5, 861–866.
- Cody, J.D., Hodson, E.M., 2016. Recombinant human erythropoietin versus placebo or no treatment for the anaemia of chronic kidney disease in people not requiring dialysis. *Cochrane Database Syst. Rev.* 1, CD003266.
- Dalle, B., Henri, A., Fessard, P.R., Bettan, M., Scherman, D., Beuzard, Y., Payen, E., 2001. Dimeric erythropoietin fusion protein with enhanced erythropoietic activity in vitro and in vivo. *Blood* 97, 3776–3782.
- Deweid, L., Avrutina, O., Kolmar, H., 2019. Microbial transglutaminase for biotechnological and biomedical engineering. *Biol. Chem.* 400, 257–274.
- Ehrenreich, H., Weissenborn, K., Begemann, M., Busch, M., Vieta, E., Miskowiak, K.W., 2020. Erythropoietin as candidate for supportive treatment of severe COVID-19. *Mol. Med.* 26, 58.
- Elliot, S., Egrie, J., Browne, J., Lorenzini, T., Busse, L., Rogers, N., Ponting, I., 2004. Control of rHuEPO biological activity: the role of carbohydrate. *Exp. Hematol.* 32, 1146–1155.
- Eschbach, J.W., Egrie, J.C., Downing, M.R., Browne, J.K., Adamson, J.W., 1987. Correction of the anemia of end-stage renal disease with recombinant human erythropoietin: results of a combined phase-I and -II clinical trial. *N. Engl. J. Med.* 316, 73–78.
- Folk, J.E., Cole, P.W., 1966. Transglutaminase: Mechanistic features of the active site as determined by kinetic and inhibitor studies. *Biochim. Biophys. Acta* 122, 244–264.
- Gao, K., Oerlemans, R., Groves, M.R., 2020. Theory and applications of differential scanning fluorimetry in early-stage drug discovery. *Biophys. Rev.* 12, 85–104.
- Glaspy, J., 2014. Current status of use of erythropoietic agents in cancer patients. *Semin. Thromb. Hemost.* 40, 306–312.
- Graber, S.E., Krantz, S.B., 1978. Erythropoietin and control of red-cell production. *Annu. Rev. Med.* 29, 51–66.
- Greindl, A., Kessler, C., Breuer, B., Haberl, U., Rybka, A., Emgenbroich, M., Pötgens, A.J.G., Frank, H.G., 2010. AGEM400 (HES), a Novel erythropoietin mimetic peptide conjugated to hydroxyethyl starch with excellent in vitro efficacy. *Open Hematol. J.* 4, 1–14.
- Guan, X.Z., Wang, L.L., Pan, X., Liu, L., Sun, X.L., Zhang, X.J., Wang, D.Q., Yu, Y., 2020. Clinical indications of recombinant human erythropoietin in a single center: a 10-year retrospective study. *Front. Pharmacol.* 11, 1110.
- Hedayati, M.H., Norouzian, D., Aminian, M., Teimourian, S., Reza Ahangari Cohan, R.A., Sardari, S., Khorramzadeh, M.R., 2017. Molecular design, expression and evaluation of pasylated human recombinant erythropoietin with enhanced functional properties. *Protein J.* 36, 36–48.

- Henry, D.H., Beall, G.N., Benson, C.A., Carey, J., Cone, L.A., Eron, L.J., Fiala, M., Fischl, M.A., Gabin, S.J., Gottlieb, M.S., 1992. Recombinant human erythropoietin in the treatment of anemia associated with human immunodeficiency virus (HIV) infections and zidovudine therapy. *Ann. Intern. Med.* 117, 739–748.
- Hoang Thi, T.T., Pilkington, E.H., Nguyen, D.H., Lee, J.S., Park, K.D., Truong, N.P., 2020. The importance of Poly(ethylene glycol) alternatives for overcoming PEG immunogenicity in drug delivery and bioconjugation. *Polymers* 12, 298.
- Höck, S., Marti, R., Riedl, R., Simeunovic, M., 2010. Thermal cleavage of the Fmoc protection group. *Chimia* 64, 200–202.
- Hoffmann, E., Streichert, K., Nischan, N., Seitz, C., Brunner, T., Schwagerus, S., Hackenberger, C.P.R., Rubini, M., 2016. Stabilization of bacterially expressed erythropoietin by single site-specific introduction of short branched PEG chains at naturally occurring glycosylation sites. *Mol. BioSyst.* 12, 1750–1755.
- Jacobs, K., Shoemaker, C., Rudersdorf, R., Neill, S.D., Kaufman, R.J., Mufson, A., Seehra, J., Jones, S.S., Hewick, R., Fritsch, E.F., 1985. Isolation and characterization of genomic and cDNA clones of human erythropoietin. *Nature* 313, 806–810.
- Jelkmann, W., 1992. Erythropoietin: structure, control of production, and function. *Physiol. Rev.* 72, 449–489.
- Jelkmann, W., 2013. Physiology and pharmacology of erythropoietin. *Transfus. Med. Hemother.* 40, 302–309.
- Kessler, C., Greindl, A., Breuer, B., Haberl, U., Rybka, A., Emgenbroich, M., Frank, H.G., Potgens, A.J., 2012. Erythropoietin mimetic compound AGEM400(HES) binds to the same receptor as erythropoietin but displays a different spectrum of activities. *Cytokine* 57, 226–237.
- Konuray, A.O., Fernández-Francos, X., Ramis, X., 2018. Curing kinetics and characterization of dual-curable thiol-acrylate-epoxy thermosets with latent reactivity. *React. Funct. Polym.* 122, 60–67.
- Lai, P.H., Everett, R., Wang, F.F., Arakawa, T., Goldwasser, E., 1986. Structural characterization of human erythropoietin. *J. Biol. Chem.* 261, 3116–3121.
- Lee, D.E., Son, W., Ha, B.J., Oh, M.S., Yoo, O.J., 2006. The prolonged half-lives of new erythropoietin derivatives via peptide addition. *Biochem. Biophys. Res. Commun.* 339, 380–385.
- Lin, F.K., Suggs, S., Lin, C.H., Browne, J.K., Smalling, R., Egrie, J.C., Chen, K.K., Fox, G. M., Martin, F., Stabinsky, Z., 1985. Cloning and expression of the human erythropoietin gene. *Proc. Natl. Acad. Sci.* 82, 7580–7584.
- Lowe, A.B., 2014. Thiol–ene “click” reactions and recent applications in polymer and materials synthesis: a first update. *Polym. Chem.* 5, 4820–4870.
- Madeddu, C., Gramignano, G., Astara, G., Demontis, R., Sanna, E., Atzeni, V., Macciò, A., 2018. Pathogenesis and treatment options of cancer related anemia: perspective for a targeted mechanism-based approach. *Front. Physiol.* 9, 1294.
- Magnusson, A.O., Szekrenyi, A., Joosten, H.J., Finnigan, J., Charnock, S., Fessner, W.D., 2019. NanoDSF as screening tool for enzyme libraries and biotechnology development. *FEBS J.* 286, 184–204.
- Malešević, M., Migge, A., Hertel, T.C., Pietzsch, M., 2015. A fluorescence-based array screen for transglutaminase substrates. *ChemBioChem* 16, 1169–1174.
- Manning, M., Colón, W., 2004. Structural basis of protein kinetic stability: resistance to sodium dodecyl sulfate suggests a central role for rigidity and a bias toward,  $\beta$ -sheet structure. *Biochemistry* 43, 11248–11254.
- Marx, C.K., Hertel, T.C., Pietzsch, M., 2008. Random mutagenesis of a recombinant microbial transglutaminase for the generation of thermostable and heat sensitive variants. *J. Biotechnol.* 136, 156–162.
- Moreno, A., Pitoc, G.A., Ganson, N.J., Layzer, J.M., Hershfield, M.S., Tarantal, A.F., Sullenger, B.A., 2019. Anti-PEG antibodies inhibit the anticoagulant activity of PEGylated aptamers. *Cell Chem. Biol.* 26, 634–644 e3.
- Neises, B., Steglich, W., 1978. Simple method for the esterification of carboxylic acids. *Angew. Chem. Int. Ed. Engl.* 17, 522–524.
- Ohtsuka, T., Sawa, A., Kawabata, R., Nio, N., Motoki, M., 2000. Substrate specificities of microbial transglutaminase for primary amines. *J. Agric. Food Chem.* 48, 6230–6233.
- Paolini, A., Leoni, L., Giannicchi, I., Abbaszadeh, Z., D’Oria, V., Mura, F., Cort, A.D., Masotti, A., 2018. MicroRNAs delivery into human cells grown on 3D-printed PLA scaffolds coated with a novel fluorescent PAMAM dendrimer for biomedical applications. *Sci. Rep.* 8, 13888.
- Pool, C. Formation of novel erythropoietin conjugates using transglutaminase, US Pat. No. 2006/0116322 A1, 2006.
- Rey, F., Balsari, A., Giallongo, T., Ottolenghi, S., Di Giulio, A.M., Samaja, M., Carelli, S., 2019. Erythropoietin as a Neuroprotective Molecule: An Overview of Its Therapeutic Potential in Neurodegenerative Diseases. *ASN neuro* 11, 1759091419871420.
- Santhi, D., Kalaikannan, A., Malairaj, P., Prabhu, S.A., 2017. Application of microbial transglutaminase in meat foods: a review. *Crit. Rev. Food Sci. Nutr.* 57, 2071–2076.
- Santoso, A., Rubiyana, Y., Sk, W., Herawati, N., Wardiana, A., Ningrum, R.A., 2013. Heterologous expression and characterization of human erythropoietin in *pichia pastoris*. *Int. J. Pharm. Biol. Sci.* 4, 187–196.
- Sato, H., 2002. Enzymatic procedure for site-specific pegylation of proteins. *Adv. Drug Deliv. Rev.* 54, 487–504.
- Skibeli, V., Nissen-Lie, G., Torjesen, P., 2001. Sugar profiling proves that human serum erythropoietin differs from recombinant human erythropoietin. *Blood* 98, 3626–3634.
- Spolaore, B., Raboni, S., Satwekar, A.A., Grigoletto, A., Mero, A., Montagner, I.M., Rosato, A., Pasut, G., Fontana, A., 2016. Site-specific transglutaminase-mediated conjugation of interferon  $\alpha$ -2b at glutamine or lysine residues. *Bioconj. Chem.* 27, 2695–2706.
- Strop, P., 2014. Versatility of Microbial Transglutaminase. *Bioconj. Chem.* 25, 855–862.
- Su, D., Zhao, H., Xia, H., 2010. Glycosylation-modified erythropoietin with improved half-life and biological activity. *Int. J. Hematol.* 91, 238–244.
- Sun, J., Martin, J.M., Vanderpoel, V., Sumbria, R.K., 2019. The promises and challenges of erythropoietin for treatment of Alzheimer’s disease. *Neuromol. Med.* 21, 12–24.
- Suresh, S., Rajvanshi, P.K., Noguchi, C.T., 2020. The many facets of erythropoietin physiologic and metabolic response. *Front. Physiol.* 10, 1534.
- Suresh Kumar, T.K., Gopalakrishna, K., Prasad, V.V.H., Pandit, M.W., 1993. Multiple bands on the sodium dodecyl sulfate-polyacrylamide gel electrophoresis gels of proteins due to intermolecular disulfide cross-linking. *Anal. Biochem.* 213, 226–228.
- Taresco, V., Creasey, R.G., Kennon, J., Mantovani, G., Alexander, C., Burley, J.C., Garnett, M.C., 2016. Variation in structure and properties of poly(glycerol adipate) via control of chain branching during enzymatic synthesis. *Polymer* 89, 41–49.

# Microbial Transglutaminase-Mediated Formation of Erythropoietin-Polyester Conjugates

Razan Alaneed <sup>a,b</sup>, Marcel Naumann <sup>c</sup>, Markus Pietzsch <sup>b,\*</sup>, and Jörg Kressler <sup>a,\*</sup>

<sup>a</sup> Department of Chemistry, Martin Luther University Halle-Wittenberg, Von-Danckelmann-Platz 4, D-06099 Halle/Saale, Germany

<sup>b</sup> Department of Pharmacy, Martin Luther University Halle-Wittenberg, Weinbergweg 22, D-06120, Halle/Saale, Germany

<sup>c</sup> Fraunhofer Institute for Cell Therapy and Immunology, Department of Drug Design and Target Validation, Biozentrum, Weinbergweg 22, D-06120 Halle/Saale, Germany

\*Corresponding author: [markus.pietzsch@pharmazie.uni-halle.de](mailto:markus.pietzsch@pharmazie.uni-halle.de); [joerg.kressler@chemie.uni-halle.de](mailto:joerg.kressler@chemie.uni-halle.de)

## Appendix A. Supplementary data

### Table of Contents

Materials and methods	2
Enzymatic synthesis of PDSA	4
Procedure used to determine TG <sup>16</sup> specific activity	4
Figures	
Fig. S1. <sup>1</sup> H NMR spectrum of Rh-labelled PDSA-g-NH <sub>2</sub> .	5
Fig. S2. GPC traces of PDSA before and after modification.	5
Fig. S3. MALDI-TOF mass spectrum acquired from LL-37 before and after modification with MDC by TG <sup>16</sup> .	6
Fig. S4. Fragment spectra acquired from the proteolytic peptides of rHuEPO-MDC.	6
Fig. S5. Fragment spectra acquired from the proteolytic peptides of rHuEPO-MDC.	7
Fig. S6. Fragment spectra acquired from the proteolytic peptides of rHuEPO-MDC.	7
Fig. S7. Fragment spectra acquired from the proteolytic peptides of rHuEPO-MDC.	8
Fig. S8. Sequence coverage for rHuEPO-MDC based on tryptic peptides identified by LC-ESI-LIT and MALDI-TOF/TOF mass spectrometry.	8
Fig. S9. SDS-PAGE analysis of rHuEPO-TG <sup>16</sup> reaction as a control.	9
Fig. S10. SDS-PAGE analysis of MDC-TG <sup>16</sup> reaction as a negative control.	9
Fig. S11. SDS-PAGE analysis of rHuEPO-MDC reaction as a control.	10
Fig. S12. SDS-PAGE analysis of rHuEPO before and after N-deglycosylation.	10
Fig. S13. Molar mass determination of rHuEPO-Rh-labelled PDSA-g-NH <sub>2</sub> conjugates.	11
Supporting references.	11

## Materials and methods

**Materials.** Recombinant human erythropoietin (rHuEPO, CHO cell-derived,  $\geq 90\%$  purity) was obtained from PeproTech GmbH (Hamburg, Germany). Peptide-*N*-glycosidase F (PNGase F) having a concentration of 500,000 U/mL was obtained from New England Biolabs GmbH (Frankfurt am Main, Germany). Glycoprotein denaturing buffer, glycol buffer, and Nonidet P-40 (NP-40) were supplied with PNGase F. Monodansylcadaverine (MDC,  $\geq 97\%$ ), D-sorbitol (98%), *N*-acetyl-L-cysteine methyl ester (Ac-L-Cys ME,  $\geq 90\%$ ), and rhodamine B-isothiocyanate were obtained from Sigma-Aldrich (Steinheim, Germany). Lipase B, commercially known as Novozyme (N435), derived from *Candida antarctica* immobilized on an acrylic resin was purchased from Sigma-Aldrich (St. Louis, MO, USA). Lipase B was dried over phosphorus pentoxide ( $P_2O_5$ ) for 24 h before use. Divinyl adipate (DVA, stabilized with 4-methoxyphenol (MEHQ),  $>99.0\%$ ) was purchased from TCI-Europe. Tris (tris(hydroxymethyl)aminomethane,  $\geq 99.9\%$ ), sodium chloride (NaCl,  $>99.5\%$ ), 4-(dimethylamino)pyridine (DMAP), 1-ethyl-3-(3-dimethylaminopropyl)carbodiimide hydrochloride (EDC·HCl), dimethyl sulfoxide (DMSO, anhydrous), phosphorus pentoxide ( $P_2O_5$ ,  $\geq 99\%$ ), dialysis membranes with a cut-off molar mass of 1000 g mol<sup>-1</sup>, acetic acid (CH<sub>3</sub>COOH, 100%), formaldehyde ( $\geq 37\%$ ), silver nitrate (AgNO<sub>3</sub>,  $\geq 99.9\%$ ), ethanol (Et-OH,  $>99.8\%$ ), methanol (Me-OH,  $>99.8\%$ ), L-glutathione (reduced form,  $\geq 98\%$ ), trichloroacetic acid (TCA,  $>99\%$ ), hydrochloric acid (HCl, 37%), sodium thiosulphate pentahydrate (Na<sub>2</sub>S<sub>2</sub>O<sub>3</sub> · 5 H<sub>2</sub>O,  $\geq 99\%$ ), and sodium carbonate (Na<sub>2</sub>CO<sub>3</sub>,  $\geq 99.5\%$ ) were purchased from Carl Roth (Karlsruhe, Germany). 6-(Fmoc-amino)hexanoic acid (6-(Fmoc-Ahx, 98%) and acetonitrile (ACN, anhydrous, 99.8%) were purchased from Alfa Aesar (Kandel, Germany). *N,N*-dimethylformamide-d<sub>7</sub> (DMF-d<sub>7</sub>, 99.5%) was purchased from Armar Chemicals (Döttingen, Switzerland). Hydroxylammoniumchloride ( $>99\%$ ) and iron (III) chloride (FeCl<sub>3</sub>,  $>99$ ) were obtained from Merck KGaA (Darmstadt, Germany). Carbobenzoxy glutamine glycine (CBZ-Gln-Gly) was purchased from Bachem (Switzerland). *N,N*-dimethylformamide (DMF, extra dry, 99.8 %) was purchased from Acros Organics. HPLC grade solvents like, tetrahydrofuran (THF) and *tert*-butylmethylether (TBME), were purchased from Carl Roth (Karlsruhe, Germany). Solvents for mass spectrometry sample preparation and high-performance liquid chromatography (HPLC) separation (ACN, H<sub>2</sub>O, and formic acid (FA)) were purchased from Biosolve (ULC/MS grade). Trifluoroacetic acid (TFA) was obtained from Merck (spectroscopy grade) and the 2,5-dihydroxybenzoic acid (DHB) matrix for MALDI-TOF/TOF mass spectrometry was from Bruker Daltonics.

## Methods

**Nuclear magnetic resonance (NMR) spectroscopy.** <sup>1</sup>H NMR spectra of all synthesized polymers were recorded on a VNMRs spectrometer 400 MHz (Agilent Technologies) at 27 °C. As an internal standard, tetramethylsilane was used. For all measurements, around 40 mg of polymer was dissolved in 700 μL of DMF-d<sub>7</sub> as deuterated solvent. Chemical shifts (δ) are given in ppm. The NMR spectral data were interpreted using MestRec (v.4.9.9.6) software (Mestrelab Research, Santiago de Compostela, Spain).

**Gel permeation chromatography (GPC).** GPC measurements for PDSA, PDSA-*g*-6-(Fmoc-Ahx), and PDSA-*g*-NH<sub>2</sub> were performed on a Viscotek GPC max VE 2002 using HHRH Guard-17360 and GMHH-N-18055 columns and refractive index detector (VE 3580 RI detector, Viscotek). DMF containing 0.01 M LiBr was used as eluent in a thermostated column kept at 25 °C. The calibration standard for all measurements was poly(methyl methacrylate). For all samples, the concentration was 3 mg mL<sup>-1</sup> and the flow rate was 1 mL min<sup>-1</sup>. For data analysis, Origin 8 software was used.

**Thermal stability studies.** Thermal unfolding study of rHuEPO as well as melting temperature determination was performed with the Prometheus NT.48 nano differential scanning fluorimeter (nanoDSF) (NanoTemper Technologies GmbH, Munich, Germany). Initially, rHuEPO was dissolved in 50 mM Tris buffer (pH = 8) with a final concentration of 500 μg/mL. Then, the capillaries were loaded

with 10  $\mu$ l of protein solution and placed into the instrument. The experiment was carried out at a temperature range of 15 to 95 °C with a heating rate of 1 °C min<sup>-1</sup>. The unfolding process of rHuEPO was monitored by measuring the changes of the intrinsic fluorescence of tryptophan and/or tyrosine residues between emission wavelengths  $\lambda$  330 and 350 nm as a function of temperature. The melting temperature  $T_m$  of rHuEPO was determined from the first derivative of the fluorescence ratio F350/F330. The measurement was done in duplicate. NT PR.ThermControl software was used for data analysis.

**Sodium dodecyl sulfate-polyacrylamide gel electrophoresis (SDS-PAGE).** SDS-PAGE was carried out as previously described by Laemmli.<sup>1</sup> In this method, the separation of proteins under constant electric current is based on the molar mass. Protein-containing samples were separated using 12.5% (w/v) polyacrylamide resolving gel with a 4.5% (w/v) polyacrylamide stacking gel. All samples were mixed in a 1:1 ratio with SDS sample buffer and incubated at 95 °C for 5 min. The sample mixtures were then cooled to room temperature. For molar mass reference, two protein ladders were used, a protein molar mass marker (Fermentas Life Sciences, St. Leon-Rot, Germany) and PageRule Prestained Protein Ladder (Thermo fisher scientific, Germany). 5  $\mu$ L of protein ladder and 10  $\mu$ L of each sample were loaded into the wells of the stacking gel. The electrophoresis was accomplished in two steps. The first electrophoresis run was at 200 V, 100 mA, for 8 min and the second run was at 200 V, 60 mA, for 45 min. Following electrophoresis, the fluorescent bands were visualized under UV light and then all bands were revealed by silver staining following the procedure used by Blum et al.<sup>2</sup> After the electrophoresis run, each gel was fixed in 100 mL of fixing solution (methanol, acetic acid, and formaldehyde) overnight. Thereafter, the gel was washed three times with 50% (v/v) ethanol, sensitized with 100 mL of sensitization solution (0.2 g/L Na<sub>2</sub>S<sub>2</sub>O<sub>3</sub> x 5 H<sub>2</sub>O) for 1 min, and then washed with distilled water. Then, the gel was stained with 100 mL of silver nitrate solution (0.4 g AgNO<sub>3</sub>) containing 150  $\mu$ L formaldehyde (37% (v/v)) for 30 min. After being washed twice with distilled water, the gel was incubated with 100 mL of developing solution (12 g Na<sub>2</sub>CO<sub>3</sub>, formaldehyde (37% (v/v)) and 4 mL of sensitization solution) for 10 min, stopped in 50% (v/v) methanol and 12% (v/v) acetic acid solution, and finally dried.

**Proteolytic digestion.** The protein band containing rHuEPO-MDC was excised from the polyacrylamide gel and destained by repeated incubation in 100 mM ammonium bicarbonate (NH<sub>4</sub>HCO<sub>3</sub>) in H<sub>2</sub>O and 100 mM NH<sub>4</sub>HCO<sub>3</sub> in ACN/H<sub>2</sub>O (500/500; v/v). Disulfide bonds were reduced with 10 mM dithiothreitol (DTT) (45 min at 50 °C) and free cysteine residues were alkylated with 55 mM iodoacetamide (60 min at RT). Trypsin (Gold, MS grade, Promega, Walldorf, Germany) was used for the proteolytic digestion (10 h at 37 °C). Proteolytic peptides were extracted by repeated incubation of the gel band in H<sub>2</sub>O, ACN/H<sub>2</sub>O/TFA (500/450/50; v/v/v) and neat ACN. The obtained extract was concentrated by rotational vacuum concentration and proteolytic peptides were purified by solid-phases extraction using a polytetrafluoroethylene (PTFE)-based C18 material (Sigma-Aldrich, St. Louis, USA). Elution of proteolytic peptides was carried out with 10  $\mu$ l of either ACN/H<sub>2</sub>O/FA (675/325/1; v/v/v) for LC-MS/MS analysis or ACN/H<sub>2</sub>O/TFA (750/250/1; v/v/v) for MALDI-TOF/TOF analysis.

**Matrix-assisted laser desorption/ionization time-of-flight/time-of-flight mass spectrometry (MALDI-TOF/TOF MS).** Proteolytic peptides were co-crystallized on a MALDI ground steel target with DHB matrix. Mass spectra were acquired on a MALDI-TOF/TOF mass spectrometer (Autoflex Speed, Bruker Daltonics, Bremen, Germany) with positive polarity in reflector mode using a Nd:YAG laser (Smart beam-II) with a pulse rate of 1 kHz and an emission wavelength of 355 nm. Spectra were recorded using flexControl (version 3.4) by accumulation of at least 10000 shots (per sample spot). Mass spectra were processed with flexAnalysis (version 3.4) by applying baseline subtraction with TopHat algorithm and peak detection with SNAP algorithm. Data analysis was carried out with PEAKS Studio (version 7.5, Bioinformatics Solutions Inc., Waterloo, Canada) using the human sequences of the UniProt/SwissProt database (release 2020\_04). The database search was performed using the following

mass tolerances: 25.0 ppm for MS and 0.5 Da for MS/MS. In a mass spectrum, the y-axis represents the abundance of ions or peak intensity and the x-axis represents the mass-to-charge ratio of the ions ( $m/z$ ).

**Liquid chromatography-electrospray-linear ion trap-tandem mass spectrometry (LC-ESI-LIT MS).** Proteolytic peptides were separated by liquid chromatography on a HPLC system (Agilent HP 1260 Infinity, Waldbronn, Germany) coupled to a hybrid Triple-Quadrupole/Linear Ion Trap (LIT) mass spectrometer (4000 QTRAP, Sciex, Darmstadt, Germany) which was controlled by Analyst (version 1.6.2). Chromatographic separations were carried out at 40 °C on a AdvanceBio Peptide Mapping column (Agilent, Waldbronn, Germany) with a C18 stationary phase (150 mm x 2.1 mm column dimension, 2.7  $\mu\text{m}$  particle size, 120 Å pore size) using a 45 min linear gradient from 3 % to 100 % of mobile phase B (ACN/FA (1000/1; v/v)) at 0.4 ml/min. The flow was directed to the ESI source (Turbo V, Sciex, Darmstadt, Germany) and peptide ions were generated in positive polarity. Mass spectra were acquired in three measurement modes: Enhanced MS (EMS), Enhanced Resolution (ER) and Enhanced Product Ion (EPI). Data analysis was carried out with PEAKS Studio (version 7.5) using the human sequences of the UniProt/SwissProt database (release 2020\_04). The database search was performed using the following mass tolerances: 150.0 ppm for MS and 0.15 Da for MS/MS.

**Enzymatic synthesis of PDSA.** Briefly, a mixture of D-sorbitol (10 g, 54.9 mmol) and an equimolar amount of divinyl adipate (10.9 g, 54.9 mmol), with respect to primary OH groups and vinyl end groups, were charged in a 250 mL three-neck round-bottom flask equipped with an overhead mechanical stirrer and a reflux condenser containing a  $\text{CaCl}_2$  tube at its outlet. Afterwards, 40 mL of acetonitrile was added to the reaction flask and the solution mixture was stirred at 50 °C for 30 min. Then, CAL-B (2.1 g, 10 wt% of total mass of monomers) was added to start the reaction. After 92 h, the reaction was quenched by the removal of enzyme beads after being diluted with 20 mL DMF. After collecting the filtrate, the solution was dialyzed against water to remove oligomers using a membrane with a cut-off molar mass of 1000  $\text{g mol}^{-1}$ .  $^1\text{H NMR}$  (400 MHz,  $\text{DMF-d}_7$ )  $\delta$  (ppm): 4.98–4.62 (m, 2H), 4.57–4.29 (m, 2H), 4.27–3.84 (m, 3H), 3.68 (d,  $J = 49$  Hz, 2H), 3.58–3.32 (m, 2H), 2.37–2.17 (m, 4H), 1.63–1.41 (m, 4H).

**Procedure used to determine  $\text{TG}^{16}$  specific activity.** Briefly, the  $\text{TG}^{16}$  precipitate was solubilized in 500  $\mu\text{L}$  of 50 mM Tris buffer + 300 mM NaCl (pH = 8) for 30 min on ice. After 5 min centrifugation at 16,000 g, the supernatant was collected to start the colorimetric assay. 90  $\mu\text{L}$  of substrate mixture containing 100 mM hydroxylamine, 10 mM reduced glutathione, and 30 mM N-CBZ-Gln-Gly in Tris buffer (pH = 6) was incubated at 37 °C for 3 min. To start the reaction, 50  $\mu\text{L}$  of  $\text{TG}^{16}$  solution was added. After 10 min incubation at 37 °C in thermomixer, the reaction was stopped with stop solution (consisting of  $\text{FeCl}_3$ , TCA, and HCl). After centrifugation for 5 min at 16,000 g, the supernatant was collected and the absorption was measured at 525 nm using microtiter plate reader (FluoStar, BMG Labtech GmbH, Offenburg, Germany). One unit of  $\text{TG}^{16}$  can form one micromole of L-glutamic acid  $\gamma$ -monohydroxamate per min at 37 °C.<sup>3</sup>

## Figures

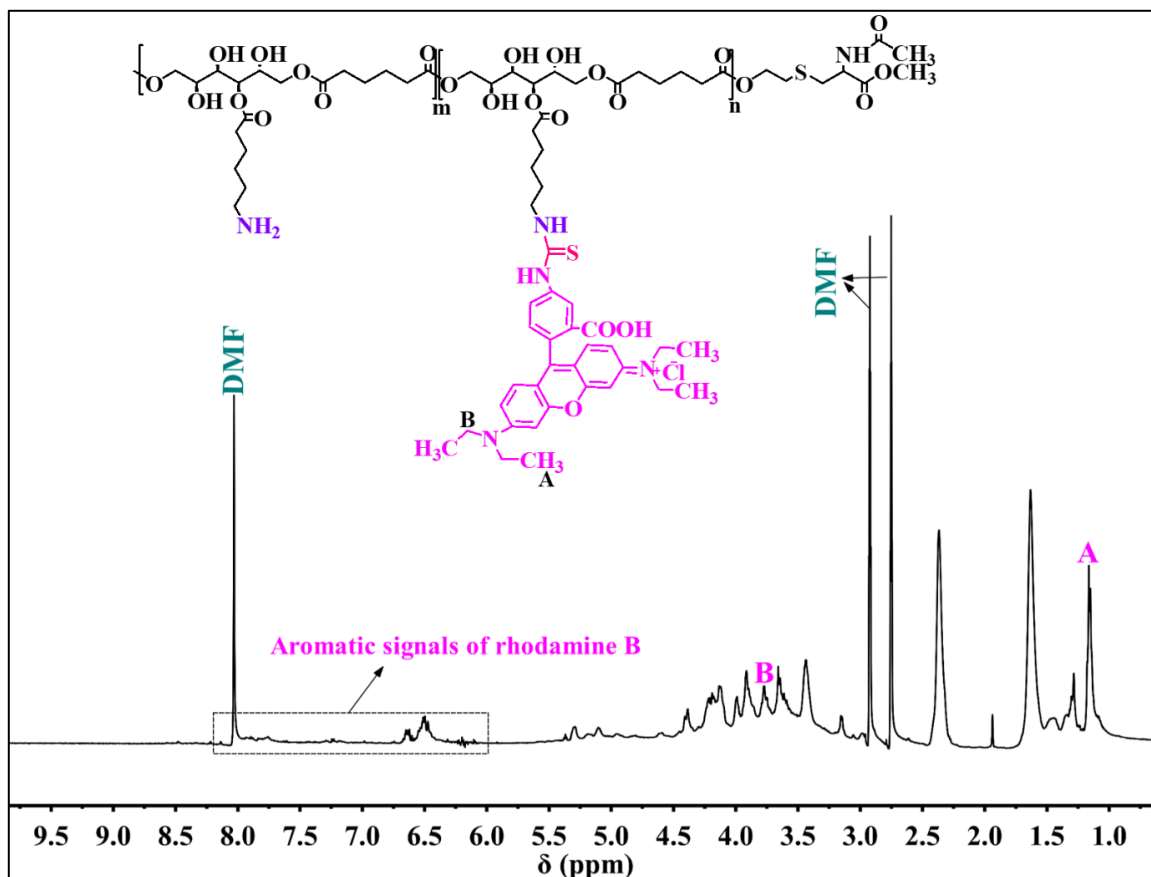


**Fig. S1.**  $^1\text{H}$  NMR spectrum of Rh-labelled PDSA-g-NH<sub>2</sub>, recorded at 27 °C, 400 MHz, using DMF-d<sub>7</sub> as solvent.

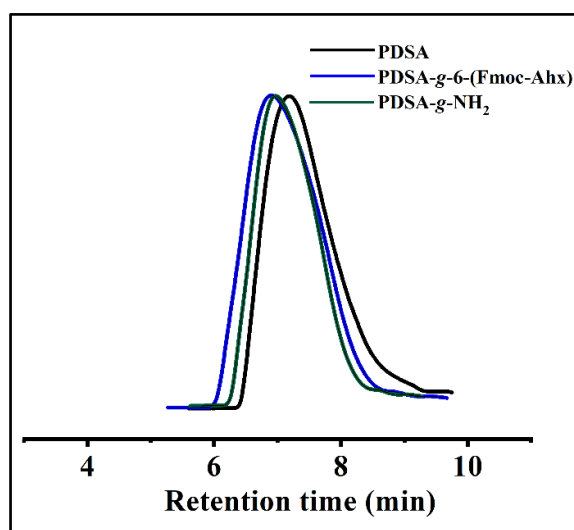


**Fig. S2.** GPC traces of PDSA before and after modification in DMF + 0.01 M LiBr at RT. Poly(methyl methacrylate) (PMMA) was used as a calibration standard for data evaluation.

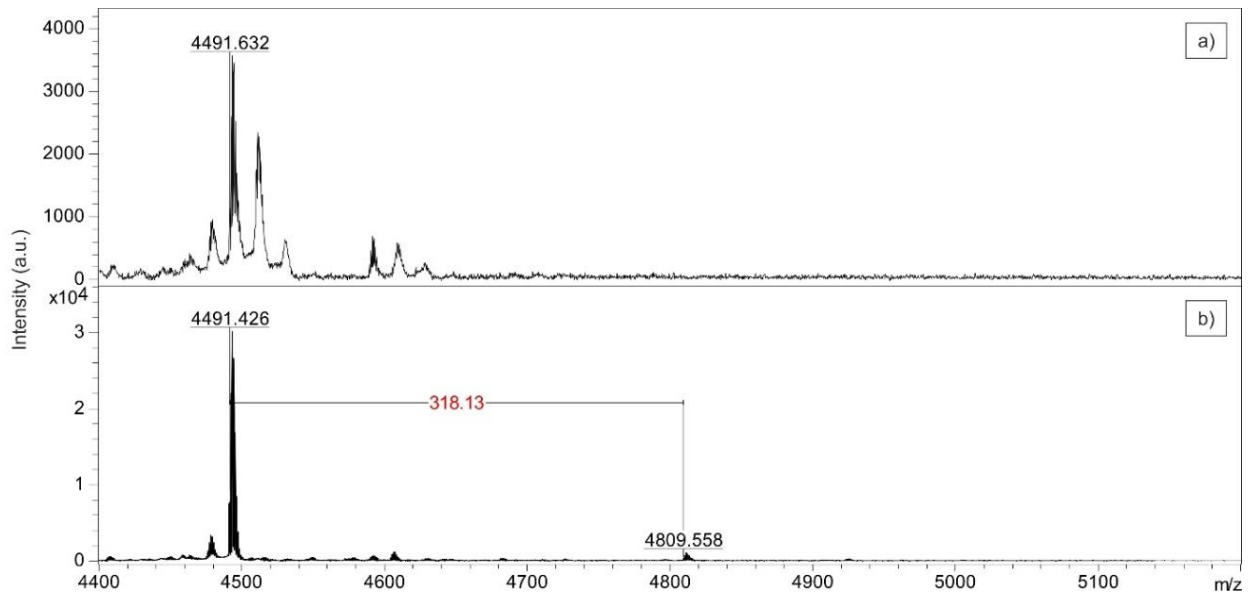


**Fig. S3.** MALDI-TOF mass spectrum acquired from LL-37 before (a) and after (b) modification with MDC by TG<sup>16</sup>. The corresponding mass shift of +318.13 Da belongs to the molar mass of MDC subtracted by the molar mass of ammonia.

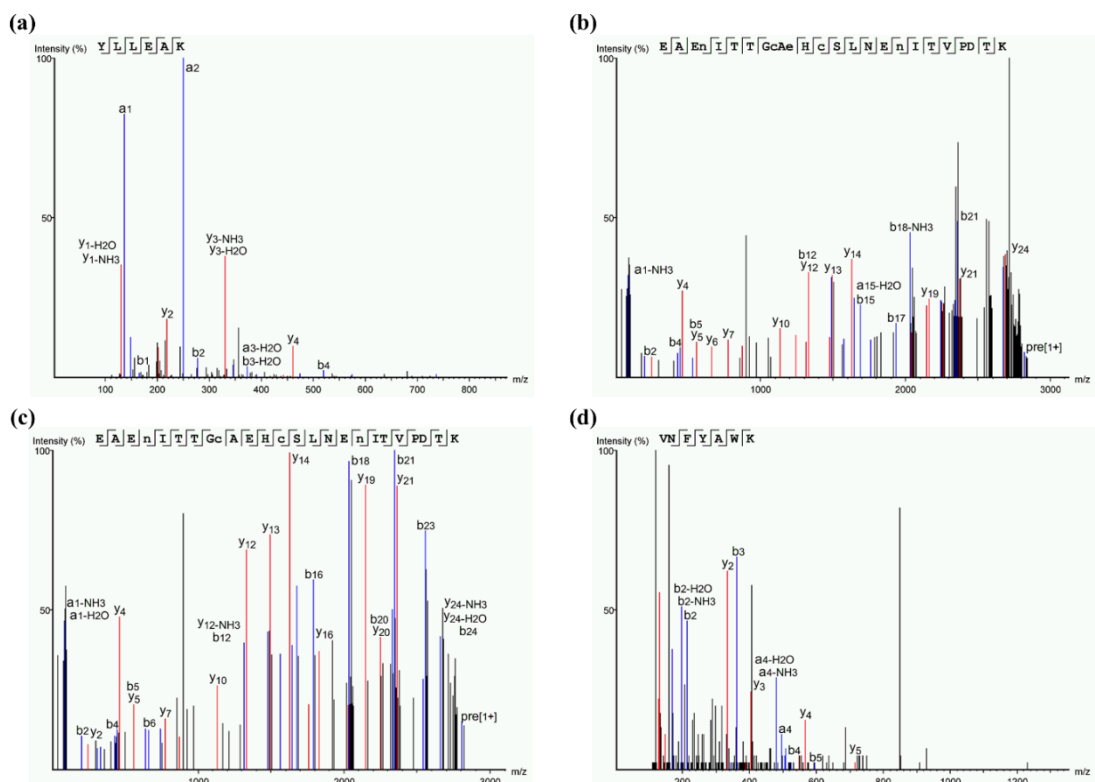


**Fig. S4.** Fragment spectrum acquired with (a) ESI-MS/MS from the peptide precursor ion with  $m/z = 736.4512$  ( $z = 1$ , amino acids 15-20 of rHuEPO-MDC), (b) MALDI-MS/MS from the peptide precursor ion with  $m/z = 2819.2278$  ( $z = 1$ , amino acids 21-45 of rHuEPO-MDC), (c) MALDI-MS/MS from the peptide precursor ion with  $m/z = 2805.2188$  ( $z = 1$ , amino acids 21-45 of rHuEPO-MDC), and (d) ESI-MS/MS from the peptide precursor ion with  $m/z = 927.4894$  ( $z = 1$ , amino acids 46-52 of rHuEPO-MDC).

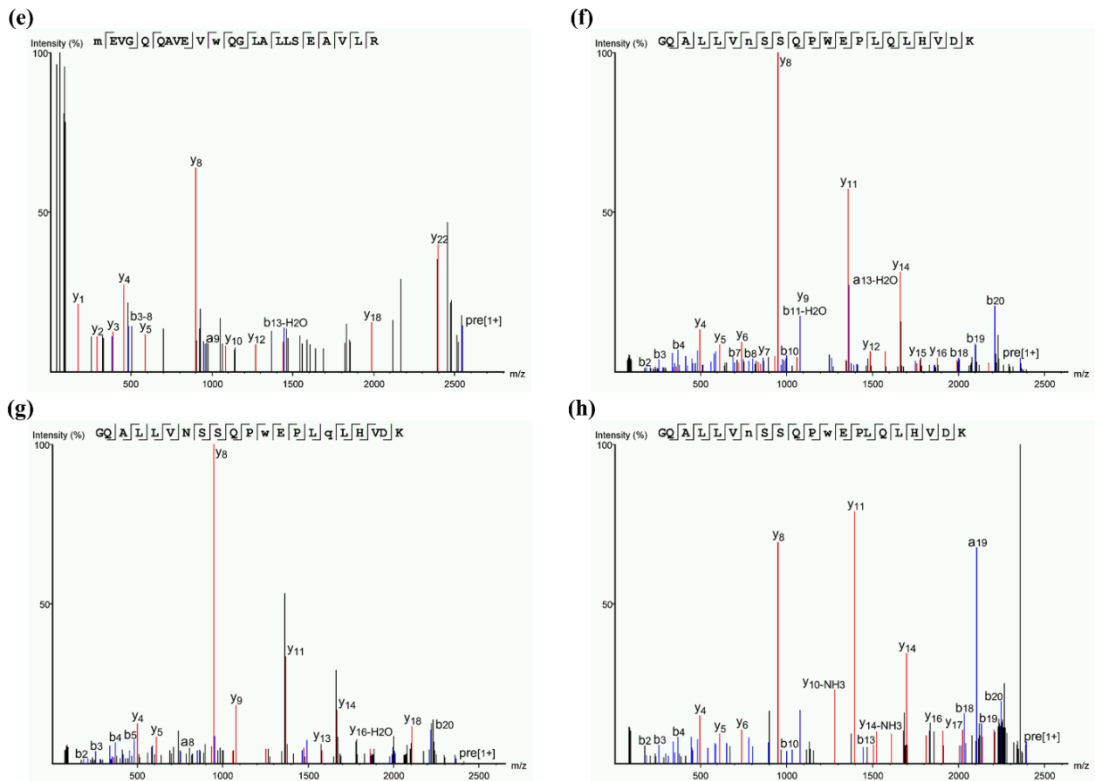


**Fig. S5.** Fragment spectrum acquired with (e) MALDI-MS/MS from the peptide precursor ion with  $m/z = 2546.3340$  ( $z = 1$ , amino acids 54-76 of rHuEPO-MDC), (f) MALDI-MS/MS from the peptide precursor ion with  $m/z = 2360.2288$  ( $z = 1$ , amino acids 77-97 of rHuEPO-MDC), (g) MALDI-MS/MS from the peptide precursor ion with  $m/z = 2364.2214$  ( $z = 1$ , amino acids 77-97 of rHuEPO-MDC), and (h) MALDI-MS/MS from the peptide precursor ion with  $m/z = 2392.2156$  ( $z = 1$ , amino acids 77-97 of rHuEPO-MDC).

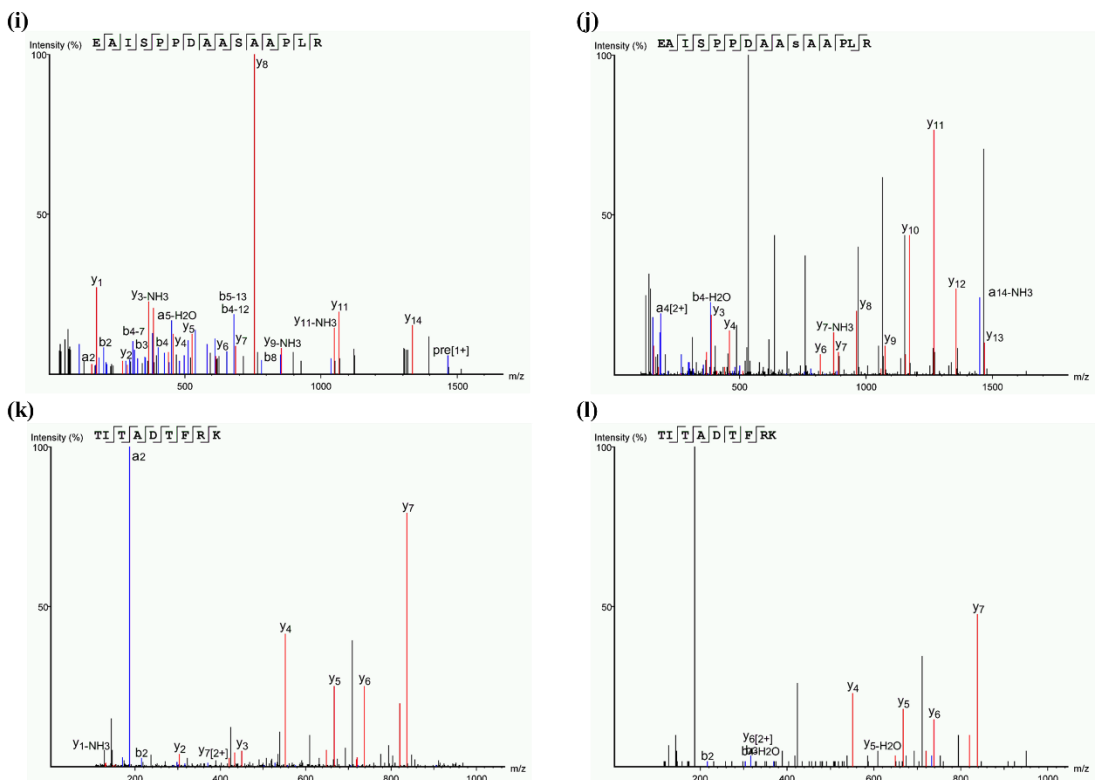


**Fig. S6.** Fragment spectrum acquired with (i) MALDI-MS/MS from the peptide precursor ion with  $m/z = 1465.7655$  ( $z = 1$ , amino acids 117-131 of rHuEPO-MDC), (j) ESI-MS/MS from the peptide precursor ion with  $m/z = 835.0251$  ( $z = 2$ , amino acids 117-131 of rHuEPO-MDC), (k) ESI-MS/MS from the peptide precursor ion with  $m/z = 526.8331$  ( $z = 2$ , amino acids 132-140 of rHuEPO-MDC), and (l) ESI-MS/MS from the peptide precursor ion with  $m/z = 526.8470$  ( $z = 2$ , amino acids 132-140 of rHuEPO-MDC).

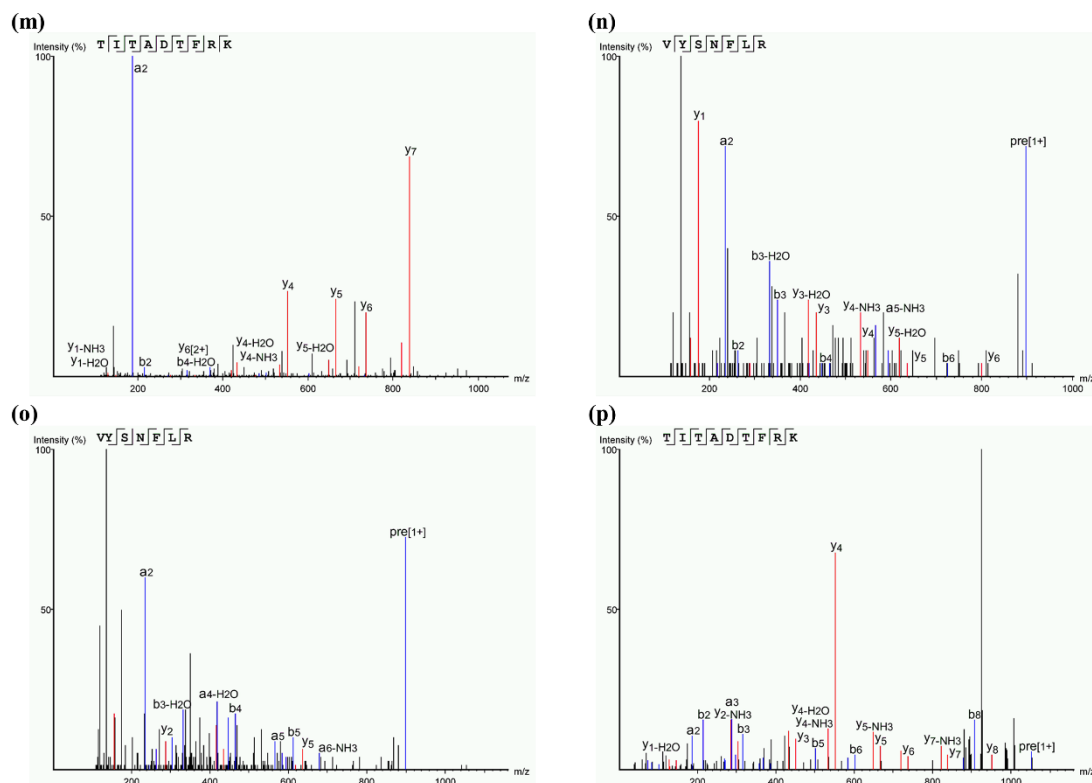


**Fig. S7.** Fragment spectrum acquired with (m) ESI-MS/MS from the peptide precursor ion with  $m/z = 526.8358$  ( $z = 2$ , amino acids 132-140 of rHuEPO-MDC), (n) ESI-MS/MS from the peptide precursor ion with  $m/z = 898.5221$  ( $z = 1$ , amino acids 144-150 of rHuEPO-MDC), (o) ESI-MS/MS from the peptide precursor ion with  $m/z = 898.4977$  ( $z = 1$ , amino acids 144-150 of rHuEPO-MDC), and (p) MALDI-MS/MS from the peptide precursor ion with  $m/z = 1052.5685$  ( $z = 1$ , amino acids 132-140 of rHuEPO-MDC).

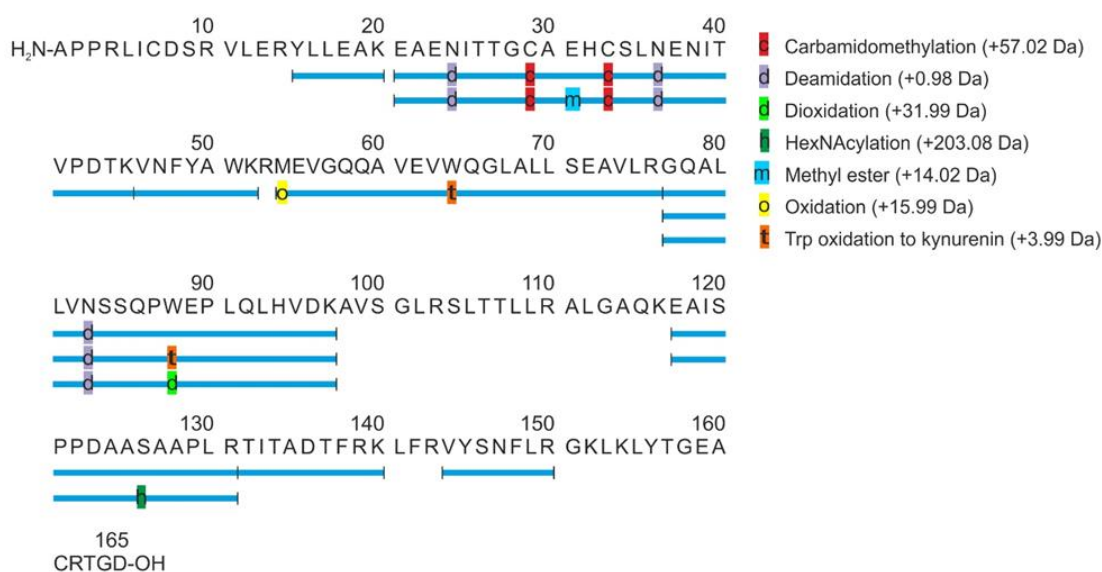


**Fig. S8.** Sequence coverage for rHuEPO-MDC based on tryptic peptides identified by LC-ESI-LIT and MALDI-TOF/TOF mass spectrometry.

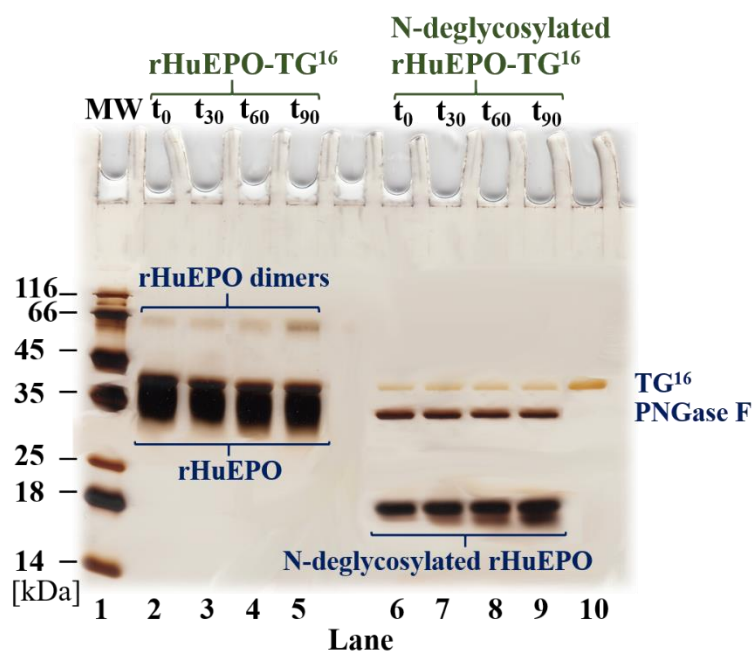


**Fig. S9.** SDS-PAGE image for the rHuEPO-TG<sup>16</sup> reaction as a control. The reaction temperature was 54 °C. Lane 1: MW marker, Lane 2-5: rHuEPO + TG<sup>16</sup> at (t<sub>0</sub>), (t<sub>30</sub>), (t<sub>60</sub>), and (t<sub>90</sub>) respectively, Lane 6-9: rHuEPO + TG<sup>16</sup> after treatment with PNGase F at (t<sub>0</sub>), (t<sub>30</sub>), (t<sub>60</sub>), and (t<sub>90</sub>) respectively, Lane 10: TG<sup>16</sup> (with higher concentration than in the reaction mixture). It is obviously noticed that the band intensity of rHuEPO dimers is increased with increasing reaction time. After N-deglycosylation, the rHuEPO dimers band disappeared as the concentration is reduced after treatment with PNGase F.

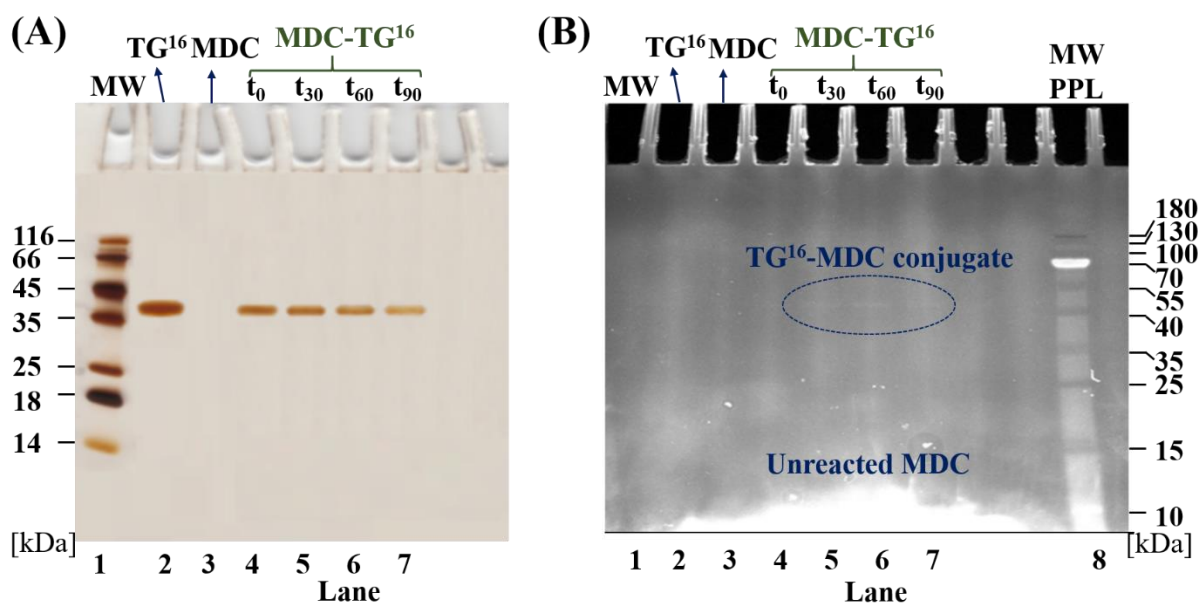


**Fig. S10.** (A) SDS-PAGE image for the MDC-TG<sup>16</sup> reaction as a negative control and (B) fluorescent visualization of the SDS-PAGE under UV light. The reaction temperature was 54 °C. Lane 1: MW marker, Lane 2: TG<sup>16</sup> (with higher concentration than in the reaction mixture), Lane 3: MDC, Lane 4-7:

MDC + TG<sup>16</sup> (t<sub>0</sub>), (t<sub>30</sub>), (t<sub>60</sub>), and (t<sub>90</sub>) respectively, Lane 8: prestained PPL protein marker (shown only in the fluorescent image (B)). The fluorescent image shows very faint fluorescence after 30, 60, and 90 min at the molar mass of TG<sup>16</sup>. Here, the TG<sup>16</sup> band intensity is observed to decrease with the reaction time as the low modification with MDC can change the interaction with silver as well as the presence of proteinase K traces can be activated on SDS at high temperature.

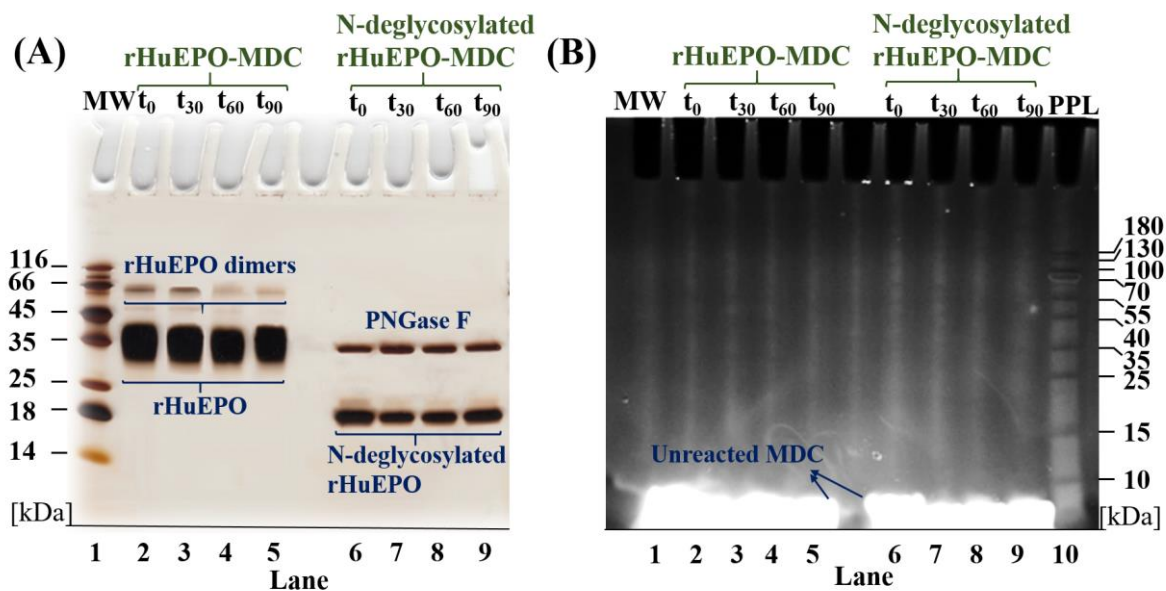


**Fig. S11.** (A) SDS-PAGE image for the rHuEPO-MDC reaction as a control and (B) fluorescent visualization of the SDS-PAGE under UV light. The reaction temperature was 54 °C. Lane 1: MW marker, Lane 2-5: rHuEPO-MDC (t<sub>0</sub>), (t<sub>30</sub>), (t<sub>60</sub>), and (t<sub>90</sub>) respectively, Lane 6-9: rHuEPO-MDC after treatment with PNGase F at (t<sub>0</sub>), (t<sub>30</sub>), (t<sub>60</sub>), and (t<sub>90</sub>) respectively, Lane 10: prestained PPL protein marker (shown only in the fluorescent image (B)). The fluorescent image shows no fluorescent bands at the molar mass of rHuEPO. Here, the band intensity of rHuEPO dimers is high before incubation (lane 2) and after incubation (lane 3) due to oxidation reaction upon storage.<sup>4</sup> After N-deglycosylation, the rHuEPO dimers band disappeared as the concentration is reduced after treatment with PNGase F.

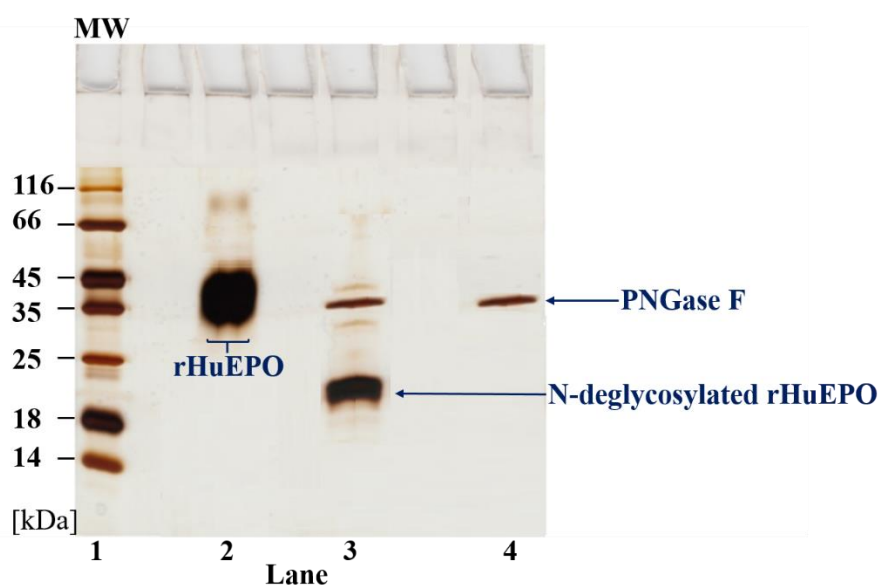


**Fig. S12.** SDS-PAGE image for rHuEPO and rHuEPO after N-deglycosylation at 37 °C. Lane 1: MW marker, Lane 2: rHuEPO (the concentration is 500 µg/mL), Lane 3: rHuEPO + PNGase F, Lane 4: PNGase F.

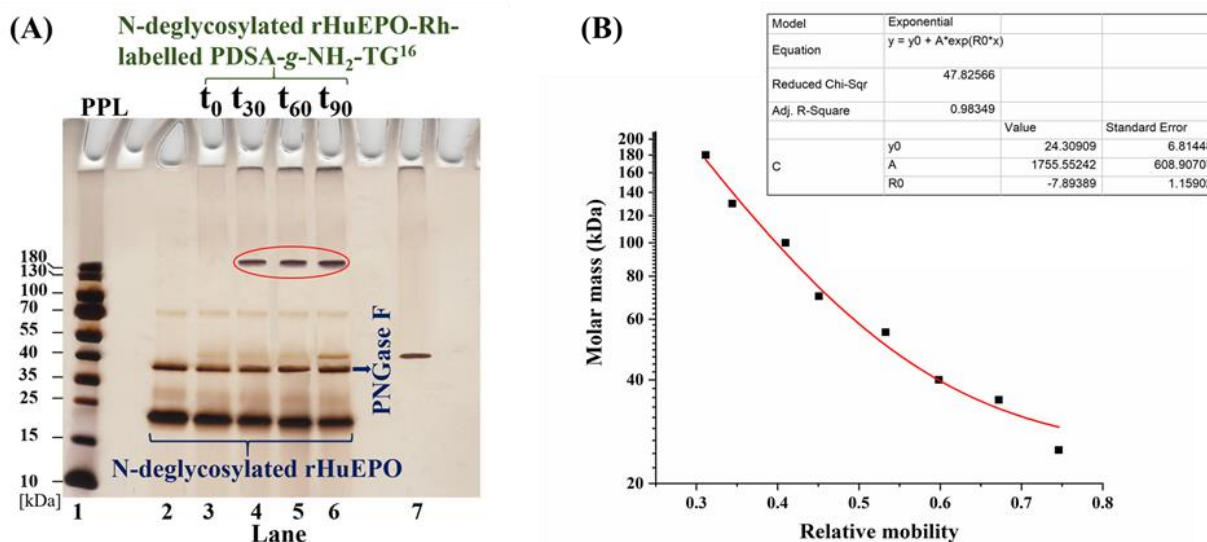


**Fig. S13.** (A) SDS-PAGE image showing silver staining for rHuEPO-Rh-labelled PDSA-g-NH<sub>2</sub> conjugation after treatment with PNGase F, Lane 1: prestained marker, Lane 2: rHuEPO + Rh-labelled PDSA-g-NH<sub>2</sub>, Lane 3-6: rHuEPO + Rh-labelled PDSA-g-NH<sub>2</sub> + TG<sup>16</sup> ( $t_0$ ), ( $t_{30}$ ), ( $t_{60}$ ), and ( $t_{90}$ ), respectively, Lane 7: Rh-labelled PDSA-g-NH<sub>2</sub> + TG<sup>16</sup> incubated for 60 min. The red circle indicates the rHuEPO-Rh-labelled PDSA-g-NH<sub>2</sub> conjugates, (B) Molar mass determination of these conjugates by a calibration curve fitted with exponential function. The curve was made using the molar masses of the protein marker PPL and their relative mobility (calculated as the distance traveled by the bands from the top of the gel divided by the distance migrated by the dye front).

### Supporting references

1. Laemmli, U. K. (1970) Cleavage of structural proteins during the assembly of the head of bacteriophage T4. *Nature* 227, 680-685.
2. Blum, H., Beier, H., and Gross, H. J. (1987) Improved silver staining of plant proteins, RNA and DNA in polyacrylamide gels. *Electrophoresis* 8, 93-99.
3. Folk, J. E. (1969) Mechanism of Action of Guinea Pig Liver Transglutaminase: VI. Order of substrate addition. *J. Biol. Chem.* 244, 3707-3713.
4. Grassi, L., and Cabrele, C. (2019) Susceptibility of protein therapeutics to spontaneous chemical modifications by oxidation, cyclization, and elimination reactions. *Amino Acids* 51, 1409-1431.

### 3.3 Paper III:

#### **Network formation by aza-Michael addition of primary amines to vinyl end groups of enzymatically synthesized poly(glycerol adipate)<sup>3</sup>**

Great attention has been drawn to the use of hydrophilic polymeric networks due to their significant industrial and biomedical applications. In particular, networks based on biodegradable and biocompatible polyesters have been widely explored in the biomedical field especially, as drug delivery carriers that can provide controlled drug release. In order to achieve these polymeric networks, several approaches have been developed. Among them, Michael addition chemistry has been a special focus since it affords mild reaction conditions, high selectivity, high product yields, and lack of by-products.

In the following publication, an efficient strategy for the synthesis of polymeric networks *via* aza-Michael addition of primary amines to  $\alpha,\beta$ -unsaturated (vinyl) end groups of enzymatically synthesized PGA is investigated. PGA is terminated with some vinyl end groups which represent suitable acceptors for aza-Michael addition reactions. In the next synthesis step, PGA was modified with amine-functionalized side chains to undergo further reaction with its vinyl end groups under catalyst-free conditions and finally form hydrophilic PGA-based networks with potential biomedical applications. Different techniques like GPC, FTIR, <sup>1</sup>H NMR and <sup>13</sup>C NMR spectroscopy, and HR MALDI-TOF mass spectrometry were used to characterize PGA before and after modification. <sup>13</sup>C SP MAS NMR relaxation studies as well as FTIR spectroscopy were used to confirm the aza-Michael addition reaction and network formation. An investigation of the network structure and free dangling chain ends was accomplished by <sup>1</sup>H DQ NMR spectroscopy.

The author contributions of the following article are: R. Alaneed and J. Kressler designed research. R. Alaneed performed the experiments, wrote the original draft, and made the final version. Y. Golitsyn carried out the solid state NMR experiments and analyzed the NMR data. D. Reichert discussed the NMR results. T. Hauenschild performed and analyzed the HR MALDI-TOF measurements. M. Pietzsch, D. Reichert and J. Kressler conceptualized the work, supervised and complemented the writing, editing and finalization of manuscript.

---

<sup>3</sup>The following article [R. Alaneed et al., Polym. Int., **70**, 135-144 (2021)] is an open access article under Wiley Creative Commons Attributions 4.0 International License (CC BY-NC-ND 4.0), which permits use and distribution of the article in any medium for non-commercial purposes. The link to the article on the publisher's website is: <https://onlinelibrary.wiley.com/doi/10.1002/pi.6102>. No changes were made.

# Network formation by aza-Michael addition of primary amines to vinyl end groups of enzymatically synthesized poly(glycerol adipate)

Razan Alaneed,<sup>a,c</sup> Yury Golitsyn,<sup>b</sup> Till Hauenschild,<sup>a</sup> Markus Pietzsch,<sup>c</sup> Detlef Reichert<sup>b</sup> and Jörg Kressler<sup>a\*</sup>



## Abstract

A highly efficient approach for the synthesis of polyester-based networks via aza-Michael addition of primary amines to  $\alpha,\beta$ -unsaturated (vinyl) end groups of poly(glycerol adipate) (PGA) was achieved. By acylation of PGA with 6-(Fmoc-amino)hexanoic acid side chains via Steglich esterification, protected amine-functionalized PGA was obtained. This was followed by the removal of fluorenylmethyloxycarbonyl (Fmoc) protecting groups and the synthesis of PGA-based networks under catalyst-free conditions. The successful conjugate addition of primary amines to vinyl end groups and network formation were confirmed using  $^{13}\text{C}$  magic angle spinning NMR and Fourier transform infrared spectroscopy. Network heterogeneity and defects were quantitatively investigated using  $^1\text{H}$  double-quantum NMR spectroscopy. Finally, a hydrogel was prepared with potential biomedical applications.

Supporting information may be found in the online version of this article.

**Keywords:** poly(glycerol adipate); vinyl end groups; aza-Michael addition; network synthesis; gels

## INTRODUCTION

Polymer networks belong to an important class of polymeric materials with a broad range of industrial and biomedical applications. By definition, polymer networks are three-dimensional structures that can be formed by crosslinking of polymer chains, by either chemical or physical crosslinks.<sup>1-3</sup> Hydrophilic polymer networks can form hydrogels with tunable water uptake capacity. They have been used and developed for various biological and biomedical purposes.<sup>4-6</sup> Specifically, biodegradable and biocompatible hydrogel systems have attracted considerable interest for their use in drug delivery, as they offer a convenient controlled drug release. Therefore, it is advantageous to use biodegradable polymer backbones in the preparation of hydrogels.<sup>7</sup> Among these biodegradable polymers, aliphatic polyesters are receiving significant attention due to their biodegradability and biocompatibility that make them favorable candidates for drug delivery systems.<sup>8-10</sup> The traditional synthetic pathways for the production of polyesters use metal-based catalysts. Under these conditions, the residual metals from the catalyst used are hard to remove, which may have harmful effects on the environment as well as the resulting polyesters with metallic traces being not suitable for biomedical use due to their potential toxicity.<sup>11-13</sup> Hence, *in vitro* synthesis of polyesters through enzymatic polymerization in organic media has been extensively developed as an important

alternative to the conventional polycondensation or ring-opening polymerization because of the high catalytic activity and high selectivity of the enzymes under mild reaction conditions.<sup>14</sup> Aliphatic functional polyester synthesis using enzymes as biocatalysts is promising for environmentally benign synthesis of polymeric materials.<sup>15</sup> In this regard, the most widely used enzyme is lipase B derived from *Candida antarctica* (CAL-B). CAL-B shows high regioselectivity towards primary hydroxyl groups rather than secondary ones.<sup>16</sup> Thus, linear polyesters can be synthesized having pendant OH groups on their backbones, which renders these polymers hydrophilic. Poly(glycerol adipate) (PGA) is a well-established, hydrophilic polyester with one pendant free OH group per repeat unit. It is generally produced from

\* Correspondence to: J Kressler, Department of Chemistry, Martin Luther University Halle-Wittenberg, D-06099 Halle (Saale), Germany. E-mail: joerg.kressler@chemie.uni-halle.de

<sup>a</sup> Department of Chemistry, Martin Luther University Halle-Wittenberg, Halle (Saale), Germany

<sup>b</sup> Department of Physics, Martin Luther University Halle-Wittenberg, Halle (Saale), Germany

<sup>c</sup> Department of Pharmaceutical Technology and Biopharmacy, Institute of Pharmacy, Martin Luther University Halle-Wittenberg, Halle (Saale), Germany

enzymatic transesterification reaction between glycerol and either dimethyl adipate or divinyl adipate. PGA has been widely investigated in the field of drug delivery.<sup>17–19</sup> Likewise, our group has reported a modified PGA, which was synthesized from activated vinyl ester monomers with various fatty acids to produce amphiphilic PGA useful for nanoparticle formation.<sup>20</sup> Recently, the conjugation between dimethylcasein and amine-functionalized PGA using microbial transglutaminase was reported.<sup>21</sup>

In the work reported in this paper, we focused on the development of an efficient strategy for the synthesis of biodegradable and biocompatible networks. Initially, we synthesized PGA with well-defined vinyl end groups. Then, 6-(Fmoc-amino)hexanoic acid (6-(Fmoc-Ahx)) side chains were introduced to the PGA backbone to produce PGA-*g*-6-(Fmoc-amino)hexanoate (PGA-*g*-6-(Fmoc-Ahx)). The use of Fmoc (fluorenylmethyloxycarbonyl) as a protecting group is crucial in order to achieve well-defined networks in the final synthesis step. The Fmoc protecting groups were subsequently removed and the synthesis of networks based on PGA was achieved via aza-Michael addition reaction of primary nucleophilic amines to the vinyl end groups of the PGA backbone. This method is simple and works efficiently under mild conditions and without using any catalyst. The chemical structures were analyzed using Fourier transform infrared (FTIR), <sup>1</sup>H NMR and <sup>13</sup>C NMR spectroscopies. Gel permeation chromatography (GPC) and high-resolution matrix-assisted laser desorption ionization time-of-flight (HR MALDI-TOF) mass spectrometry were performed in order to determine the molar mass and polydispersity index. Special focus was given to the quantitative determination of vinyl end groups using <sup>13</sup>C NMR spectroscopy and HR MALDI-TOF mass spectrometry. Michael addition reaction was followed via the complete disappearance of vinyl end groups after network formation as estimated based on FTIR and <sup>13</sup>C single pulse (SP) magic angle spinning (MAS) NMR spectroscopic data. For the characterization of the network structure and free dangling chain ends, <sup>1</sup>H double-quantum (DQ) NMR spectroscopy was employed. Finally, a hydrogel with potential biomedical applications was synthesized.

## EXPERIMENTAL

### Materials

CAL-B immobilized on an acrylic resin (Sigma-Aldrich, St Louis, MO, USA), commercially known as Novozyme (N435), was dried over phosphorus pentoxide (P<sub>2</sub>O<sub>5</sub>) at 4 °C for 24 h prior to use. 6-(Fmoc-Ahx) (98%) was purchased from Alfa Aesar (Kandel, Germany). Divinyl adipate (DVA; stabilized with 4-methoxyphenol, >99.0%) was purchased from TCI-Europe. Tetrahydrofuran (THF; anhydrous, 99.5%) and dichloromethane (DCM; anhydrous, 99.9%) were purchased from Acros Organics (Schwerte, Germany). P<sub>2</sub>O<sub>5</sub> (≥99%), 4-(dimethylamino)pyridine (DMAP), 1-ethyl-3-(3-dimethylaminopropyl)carbodiimide hydrochloride (EDC-HCl), silica gel (SiO<sub>2</sub>; 0.03–0.2 mm), dimethylsulfoxide (DMSO)-*d*<sub>6</sub> (99.8%) and CDCl<sub>3</sub> (99.8%) were purchased from Carl Roth (Karlsruhe, Germany). Glycerol (≥99.5%), deuterium oxide (D<sub>2</sub>O; 99.9%) and anhydrous DMSO were obtained from Sigma-Aldrich (Steinheim, Germany). All chemicals were used as received without further purification. All HPLC-grade solvents like THF, ethyl acetate, *tert*-butylmethyl ether, diethyl ether and acetone were purchased from Carl Roth (Karlsruhe, Germany).

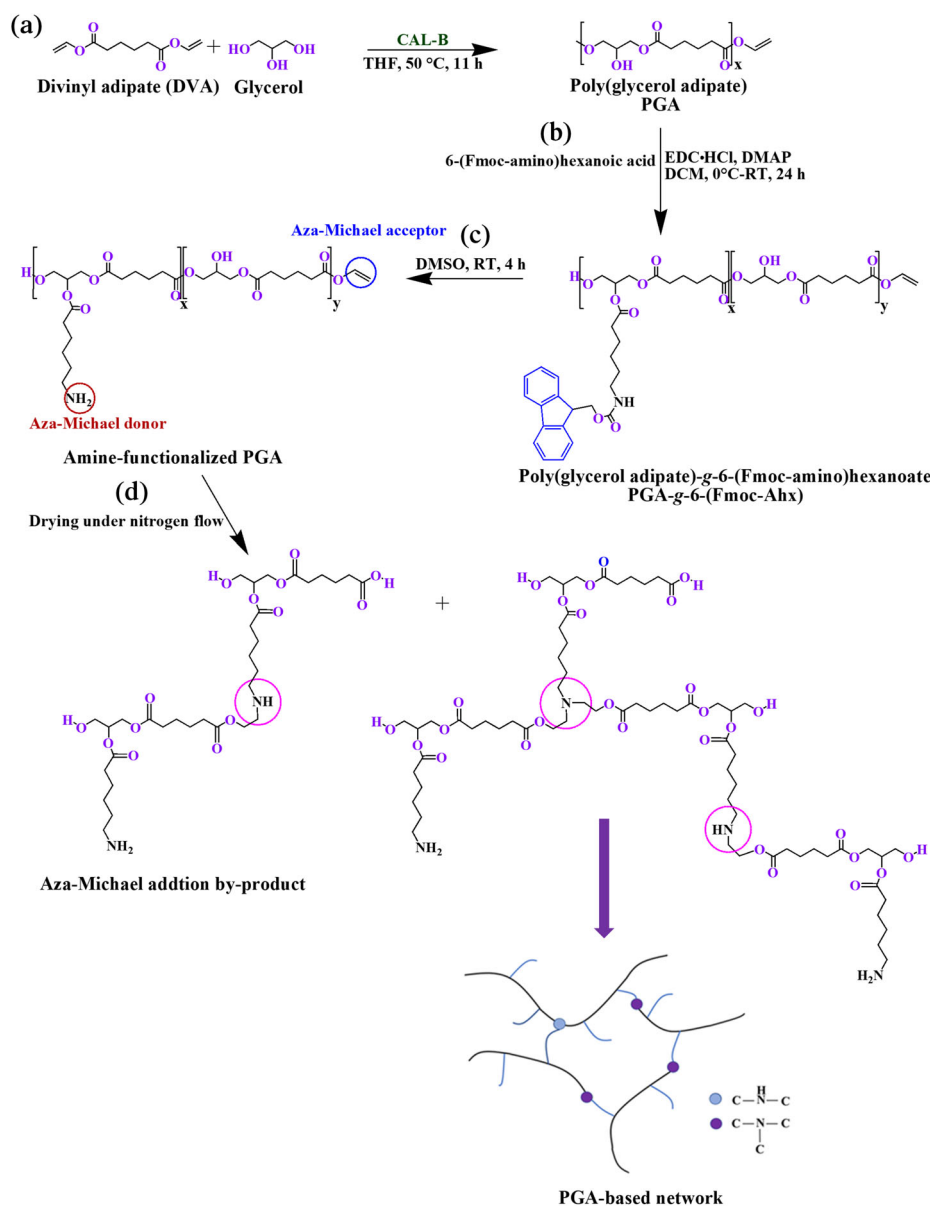
### Synthesis of PGA

PGA backbone was synthesized following the same procedure described by Kallinteri et al.<sup>17</sup> as shown in Scheme 1(A). Glycerol

and DVA were used in equimolar amounts in the presence of CAL-B. The amounts used for this reaction were as follows: glycerol (11 g, 120 mmol), DVA (23.8 g, 120 mmol), 23 mL of anhydrous THF and Novozyme (N435) (0.72 g, 2 wt% of the total monomers mass). The reaction was carried out for 11 h at 50 °C. At the end, the reaction was quenched by adding 50 mL of THF at room temperature, followed by filtration in order to remove the enzyme beads. The solvent was removed by rotary evaporation at 60 °C under vacuum. The polymer was used for further modification without any additional purification steps. The molar mass of PGA was determined using GPC in THF as  $M_n = 6000 \text{ g mol}^{-1}$  with a polydispersity index (PDI) of 1.8 and using HR MALDI-TOF mass spectrometry as  $m/z 5696.65 \text{ g mol}^{-1}$  with a repeat unit of  $m/z 202 \text{ g mol}^{-1}$ . The <sup>1</sup>H NMR spectrum of PGA is given in Fig. 1. <sup>1</sup>H NMR (400 MHz, CDCl<sub>3</sub>;  $\delta$ , ppm): 5.26 (m, 1H), 5.10 (m, 1H), 4.37–3.9 (m, 6H), 3.60 (dd,  $J = 11.5, 6.2 \text{ Hz}$ , 2H), 2.45–2.26 (m, 4H), 1.75–1.56 (m, 4H). IR (KBr;  $\nu$ , cm<sup>-1</sup>): 3470 ( $\nu$ (–OH)), 2953 ( $\nu_{\text{as}}$ (C–H)), 2875 ( $\nu_{\text{s}}$ (C–H)), 1726 ( $\nu$ (C=O)), 1646 ( $\nu$ (R–CH=CH<sub>2</sub>)), 1463 ( $\delta_{\text{s}}$ (C–H)), 1392–1280 (C–H ( $\omega, \tau$ )), 1264–1180 ( $\nu_{\text{as}}$ (C–O–C)), 1144–1080 ( $\nu_{\text{s}}$ (C–O–C)) and (C–H ( $\rho$ )), 1075–1055 ( $\delta$ (–OH)), 982–800 (C–H ( $\rho$ )), 980, 733 (R–CH=CH<sub>2</sub> ( $\gamma$ )).

### Synthesis of PGA-*g*-6-(Fmoc-Ahx)

PGA with a molar mass  $M_n$  of 6000 g mol<sup>-1</sup> was used for further modification with 6-(Fmoc-Ahx) according to the procedure described by Neises and Steglich,<sup>22</sup> shown in Scheme 1(B). PGA (1.5 g, 7.42 mmol) was dissolved in 20 mL of anhydrous DCM and then charged into a 100 mL three-neck round-bottom flask. The solution was cooled to 0 °C using an ice bath for 20 min. Then, a weighed amount of 6-(Fmoc-Ahx) (15 mol% of all OH groups, 0.4 g, 1.13 mmol) was added. Thereafter, weighed amounts of EDC-HCl (0.84 g, 4.4 mmol) and DMAP (40 mg, 0.33 mmol) were dissolved in 10 mL of anhydrous DCM and added dropwise. Under inert gas conditions, the reaction mixture was stirred for 24 h at room temperature. The reaction solution was filtered and the filtrate was concentrated to a volume of 4 mL using a rotary evaporator. The crude product was purified by silica gel column chromatography using HPLC-grade ethyl acetate as an eluent, in order to remove the unreacted 6-(Fmoc-Ahx), followed by HPLC-grade acetone which contained the grafted polymer. The solvent was removed using a rotary evaporator under reduced pressure. Further purification was done by precipitation into cold diethyl ether two times. After drying under vacuum at 35 °C, a slightly yellowish and viscous product was obtained. Product yield was 84 wt %. The molar mass of PGA-*g*-6-(Fmoc-Ahx) was calculated based on degree of grafting (mol%) from the <sup>1</sup>H NMR spectrum, given in Fig. 5, as  $M_n = 7000 \text{ g mol}^{-1}$ . The average molar mass of PGA-*g*-6-(Fmoc-Ahx) was also estimated using HR MALDI-TOF mass spectrometry as  $m/z 5739.72 \text{ g mol}^{-1}$  with a repeat unit of  $m/z 537.24 \text{ g mol}^{-1}$ . The PDI was determined using GPC in THF to be 1.7. <sup>1</sup>H NMR (400 MHz, CDCl<sub>3</sub>;  $\delta$ , ppm): 7.75 (d,  $J = 7.5 \text{ Hz}$ , 2H), 7.58 (d,  $J = 7.4 \text{ Hz}$ , 2H), 7.38 (t,  $J = 7.5 \text{ Hz}$ , 2H), 7.29 (t,  $J = 7.4 \text{ Hz}$ , 2H), 5.24 (q,  $J = 5 \text{ Hz}$ , 1H), 5.08 (q,  $J = 5 \text{ Hz}$ , 1H), 4.38–3.58 (m, 9H), 3.71 (s, 1H), 3.17 (q,  $J = 6.8 \text{ Hz}$ , 2H), 2.42–2.26 (m, 6H), 1.75–1.57 (m, 6H), 1.51 (s, 2H), 1.38–1.24 (m, 2H). IR (KBr;  $\nu$ , cm<sup>-1</sup>): 3470 ( $\nu$ (–OH)), 3455 ( $\nu$ (–NH)), 2953 ( $\nu_{\text{as}}$ (C–H)), 2875 ( $\nu_{\text{s}}$ (C–H)), 1726 ( $\nu$ (C=O)), 1646 ( $\nu$ (R–CH=CH<sub>2</sub>)), 1535 ( $\delta$ (–NH)), 1452 ( $\delta_{\text{s}}$ (C–H)), 1384–1280 (C–H ( $\omega, \tau$ )), 1260–1180 ( $\nu_{\text{as}}$ (C–O–C)), 1144–1075 ( $\nu_{\text{s}}$ (C–O–C)) and (C–H ( $\rho$ )), 1075–1055 ( $\delta$ (–OH)), 980, 733 (R–CH=CH<sub>2</sub> ( $\gamma$ )), 762, 733 (=C–H ( $\gamma$ )).



**Scheme 1.** Synthetic pathways for (a) PGA, (b) PGA-g-6-(Fmoc-Ahx), (c) deprotection of Fmoc groups and (d) aza-Michael addition byproduct and schematic representation of PGA-based network. The black chains correspond to PGA backbone with vinyl end groups and the blue chains correspond to the side chains that bear primary amine groups. A full presentation of PGA-based network structure is shown in the supporting information (Fig. S1).

### Deprotection of Fmoc groups and network formation

Fmoc protecting groups were removed applying the same method as described by Höck *et al.*,<sup>23</sup> with a slight modification. PGA-g-6-(Fmoc-Ahx) with a molar mass  $M_n$  of 7000 g mol<sup>-1</sup> (1 g, 1.86 mmol) was dissolved in 8 mL of anhydrous DMSO and the solution was agitated for 4 h at room temperature. To remove the formed byproduct, dibenzofulvene and most of DMSO, the polymer solution was precipitated twice into excess of cold *tert*-butylmethyl ether to yield amine-functionalized PGA (Scheme 1(C)). After drying under nitrogen flow for 30 min, 10 wt% of aza-Michael addition byproduct (sol content) and 90 wt% of yellowish PGA-based network were obtained as shown in Scheme 1(D). A schematic of the network is given in the supporting information (Fig. S1). This process occurred according to a typical Michael addition reaction since PGA has acceptor sites, i.e. vinyl end groups, in addition to the primary amine groups along the repeat units, which can act as aza-Michael donors. For network

characterization, the byproduct was dissolved again in DMSO and extracted from the network. IR (KBr;  $\nu$ , cm<sup>-1</sup>): 3482 ( $\nu$ (—OH)), 3387 ( $\nu$ (—NH)), 2941 ( $\nu_{\text{as}}$ (C—H)), 2871 ( $\nu_{\text{s}}$ (C—H)), 1737 ( $\nu$ (C=O)), 1651 ( $\delta_{\text{s}}$ (—NH<sub>2</sub>)), 1550 ( $\delta$ (N—H)), 1456 ( $\delta_{\text{s}}$ (C—H)), 1385–1280 (C—H ( $\omega$ , $\tau$ )), 1258–1170 ( $\nu_{\text{as}}$ (C—O—C)), 1144–1075 ( $\nu_{\text{s}}$ (C—O—C) and (C—H ( $\rho$ )), 1142, 1059 ( $\nu$ (C—N)), 759 (—NH<sub>2</sub> ( $\omega$ )). For <sup>1</sup>H DQ measurements, the network was swollen to equilibrium in DMSO-*d*<sub>6</sub>. In addition, the network was swollen in D<sub>2</sub>O in order to obtain hydrogels.

### Characterization

#### FTIR spectroscopy

FTIR measurements were performed with a Bruker Vector 22 FTIR spectrometer at room temperature with 256 scans using dry KBr for sample preparation. For all measurements, the sample concentration was 1.5 mg per 150 mg of KBr. FTIR spectral data were

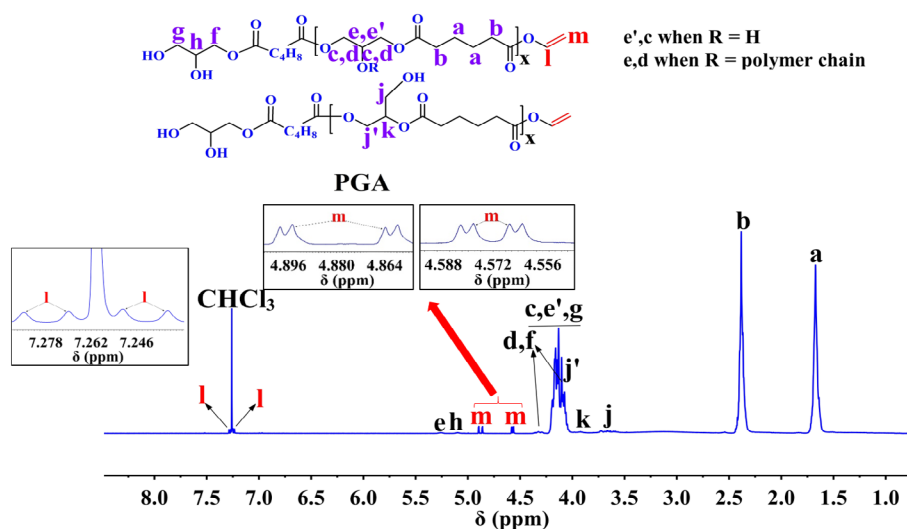


**Figure 1.**  $^1\text{H}$  NMR spectrum of PGA in  $\text{CDCl}_3$  at  $27^\circ\text{C}$ . The three insets show expansions of the peaks corresponding to vinyl end groups.

interpreted using OMNIC 7.2 Spectra software. All FTIR spectra were recorded in the range  $400\text{--}4000\text{ cm}^{-1}$ .

#### NMR spectroscopy

Solution NMR spectra ( $^1\text{H}$  NMR and  $^{13}\text{C}$  NMR) were recorded with a VNMR5 spectrometer operating at 400 MHz for  $^1\text{H}$  NMR and 100 MHz for  $^{13}\text{C}$  NMR at  $27^\circ\text{C}$ , using an internal calibration standard, tetramethylsilane. Samples (*ca* 30 mg) were dissolved in 0.7 mL of deuterated solvents. The inversion-recovery method was performed in order to obtain the quantitative  $^{13}\text{C}$  NMR spectrum of PGA backbone by measuring the spin-lattice relaxation time ( $T_1$ ). For this, PGA sample (*ca* 300 mg) was dissolved in 0.7 mL of  $\text{CDCl}_3$ . The NMR spectral data were interpreted using MestRec (v.4.9.9.6) software (Mestrelab Research, Santiago de Compostela, Spain).

#### $^{13}\text{C}$ MAS NMR spectroscopy

$^{13}\text{C}$  SP MAS experiments were performed with a Bruker Avance 400 spectrometer at a frequency of 100.6 MHz, with a standard Bruker 4 mm MAS probe. A MAS spinning frequency of 10 kHz was applied in all experiments. Swollen network samples (in  $\text{DMSO-}d_6$  and  $\text{D}_2\text{O}$ ) were filled into a Bruker Kel-F MAS insert,<sup>24</sup> for liquid samples. The sample temperature was controlled with a standard Bruker VT controller and calibrated with methanol. The experimental temperature was regulated to  $30^\circ\text{C}$ . The  $^{13}\text{C}$  NMR  $\pi/2$  pulse length varied between 2.5 and 3.0  $\mu\text{s}$ . The recycle delay was set to 10 s for all samples.

#### $^1\text{H}$ DQ NMR measurements

$^1\text{H}$  DQ NMR experiments were run with a 200 MHz Bruker Avance III spectrometer using a static 5 mm Bruker probe with a short dead time (2.5  $\mu\text{s}$ ). The temperature was controlled with a BVT-3000 heating device with  $\pm 1^\circ\text{C}$  and was set to  $30^\circ\text{C}$  for all measurements. The  $^1\text{H}$  pulse length for the  $\pi/2$  and  $\pi$  pulses was set to 3.0 and 6.0  $\mu\text{s}$ , respectively. The sample was swollen to equilibrium in  $\text{DMSO-}d_6$  and  $\text{D}_2\text{O}$  at room temperature and the NMR tubes were sealed. The swelling ratio of PGA-based networks was measured after soaking the dried network in  $\text{D}_2\text{O}$  and in  $\text{DMSO-}d_6$  at room temperature for 24 h. The swelling ratio ( $Q$ ) can be calculated as follows:

$$Q = \frac{m_s - m_d}{m_d}$$

where  $m_s$  is the mass of swollen network and  $m_d$  represents the mass of dry network. The swelling ratio of PGA-based networks in  $\text{D}_2\text{O}$  and in  $\text{DMSO-}d_6$  was 4.8 and 8.5, respectively.

#### GPC measurements

GPC measurements for PGA and PGA-*g*-6-(Fmoc-Ahx) were performed with a Viscotek GPC max VE 2002 using HHRH Guard-17360 and GMHH-N-18055 columns and refractive index detector (VE 3580, Viscotek). THF was used as mobile phase in a thermostatically controlled column at  $25^\circ\text{C}$ . For both samples, the concentration was  $3\text{ mg mL}^{-1}$ , and the flow rate was  $1\text{ mL min}^{-1}$ . The calibration standard for both measurements was polystyrene. The data were analyzed using Origin 8 software.

#### MALDI-TOF mass spectrometry

The HR MALDI-TOF mass spectra were recorded with a REFLEX-TOF mass spectrometer (Bruker Daltonik GmbH, Bremen), equipped with a 337 nm nitrogen laser, which was operated at a pulse frequency of 3 Hz. The ions were accelerated using pulsed ion extraction after a delay of 50 ns by a voltage of 28.5 kV. The analyzer was operated in HR reflectron mode, and generated ions were detected with a microchannel plate detector. For calibration of the mass spectrometer, a polystyrene standard was used. The sample preparation for the recorded HR mass spectra was carried out by mixing of the samples (PGA and PGA-*g*-6-(Fmoc-Ahx)) with a suitable matrix, namely 2-[(2*E*)-3-(4-*tert*-butylphenyl)-2-methylprop-2-enylidene]malononitrile (DCTB), in a ratio of 1:1000 in THF. For preparing the sample, a stock solution of  $10\text{ mg mL}^{-1}$  DCTB in THF and  $10\text{ }\mu\text{g mL}^{-1}$  sample in the same solvent were used. Before the measurement, the prepared sample was crystallized on a stainless steel target. The resulting mass spectra were smoothed, and baseline-corrected with the XMASS data processing program (Bruker). mMass was used to evaluate the spectra. In a mass spectrum, the vertical  $y$ -axis represents the peak intensity (abundance of ions) and the horizontal  $x$ -axis represents the mass-to-charge ratio of the ions ( $m/z$ ). The molar mass of the ionized molecule was determined by the value of  $m/z$  ( $z = 1$ ).

## RESULTS AND DISCUSSION

### Enzymatic polymerization and grafting of PGA with 6-(Fmoc-Ahx) side chains

Enzymatic synthesis of PGA backbone can be achieved through transesterification reaction between glycerol and DVA in the presence of CAL-B. Although vinyl esters are considered to be more costly than alkyl esters (see supporting information), they are particularly suitable monomers for this synthesis as vinyl alcohol is released as a byproduct and tautomerizes promptly into acetaldehyde which can be removed easily at the reaction temperature making the reaction irreversible.<sup>25,26</sup> Thus, polymers with high molar mass are obtained. Compared to the use of dimethyl adipate instead of DVA in PGA synthesis, polymers with lower molar mass are produced.<sup>27</sup> Figure 1 presents the <sup>1</sup>H NMR spectrum of PGA synthesized from glycerol and DVA with peak assignments.

Analysis of the <sup>1</sup>H NMR spectrum shows characteristic signals of PGA, i.e. the methylene and methine proton signals, corresponding to the substituted glyceride and adipate units. Since the enzyme active site contains bound water molecules, which are crucial for enzyme activation, most vinyl end groups are hydrolyzed into carboxylic acid end groups during the polymerization reaction,<sup>28</sup> and some remain and can be recognized as three signals in the <sup>1</sup>H NMR spectrum at 7.29, 4.86 and 4.56 ppm as shown in the insets of Fig. 1. The methylene protons of vinyl end groups, labelled as (m), show two doublet of doublets at 4.86 and 4.56 ppm due to the unequal proton–proton coupling constants.

Although the enzyme shows high reactivity towards primary hydroxyl groups rather than secondary ones, some lack of enzyme regioselectivity is observed by the presence of several methine proton signals.<sup>29</sup> Kline *et al.*<sup>30</sup> reported the high reactivity of lipase towards primary OH groups (*ca* 95%) compared to secondary ones at 50 °C. These investigations explain the formation of differently substituted glyceride units, i.e. 1,2-disubstituted and 1,2,3-trisubstituted glyceride units in addition to 1,3-disubstituted and 1-substituted glyceride units that would

occur in the case of perfect enzyme regioselectivity towards primary OH groups. Similarly, our group has determined the regioselectivity of acylation of lipase toward primary OH groups as 96% in relation to secondary OH groups, which is highly dependent on the reaction temperature.<sup>31</sup> Additionally, PGA was analyzed using <sup>13</sup>C NMR spectroscopy. The spectrum reveals two signals at 141.2 and 97.9 ppm arising from vinyl end groups as can be seen in the inset of Fig. 2. The percentage of vinyl end groups was calculated quantitatively by the ratio of integrals between the adipate repeat unit carbons ( $\int a = 2$ ) and vinyl carbons at 97.9 ppm ( $\int m = 0.08$ ) to be estimated as 8% of the total end groups.

The molar mass and PDI of PGA were determined using GPC with THF as an eluent and polystyrene as calibration standard. The GPC traces are shown in the supporting information (Fig. S2). Along with GPC measurements, PGA was further analyzed using HR MALDI-TOF mass spectrometry in order to determine the absolute molar mass distribution. Figure 3 shows a representative HR MALDI-TOF mass spectrum of PGA molar mass distribution extending from *m/z* 4500 to *m/z* 7000, with a central intense peak at *m/z* 5696.65, which corresponds to the average molar mass of PGA. The HR MALDI-TOF mass spectrum is characterized by a number of peaks separated by regular intervals of *m/z* 202, which is the expected molar mass of PGA repeat units. This confirms the predominant linearity of PGA. The expanded view of the spectrum in the mass range *m/z* 5875–6050 reveals the presence of several series of peaks that can be assigned to different end groups of PGA chains, i.e. hydroxyl (OH) + H (18 + 202*n*), hydroxyl (OH) + vinyl (CH=CH<sub>2</sub>) (44 + 202*n*), adipate part + H (129 + 202*n*) and glycerol part + H (92 + 202*n*) terminated polymer chains wherein *n* is the number of repeat units per polymer chain. The highest intensity peak at *m/z* 5916.70 contains hydroxyl (OH) + H terminated polymer chains, which is in agreement with the PGA synthesis mechanism.

In the second step, side chains terminated with protected amine groups were introduced to the PGA backbone via Steglich

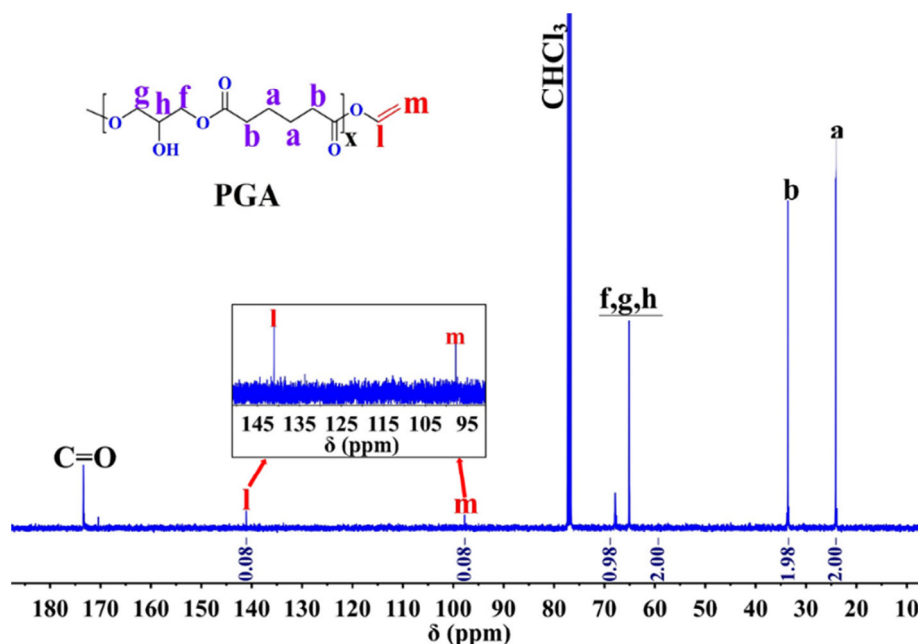


**Figure 2.** Quantitative <sup>13</sup>C NMR spectrum of PGA synthesized from DVA and glycerol in CDCl<sub>3</sub> at 27 °C. The inset shows an expansion of the peaks corresponding to vinyl end groups.

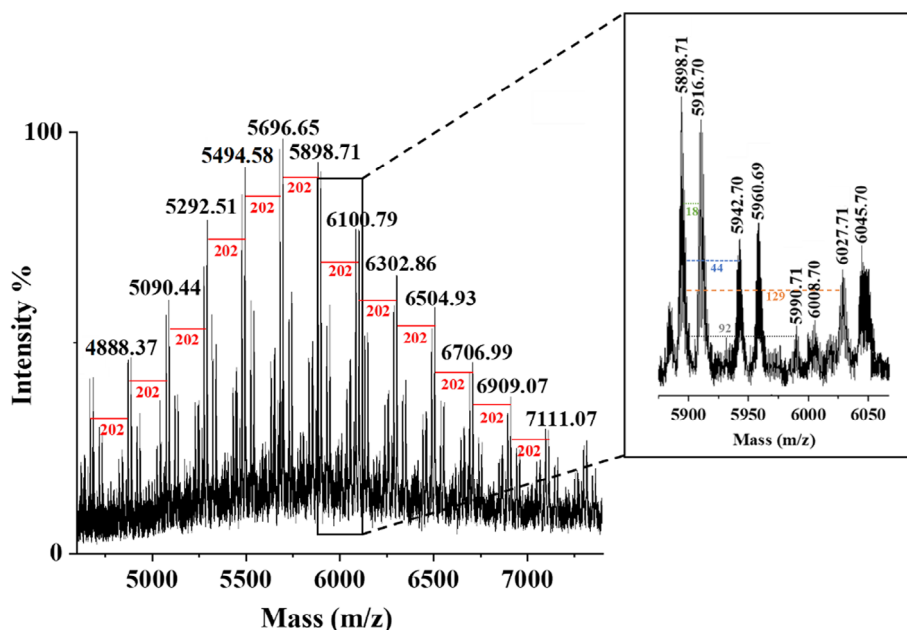


**Figure 3.** HR MALDI-TOF mass spectrum of PGA, using DCTB as a matrix. The molar mass of the repeat unit is  $202 \text{ g mol}^{-1}$ . The expanded view of the  $m/z$  5875–6050 region (right) shows different types of PGA end groups.

esterification between the secondary hydroxyl groups on PGA backbone and 6-(Fmoc-Ahx) with the help of DMAP as a catalyst and EDC-HCl as a coupling agent, as shown in Scheme 1(B). In addition, an excess of EDC-HCl was applied as a drying agent. The GPC traces, shown in the supporting information (Fig. S2), indicate that the grafted polymer has a higher molar mass than the unmodified PGA, indicating the successful acylation reaction. The molar mass and PDI of PGA and PGA-*g*-6-(Fmoc-Ahx) are given in the supporting information (Table S1). In addition to GPC measurements, PGA-*g*-6-(Fmoc-Ahx) was also investigated using HR MALDI-TOF mass spectrometry to determine the molar mass of the new repeat unit after modification. Figure 4 illustrates a full HR MALDI-TOF mass spectrum of the PGA-*g*-6-(Fmoc-Ahx) distribution in the range from  $m/z$  4600 to  $m/z$  7400. The expanded view in the mass range  $m/z$  5000–6750 in Fig. 4 shows the appearance of new peaks separated from the central intense peak by intervals of  $m/z$  537.24 due to the introduction of 6-(Fmoc-Ahx) side chains.

The chemical structure of PGA-*g*-6-(Fmoc-Ahx) was further confirmed using  $^1\text{H}$  NMR and  $^{13}\text{C}$  NMR spectroscopy. The  $^{13}\text{C}$  NMR spectrum is given in the supporting information (Fig. S3). The  $^1\text{H}$  NMR spectrum of PGA-*g*-6-(Fmoc-Ahx) is shown in Fig. 5. Analysis of the  $^1\text{H}$  NMR spectrum reveals the presence of proton signals, labelled with (n, o, p, q and r), which belong to the methylene protons of 6-(Fmoc-Ahx) side chains. The resonance of Fmoc (RNHC=O) proton, labelled with (s), appears as a weak and broad signal at 3.6 ppm. The resonance of aromatic rings labelled with (u, v, w, x and y), and the peak labelled with (t), reflect the protons of the Fmoc protecting group. The degree of grafting of OH groups of PGA is determined quantitatively using selective known peak integration represented in the corresponding  $^1\text{H}$  NMR spectrum. From the integrals of peaks (a) in the polymer backbone and (q) in the side chain, the degree of grafting (*g*) is calculated as 12 mol% with respect to all OH groups of the polymer backbone (where a theoretical value of 15 mol% grafting was used in the feed composition). The molar mass calculations are based on

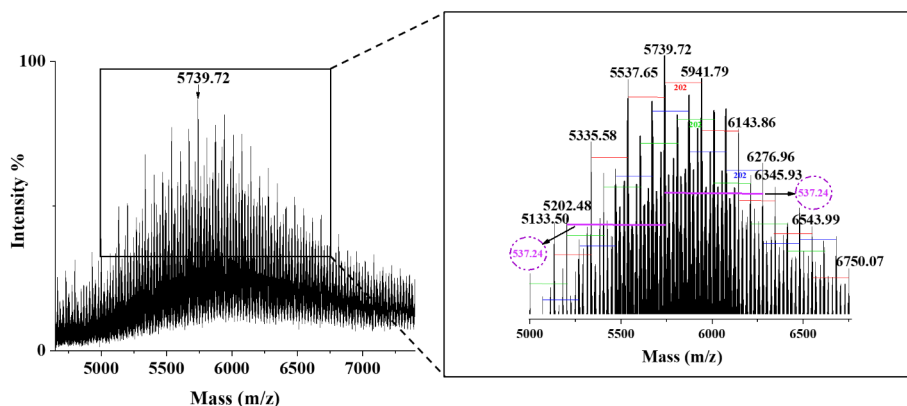


**Figure 4.** HR MALDI-TOF mass spectrum of PGA-*g*-6-(Fmoc-Ahx), using DCTB as a matrix. The expanded view in the mass range  $m/z$  5000–6750 (right) shows the molar mass of the new repeat unit as  $537.24 \text{ g mol}^{-1}$ .

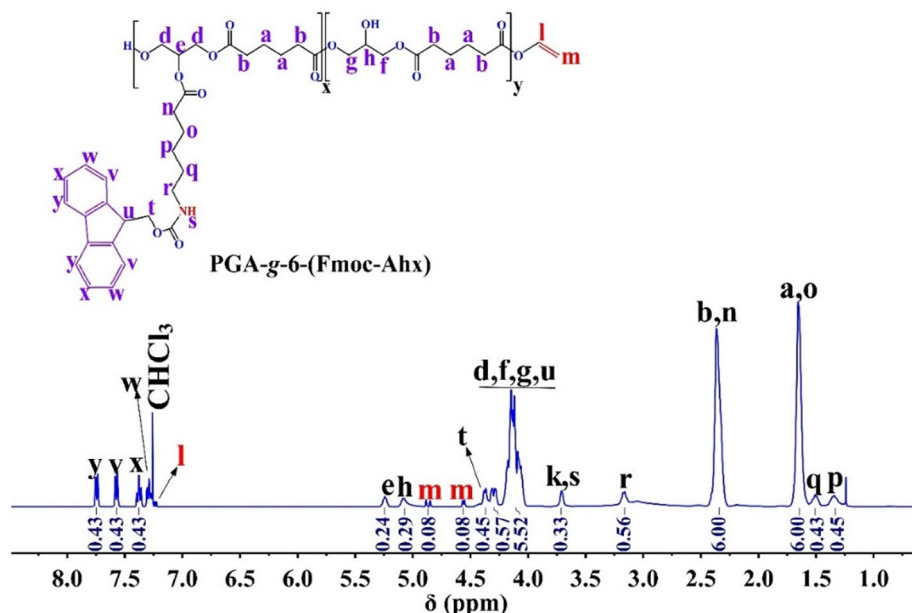


**Figure 5.**  $^1\text{H}$  NMR spectrum of PGA-*g*-6-(Fmoc-Ahx) in  $\text{CDCl}_3$  at 27 °C.

$x$  to  $y$  ratio (given in the chemical structure of Fig. 5). Since  $y + x = 100\%$ , it follows that  $y = 88\%$  and  $x = g = 12\text{ mol}\%$ . Accordingly, the molar mass is calculated as  $7000\text{ g mol}^{-1}$ .

A comparison between the FTIR spectra of PGA and PGA-*g*-6-(Fmoc-Ahx) is shown in Fig. 6. For PGA, all major peaks are assigned. For instance, the spectrum shows a broad and strong peak for the hydroxyl ( $-\text{OH}$ ) stretching band at  $3470\text{ cm}^{-1}$  as a result of hydrogen bonds,  $\text{C}-\text{H}$  alkyl stretching bands between  $2953$  and  $2875\text{ cm}^{-1}$ , carbonyl ( $\text{C}=\text{O}$ ) stretching band at  $1726\text{ cm}^{-1}$  of the ester groups, vinyl end group stretching band at  $1646\text{ cm}^{-1}$ ,  $\text{C}-\text{H}$  bending between  $1463$  and  $1392\text{ cm}^{-1}$ , and  $\text{C}-\text{O}-\text{C}$  stretching bands between  $1264$  and  $1055\text{ cm}^{-1}$ .

After modification of PGA with 6-(Fmoc-Ahx), the stretching bands of  $-\text{OH}$ ,  $\text{C}-\text{H}$  and  $\text{C}=\text{O}$  are observed at the same wavenumber. The presence of ( $\text{RNHC}=\text{O}$ ) stretching band at  $3455\text{ cm}^{-1}$  which is overlapped with ( $-\text{OH}$ ) stretching band,  $\text{C}-\text{H}$  (aromatic) bands at  $762$  and  $743\text{ cm}^{-1}$  and amide II ( $-\text{NH}$ ) bending band at  $1535\text{ cm}^{-1}$  confirms the formation of PGA-*g*-6-(Fmoc-Ahx). Since the modification of PGA with 6-(Fmoc-Ahx)

is only  $12\text{ mol}\%$ , i.e.  $x = g = 12\text{ mol}\%$  with respect to all OH groups of the polymer backbone, it can be observed that the stretching bands of ( $\text{C}-\text{H}$ ) alkyl chains and ( $\text{C}=\text{O}$ ) carbonyl of the ester groups become slightly sharper after this modification.

#### Deprotection of Fmoc protecting group

A mild method for the cleavage of Fmoc protecting group was applied under base-free conditions. This reaction was conducted in anhydrous DMSO and at room temperature, which resulted in a quantitative cleavage of Fmoc groups.<sup>23</sup> The cleavage process was monitored by increasing the olefin signal of the formed byproduct, dibenzofulvene, which appears in the  $^1\text{H}$  NMR spectrum as singlet at  $6.21\text{ ppm}$ , with the aromatic signals in the range  $7-8\text{ ppm}$ . The monitoring process of Fmoc cleavage was carried out in an NMR tube using deuterated DMSO. The  $^1\text{H}$  NMR spectrum is given in the supporting information (Fig. S4).

#### Network characterization

##### FTIR spectroscopy

PGA is a hydrophilic but water-insoluble linear polyester terminated with different end groups. Among them, some electron-deficient alkenes represent proper aza-Michael acceptors and can be involved in a nucleophilic addition reaction with free primary amines (aza-Michael donors),<sup>32-36</sup> to produce a hydrophilic polymer network under mild conditions. FTIR spectroscopy was used to investigate the network formation. Figure 7 depicts the FTIR spectrum of the PGA-based network, the structure of which is shown in Scheme 1(D). The complete disappearance of vinyl end group vibration band at  $1646\text{ cm}^{-1}$  after deprotection reaction and the appearance of  $\text{C}-\text{N}$  vibration band indicate the successful addition reaction of primary amines to vinyl end groups of the PGA backbone. In addition, the carbonyl  $\text{C}=\text{O}$  stretching band of the ester groups shifts to a higher wavenumber ( $1737\text{ cm}^{-1}$ ) due to electronegativity changes as all vinyl end groups disappear.<sup>37</sup> The presence of secondary and tertiary amine bands at  $1556$  and  $1059\text{ cm}^{-1}$ , respectively, represents the aza-Michael mono- and bis-addition products. The presence of primary amine

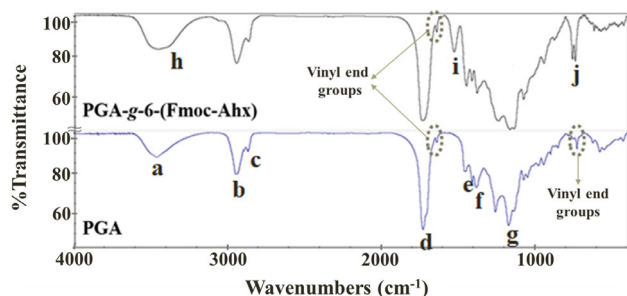


**Figure 6.** FTIR spectra of PGA and PGA-*g*-6-(Fmoc-Ahx) at room temperature. For PGA: (a) OH stretching,  $\nu(-\text{OH})$ , (b)  $\text{C}-\text{H}$  asymmetric stretching,  $\nu_{\text{as}}(\text{C}-\text{H})$ , (c)  $\text{C}-\text{H}$  symmetric stretching,  $\nu_{\text{s}}(\text{C}-\text{H})$ , (d)  $\text{C}=\text{O}$  stretching,  $\nu(\text{C}=\text{O})$ , (e)  $\text{C}-\text{H}$  scissoring bending,  $\delta_{\text{s}}(\text{C}-\text{H})$ , (f)  $\text{C}-\text{H}$  wagging and twisting,  $\text{C}-\text{H}$  ( $\omega$ ,  $\tau$ ), (g)  $\text{C}-\text{O}-\text{C}$  asymmetric and symmetric stretching,  $\nu_{\text{as,s}}(\text{C}-\text{O}-\text{C})$ . For PGA-*g*-6-(Fmoc-Ahx): (h)  $-\text{NH}$  stretching,  $\nu(-\text{NH})$ , (i) amide II bending,  $\delta(-\text{NH})$  and (j)  $=\text{CH}$  out-of-plane bending,  $=\text{CH}(\gamma)$ .

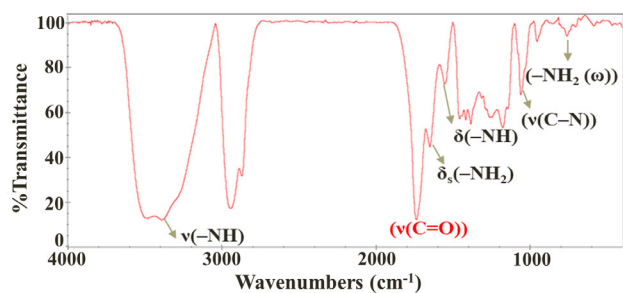


**Figure 7.** FTIR spectrum of PGA-based network at room temperature. Assignments ( $\text{cm}^{-1}$ ): 3387  $\nu(-\text{NH})$ , 1737  $\nu(\text{C}=\text{O})$ , 1651  $\delta_s(-\text{NH}_2)$ , 1550  $\delta(-\text{NH})$ , 1142, 1059  $\nu(\text{C}-\text{N})$ , 759  $-\text{NH}_2(\omega)$ . The spectrum shows the disappearance of vinyl end group vibration at  $1646\text{ cm}^{-1}$  after deprotection reaction and the appearance of  $(-\text{NH}_2)$  vibration band.

$(-\text{NH}_2)$  vibration bands explains that some free amine groups were not involved in the addition reaction.

### <sup>13</sup>C SP MAS spectra

<sup>13</sup>C SP MAS NMR measurements were performed in order to confirm the network structure. Figure 8 shows the <sup>13</sup>C SP MAS spectrum of PGA-based network in DMSO-*d*<sub>6</sub>. It is clearly visible that after network formation, there is no resonance arising from vinyl end groups in the regions of 141.2 and 97.9 ppm (shown in the inset of Fig. 8), which is in complete agreement with the FTIR results (Fig. 7).

Since the spectrum is well resolved, it is possible to determine the degree of grafting with 6-(Fmoc-Ahx) side chains. Therefore, the resonances labelled as (a), (b) and the carbonyl signal (C=O) which belong to the polymer backbone and the resonance labelled as (q) which is assigned to the side chain were integrated. All integration values and detailed calculations can be found in the supporting information. The degree of grafting represents the amount of the modified monomers *x* with 6-(Fmoc-Ahx) side chains. The degree of grafting is calculated as  $x = g = (9.8 \pm 5.0)\text{ mol\%}$  with respect to OH groups that corresponds well with the results of solution NMR spectroscopy. The <sup>13</sup>C SP MAS spectrum of PGA-based network after swelling in D<sub>2</sub>O is given in the supporting information (Fig. S5).

<sup>13</sup>C SP MAS NMR measurements together with FTIR results clearly demonstrate that the possibility of amine groups reacting with ester groups via amide formation is not relevant in our system. Since the reaction was carried out under mild conditions, it guarantees the stability of PGA.

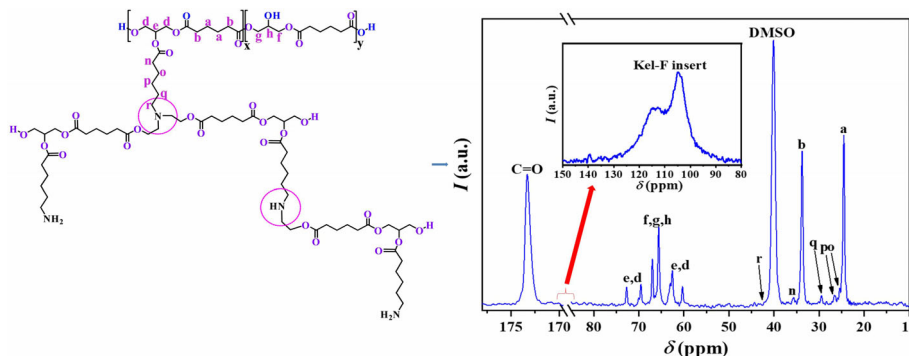


**Figure 8.** <sup>13</sup>C SP MAS NMR spectrum of network swollen to equilibrium in DMSO-*d*<sub>6</sub> measured at 30 °C. The inset shows the spectrum in the range 80 to 150 ppm. The broad signal corresponds to the sample insert,<sup>24</sup> but no vinyl resonances are present at 141.2 and 97.9 ppm.

### <sup>1</sup>H DQ NMR spectroscopy

The <sup>1</sup>H DQ NMR experiment<sup>38</sup> provides information about the structure, defects and dynamics of polymer networks.<sup>39</sup> This method is able to describe systems with well-defined topology as well as systems with randomly distributed loop lengths.<sup>40,41</sup>

In the first step, the isotropically mobile uncoupled components, the so-called *tails*, are removed from the DQ signal. Figure 9(a) shows the procedure of the *tail* determination. Two components with significantly different decay times  $\tau$  could be identified. The component with the slow decay is assigned to the mobile *tail*, i.e. the mobile solvent molecules (non-deuterated solvent *ca* 13% of water, due to the hydrophilicity of the polymer backbone). The fast decaying component with 7% intensity corresponds to network defects such as loops and dangling chains, which are elastically inactive and do not contribute to the network structure. After subtraction of the two *tail* fractions and renormalization of the DQ data, the residual coupling constants (RDCs),  $D_{\text{res}}$ , can be estimated.<sup>39</sup>

Since the grafted side chains are randomly distributed along the polymer backbone, this can result in different mesh sizes, which means that the RDCs will also have a wide distribution according to the equation  $D_{\text{res}} \sim M_c^{-1}$ , where  $M_c$  is the chain molar mass between crosslinks or entanglements. In addition, the swollen elastomers always exhibit a broad  $D_{\text{res}}$  distribution, which is caused by inhomogeneous swelling and the resulting variations in local chain stretching.<sup>42</sup> The DQ data were directly evaluated with the help of a simultaneous fitting procedure:

$$I_{\Sigma\text{DQ}}(\tau_{\text{DQ}}) = \exp\left\{-\left(\tau_{\text{DQ}}/\tau\right)^\beta\right\} I_{\text{DQ}}(\tau_{\text{DQ}})$$

$$= \int_0^\infty I_{\text{DQ}}(\tau_{\text{DQ}}, D_{\text{res}}) p(D_{\text{res}}, \sigma) dD_{\text{res}} = \int_0^\infty \frac{1}{2} \left[1 - \exp\left\{-\left(0.378 \cdot D_{\text{res}} \tau_{\text{DQ}}\right)^{1.5}\right\} \cos(0.583 D_{\text{res}} \tau_{\text{DQ}})\right] \exp\left\{-\left(\tau_{\text{DQ}}/\tau\right)^\beta\right\} p(D_{\text{res}}, \sigma) dD_{\text{res}}$$

Fitting parameters are the time constant  $\tau$ , which corresponds to the characteristic decay time  $T_2^*$ , the exponent  $\beta$  of the Kohlrausch–Williams–Watts function, the RDC  $D_{\text{res}}$  and the width of the log-normal distribution  $\sigma$ . In the given formula, a log-normal distribution was used.

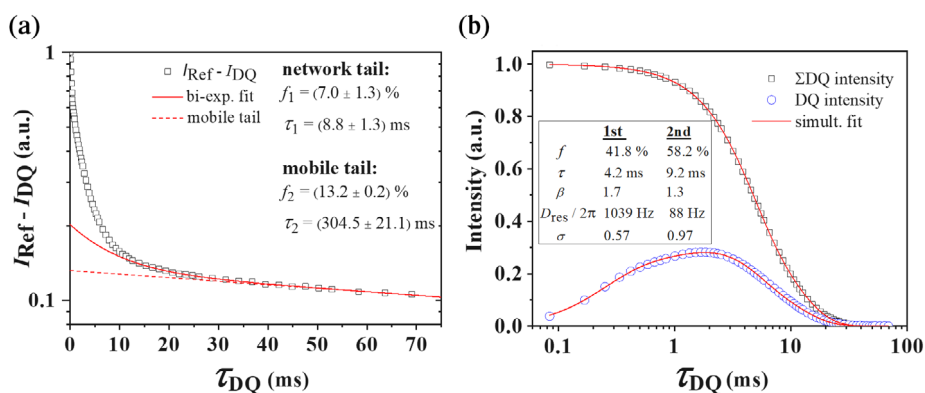


**Figure 9.** (a) Procedure of *tail* determination for the network, swollen to equilibrium in DMSO- $d_6$ . The red line represents the bi-exponential fit to the  $I_{Ref} - I_{DQ}$  intensity. The dashed line represents the mobile tail fraction. The fitting parameters are given in the inset. The fitting area begins at short time where the DQ intensity is already decayed and only a signal from the reference is present. (b) Simultaneous multicomponent fitting to the sum and DQ intensity after *tail* subtraction of the swollen-to-equilibrium network sample. The inset shows the fitting parameters. The component fractions  $f$  are given without taking into account the network *tail* of 7%.

According to the results in Fig. 9(b), we found two components arising from the elastic network structure. A comparison between the simultaneous fit with one and two network components in DMSO- $d_6$  is shown in the supporting information (Fig. S6(a)). These components are well separated due to the different relaxation times  $\tau$  and dipolar coupling constants  $D_{res}$ . Since the strength of the dipolar coupling decreases with increasing length of the network segment,<sup>43,44</sup> we can conclude that the first component with the larger coupling constant is the smallest possible mesh size. The second component represents larger mesh sizes and entanglements that make up the network. Taking the network *tail* into account, the composition of the sample is as follows: strongly coupled network component of 39%, weakly coupled network component of 54%, network defects of 7%. The existence of two well-distinguishable network components as well as the large distribution widths  $\sigma$  of the RDC indicate an inhomogeneous network structure, for example areas of high and low polymer concentration. The  $^1\text{H}$  DQ NMR data and the comparison between the simultaneous fit with one and two network components in  $\text{D}_2\text{O}$  are shown in the supporting information (Figs S7 and S6(b), respectively). Table S2 (supporting information) summarizes the results of the  $^1\text{H}$  DQ NMR data of PGA-based networks in DMSO- $d_6$  and  $\text{D}_2\text{O}$ .

To summarize, from the  $^{13}\text{C}$  SP MAS data it was possible to determine the degree of grafting of the modified PGA as  $(9.8 \pm 5)$  mol%. This corresponds to the value calculated from solution  $^1\text{H}$  NMR spectroscopy. With the help of the  $^1\text{H}$  DQ NMR measurements, the structure of the networks could be determined. Two

components with different RDC and large distribution widths were detected.

## CONCLUSIONS

We present a simple and catalyst-free approach towards the one-pot synthesis of polymer networks based on a biodegradable and biocompatible polyester, PGA. Initially, the lipase-catalyzed transesterification reaction between glycerol and DVA resulted in a hydrophilic polyester carrying  $\alpha,\beta$ -unsaturated (vinyl) end groups that acted as aza-Michael acceptors. In the next step, the pendant hydroxyl groups on the PGA backbone were partially modified by introducing protected amine-terminated side groups and the degree of grafting was calculated to be 10 mol% of total OH groups. It should be noted that grafting with non-protected amino acid leads to immediate but not well-defined network formation. The use of Fmoc as a protecting group offered the opportunity to generate a well-defined network in the final synthesis step. Subsequent removal of Fmoc protecting groups produced a modified PGA with side chains terminated with primary amine groups that served as aza-Michael donors resulting in polymer gelation and formation of a well-defined and hydrophilic network under mild reaction conditions in DMSO.

FTIR and  $^{13}\text{C}$  MAS NMR spectroscopic measurements confirm the network formation by the complete disappearance of vinyl end groups and the appearance of C–N bonds accordingly. Network heterogeneity and defects were determined using  $^1\text{H}$  DQ NMR spectroscopy in DMSO- $d_6$ , which reveals that two components form the elastic network structure, a strongly coupled network component of 39% and a weakly coupled network component of 54% with network defects of 7%. Besides, it was possible to perform the measurements in  $\text{D}_2\text{O}$  by removing DMSO from the synthesized networks and re-swelling in  $\text{D}_2\text{O}$ .  $^{13}\text{C}$  MAS NMR and  $^1\text{H}$  DQ NMR data of PGA-based networks in  $\text{D}_2\text{O}$  are presented in the supporting information that explain the presence of network components with lower coupling constant and shorter relaxation time comparing with the results obtained in DMSO- $d_6$  due to the poor water insolubility of the polymer backbone.

Figure 10 shows images of PGA-based hydrogels. It can be seen that the sample shows a high tack, which makes it suitable for typical pharmaceutical applications of hydrogels in combination with wet tissues. The tack properties of PGA-based hydrogels together



**Figure 10.** Appearance of PGA-based hydrogels.

with their biodegradability mean that they could have significant applications as barrier to prevent postoperative adhesions that may cause medical complications.<sup>45</sup>

Finally, the present protocol exhibits some significant benefits as being operationally simple, mild and catalyst-free, making it a promising approach for the synthesis of polyester-based networks with good water uptake capacity, which can be used for potential pharmaceutical applications such as carriers for sustained release of hydrophilic drugs<sup>46</sup> and biodegradable implants for controlled drug delivery.<sup>47</sup>

## ACKNOWLEDGEMENTS

This work was financially supported by Deutscher Akademischer Austauschdienst (DAAD) under a Research Grants – Doctoral Programs in Germany, 2017/18 (57299294). JK and DR thank Deutsche Forschungsgemeinschaft (JK 1714/9-2, RE 1025/19-2). Open access funding enabled and organized by Projekt DEAL.

## SUPPORTING INFORMATION

Supporting information may be found in the online version of this article.

## REFERENCES

- Dhandayuthapani B, Yoshida Y, Maekawa T and Kumar DS, *Int J Polym Sci* **2011**:1–19 (2011).
- Rezwan K, Chen QZ, Blaker JJ and Boccaccini AR, *Biomaterials* **27**:3413–3431 (2006).
- Gu Y, Zhao J and Johnson JA, *Angew Chem Int Ed* **59**:5022–5049 (2020).
- Peppas NA and Khare AR, *Adv Drug Deliv Rev* **11**:1–35 (1993).
- Buwalda SJ, Vermonden T and Hennink WE, *Biomacromolecules* **18**:316–330 (2017).
- Hirst AR, Escuder B, Miravet JF and Smith DK, *Angew Chem Int Ed* **47**:8002–8018 (2008).
- Kamath KR and Park K, *Adv Drug Deliv Rev* **11**:59–84 (1993).
- Coulember O, Degée P, Hedrick JL and Dubois P, *Prog Polym Sci* **31**:723–747 (2006).
- Jeske RC, DiCiccio AM and Coates GW, *J Am Chem Soc* **129**:11330–11331 (2007).
- Amass W, Amass A and Tighe B, *Polym Int* **47**:89–144 (1998).
- Azim H, Dekhterman A, Jiang Z and Gross RA, *Biomacromolecules* **7**:3093–3097 (2006).
- Cao H, Han H, Li G, Yang J, Zhang L, Yang Y et al., *Int J Mol Sci* **13**:12232–12241 (2012).
- Jiang Y, Woortman AJ, van Ekenstein GO and Loos K, *Biomolecules* **3**:461–480 (2013).
- Kobayashi S, *Proc Jpn Acad Ser B* **86**:338–365 (2010).
- Kobayashi S, Uyama H and Kimura S, *Chem Rev* **101**:3793–3818 (2001).
- Uyama H, Kleggraf E, Wada S and Kobayashi S, *Chem Lett* **29**:800–801 (2000).
- Kallinteri P, Higgins S, Hutcheon GA, St Pourçain CB and Garnett MC, *Biomacromolecules* **6**:1885–1894 (2005).
- Weisig T, Hacker MC, Kressler J and Mäder K, *Int J Pharm* **531**:225–234 (2017).
- Swainson SME, Taresco V, Pearce AK, Clapp LH, Ager B, McAllister M et al., *Eur J Pharm Biopharm* **142**:377–386 (2019).
- Weiss VM, Naolou T, Hause G, Kuntsche J, Kressler J and Mäder K, *J Control Release* **158**:156–164 (2012).
- Alaneed R, Hauenschild T, Mäder K, Pietzsch M and Kressler J, *J Pharm Sci* **109**:981–991 (2020).
- Neises B and Steglich W, *Angew Chem Int Ed* **17**:522–524 (1978).
- Höck S, Marti R, Riedl R and Simeunovic M, *Chimia* **64**:200–202 (2010).
- Smernik RJ and Oades JM, *Solid State Nucl Magn Reson* **20**:74–84 (2001).
- Puskas JE, Seo KS and Sen MY, *Eur Polym J* **47**:524–534 (2011).
- Castano M, Seo KS, Guo K, Becker ML, Wesdemiotis C and Puskas JE, *Polym Chem* **6**:1137–1142 (2015).
- Naolou T, Weiss VM, Conrad D, Busse K, Mäder K and Kressler J, Fatty acid modified poly(glycerol adipate): polymeric analogues of glycerides, in *Tailored Polymer Architectures for Pharmaceutical and Biomedical Applications*, Vol. **1135**, ed. by Scholz C and Kressler J. American Chemical Society, Washington, DC, pp. 39–52 (2013).
- Chaudhary AK, Lopez J, Beckman EJ and Russell AJ, *Biotechnol Prog* **13**:318–325 (1997).
- Taresco V, Suksirworapong J, Creasey R, Burley JC, Mantovani G, Alexander C et al., *J Polym Sci A Polym Chem* **54**:3267–3278 (2016).
- Kline BJ, *J Am Chem Soc* **120**:9475–9480 (1998).
- Bilal MH, Hussain H, Prehm M, Baumeister U, Meister A, Hause G et al., *Eur Polym J* **91**:162–175 (2017).
- Rulev AY, *Russ Chem Rev* **80**:197–218 (2011).
- Yadav JS, Ramesh Reddy A, Gopal Rao Y, Narsaiah AV and Reddy BVS, *Lett Org Chem* **4**:462–464 (2007).
- Ying AG, Liu L, Wu GF, Chen G, Chen XZ and Ye WD, *Tetrahedron Lett* **50**:1653–1657 (2009).
- Reddick JJ, *Org Lett* **5**:1967–1970 (2003).
- Matveeva EV, Petrovskii PV and Odinetz IL, *Tetrahedron Lett* **49**:6129–6133 (2008).
- Kagarise RE, *J Am Chem Soc* **77**:1377–1379 (1955).
- Baum J and Pines A, *J Am Chem Soc* **108**:7447–7454 (1986).
- Saalwächter K, *Prog Nucl Magn Reson Spectrosc* **51**:1–35 (2007).
- Lange F, Schwenke K, Kurakazu M, Akagi Y, Chung U, Lang M et al., *Macromolecules* **44**:9666–9674 (2011).
- Golitsyn Y, Pulst M, Samiullah MH, Busse K, Kressler J and Reichert D, *Polymer* **165**:72–82 (2019).
- Saalwächter K, *J Am Chem Soc* **125**:14684–14685 (2003).
- Saalwächter K, Multiple-quantum NMR studies of anisotropic polymer chain dynamics, in *Modern Magnetic Resonance*, ed. by Webb GA. Springer, Cham, pp. 1–28 (2017).
- Samiullah MH, Reichert D, Zinkevich T and Kressler J, *Macromolecules* **46**:6922–6930 (2013).
- Jiang A, Hussain H and Kressler J, *Macromol Mater Eng* **300**:181–190 (2015).
- Hu Y, Liu Y, Qi X, Liu P, Fan Z and Li S, *Polym Int* **61**:74–81 (2012).
- Lehner E, Gündel D, Liebau A, Plontke S and Mäder K, *Int J Pharm X* **1**:100015 (2019).

# Network formation by aza-Michael addition of primary amines to vinyl end groups of enzymatically synthesized poly(glycerol adipate)

Razan Alaneed,<sup>a,c</sup> Yury Golitsyn,<sup>b</sup> Till Hauenschild,<sup>a</sup> Markus Pietzsch,<sup>c</sup> Detlef Reichert<sup>b</sup> and Jörg Kressler<sup>a\*</sup>

<sup>a</sup> Department of Physical Chemistry, Institute of Chemistry, Martin Luther University Halle-Wittenberg, D-06099 Halle/Saale, Germany

<sup>b</sup> Department of Physics, Martin Luther University Halle-Wittenberg, D-06099, Halle (Saale), Germany

<sup>c</sup> Department of Pharmaceutical Technology and Biopharmacy, Institute of Pharmacy, Martin Luther University Halle-Wittenberg, Wolfgang-Langenbeck-Str. 4, D-06120 Halle/Saale, Germany

\* Corresponding author: [joerg.kressler@chemie.uni-halle.de](mailto:joerg.kressler@chemie.uni-halle.de)

## Supporting Information

### PGA-based network.

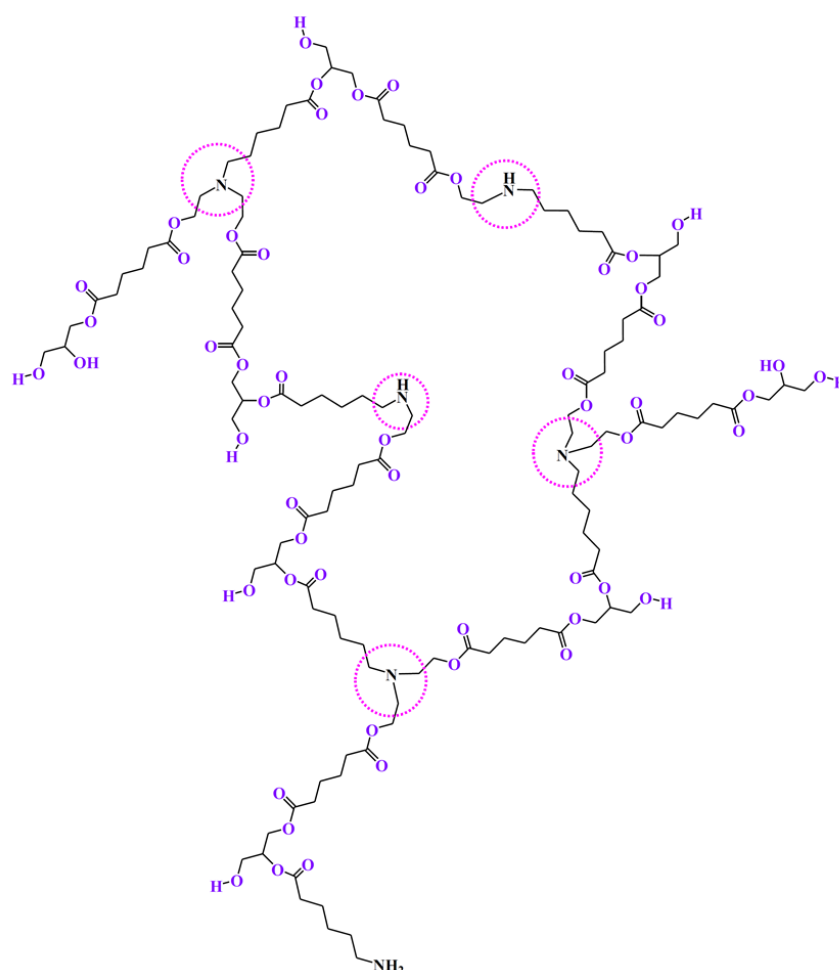


**Figure S1.** Schematic presentation of PGA-based network structure.

### GPC results.

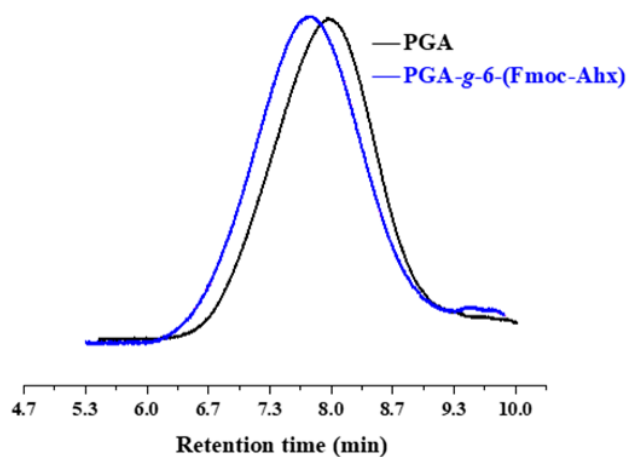


Figure S2. GPC traces of PGA and PGA-g-6-(Fmoc-Ahx) in THF at RT (polystyrene as a calibration standard).

Table S1. Molar mass and PDI of PGA and PGA-g-6-(Fmoc-Ahx).

Polymer	$M_n$ (g mol <sup>-1</sup> )	PDI
PGA	6,000 <sup>a</sup> (DP = 30)	1.8 <sup>a</sup>
PGA-g-6-(Fmoc-Ahx)	7,000 <sup>b</sup>	1.7 <sup>a</sup>

<sup>a</sup>  $M_n$  of PGA backbone and polydispersity index (PDI) are obtained from GPC using THF as an eluent and polystyrene as a calibration standard.

<sup>b</sup>  $M_n$  is calculated on the basis of mol% degree of grafting from <sup>1</sup>H NMR spectrum.

### <sup>13</sup>C NMR spectrum of PGA-g-6-(Fmoc-Ahx).

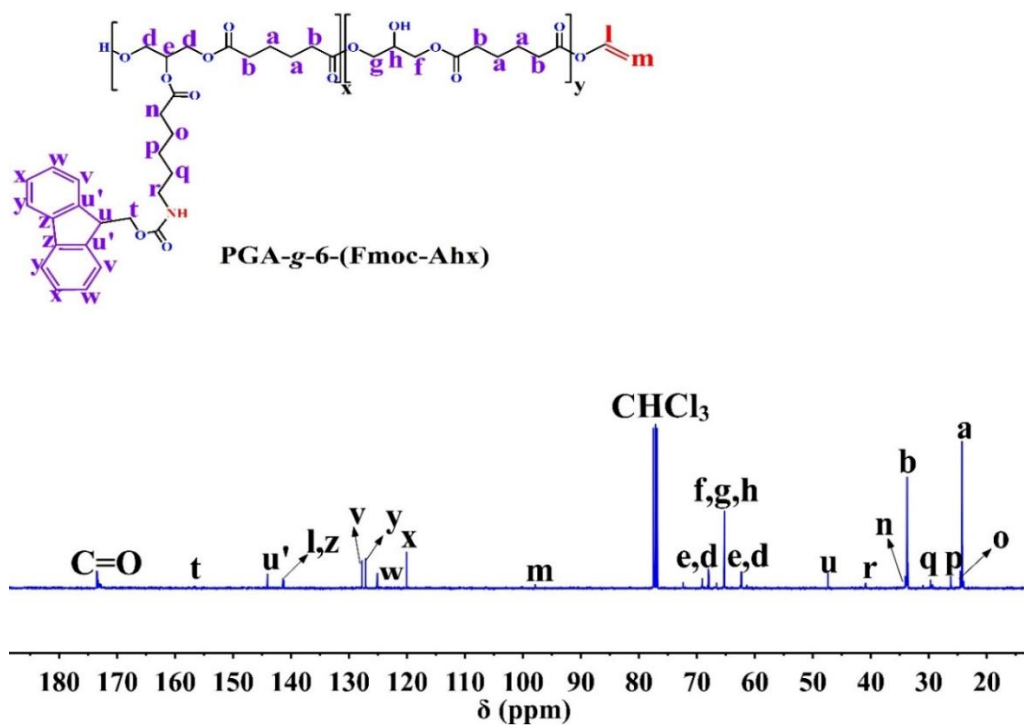


Figure S3. <sup>13</sup>C NMR spectrum of PGA-g-6-(Fmoc-Ahx) in CDCl<sub>3</sub> at 27 °C.

### Monitoring of Fmoc deprotection using $^1\text{H}$ NMR in $\text{DMSO-d}_6$ .

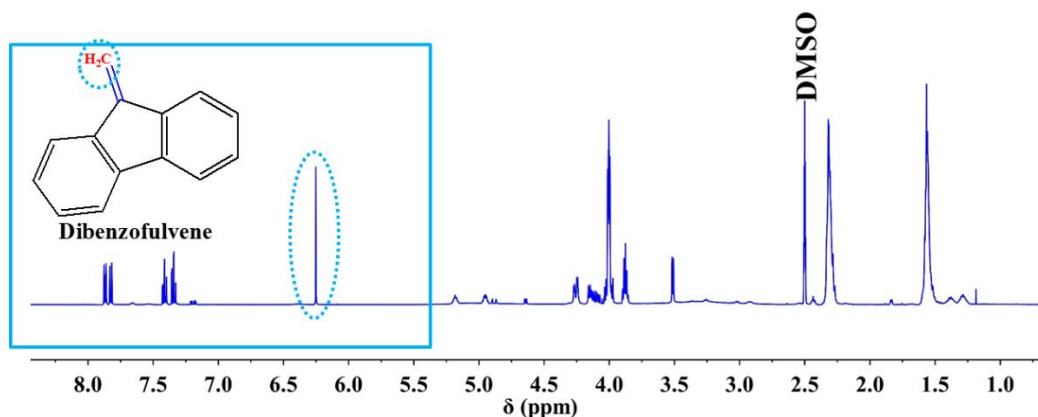


Figure S4.  $^1\text{H}$  NMR spectrum of Fmoc deprotection process in  $\text{DMSO-d}_6$  at  $27^\circ\text{C}$ .

### $^{13}\text{C}$ MAS NMR calculations (x:y ratio).

To determine the degree of grafting with 6-(Fmoc-Ahx) side chains, the separate resonances in the  $^{13}\text{C}$  SP MAS spectrum (Figure 8) were integrated and normalized to the peak (q):  $I_a = 20.56$ ,  $I_b = 20.25$ ,  $I_{\text{C=O}} = 21.66$ ,  $I_q = 1$ . The first three resonances belong to the polymer backbone and the last to the side chain. Since the resonances (a) and (b) occur twice in unmodified monomers  $y$  and in modified monomers  $x$ , the following relationships apply:  $I_a = I_b = 2 \cdot (y+x)$ , where  $y$  and  $x$  are the number of monomers. Resonance (q) occurs only in the modified monomers, so  $I_q = x = 1$ . Thus, the following applies:  $y = 0.5 \cdot I_a - I_q = 0.5 \cdot I_b - I_q$ . The mean value results to  $y = 9.2$ .

Since  $y + x = 100\%$ , it follows  $y = 90.2\%$  and  $x = g = (9.8 \pm 5.0)\text{ mol}\%$ , where  $g$  is the degree of grafting. This result can be checked using the resonance (C=O):  $I_{\text{C=O}} = 2 \cdot y + 3 \cdot x = 21.4$ . This value agrees well with the integrated value  $I_{\text{C=O}} = 21.66$ .

In the same way, the degree of grafting was determined from the  $^{13}\text{C}$  MAS NMR spectrum in  $\text{D}_2\text{O}$ . The separate resonances in the  $^{13}\text{C}$  SP MAS spectrum (Figure S5) were integrated and normalized to the peak (q) and (r). For (q) peak,  $g = (7.7 \pm 5.0)\text{ mol}\%$ . For (r) peak,  $g = (10.3 \pm 5)\text{ mol}\%$ . The difference between two values is due to the small peak intensities and broad line width.

### $^{13}\text{C}$ single-pulse MAS NMR spectrum of the network swollen to equilibrium in $\text{D}_2\text{O}$ .

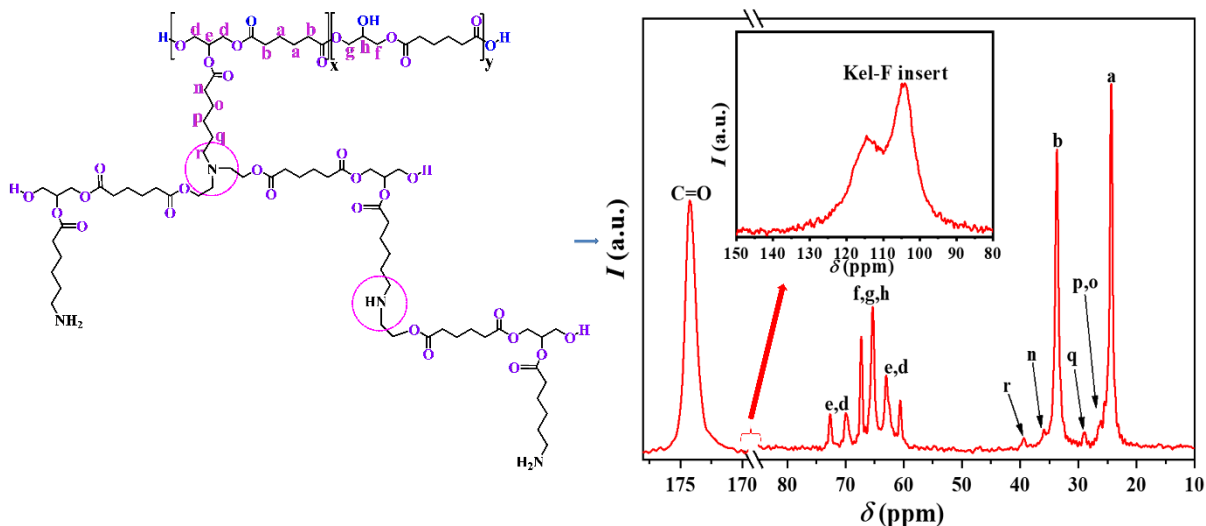


**Figure S5.**  $^{13}\text{C}$  single-pulse MAS NMR spectrum of the network swollen to equilibrium in  $\text{D}_2\text{O}$  measured at  $30^\circ\text{C}$ . The inset shows the spectrum in the range of 80 to 150 ppm. The broad signal corresponds to the sample insert, but no vinyl resonances are present at 141.2 and 97.9 ppm.

Single and two component fitting of  $^1\text{H}$  DQ NMR data in  $\text{DMSO-d}_6$  and  $\text{D}_2\text{O}$ .

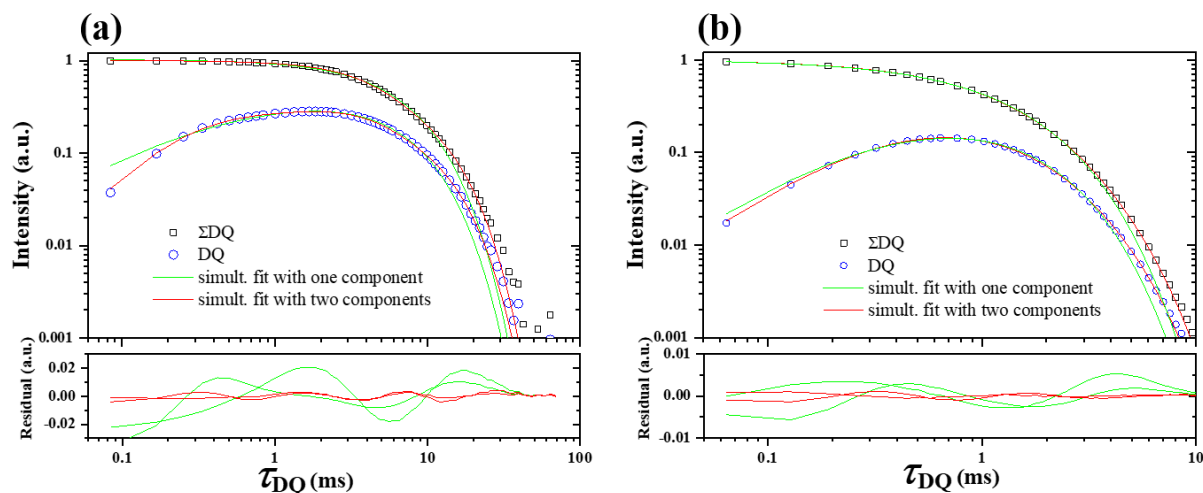


**Figure S6.** Comparison between single and two component fitting for  $^1\text{H}$  DQ NMR data in a)  $\text{DMSO-d}_6$  and b)  $\text{D}_2\text{O}$ .

$^1\text{H}$  DQ NMR data of PGA-based network in  $\text{D}_2\text{O}$ .

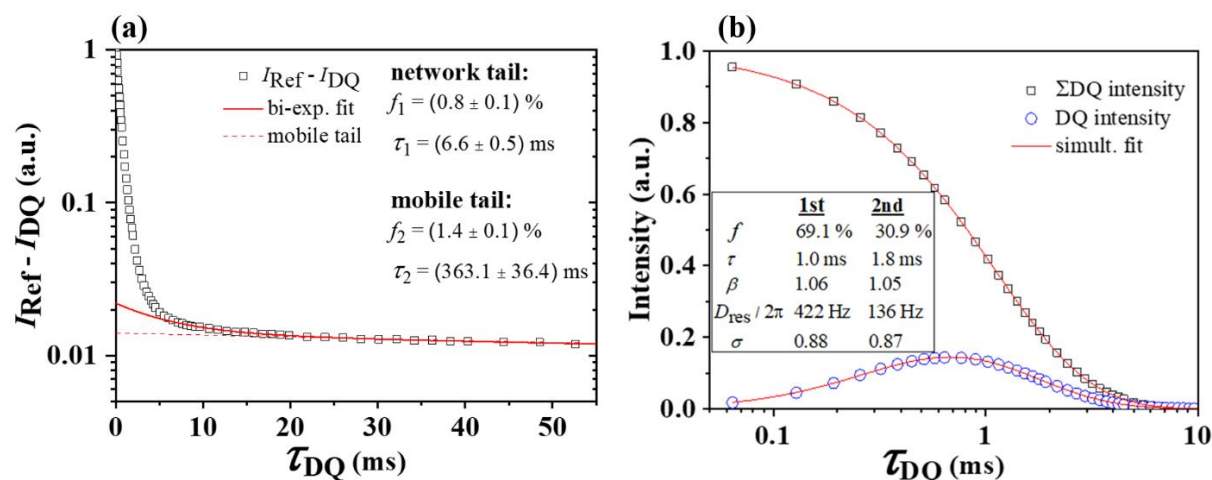


**Figure S7.** (a) Procedure of *tail* determination for the network, swollen to equilibrium in  $\text{D}_2\text{O}$ . The red line represents the bi-exponential fit to the  $I_{\text{Ref}} - I_{\text{DQ}}$  intensity. The dashed line represents the mobile tail fraction. The fitting parameters are given in the inset. The fitting area begins at short time where the DQ intensity is already decayed and only a signal from the reference is present, (b) Simultaneous multicomponent fitting to the sum and DQ intensity after *tail* subtraction of the swollen to equilibrium network sample. The inset shows the fitting parameters. The network tail is much lower than in  $\text{DMSO-d}_6$ . In addition, the differences between the components from the two-component fit are small, which means that  $\text{D}_2\text{O}$  is not a good solvent for the network.

**Table S2.** Summary of  $^1\text{H}$  DQ NMR data of PGA-based network in DMSO- $d_6$  and  $\text{D}_2\text{O}$ .

The network tail is much lower than in DMSO- $d_6$  as well as the coupling constant  $D_{\text{res}}$  as the network tail was not resolved from the network structure. In addition, the differences between the components from the two-component fit are small which means that  $\text{D}_2\text{O}$  is not a good solvent for the network.

Fitting parameters	Network components in DMSO- $d_6$			Network components in $\text{D}_2\text{O}$		
	1st	2nd	Network tail	1st	2nd	Network tail
$f$ (%)	39	54	7	68.5	30.7	0.8
$\tau$ (ms)	4.2	9.2	8.8	1	1.8	6.6
$\beta$	1.7	1.3	1	1.06	1.05	1
$D_{\text{res}} / 2\pi$ (Hz)	1039	88	-	422	136	-
$\sigma$	0.57	0.97	-	0.88	0.87	-

### Additional information on divinyl adipate (DVA) from TCI.

Divinyl adipate (DVA, stabilized with 4-methoxyphenol (MEHQ), >99.0%) was purchased from TCI-Europe.

Product Number: A1188.

CAS RN: 4074-90-2.

Price: it costs 168 Euro per 500 G of DVA.

## Figure Legends

**Figure S1.** Schematic presentation of PGA-based network structure.

**Figure S2.** GPC traces of PGA and PGA-*g*-6-(Fmoc-Ahx) in THF at RT (polystyrene as a calibration standard).

**Figure S3.**  $^{13}\text{C}$  NMR spectrum of PGA-*g*-6-(Fmoc-Ahx) in  $\text{CDCl}_3$  at 27 °C.

**Figure S4.**  $^1\text{H}$  NMR spectrum of Fmoc deprotection process in DMSO- $d_6$  at 27 °C.

**Figure S5.**  $^{13}\text{C}$  single-pulse MAS NMR spectrum of the network swollen to equilibrium in  $\text{D}_2\text{O}$  measured at 30 °C. The inset shows the spectrum in the range of 80 to 150 ppm. The broad signal corresponds to the sample insert, but no vinyl resonances are present at 141.2 and 97.9 ppm.

**Figure S6.** Comparison between single and two component fitting for  $^1\text{H}$  DQ NMR data in a) DMSO- $d_6$  and b)  $\text{D}_2\text{O}$ .

**Figure S7.** (a) Procedure of *tail* determination for the network, swollen to equilibrium in  $\text{D}_2\text{O}$ . The red line represents the bi-exponential fit to the  $I_{\text{Ref}} - I_{\text{DQ}}$  intensity. The dashed line represents the mobile tail fraction. The fitting parameters are given in the inset. The fitting area begins at short time where the DQ intensity is already decayed and only a signal from the reference is present, (b) Simultaneous multicomponent fitting to the sum and DQ intensity after *tail* subtraction of the swollen to equilibrium network sample. The inset shows the fitting parameters. The network tail is much lower than in DMSO- $d_6$ . In addition, the differences between the components from the two-component fit are small, which means that  $\text{D}_2\text{O}$  is not a good solvent for the network.

## Table Legends

**Table S1.** Molar mass and PDI of PGA and PGA-*g*-6-(Fmoc-Ahx).

**Table S2.** Summary of  $^1\text{H}$  DQ NMR data of PGA-based network in DMSO- $d_6$  and  $\text{D}_2\text{O}$ .

The network tail is much lower than in DMSO- $d_6$  as well as the coupling constant  $D_{\text{res}}$  as the network tail was not resolved from the network structure. In addition, the differences between the components from the two-component fit are small which means that  $\text{D}_2\text{O}$  is not a good solvent for the network.

## 4 | Summary and outlook

Enzymatic synthesis of polyesters as a green alternative to the conventional chemical polymerization procedures has resulted in a highly elegant and versatile strategy to produce biodegradable, biocompatible, and functionalizable polyesters suitable for a wide range of pharmaceutical applications. The thesis presented here describes an environmentally benign approach for the production of aliphatic biodegradable polyesters using CAL-B as a biocatalyst. In this regard, CAL-B-catalyzed polytransesterification reaction of glycerol and either DVA or DMA yielded biodegradable PGA and PGA(M) of molar masses 6,000 and 2,600 g mol<sup>-1</sup>, respectively. While, CAL-B-catalyzed polytransesterification reaction of D-sorbitol and DVA yielded a biodegradable sugar-based polyester, PDSA, having a molar mass of 12,000 g mol<sup>-1</sup>. Due to the significant selectivity of CAL-B toward primary OH-groups rather than secondary ones, linear polyesters were obtained with free pendant secondary OH-groups capable of being used for post-modification reactions and thus, adjusting the physicochemical properties of these polyesters. By esterification of OH-groups along the three polyester backbones with side chains bearing protected amine groups, namely 6-(fluorenylmethyloxycarbonyl-amino)hexanoic acid (6-(Fmoc-Ahx)) *via* a simple carbodiimide coupling reaction (Steglich esterification), protected amine-modified polyesters were successfully synthesized. This was followed by the removal of the protective group, Fmoc, under mild reaction conditions in dimethyl sulfoxide (DMSO) at room temperature to generate primary amine-modified polyesters for further applications in the field of enzymatic-mediated protein-polymer conjugation and polymeric networks formation.

In the first part of this work, amine-modified PGA(M), namely PGA(M)-g-NH<sub>2</sub> was further modified with hydrophilic succinylated mPEG12 side chains *via* Steglich esterification to yield water soluble graft copolymers, PGA(M)-g-NH<sub>2</sub>-g-mPEG12. Such techniques like <sup>1</sup>H NMR and FTIR spectroscopy were used to investigate their chemical structures. The degree of primary amine and mPEG12 functionalization was determined from <sup>1</sup>H NMR measurements as 16 mol% (with nearly two amine groups per polymer chain) and ~80 mol% of total OH-groups, respectively. Moreover, the molar mass distribution of these polymers was characterized by GPC. Subsequently, PGA(M)-g-NH<sub>2</sub>-g-mPEG12 was subjected for the conjugation reaction with a model protein, DMC, mediated by a variant of thermoresistant mTGase-S2P at 37 °C and the formed conjugates were analyzed by SDS-PAGE stained with Coomassie blue as a

direct proof technique. A new band of higher molar mass appeared on the SDS-PAGE associated with the disappearance of pure DMC band at the end of the reaction, thus, confirming the efficient formation of DMC-PGA(M) conjugates in the presence of mTGase-S2P. Furthermore, a series of control experiments were conducted. For instance, (i) DMC was incubated with a fluorescent dye bearing primary amine group, monodansyl cadaverine (MDC), in the presence of mTGase-S2P and the SDS-PAGE results revealed a shift of the protein band to a higher molar mass fluorescent band detected under UV light demonstrating the successful conjugation of DMC with MDC, (ii)  $\beta$ -casein was incubated with mTGase-S2P to yield cross-linked aggregates of high molar masses observed on SDS-PAGE which can be explained by the self-cross-linking between the Lys residue of one  $\beta$ -casein molecule and the Gln residue of another  $\beta$ -casein molecule, and finally (iii) DMC was incubated with mTGase-S2P as a negative control and no significant self-cross-linking of DMC was observed on SDS-PAGE. These results were very promising to further expand the application of this enzymatic approach using therapeutic proteins that can improve their *in vivo* therapeutic efficiency.

In the second part of the present work, the potential of mTGase-mediated conjugation reaction using a therapeutic protein, rHuEPO, at the level of Gln residues with the aim to generate new rHuEPO conjugates was explored. Since the accessible Gln residues by TGases should be located in highly flexible and unfolded segments of the protein, thermal stability analysis of rHuEPO was conducted by nano differential scanning fluorimetry (nanoDSF) and the results showed a reversible thermal unfolding of rHuEPO without protein aggregation, i.e. it retains its native folded state upon cooling down. The  $T_m$  of rHuEPO was further investigated as 54.3 °C, where half of rHuEPO molecules are in the unfolded state. Accordingly, variant mTGase-TG<sup>16</sup>, with higher thermostability than mTGase-S2P was applied for the conjugation reactions. As a proof of principle study, the reactivity of rHuEPO towards mTGase-TG<sup>16</sup> using MDC substrate was studied at 54 °C before and after treatment with PNGase F which releases the N-linked glycan. The presence of fluorescent bands under UV light at the molar mass of glycosylated (~ 35 kDa) and N-deglycosylated rHuEPO (~ 18.4 kDa), verified the successful conjugation. After that, another mTGase-TG<sup>16</sup>-recognizable substrate based on the biodegradable and water soluble polyester, PDSA, was prepared for the conjugation reaction with rHuEPO. Since PDSA was synthesized using DVA as a monomer, some vinyl end groups were remaining at the end of enzymatic polymerization and able to undergo aza-Michael addition reaction of primary amine groups to these end groups after modification. Accordingly, and in order to avoid this possibility, vinyl end groups were protected with *N*-acetyl-L-cysteine methyl ester (Ac-L-Cys

ME) *via* thiol-ene based Michael reaction as a critical step in this study. Afterwards, amine-modified PDSA, namely PDSA-*g*-NH<sub>2</sub> was synthesized and well characterized by <sup>1</sup>H NMR spectroscopy. On the basis of <sup>1</sup>H NMR measurements, the grafting degree of primary amine was determined as ~13 mol% with respect to all OH-groups along the polymer backbone, which results in about five amine groups per polymer chain. Further, PDSA-*g*-NH<sub>2</sub> was partially modified with a fluorescent dye, rhodamine B-isothiocyanate, and thoroughly characterized by <sup>1</sup>H NMR spectroscopy. Then, both synthesized polyesters, i.e. PDSA-*g*-NH<sub>2</sub> and Rhodamine-labelled PDSA-*g*-NH<sub>2</sub> were subjected for mTGase-TG<sup>16</sup>-mediated conjugation reaction with rHuEPO at 54 °C before and after treatment with PNGase F and the formed conjugates were analyzed by SDS-PAGE. After separation by electrophoresis, all fluorescent bands were visualized under UV light and then stained with silver nitrate. From SDS-PAGE analysis, the conjugated species displayed a high molar mass band ~ 184 kDa in addition to the appearance of cross-linked aggregates accompanied with a subsequent decrease of the pure rHuEPO band. These results were confirmed by the presence of high molar mass fluorescent bands under UV light corresponding to the investigated conjugates. Thus, the preparation of novel rHuEPO-PDSA conjugates was achievable by the use of mTGase-TG<sup>16</sup> at the *T<sub>m</sub>* of rHuEPO and even in the presence of N- and O-glycans. The biodegradability of PDSA exhibits a potential advantage over the well-established PEG to produce biodegradable rHuEPO conjugates that may have a positive impact on rHuEPO *in vivo* performance. Additionally, various control experiments were performed, (i) the reaction of rHuEPO with mTGase-TG<sup>16</sup> revealed that no self-cross-linking of rHEPO has occurred, (ii) the reaction of MDC with mTGase-TG<sup>16</sup> resulted in the conjugate formation, and finally (iii) the reaction of PDSA-*g*-NH<sub>2</sub> with mTGase-TG<sup>16</sup> resulted in the formation of cross-linked aggregates.

In short, two enzymatically synthesized polyesters, PGA(M) and PDSA, modified with the same functional linker group were successfully conjugated to DMC and rHuEPO, respectively, using mTGase as a cross-linker catalyst, hence, establishing one approach to develop new acceptable substrates for mTGase. In both respects, protein-polymer conjugates of higher molar mass were obtained due to the presence of multiple reactive sites, i.e. amine groups along the polymer backbones as well as Gln residues on the protein substrates. On the basis of these promising results, further research should be conducted to first identify the site of reaction on rHuEPO, i.e. the Gln residues that were specifically modified by mTGase-TG<sup>16</sup> and second to investigate the impact of polymer conjugation on protein solubility, activity, stability against enzymatic cleavage, and bioavailability.

In the last part of this work, well-defined and hydrophilic PGA-based networks were synthesized using highly efficient aza-Michael addition chemistry. Initially, the CAL-B-catalyzed polytransesterification reaction between DVA and glycerol has resulted a linear PGA having some  $\alpha,\beta$ -unsaturated (vinyl) end groups able to serve as aza-Michael acceptors. By esterification with side chains terminated with protected amine groups, modified PGA was successfully synthesized and comprehensively characterized by  $^1\text{H}$  NMR,  $^{13}\text{C}$  NMR, and FTIR spectroscopy. HR MALDI-TOF mass spectrometry was also conducted in order to determine the molar mass of PGA before and after modification as well as to confirm the presence of vinyl end groups beside hydroxyl end groups. After Fmoc deprotection process, free primary amine groups along the PGA backbone were obtained to serve as aza-Michael donors. These nucleophilic amines subsequently reacted with vinyl end groups of PGA *via* aza-Michael addition reaction to produce hydrogel under catalyst-free conditions and without the formation of by-products. The successful aza-Michael addition of primary amines to vinyl end groups of PGA and the formation of PGA-based networks were confirmed by solid state  $^{13}\text{C}$  SP MAS NMR and FTIR spectroscopy, which showed a complete disappearance of vinyl end groups and the appearance of new carbon–nitrogen bonds. On the basis of  $^{13}\text{C}$  SP MAS NMR measurements, the degree of grafting of amine groups was calculated as 10 mol% of total OH-groups. Network heterogeneity and defects were investigated using  $^1\text{H}$  DQ NMR spectroscopy and the results revealed that two main components with distinct relaxation times and dipolar coupling constants form the elastic network structure, i.e. a strongly coupled network component of 39% and a weakly coupled network component of 54% with network defects of 7%. These novel PGA-based networks with promising properties such as biocompatibility and biodegradability can serve as a tunable platform for sustained release of many hydrophilic therapeutics. However, further studies will be necessary on investigation of the therapeutic *in vitro* release from these networks under different conditions, followed by *in vivo* release behavior study and thus, improve their role within the field of controlled drug delivery in addition to extend its application for cell imaging, tissue engineering, and regenerative medicine.

Overall it has been shown that enzymatically synthesized polyesters offer an interesting tool for the preparation of various biocompatible and biodegradable protein-polymer conjugates as well as polymeric networks with a great potential to be applied as carriers for controlled delivery of proteins and drugs.

## Bibliography

- [1]. Boni, R., Ali, A., Shavandi, A., and Clarkson, A. N. (2018). Current and novel polymeric biomaterials for neural tissue engineering. *J. Biomed. Sci.* 25, 90.
- [2]. Teo, A. J. T., Mishra, A., Park, I., Kim, Y. -J., Park, W. -T., and Yoon, Y. -J. (2016). Polymeric biomaterials for medical implants and devices. *ACS Biomater. Sci. Eng.* 2, 454–472.
- [3]. Gupta, S., Sharma, A., and Verma, R. S. (2020). Polymers in biosensor devices for cardiovascular applications. *Curr. Opin. Biomed. Eng.* 13, 69–75.
- [4]. Sung, Y. K. and Kim, S. W. (2020). Recent advances in polymeric drug delivery systems. *Biomater. Res.* 24, 12.
- [5]. Albertsson, A. C. and Varma, I. K. (2003). Recent developments in ring opening polymerization of lactones for biomedical applications. *Biomacromolecules* 4, 1466–1486.
- [6]. Seyednejad, H., Ghassemi, A. H., van Nostrum, C. F., Vermonden, T., and Hennink W. E. (2011). Functional aliphatic polyesters for biomedical and pharmaceutical applications. *J. Controlled Release* 152, 168–176.
- [7]. Díaz, A., Katsarava, R., and Puiggali, J. (2014). Synthesis, properties and applications of biodegradable polymers derived from diols and dicarboxylic acids: From polyesters to poly(ester amide)s. *Int. J. Mol. Sci.* 15, 7064–7123.
- [8]. Weiss, V. M., Naolou, T., Groth, T., Kressler, J., and Mäder, K. (2012). In vitro toxicity of stearyl-poly(glycerol adipate) nanoparticles. *J. Appl. Biomater. Function Mater.* 10, 163–169.
- [9]. Weiss, V. M., Lucas, H., Mueller, T., Chytil, P., Etrych, T., Naolou, T., Kressler, J., and Mäder, K. (2018). Intended and unintended targeting of polymeric nanocarriers: The case of modified poly(glycerol adipate) nanoparticles. *Macromol. Biosci.* 18, 1700240.
- [10]. Swainson, S. M. E., Taresco, V., Pearce, A. K., Clapp, L. H., Ager, B., McAllister, M., Bosquillon, C., and Garnett, M. C. (2019). Exploring the enzymatic degradation of poly(glycerol adipate). *Eur. J. Pharm. Biopharm.* 142, 377–386.
- [11]. Naves, L., Dhand, C., Almeida, L., Rajamani, L., Ramakrishna, S., and Soares, G. (2017). Poly(lactic-co-glycolic) acid drug delivery systems through transdermal pathway: An overview. *Prog. Biomater.* 6, 1–11.
- [12]. Emami, F., Mostafavi Yazdi, S. J., and Na, D. H. (2019). Poly(lactic acid)/poly(lactic-co-glycolic acid) particulate carriers for pulmonary drug delivery. *J. Pharm. Investig.* 49, 427–442.
- [13]. Su, Y., Zhang, B., Sun, R., Liu, W., Zhu, Q., Zhang, X., Wang, R., and Chen, C. (2021). PLGA-based biodegradable microspheres in drug delivery: Recent advances in research and application. *Drug Deliv.* 28, 1397–1418.

- [14]. Govender, T., Stolnik, S., Garnett, M. C., Illum, L., and Davis, S. S. (1999). PLGA nanoparticles prepared by nanoprecipitation: Drug loading and release studies of a water soluble drug. *J. Controlled Release* 57, 171–185.
- [15]. Dean Allison, S. (2008). Analysis of initial burst in PLGA microparticles. *Expert Opin. Drug Deliv.* 5, 615–628.
- [16]. Danhier, F., Ansorena, E., Silva, J. M., Coco, R., Breton, A. L., and Préat, V. (2012). PLGA-based nanoparticles: An overview of biomedical applications. *J. Controlled Release* 161, 505–522.
- [17]. Yoo, J. and Won, Y. Y. (2020). Phenomenology of the initial burst release of drugs from PLGA microparticles. *ACS Biomater. Sci. Eng.* 6, 6053–6062.
- [18]. Van de Weert, M., Hennink, W. E., and Jiskoot, W. (2000). Protein instability in poly(lactic-co-glycolic acid) microparticles. *Pharm. Res.* 17, 1159–1167.
- [19]. Ding, A. G. and Schwendeman, S. P. (2008). Acidic microclimate pH distribution in PLGA microspheres monitored by confocal laser scanning microscopy. *Pharm. Res.* 25, 2041–2052.
- [20]. Rosario-Meléndez, R., Yu, W., and Uhrich, K. E. (2013). Biodegradable polyesters containing ibuprofen and naproxen as pendant groups. *Biomacromolecules* 14, 3542–3548.
- [21]. Stebbins, N. D., Yu, W., and Uhrich, K. E. (2015). Enzymatic polymerization of an ibuprofen-containing monomer and subsequent drug release. *Macromol. Biosci.* 15, 1115–1124.
- [22]. Griffin, J., Delgado-Rivera, R., Meiners, S., and Uhrich, K. E. (2011). Salicylic acid-derived poly(anhydride-ester) electrospun fibers designed for regenerating the peripheral nervous system. *J. Biomed. Mater. Res. A* 97, 230–242.
- [23]. Kallinteri, P., Higgins, S., Hutcheon, G. A., St. Pourçain, C. B., and Garnett, M. C. (2005). Novel functionalized biodegradable polymers for nanoparticle drug delivery systems. *Biomacromolecules* 6, 1885–1894.
- [24]. Swainson, S. M. E., Styliari, I. D., Taresco, V., and Garnett, M. C. (2019). Poly(glycerol adipate) (PGA), an enzymatically synthesized functionalizable polyester and versatile drug delivery carrier: A literature update. *Polymers* 11, 1561.
- [25]. Bilal, M. H., Prehm, M., Njau, A. E., Samiullah, M. H., Meister, A., and Kressler, J. (2016). Enzymatic synthesis and characterization of hydrophilic sugar based polyesters and their modification with stearic acid. *Polymers* 8, 80.
- [26]. Rashid, H., Golitsyn, Y., Bilal, M. H., Mäder, K., Reichert, D., and Kressler, J. (2021). Polymer networks synthesized from poly(sorbitol adipate) and functionalized poly(ethylene glycol). *Gels* 7, 22.
- [27]. Alaneed, R., Hauenschild, T., Mäder, K., Pietzsch, M., and Kressler, J. (2020). Conjugation of amine-functionalized polyesters with dimethylcasein using microbial transglutaminase. *J. Pharm. Sci.* 109, 981–991.

- [28]. Alaneed, R., Naumann, M., Pietzsch, M., and Kressler, J. (2022). Microbial transglutaminase-mediated formation of erythropoietin-polyester conjugates. *J. Biotechnol.* *346*, 1–10.
- [29]. Olsson, A., Lindstro, M., and Iversen, T. (2007). Lipase-catalyzed synthesis of an epoxy-functionalized polyester from the suberin monomer cis-9,10-epoxy-18-hydroxyoctadecanoic acid. *Biomacromolecules* *8*, 757–760.
- [30]. Jiang, Y. and Loos, K. (2016). Enzymatic synthesis of biobased polyesters and polyamides. *Polymers (Basel)* *8*, 243.
- [31]. Gross, R. A., Ganesh, M., and Lu, W. (2010). Enzyme-catalysis breathes new life into polyester condensation polymerizations. *Trends Biotechnol.* *28*, 435–443.
- [32]. Stjerndahl, A., Wistrand, A. F., and Albertsson, A. -C. (2007). Industrial utilization of tin-initiated resorbable polymers: Synthesis on a large scale with a low amount of initiator residue. *Biomacromolecules* *8*, 937–940.
- [33]. Gross, R. A., Kumar, A., and Kalra, B. (2001). Polymer synthesis by in vitro enzyme catalysis. *Chem. Rev.* *101*, 2097–2124.
- [34]. Kobayashi, S. (2010). Lipase-catalyzed polyester synthesis— A green polymer chemistry. *Proc. Jpn. Acad. Ser. B* *86*, 338–365.
- [35]. Yu, Y., Wu, D., Liu, C., Zhao, Z., Yang, Y., and Li, Q. (2012). Lipase/esterase-catalyzed synthesis of aliphatic polyesters via polycondensation: A review. *Process Biochem.* *47*, 1027–1036.
- [36]. Kobayashi, S. (2015). Enzymatic ring-opening polymerization and polycondensation for the green synthesis of polyesters. *Polym. Adv. Technol.* *26*, 677–686.
- [37]. Liu, Y., Song, L., Feng, N., Jiang, W., Jin, Y., and Xuwen Li, X. (2020). Recent advances in the synthesis of biodegradable polyesters by sustainable polymerization: Lipase-catalyzed polymerization. *RSC Adv.* *10*, 36230.
- [38]. Wu, R., Al-Azemi, T. F., and Bisht, K. S. (2008). Functionalized polycarbonate derived from tartaric acid: Enzymatic ring-opening polymerization of a seven-membered cyclic carbonate. *Biomacromolecules* *9*, 2921–2928.
- [39]. Park, H. G., Do, J. H., and Chang, H. N. (2003). Regioselective enzymatic acylation of multi-hydroxyl compounds in organic synthesis. *Biotechnol. Bioprocess Eng.* *8*, 1–8.
- [40]. Hagström, A. E. V., Nordblad, M., and Adlercreutz, P. (2009). Biocatalytic polyester acrylation—process optimization and enzyme stability. *Biotechnol. Bioeng.* *102*, 693–699.
- [41]. Yang, Y., Yu, Y., Zhang, Y., Liu, C., Shi, W., and Li, Q. (2011). Lipase/esterase-catalyzed ring-opening polymerization: A green polyester synthesis technique. *Process Biochem.* *46*, 1900–1908.
- [42]. Stavila, E., van Ekenstein, G. O. R. A., Woortman, A. J. J., and Loos, K. (2014). Lipase-catalyzed ring-opening copolymerization of  $\epsilon$ -caprolactone and  $\beta$ -lactam. *Biomacromolecules* *15*, 234–241.

- [43]. Reetz, M. T. (2016). What are the limitations of enzymes in synthetic organic chemistry?. *Chem. Rec.* 16, 2449–2459.
- [44]. Kobayashi, S., Uyama, H., and Kimura, S. (2001). Enzymatic polymerization. *Chem. Rev.* 101, 3793–3818.
- [45]. Blanco, A. and Blanco, G. *Enzymes*. In *Medical Biochemistry*; Blanco, A. and Blanco, G., Eds.; Academic Press, 2017; pp. 153–175; Chapter 8.
- [46]. Fischer, E. (1894). Einfluss der configuration auf die wirkung der enzyme. *Ber. Dtsch. Chem. Ges.* 27, 2985–2993.
- [47]. McDonald, A. G. and Tipton, K. F. (2014). Fifty-five years of enzyme classification: Advances and difficulties. *FEBS J.* 281, 583–592.
- [48]. Ohtsuka, T., Sawa, A., Kawabata, R., Nio, N., and Motoki, M. (2000). Substrate specificities of microbial transglutaminase for primary amines. *J. Agric. Food Chem.* 48, 6230–6233.
- [49]. Lowe, M. E. (1997). Structure and function of pancreatic lipase and colipase. *Annu. Rev. Nutr.* 17, 141–158.
- [50]. Loos, K. In *Biocatalysis in Polymer Chemistry*; Loos, K., Ed.; Wiley-VCH Verlag GmbH & Co. KGaA: Weinheim, Germany, 2010; pp. i–xxix.
- [51]. Miletić, N., Loos, K., and Gross, R. A. *Enzymatic polymerization of polyester*. In *Biocatalysis in Polymer Chemistry*; Loos, K., Ed.; Wiley-VCH Verlag GmbH & Co. KGaA: Weinheim, Germany, 2010; pp. 83–129.
- [52]. Stavila, E. and Loos, K. (2015). Synthesis of polyamides and their copolymers via enzymatic polymerization. *J. Renew. Mater.* 3, 268–280.
- [53]. Hollmann, F. *Enzymatic polymerization of vinyl polymers*. In *Biocatalysis in Polymer Chemistry*; Loos, K., Ed.; Wiley-VCH Verlag GmbH & Co. KGaA: Weinheim, Germany, 2010; pp. 143–163.
- [54]. Ciric, J., Petrovic, D. M., and Loos, K. (2014). Polysaccharide biocatalysis: From synthesizing carbohydrate standards to establishing characterization methods. *Macromol. Chem. Phys.* 215, 931–944.
- [55]. Kapoor, M. and Gupta, M. N. (2012). Lipase promiscuity and its biochemical applications. *Process Biochem.* 47, 555–569.
- [56]. Kadokawa, J. and Kobayashi, S. (2010). Polymer synthesis by enzymatic catalysis. *Curr. Opin. Chem. Biol.* 14, 145–153.
- [57]. Szymczak, T., Cybulska, J., Podleśny, M., and Frąć, M. (2021). Various perspectives on microbial lipase production using agri-food waste and renewable products. *Agriculture* 11, 540.
- [58]. Okumura, S., Iwai, M., and Tominaga, Y. (1984). Synthesis of ester oligomer by *Aspergillus niger* lipase. *Agric. Biol. Chem.* 48, 2805–2808.
- [59]. Shoda, S., Uyama, H., Kadokawa, J., Kimura, S., and Kobayashi, S. (2016). Enzymes as green catalysts for precision macromolecular synthesis. *Chem. Rev.* 116, 2307–2413.

- [60]. Stauch, B., Fisher, S. J., and Cianci, M. (2015). Open and closed states of *Candida antarctica* lipase B: Protonation and the mechanism of interfacial activation. *J. Lipid Res.* 56, 2348–2358.
- [61]. Douka, A., Vouyiouka, S., Papaspyridi, L. -M., and Papaspyrides, C. D. (2018). A review on enzymatic polymerization to produce polycondensation polymers: The case of aliphatic polyesters, polyamides and polyesteramides. *Prog. Polym. Sci.* 79, 1–25.
- [62]. Hedfors, C., Hult, K., and Martinelle, M. (2010). Lipase chemoselectivity towards alcohol and thiol acyl acceptors in a transacylation reaction. *J. Mol. Catal. B Enzym.* 66, 120–123.
- [63]. Kline, B. J., Beckman, E. J., and Russell, A. J. (1998). One-step biocatalytic synthesis of linear polyesters with pendant hydroxyl groups. *J. Am. Chem. Soc.* 120, 9475–9480.
- [64]. Sharma, R. K., Aggarwal, N., Arya, A., Olsen, C. E., Parmar, V. S., and Prasad, A. K. (2009). Lipase-catalyzed regio- and stereoselective deacylation: Separation of anomers of peracylated  $\alpha,\beta$ -D-ribofuranosides. *Indian J. Chem.* 48B, 1727–1731.
- [65]. Uppenberg, J., Trier Hanse, M., Patkar, S., and Jones, T. A. (1994). The sequence, crystal structure determination and refinement of two crystal forms of lipase B from *Candida antarctica*. *Structure* 2, 293–308.
- [66]. Xie, Y., An, J., Yang, G., Wu, G., Zhang, Y., Cui, L., and Feng, Y. (2014). Enhanced enzyme kinetic stability by increasing rigidity within the active site. *J. Biol. Chem.* 289, 7994–8006.
- [67]. Bezborodov, A. M. and Zagustina, N. A. (2014). Lipases in catalytic reactions of organic chemistry. *Appl. Biochem. Microbiol.* 50, 313–337.
- [68]. Zisis, T., Freddolino, P. L., Turunen, P., van Teeseling, M. C. F., Rowan, A. E., and Blank, K. G. (2015). Interfacial activation of *Candida antarctica* lipase B: Combined evidence from experiment and simulation. *Biochemistry* 54, 5969–5979.
- [69]. Castillo, E., Casas-Godoy, L., and Sandoval, G. (2016). Medium-engineering: A useful tool for modulating lipase activity and selectivity. *Biocatalysis* 1, 178–188.
- [70]. Sheldon, R. A. and van Pelt, S. (2013). Enzyme immobilisation in biocatalysis: Why, what and how. *Chem. Soc. Rev.* 42, 6223–6235.
- [71]. Franssen, M. C. R., Steunenberg, P., Scott, E. L., Zuilhof, H., and Sanders, J. P. M. (2013). Immobilised enzymes in biorenewables production. *Chem. Soc. Rev.* 42, 6491–6533.
- [72]. Miletic´, N., Nastasovic´, A., and Loos, K. (2012). Immobilization of biocatalysts for enzymatic polymerizations: Possibilities, advantages, applications. *Bioresour. Technol.* 115, 126–135.
- [73]. Mahapatro, A., Kumar, A., Kalra, B., and Gross, R. A. (2004). Solvent-free adipic acid/1,8-octanediol condensation polymerizations catalyzed by *Candida antartica* lipase B. *Macromolecules* 37, 35–40.
- [74]. Ortiz, C., Ferreira, M. L., Barbosa, O., dos Santos, J. C. S., Rodrigues, R. C., Berenguer-Murcia, Á., Briand, L. E., and Fernandez-Lafuente, R. (2019). Novozym 435: The “perfect” lipase immobilized biocatalyst?. *Catal. Sci. Technol.* 9, 2380–2420.

- [75]. Uyama, H., Inada, K., and Kobayashi, S. (2000). Lipase-catalyzed synthesis of aliphatic polyesters by polycondensation of dicarboxylic acids and glycols in solvent-free system. *Polym. J.* 32, 440–443.
- [76]. Kanelli, M., Douka, A., Vouyiouka, S., Papaspyrides, C. D., Topakas, E., Papaspyridi, L. -M., and Christakopoulos, P. (2014). Production of biodegradable polyesters via enzymatic polymerization and solid state finishing. *J. Appl. Polym. Sci.* 131, 40820.
- [77]. Perin, G. B. and Felisberti, M. I. (2020). Enzymatic synthesis of poly(glycerol sebacate): Kinetics, chain growth, and branching behavior. *Macromolecules* 53, 7925–7935.
- [78]. Varma, I. K., Albertsson, A. -C., Rajkhowa, R., and Srivastava, R. K. (2005). Enzyme catalyzed synthesis of polyesters. *Prog. Polym. Sci.* 30, 949–981.
- [79]. Hunsen, M., Azim, A., Mang, H., Wallner, S. R., Ronkvist, A., Xie, W., and Gross, R. A. (2007). A cutinase with polyester synthesis activity. *Macromolecules* 40, 148–150.
- [80]. Azim, H., Dekhterman, A., Jiang, Z., and Gross, R. A. (2006). *Candida antarctica* lipase B-catalyzed synthesis of poly(butylene succinate): Shorter chain building blocks also work. *Biomacromolecules* 7, 3093–3097.
- [81]. Wu, W. -X., Li, J., Yang, X. -L., Wang, N., and Yu, X. -Q. (2019). Lipase-catalyzed synthesis of renewable acid-degradable poly( $\beta$ -thioether ester) and poly( $\beta$ -thioether ester-co-ricinoleic acid) copolymers derived from castor oil. *Eur. Polym. J.* 121, 109315.
- [82]. Taresco, V., Creasey, R. G., Kennon, J., Mantovani, G., Alexander, C., Burley, J. C., and Garnett, M. C. (2016). Variation in structure and properties of poly(glycerol adipate) via control of chain branching during enzymatic synthesis. *Polymer* 89, 41–49.
- [83]. Dong, H., Cao, S. -G., Li, Z. -Q., Han, S. -P., You, D. -L., and Shen, J. -C. (1999). Study on the enzymatic polymerization mechanism of lactone and the strategy for improving the degree of polymerization. *J. Polym. Sci. A* 37, 1265–1275.
- [84]. Kumar, A. and Gross, R. A. (2000). *Candida antartica* lipase B catalyzed polycaprolactone synthesis: Effects of organic media and temperature. *Biomacromolecules* 1, 133–138.
- [85]. Linko, Y. -Y., Wang, Z. -L., and Seppälä, J. (1995). Lipase-catalyzed synthesis of poly(1,4-butyl sebacate) from sebacic acid or its derivatives with 1,4-butanediol. *J. Biotechnol.* 40, 133–138.
- [86]. Jiang, Y., Woortman, A. J. J., van Ekenstein, G. O. R. A., and Loos, K. (2013). Enzyme-catalyzed synthesis of unsaturated aliphatic polyesters based on green monomers from renewable resources. *Biomolecules* 3, 461–480.
- [87]. Yoshizawa-Fujita, M., Saito, C., Takeoka, Y., and Rikukawa, M. (2008). Lipase-catalyzed polymerization of L-lactide in ionic liquids. *Polym. Adv. Technol.* 19, 1396–1400.
- [88]. Uyama, H., Inada, K., and Kobayashi, S. (1999). Regioselective polymerization of divinyl sebacate and triols using lipase catalyst. *Macromol. Rapid Commun.* 20, 171–174.
- [89]. Lang, K., Bhattacharya, S., Ning, Z., Sánchez-Leija, R. J., Bramson, M. T. K., Centore, R., Corr, D. T., Linhardt, R. J., and Gross, R. A. (2020). Enzymatic polymerization of poly(glycerol-1,8-

- octanediol-sebacate): Versatile poly(glycerol sebacate) analogues that form monocomponent biodegradable fiber scaffolds. *Biomacromolecules* 21, 3197–3206.
- [90]. Chaudhary, A. K., Lopez, J., Beckman, E. J., and Russell, A. J. (1997). Biocatalytic solvent-free polymerization to produce high molecular weight polyesters. *Biotechnol. Prog.* 13, 318–325.
- [91]. Uyama, H. and Kobayashi, S. (1994). Lipase-catalyzed polymerization of divinyl adipate with glycols to polyesters. *Chem. Lett.* 23, 1687–1690.
- [92]. Mahapatro, A., Kalra, B., Kumar, A., and Gross, R. A. (2003). Lipase-catalyzed polycondensations: Effect of substrates and solvent on chain formation, dispersity, and end-group structure. *Biomacromolecules* 4, 544–551.
- [93]. Yadav, G. D. and Trivedi, A. H. (2003). Kinetic modeling of immobilized-lipase catalyzed transesterification of *n*-octanol with vinyl acetate in non-aqueous media. *Enzyme Microb. Technol.* 32, 783–789.
- [94]. Yadav, G. D. and Lathi, P. S. (2005). Lipase catalyzed transesterification of methyl acetoacetate with *n*-butanol. *J. Mol. Catal. B: Enzym.* 32, 107–113.
- [95]. Rizzi, M., Stylos, P., Riek, A., and Reuss, M. (1992). A kinetic study of immobilized lipase catalysing the synthesis of isoamyl acetate by transesterification in *n*-hexane. *Enzyme Microb. Technol.* 14, 709–714.
- [96]. Yang, Y., Lu, W., Cai, J., Hou, Y., Ouyang, S., Xie, W., and Gross, R. A. (2011). Poly(oleic diacid-co-glycerol): Comparison of polymer structure resulting from chemical and lipase catalysis. *Macromolecules* 44, 1977–1985.
- [97]. Uyama, H. and Kobayashi, S. (2002). Enzyme-catalyzed polymerization to functional polymers. *J. Mol. Catal. B Enzym.* 19–20, 117–127.
- [98]. Kobayashi, S. (2009). Recent developments in lipase-catalyzed synthesis of polyesters. *Macromol. Rapid Commun.* 30, 237–266.
- [99]. Meier, M. A. R., Metzger, J. O., and Schubert, U. S. (2007). Plant oil renewable resources as green alternatives in polymer science. *Chem. Soc. Rev.* 36, 1788–1802.
- [100]. Montero de Espinosa, L. and Meier, M. A. R. (2011). Plant oils: The perfect renewable resource for polymer science?!. *Eur. Polym. J.* 47, 837–852.
- [101]. Tsujimoto, T., Uyama, H., and Kobayashi, S. (2000). Enzymatic synthesis of cross-linkable polyesters from renewable resources. *Biomacromolecules* 2, 29–31.
- [102]. Park, O. -J., Kim, D. -Y., and Dordick, J. S. (2000). Enzyme-catalyzed synthesis of sugar-containing monomers and linear polymers. *Biotechnol. Bioeng.* 70, 208–216.
- [103]. Wang, Y. -F., Lalonde, J. J., Momongan, M., Bergbreiter, D. E., and Wong, C. -H. (1988). Lipase-catalyzed irreversible transesterifications using enol esters as acylating reagents: Preparative enantio- and regioselective syntheses of alcohols, glycerol derivatives, sugars, and organometallics. *J. Am. Chem. Soc.* 110, 7200–7205.

- [104]. Naolou, T., Weiss, V. M., Conrad, D., Busse, K., Mäder, K., and Kressler, J. *Fatty acid modified poly(glycerol adipate): polymeric analogues of glycerides*. In *Tailored Polymer Architectures for Pharmaceutical and Biomedical Applications*; Scholz, C. and Kressler, J., Eds.; American Chemical Society, Washington, DC, 2013; Vol. 1135; pp. 39–52.
- [105]. Urszula Piotrowska, U. and Sobczak, M. (2015). Enzymatic polymerization of cyclic monomers in ionic liquids as a prospective synthesis method for polyesters used in drug delivery systems. *Molecules* 20, 1–23.
- [106]. Uyama, H. and Kobayashi, S. (1993). Enzymatic ring-opening polymerization of lactones catalyzed by lipase. *Chem. Lett.* 22, 1149–1150.
- [107]. Uyama, H., Takeya, K., and Kobayashi, S. (1993). Synthesis of polyesters by enzymatic ring-opening copolymerization using lipase catalyst. *Proc. Jpn. Acad., Ser. B* 69, 203–207.
- [108]. Knani, D., Gutman, A. L., and Kohn, D. H. (1993). Enzymatic polyesterification in organic media. Enzyme-catalyzed synthesis of linear polyesters. I. Condensation polymerization of linear hydroxyesters. II. Ring-opening polymerization of  $\epsilon$ -caprolactone. *J. Polym. Sci., Part A: Polym. Chem.* 31, 1221–1232.
- [109]. Uyama, H., Namekawa, S., and Kobayash, S. (1997). Mechanistic studies on the lipase-catalyzed ring-opening polymerization of lactones. *Polym. J.* 29, 299–301.
- [110]. van Der Mee, L., Helmich, F., De Bruijn, R., Vekemans, J. A. J. M., Palmans, A. R. A., and Meijer, E. W. (2006). Investigation of lipase-catalyzed ring-opening polymerizations of lactones with various ring sizes: Kinetic evaluation. *Macromolecules* 39, 5021–5027.
- [111]. Namekawa, S., Uyama, H., and Kobayashi, S. (2000). Enzymatic synthesis of polyesters from lactones, dicarboxylic acid divinyl esters, and glycols through combination of ring-opening polymerization and polycondensation. *Biomacromolecules* 1, 335–338.
- [112]. Feng, C., Li, Y., Yang, D., Hu, J., Zhang, X., and Huang, X. (2011). Well-defined graft copolymers: From controlled synthesis to multipurpose applications. *Chem. Soc. Rev.* 40, 1282–1295.
- [113]. Li, C., Ge, Z., Fang, J., and Liu, S. (2009). Synthesis and self-assembly of coil-rod double hydrophilic diblock copolymer with dually responsive asymmetric centipede-shaped polymer brush as the rod segment. *Macromolecules* 42, 2916–2924.
- [114]. Williams, C. K. (2007). Synthesis of functionalized biodegradable polyesters. *Chem. Soc. Rev.* 36, 1573–1580.
- [115]. Parrish, B., Breitenkamp, R. B., and Emrick, T. (2005). PEG- and peptide-grafted aliphatic polyesters by click chemistry. *J. Am. Chem. Soc.* 127, 7404–7410.
- [116]. Lenoir, S., Riva, R., Lou, X., Detrembleur, C., Jérôme, R., and Lecomte, P. (2004). Ring-opening polymerization of  $\alpha$ -chloro- $\epsilon$ -caprolactone and chemical modification of poly( $\alpha$ -chloro- $\epsilon$ -caprolactone) by atom transfer radical processes. *Macromolecules* 37, 4055–4061.

- [117]. Riva, R., Schmeits, S., Jérôme, C., Jérôme, R., and Lecomte, P. (2007). Combination of ring-opening polymerization and “click chemistry”: Toward functionalization and grafting of poly( $\epsilon$ -caprolactone). *Macromolecules* 40, 796–803.
- [118]. Naolou, T., Busse, K., and Kressler, J. (2010). Synthesis of well-defined graft copolymers by combination of enzymatic polycondensation and “click” chemistry. *Biomacromolecules* 11, 3660–3667.
- [119]. Orafi, H., Kallinteri, P., Garnett, M., Huggins, S., Hutcheon, G., and Pourcain, C. (2008). Novel poly(glycerol adipate) polymers used for nanoparticle making: A study of surface free energy. *Iran. J. Pharm. Res.* 7, 11–19.
- [120]. Weiss, V. M., Naolou, T., Hause, G., Kuntsche, J., Kressler, J., and Mäder, K. (2012). Poly(glycerol adipate)-fatty acid esters as versatile nanocarriers: From nanocubes over ellipsoids to nanospheres. *J. Control. Release* 158, 156–164.
- [121]. Weiss, V. M., Naolou, T., Amado, E., Busse, K., Mäder, K., and Kressler, J. (2012). Formation of structured polygonal nanoparticles by phase-separated comb-like polymers. *Macromol. Rapid Commun.* 33, 35–40.
- [122]. Naolou, T., Hussain, H., Baleed, S., Busse, K., Lechner, B. D., and Kressler, J. (2015). The behavior of fatty acid modified poly(glycerol adipate) at the air/water interface. *Colloids Surfaces A Physicochem. Eng. Asp.* 468, 22–30.
- [123]. Naolou, T., Meister, A., Schöps, R., Pietzsch, M., and Kressler, J. (2013). Synthesis and characterization of graft copolymers able to form polymersomes and worm-like aggregates. *Soft Matter* 9, 10364.
- [124]. Pfefferkorn, D., Pulst, M., Naolou, T., Busse, K., Balko, J., and Kressler, J. (2013). Crystallization and melting of poly(glycerol adipate)-based graft copolymers with single and double crystallizable side chains. *J. Polym. Sci. Part B Polym. Phys.* 51, 1581–1591.
- [125]. Naolou, T., Busse, K., Lechner, B. D., and Kressler, J. (2014). The behavior of poly( $\epsilon$ -caprolactone) and poly(ethylene oxide)-b-poly( $\epsilon$ -caprolactone) grafted to a poly(glycerol adipate) backbone at the air/water interface. *Colloid Polym. Sci.* 292, 1199–1208.
- [126]. Tawfeek, H., Khidr, S., Samy, E., Ahmed, S., Murphy, M., Mohammed, A., Shabir, A., Hutcheon, G., and Saleem, I. (2011). Poly(glycerol adipate-co- $\omega$ -pentadecalactone) spray-dried microparticles as sustained release carriers for pulmonary delivery. *Pharm. Res.* 28, 2086–2097.
- [127]. Tawfeek, H. M., Evans, A. R., Iftikhar, A., Mohammed, A. R., Shabir, A., Somavarapu, S., Hutcheon, G. A., and Saleem, I. Y. (2013). Dry powder inhalation of macromolecules using novel PEG-co-polyester microparticle carriers. *Int. J. Pharm.* 441, 611–619.
- [128]. Mohamed, A., Kunda, N. K., Ross, K., Hutcheon, G. A., and Saleem, I. Y. (2019). Polymeric nanoparticles for the delivery of miRNA to treat chronic obstructive pulmonary disease (COPD). *Eur. J. Pharm. Biopharm.* 136, 1–8.

- [129]. Jbeily, M., Naolou, T., Bilal, M., Amado, E., and Kressler, J. (2014). Enzymatically synthesized polyesters with pendent OH groups as macroinitiators for the preparation of well-defined graft copolymers by atom transfer radical polymerization. *Polym. Int.* 63, 894–901.
- [130]. Bilal, M., Alaneed, R., Steiner, J., Mäder, K., Pietzsch, M., and Kressler, J. *Multiple grafting to enzymatically synthesized polyesters*. In *Methods in Enzymology*; Bruns, N. and Loos, K., Eds.; Elsevier: Amsterdam, Netherlands, 2019; Volume 627, pp. 57–97.
- [131]. Thompson, C. J., Hansford, D., and Munday, D. L. (2008). Synthesis and evaluation of novel polyester-ibuprofen conjugates for modified drug release. *Drug Dev. Ind. Pharm.* 34, 877–884.
- [132]. Wersig, T., Hacker, M. C., Kressler, J., and Mäder, K. (2017). Poly(glycerol adipate)–indomethacin drug conjugates – synthesis and *in vitro* characterization. *Int. J. Pharm.* 531, 225–234.
- [133]. Suksiriworapong, J., Taresco, V., Ivanov, D. P., Styliari, I. D., Sakchaisri, K., Junyaprasert, V. B., and Garnett, M. C. (2018). Synthesis and properties of a biodegradable polymer-drug conjugate: Methotrexate-poly(glycerol adipate). *Colloids Surf. B Biointerfaces* 167, 115–125.
- [134]. Duncan, R. (2003). The dawning era of polymer therapeutics. *Nat. Rev. Drug Discov.* 2, 347–360.
- [135]. Leader, B., Baca, Q. J., and Golan, D. E. (2008). Protein therapeutics: A summary and pharmacological classification. *Nat. Rev. Drug Discov.* 7, 21–39.
- [136]. Zhao, W., Liu, F., Chen, Y., Bai, J., and Gao, W. (2015). Synthesis of well-defined protein-polymer conjugates for biomedicine. *Polymer* 66, A1–A10.
- [137]. Graber, S. E. and Krantz, S. B. (1978). Erythropoietin and control of red-cell production. *Annu. Rev. Med.* 29, 51–66.
- [138]. Cody, J. D. and Hodson, E. M. (2016). Recombinant human erythropoietin versus placebo or no treatment for the anaemia of chronic kidney disease in people not requiring dialysis. *Cochrane Database Syst. Rev.* 1, CD003266.
- [139]. Suresh, S., Rajvanshi, P. K., and Noguchi, C. T. (2020). The Many facets of erythropoietin physiologic and metabolic response. *Front. Physiol.* 10, 1534.
- [140]. Su, D., Zhao, H., and Xia, H. (2010). Glycosylation-modified erythropoietin with improved half-life and biological activity. *Int. J. Hematol.* 91, 238–244.
- [141]. Zaman, R., Islam, R. A., Ibnat, N., Othman, I., Zaini, A., Lee, C. Y., and Chowdhury, E. H. (2019). Current strategies in extending half-lives of therapeutic proteins. *J. Control Release* 301, 176–189.
- [142]. Takahara, M., Mochizuki, S., Wakabayashi, R., Minamihata, K., Goto, M., Sakurai, K., and Kamiya, N. (2021). Extending the half-life of a protein *in vivo* by enzymatic labeling with amphiphilic lipopeptides. *Bioconjugate Chem.* 32, 655–660.
- [143]. Thordarson, P., Le Droumaguet, B., and Velonia, K. (2006). Well-defined protein-polymer conjugates-synthesis and potential applications. *Appl. Microbiol. Biotechnol.* 73, 243–254.

- [144]. Abuchowski, A., van Es, T., Palczuk, N. C., and Davis, F. F. (1977). Alteration of immunological properties of bovine serum albumin by covalent attachment of polyethylene glycol. *J. Biol. Chem.* 252, 3578–3581.
- [145]. Abuchowski, A., McCoy, J. R., Palczuk, N. C., van Es, T., and Davis, F. F. (1977). Effect of covalent attachment of polyethylene glycol on immunogenicity and circulating life of bovine liver catalase. *J. Biol. Chem.* 252, 3582–3586.
- [146]. Do, B. H., Kang, H. J., Song, J. A., Nguyen, M. T., Park, S., Yoo, J., Nguyen, A. N., Kwon, G. G., Jang, J., Jang, M., et al. (2017). Granulocyte colony-stimulating factor (GCSF) fused with Fc domain produced from *E. coli* is less effective than polyethylene glycol-conjugated GCSF. *Sci. Rep.* 7, 6480.
- [147]. Cao, X., Chen, Z., Yu, Z., Ge, Y., and Zeng, X. (2014). Pharmacokinetics of PEGylated recombinant human erythropoietin in rats. *J. Anal. Methods Chem.* 2014, 918686.
- [148]. Hoffmann, E., Streichert, K., Nischan, N., Seitz, C., Brunner, T., Schwagerus, S., Hackenberger, C. P. R., and Rubini, M. (2016). Stabilization of bacterially expressed erythropoietin by single site-specific introduction of short branched PEG chains at naturally occurring glycosylation sites. *Mol. BioSyst.* 12, 1750–1755.
- [149]. Hinds, K., Koh, J. J., Joss, L., Liu, F., Baudyš, M., and Kim, S. W. (2000). Synthesis and characterization of poly(ethylene glycol)-insulin conjugates. *Bioconjugate Chem.* 11, 195–201.
- [150]. Knop, K., Hoogenboom, R., Fischer, D., and Schubert, U. S. (2010). Poly(ethylene glycol) in drug delivery: Pros and cons as well as potential alternatives. *Angew. Chem. Int. Ed. Engl.* 49, 6288–6308.
- [151]. Xu, L., Yang, J. P., Xue, B., Zhang, C., Shi, L. L., Wu, C. W., Su, Y., Jin, X., Liu, Y. M., and Zhu, X. Y. (2017). Molecular insights for the biological interactions between polyethylene glycol and cells. *Biomaterials* 147, 1–13.
- [152]. Abu Lila, A. S., Kiwada, H., and Ishida, T. (2013). The accelerated blood clearance (ABC) phenomenon: Clinical challenge and approaches to manage. *J. Controlled Release* 172, 38–47.
- [153]. Zhang, P., Sun, F., Liu, S., and Jiang, S. (2016). Anti-PEG antibodies in the clinic: Current issues and beyond PEGylation. *J. Controlled Release* 244, 184–193.
- [154]. Mohamed, M., Abu Lila A. S., Shimizu, T., Alaaeldin, E., Hussein, A., Sarhan, H. A., Szebeni, J., and Ishida, T. (2019). PEGylated liposomes: Immunological responses. *Sci. Technol. Adv. Mater.* 20, 710–724.
- [155]. Hou, Y. and Lu, H. (2019). Protein PEPylation: A new paradigm of protein–polymer conjugation. *Bioconjugate Chem.* 30, 1604–1616.
- [156]. Ge, J., Yan, M., Lu, D., Zhang, M., and Liu, Z. (2007). Hyperbranched polymer conjugated lipase with enhanced activity and stability. *Biochem. Eng. J.* 36, 93–99.
- [157]. Canalle, L. A., Löwik, D. W. P. M., and van Hest, J. C. M. (2010). Polypeptide–polymer bioconjugates. *Chem. Soc. Rev.* 39, 329–353.

- [158]. Broyer, R. M., Grover, G. N., and Maynard, H. D. (2011). Emerging synthetic approaches for protein–polymer conjugations. *Chem. Commun.* *47*, 2212–2226.
- [159]. Stenzel, M. H. (2013). Bioconjugation using thiols: Old chemistry rediscovered to connect polymers with nature’s building blocks. *ACS Macro Lett.* *2*, 14–18.
- [160]. Joshi, N. S., Whitaker, L. R., and Francis, M. B. (2004). A three-component Mannich-type reaction for selective tyrosine bioconjugation. *J. Am. Chem. Soc.* *126*, 15942–15943.
- [161]. Gilmore, J. M., Scheck, R. A., Esser-Kahn, A. P., Joshi, N. S., and Francis, M. B. (2006). N-terminal protein modification through a biomimetic transamination reaction. *Angew. Chem. Int. Ed.* *45*, 5307–5311.
- [162]. Chen, C., Ng, D. Y. W., and Weil, T. (2020). Polymer bioconjugates: Modern design concepts toward precision hybrid materials. *Prog. Polym. Sci.* *105*, 101241.
- [163]. Gao, W. P., Liu, W. G., Mackay, J. A., Zalutsky, M. R., Toone, E. J., and Chilkoti, A. (2009). In situ growth of a stoichiometric PEG-like conjugate at a protein’s N-terminus with significantly improved pharmacokinetics. *Proc. Natl. Acad. Sci. U S A* *106*, 15231–15236.
- [164]. Gao, W. P., Liu, W. G., Christensen, T., Zalutsky, M. R., and Chilkoti, A. (2010). In situ growth of a PEG-like polymer from the C terminus of an intein fusion protein improves pharmacokinetics and tumor accumulation. *Proc. Natl. Acad. Sci. U S A* *107*, 16432–16437.
- [165]. Yin, J., Liu, F., Li, X., and Walsh, C. T. (2004). Labeling proteins with small molecules by site-specific posttranslational modification. *J. Am. Chem. Soc.* *126*, 7754–7755.
- [166]. Wu, P., Shui, W., Carlson, B. L., Hu, N., Rabuka, D., Lee, J., and Bertozzi, C. R. (2009). Site-specific chemical modification of recombinant proteins produced in mammalian cells by using the genetically encoded aldehyde tag. *Proc. Natl. Acad. Sci. U S A* *106*, 3000–3005.
- [167]. Tanaka, T., Yamamoto, T., Tsukiji, S., and Nagamune, T. (2008). Site-specific protein modification on living cells catalyzed by sortase. *ChemBioChem.* *9*, 802–807.
- [168]. Rashidian, M., Dozier, J. K., Lenevich, S., and Distefano, M. D. (2010). Selective labeling of polypeptides using protein farnesyltransferase via rapid oxime ligation. *Chem. Commun.* *46*, 8998–9000.
- [169]. Sueda, S., Yoneda, S., and Hayashi, H. (2011). Site-specific labeling of proteins by using biotin protein ligase conjugated with fluorophores. *ChemBioChem.* *12*, 1367–1375.
- [170]. Cohen, J. D., Zou, P., and Ting, A. Y. (2012). Site-specific protein modification using lipoic acid ligase and bis-aryl hydrazine formation. *ChemBioChem.* *13*, 888–894.
- [171]. Heal, W. P., Wickramasinghe, S. R., Leatherbarrow, R. J., and Tate, E. W. (2008). N-Myristoyl transferase-mediated protein labelling in vivo. *Org. Biomol. Chem.* *6*, 2308.
- [172]. Sato, H. (2002). Enzymatic procedure for site-specific pegylation of proteins. *Adv. Drug Deliv. Rev.* *54*, 487–504.
- [173]. Rashidian, M., Dozier, J. K., and Distefano, M. D. (2013). Enzymatic labeling of proteins: Techniques and approaches. *Bioconjugate Chem.* *24*, 1277–1294.

- [174]. Strop, P. (2014). Versatility of microbial transglutaminase. *Bioconjugate Chem.* 25, 855–862.
- [175]. Facchiano, A. and Facchiano, F. (2009). Transglutaminases and their substrates in biology and human diseases: 50 years of growing. *Amino Acids* 36, 599–614.
- [176]. Kieliszek, M. and Misiewicz, A. (2014). Microbial transglutaminase and its application in the food industry. A review. *Folia Microbiol.* 59, 241–250.
- [177]. Ando, H., Adachi, M., Umeda, K., Matsuura, A., Nonaka, M., Uchio, R., Tanaka, H., and Motoki, M. (1989). Purification and characteristics of a novel transglutaminase derived from microorganisms. *Agric. Biol. Chem.* 53, 2613–2617.
- [178]. Kashiwagi, T., Yokoyama, K., Ishikawa, K., Ono, K., Ejima, D., Matsui, H., and Suzuki, E. (2002). Crystal structure of microbial transglutaminase from *Streptovorticillium mobaraense*. *J. Biol. Chem.* 277, 44252–44260.
- [179]. Malešević, M., Migge, A., Hertel, T. C., and Pietzsch, M. (2015). A fluorescence-based array screen for transglutaminase substrates. *ChemBioChem.* 16, 1169–1174.
- [180]. Spolaore, B., Damiano, N., Raboni, S., and Fontana, A. (2014). Site-specific derivatization of avidin using microbial transglutaminase. *Bioconjugate Chem.* 25, 470–480.
- [181]. Spolaore, B., Raboni, S., Satwekar, A. A., Grigoletto, A., Mero, A., Montagner, I. M., Rosato, A., Pasut, G., and Fontana, A. (2016). Site-specific transglutaminase-mediated conjugation of interferon  $\alpha$ -2b at glutamine or lysine residues. *Bioconjugate Chem.* 27, 2695–2706.
- [182]. Mariniello, L. and Porta, R. (2005). Transglutaminases as biotechnological tools. *Prog. Exp. Tumor Res.* 38, 174–191.
- [183]. Akbari, M., Razavi, S. H., and Kieliszek, M. (2021). Recent advances in microbial transglutaminase biosynthesis and its application in the food industry. *Trends Food Sci. Technol.* 110, 458–469.
- [184]. Cardamone, J. M. (2007). Enzyme-mediated crosslinking of wool. Part I: transglutaminase. *Text. Res. J.* 77, 214–221.
- [185]. Patzsch, K., Riedel, K., and Pietzsch, M. (2010). Parameter optimization for protein film production using microbial transglutaminase. *Biomacromolecules* 11, 896–903.
- [186]. Sato, H., Hayashi, E., Yamada, N., Yatagai, M., and Takahara, Y. (2001). Further studies on the site-specific protein modification by microbial transglutaminase. *Bioconjugate Chem.* 12, 701–710.
- [187]. Maullu, C., Raimondo, D., Caboi, F., Giorgetti, A., Sergi, M., Valentini, M., Tonon, G., and Tramontano, A. (2009). Site-directed enzymatic PEGylation of the human granulocyte colony-stimulating factor. *FEBS J.* 276, 6741–6750.
- [188]. Mero, A., Spolaore, B., Veronese, F. M., and Fontana, A. (2009). Transglutaminase-mediated PEGylation of proteins: Direct identification of the sites of protein modification by mass spectrometry using a novel monodisperse PEG. *Bioconjugate Chem.* 20, 384–389.

- [189]. Mero, A., Schiavon, M., Veronese, F. M., and Pasut, G. (2011). A new method to increase selectivity of transglutaminase mediated PEGylation of salmon calcitonin and human growth hormone. *J. Controlled Release* 154, 27–34.
- [190]. Zhou, J. Q., He, T., and Wang, J. W. (2016). PEGylation of cytochrome *c* at the level of lysine residues mediated by a microbial transglutaminase. *Biotechnol. Lett.* 38, 1121–1129.
- [191]. Besheer, A., Hertel, T. C., Kressler, J., Mäder, K., and Pietzsch, M. (2009). Enzymatically catalyzed HES conjugation using microbial transglutaminase: Proof of feasibility. *J. Pharm. Sci.* 98, 4420–4428.
- [192]. Wakabayashi, R., Yahiro, K., Hayashi, K., Masahiro Goto, M., and Kamiya, N. (2017). Protein-grafted polymers prepared through a site-specific conjugation by microbial transglutaminase for an immunosorbent assay. *Biomacromolecules* 18, 422–430.
- [193]. Takahara, M., Wakabayashi, R., Minamihata, K., Goto, M., and Kamiya, N. (2017). Primary amine-clustered DNA aptamer for DNA–protein conjugation catalyzed by microbial transglutaminase. *Bioconjugate Chem.* 28, 2954–2961.
- [194]. Strop, P., Liu, S. H., Dorywalska, M., Delaria, K., Dushin, R. G., Tran, T. T., Ho, W. H., Farias, S., Casas, M. G., Abdiche, Y., et al. (2013). Location matters: Site of conjugation modulates stability and pharmacokinetics of antibody drug conjugates. *Chem. Biol.* 20, 161–167.
- [195]. Dickgiesser, S., Rieker, M., Mueller-Pompalla, D., Schröter, C., Tonillo, J., Warszawski, S., Raab-Westphal, S., Kühn, S., Knehans, T., Könning, D., et al. (2020). Site-specific conjugation of native antibodies using engineered microbial transglutaminases. *Bioconjugate Chem.* 31, 1070–1076.
- [196]. Kamiya, N., Doi, S., Tominaga, J., Ichinose, H., and Goto, M. (2005). Transglutaminase-mediated protein immobilization to casein nanolayers created on a plastic surface. *Biomacromolecules* 6, 35–38.
- [197]. Moriyama, K., Sung, K., Goto, M., and Kamiya, M. (2011). Immobilization of alkaline phosphatase on magnetic particles by site-specific and covalent cross-linking catalyzed by microbial transglutaminase. *J. Biosci. Bioeng.* 111, 650–653.
- [198]. Marx, C. K., Hertel, T. C., and Pietzsch, M. (2008). Random mutagenesis of a recombinant microbial transglutaminase for the generation of thermostable and heat-sensitive variants. *J. Biotechnol.* 136, 156–162.
- [199]. Buettner, K., Hertel, T. C., and Pietzsch, M. (2011). Increased thermostability of microbial transglutaminase by combination of several hot spots evolved by random and saturation mutagenesis. *Amino Acids* 42, 987–996.
- [200]. Liu, Y., Huang, L., Shan, M., Sang, J., Li, Y., Jia, L., Wang, N., Wang, S., Shao, S., Liu, F., et al. (2019). Enhancing the activity and thermostability of *Streptomyces mobaraensis* transglutaminase by directed evolution and molecular dynamics simulation. *Biochem. Eng. J.* 151, 107333.

- [201]. Jiang, Y., Shang, Y. P., Li, H., Zhang, C., Pan, J., Bai, Y. P., Li, C. X., and Xu, J. H. (2017). Enhancing transglutaminase production of *Streptomyces mobaraensis* by iterative mutagenesis breeding with atmospheric and room-temperature plasma (ARTP). *Bioresour. Bioprocess.* 4, 37.
- [202]. Ohtake, K., Mukai, T., Iraha, F., Takahashi, M., Ken-ichi Haruna, K. -i., Date, M., Yokoyama, K., and Sakamoto, K. (2018). Engineering an automaturing transglutaminase with enhanced thermostability by genetic code expansion with two codon reassignments. *ACS Synth. Biol.* 7, 2170–2176.
- [203]. Böhme, B., Moritz, B., Wendler, J., Hertel, T. C., Ihling, C., Brandt, W., and Pietzsch, M. (2020). Enzymatic activity and thermoresistance of improved microbial transglutaminase variants. *Amino Acids* 52, 313–326.
- [204]. Gu, Y., Zhao, J., and Johnson, J. A. (2020). Polymer networks: From plastics and gels to porous frameworks. *Angew. Chem. Int. Ed.* 59, 5022–5049.
- [205]. Peppas, N. A. and Khare, A. R. (1993). Preparation, structure and diffusional behavior of hydrogels in controlled release. *Adv. Drug Delivery Rev.* 11, 1–35.
- [206]. Buwalda, S. J., Boere, K. W. M., Dijkstra, P. J., Feijen, J., Vermonden, T., and Hennink, W. E. (2014). Hydrogels in a historical perspective: From simple networks to smart materials. *J. Controlled Release* 190, 254–273.
- [207]. Wichterle, O. and Lím, D. (1960). Hydrophilic gels for biological use. *Nature* 185, 117–118.
- [208]. Caló, E. and Khutoryanskiy, V. V. (2015). Biomedical applications of hydrogels: A review of patents and commercial products. *Eur. Polym. J.* 65, 252–267.
- [209]. Xinming, L., Yingde, C., Lloyd, A. W., Mikhalovsky, S. V., Sandeman, S. R., Howel, C. A., and Liewen, L. (2008). Polymeric hydrogels for novel contact lens-based ophthalmic drug delivery systems: A review. *Cont. Lens Anterior Eye* 31, 57–64.
- [210]. Lin, C. -C. and Metters, A. T. (2006). Hydrogels in controlled release formulations: Network design and mathematical modeling. *Adv. Drug Deliv. Rev.* 58, 1379–1408.
- [211]. McNeill, M. E. and Graham, N. B. (1984). Vaginal pessaries from crystalline/rubbery hydrogels for the delivery of prostaglandin E2. *J. Controlled Release* 1, 99–117.
- [212]. Graham, N. B. and McNeil, M. E. (1984). Hydrogels for controlled drug delivery. *Biomaterials* 5, 27–36.
- [213]. Jeong, B., Bae, Y. H., and Kim, S. W. (2000). In situ gelation of PEG-PLGA-PEG triblock copolymer aqueous solutions and degradation thereof. *J. Biomed. Mater. Res.* 50, 171–177.
- [214]. Hiemstra, C., Zhong, Z., van Tomme, S. R., van Steenberg, M. J., Jacobs, J. J. L., Otter, W. D., Hennink, W. E., and Feijen, J. (2007). In vitro and in vivo protein delivery from in situ forming poly(ethylene glycol)–poly(lactide) hydrogels. *J. Controlled Release* 119, 320–327.

- [215]. Josef, E., Zilberman, M., and Bianco-Peled, H. (2010). Composite alginate hydrogels: An innovative approach for the controlled release of hydrophobic drugs. *Acta Biomater.* 6, 4642–4649.
- [216]. Liu, S., Huang, D., Hu, Y., Zhang, J., Chen, B., Zhang, H., Dong, X., Tong, R., Lid, Y., and Zhou, W. (2020). Sodium alginate/collagen composite multiscale porous scaffolds containing poly(3-caprolactone) microspheres fabricated based on additive manufacturing technology. *RSC Adv.* 10, 39241.
- [217]. Tsou, Y. -H, Khoneisser, J., Huang, P. -C, and Xu, X. (2016). Hydrogel as a bioactive material to regulate stem cell fate. *Bioact. Mater.* 1, 39–55.
- [218]. Cascone, M. G., Sim, B., and Sandra, D. (1995). Blends of synthetic and natural polymers as drug delivery systems for growth hormone. *Biomaterials* 16, 569–574.
- [219]. Rivera-Hernández, G., Antunes-Ricardo, M., Martínez-Morales, P., and Sánchez, M. L. (2021). Polyvinyl alcohol based-drug delivery systems for cancer treatment. *Int. J. Pharm.* 600, 120478.
- [220]. Munim, S. A. and Raza, Z. A. (2019). Poly(lactic acid) based hydrogels: Formation, characteristics and biomedical applications. *J. Porous Mater.* 26, 881–901.
- [221]. Alaneed, R., Golitsyn, Y., Hauenschild, T., Pietzsch, M., Reichert, D., and Kressler, J. (2021). Network formation by aza-Michael addition of primary amines to vinyl end groups of enzymatically synthesized poly(glycerol adipate). *Polym. Int.* 70, 135–144.
- [222]. Faheem Ullah, F., Othman, M. B. H., Javed, F., Ahmad, Z., and Md. Akil, H. (2015). Classification, processing and application of hydrogels: A review. *Mater. Sci. Eng. C* 57, 414–433.
- [223]. Bashir, S., Hina, M., Iqbal, J., Rajpar, A. H., Mujtaba, M. A., Alghamdi, N. A., Wageh, S., Ramesh, K., and Ramesh, S. (2020). Fundamental concepts of hydrogels: Synthesis, properties, and their applications. *Polymers* 12, 2702.
- [224]. Hu, W., Wang, Z., Xiao, Y., Zhang, S., and Wang, J. (2019). Advances in crosslinking strategies of biomedical hydrogels. *Biomater. Sci.* 7, 843.
- [225]. Ono, K., Saito, Y., Yura, H., Ishikawa, K., Kurita, A., Akaike, T., and Ishihara, M. (2000). Photocrosslinkable chitosan as a biological adhesive. *J. Biomed. Mater. Res.* 49, 289–295.
- [226]. Sperinde, J. J. and Griffith, L. G. (1997). Synthesis and characterization of enzymatically-cross-linked poly(ethylene glycol) hydrogels. *Macromolecules* 30, 5255–5264.
- [227]. Jiang, Y., Chen, J., Deng, C., Suuronen, E. J., and Zhong, Z. (2014). Click hydrogels, microgels and nanogels: Emerging platforms for drug delivery and tissue engineering. *Biomaterials* 35, 4969–4985.
- [228]. Sui, X., van Ingen, L., Hempenius, M. A., and Vancso, G. J. (2010). Preparation of a rapidly forming poly(ferrocenylsilane)-poly(ethylene glycol)-based hydrogel by a thiol-Michael addition click reaction. *Macromol. Rapid Commun.* 31, 2059–2063.

- [229]. Cheng, W., Wu, D., and Liu, Y. (2016). Michael addition polymerization of trifunctional amine and acrylic monomer: A versatile platform for development of biomaterials. *Biomacromolecules* 17, 3115–3126.
- [230]. Lutolf, M. P. and Hubbell, J. A. (2003). Synthesis and physicochemical characterization of end-linked poly(ethylene glycol)-co-peptide hydrogels formed by Michael-type addition. *Biomacromolecules* 4, 713–722.
- [231]. Rulev, A. Y. (2011). Aza-Michael reaction: Achievements and prospects. *Russ. Chem. Rev.* 80, 197–218.
- [232]. Bosica, G. and Abdilla, R. (2016). Aza-Michael mono-addition using acidic alumina under solventless conditions. *Molecules* 21, 815.
- [233]. Steunenbergh, P., Sijm, M., Zuilhof, H., Sanders, J. P., Scott, E. L., and Franssen, M. C. (2013). Lipase-catalyzed aza-Michael reaction on acrylate derivatives. *J. Org. Chem.* 78, 3802–3813.
- [234]. Love, D., Kim, K., Domaille, D. W., Williams, O., Stansbury, J., Charles Musgrave, C., and Bowman, C. (2019). Catalyst-free, aza-Michael polymerization of hydrazides: Polymerizability, kinetics, and mechanistic origin of an  $\alpha$ -effect. *Polym. Chem.* 10, 5790–5804.
- [235]. Southan, A., Mateescu, M., Hagel, V., Bach, M., Schuh, C., Kleinhans, C., Kluger, P. J., Tussetschläger, S., Nuss, I., Haraszti, T., et al. (2013). Toward controlling the formation, degradation behavior, and properties of hydrogels synthesized by aza-Michael reactions. *Macromol. Chem. Phys.* 214, 1865–1873.
- [236]. Zhang, Z., Loebus, A., de Vicente, G., Ren, F., Arafteh, M., Ouyang, Z., and Lensen, M. C. (2014). Synthesis of poly(ethylene glycol)-based hydrogels via amine-Michael type addition with tunable stiffness and postgelation chemical functionality. *Chem. Mater.* 26, 3624–3630.
- [237]. Hoffmann, C., Stuparu, M. C., Daugaard, A., and Khan, A. (2015). Aza-Michael addition reaction: Post-polymerization modification and preparation of PEI/PEG-based polyester hydrogels from enzymatically synthesized reactive polymers. *J. Polym. Sci. Part A: Polym. Chem.* 53, 745–749.
- [238]. Retailleau, M., Ibrahim, A., Croutxé-Barghorn, C., Allonas, X., Ley, C., and Nouen, D. L. (2015). One-pot three-step polymerization system using double click Michael addition and radical photopolymerization. *ACS Macro Lett.* 4, 1327–1331.
- [239]. Wang, J., He, H., Cooper, R. C., and Yang, H. (2017). In situ-forming polyamidoamine dendrimer hydrogels with tunable properties prepared via aza-Michael addition reaction. *ACS Appl. Mater. Interfaces* 9, 10494–1050.

## **Erklärung**

Hiermit versichere ich, die vorliegende Arbeit selbstständig und ohne fremde Hilfe verfasst und keine anderen als die von mir angegebenen Quellen und Hilfsmittel verwendet zu haben. Die den benutzten Werken wörtlich oder inhaltlich entnommenen Stellen habe ich als solche kenntlich gemacht.

Ich erkläre, keine anderweitigen Promotionsversuche unternommen und die vorliegende Dissertation weder in der jetzigen noch in einer anderen Fassung einer anderen wissenschaftlichen Einrichtung vorgelegt zu haben.

Halle (Saale), den 30.03.2022

Razan Alaneed

## Acknowledgments

I would like to thank and acknowledge everyone who has supported me throughout my doctoral studies over the years.

First of all, I have to express my deep gratitude and appreciation to my two academic supervisors, **Prof. Dr. Jörg Kressler**, Institute of Chemistry of the Martin-Luther-University Halle-Wittenberg, and **Prof. Dr. Markus Pietzsch**, Institute of Pharmacy of the Martin-Luther-University Halle-Wittenberg, for their assistance at every stage of my research project.

**Prof. Dr. Jörg Kressler** for giving me the opportunity to carry out my research project under his mentorship and to work on this interesting interdisciplinary topic. I highly appreciated his patience, continuous scientific guidance, support, and inspiration throughout my research.

His office door was always open to me for various discussions about my research and problems that needed to be solved. His humility and respect for others have been the greatest source of inspiration for me during these years. I will be forever grateful to Prof. Kressler for his incredible support.

**Prof. Dr. Markus Pietzsch** for the fruitful cooperation and for giving me the opportunity to work in the field of enzymatic protein-polymer conjugation. I highly appreciated his support, motivation, and the helpful discussions and suggestions. It was a privilege for me to work in his laboratory at Martin-Luther-University Halle-Wittenberg.

Without their guidance and constant feedback, this Ph.D. thesis would not have been achievable.

Many thanks go to **Dr. Elkin Amado** and **Dr. Mark Jbeily** for the great scientific discussions and for the pleasant office atmosphere.

My sincere thanks to **all members of Prof. Jörg Kressler's group** for the comfortable atmosphere at work as well as for their insightful comments and suggestions.

I am also thankful for the inspiration and learning experience I gained from working with **Dr. Muhammad Humayun Bilal**.

Special thanks go to **Nazmul Hasan, Rana Hore, and Haroon Rashid** for their encouragement and support all through my doctoral studies. I enjoyed the time we had together and with the whole group.

I have also to thank **all my colleagues in the groups of Prof. Markus Pietzsch** for their kind help and assistance in lab as well as for the helpful discussions of our results on protein-polymer conjugation.

I have also to thank **Dr. Franziska Seifert** for the useful discussions and instructions regarding nanoDSF experiments.

I offer my thanks to **Dr. Marcel Naumann**, Fraunhofer Institute for Cell Therapy and immunology, Halle for the MALDI-TOF and LC-ESI-LIT MS measurements.

My sincere thanks go also to **Frau Susanne Tanner** and **Julia Weichhold** for the GPC measurements.

I would like to offer my special thanks to **Dr. D. Ströhl** for the technical support in terms of NMR spectroscopy.

I would like to extend my sincere thanks to **Prof. Dr. Karsten Mäder** and his student **Jonas Steiner**, Institute of Pharmacy of the Martin-Luther-University Halle-Wittenberg, for our successful collaborative work on the synthesis of fatty acid-modified poly(glycerol adipate) microparticles for controlled drug delivery.

I have to express my gratitude to **Prof. Dr. Detlef Reichert** and his student **Yury Golitsyn**, Institute of Physics of the Martin-Luther-University Halle-Wittenberg, for our successful collaborative work on the network characterization by solid state NMR spectroscopy and the helpful explanations of NMR results.

Lastly, my family deserves endless gratitude; my **Dad, Mom, Grandparents, Maria, Raghda,** and **Alaa** for their unconditional love, their never ending support and encouragement over the years and their appreciation for my work. You are always there for me!

My warmest and dearest gratitude goes to my beloved husband **Dr. Till Hauenschild** for his endless support, patience, respect, love, and faith in me.

Words will never be enough to express how much I love you!

I gratefully acknowledge the funding received towards my Ph.D. from Deutscher Akademischer Austauschdienst (DAAD) under a Research Grant - Doctoral Programs in Germany, 2017/18 (57299294).

My thanks also go to the financial support I received from Sonderforschungsbereich SFB/Transregio TRR 102.

This dissertation would not have been possible without the support of all these wonderful people!

*I dedicate this thesis to my father Saeed for his constant support and unconditional love.*

## List of publications

1. M. Bilal, **R. Alaneed\***, J. Steiner, K. Mäder, M. Pietzsch and J. Kressler. “Multiple grafting to enzymatically synthesized polyesters”. In *Methods in Enzymology*; Elsevier: Amsterdam, The Netherlands, 2019; Volume 627, pp. 57-97.
2. **R. Alaneed\***, T. Hauenschild, K. Mäder, M. Pietzsch and J. Kressler. “Conjugation of amine-functionalized polyesters with dimethylcasein using microbial transglutaminase”. *J. Pharm. Sci.* **109**, 981-991 (2020).
3. J. Steiner, **R. Alaneed**, J. Kressler and K. Mäder. “Fatty acid-modified poly(glycerol adipate) microparticles for controlled drug delivery”. *J. Drug Deliv. Sci. Technol.* **61**, 102206 (2021).
4. **R. Alaneed\***, Y. Golitsyn, T. Hauenschild, M. Pietzsch, D. Reichert and J. Kressler. “Network formation by aza-Michael addition of primary amines to vinyl end groups of enzymatically synthesized poly(glycerol adipate)”. *Polym. Int.* **70**, 135-144 (2021).
5. W. Purahong, S. F. M. Wahdan, D. Heinz, K. Jariyavidyanont, C. Sungkapreecha, B. Tanunchai, C. Sansupa, D. Sadubsarn, **R. Alaneed**, A. Buschart, M. Schädler, A. Geissler, J. Kressler and F. Buscot. “Back to the future: decomposability of a biobased and biodegradable plastic in field soil environments and its microbiome under ambient and future climates”. *Environ. Sci. Technol.* **55**, 12337-12351 (2021).
6. **R. Alaneed\***, M. Naumann, M. Pietzsch and J. Kressler. “Microbial transglutaminase-mediated formation of erythropoietin-polyester conjugates”. *J. Biotechnol.* **346**, 1-10 (2022).
7. R. Hore, **R. Alaneed\***, M. Pietzsch and J. Kressler. “Enzymatic HES conjugation with recombinant human erythropoietin *via* variant microbial transglutaminase TG<sup>16</sup>”. *Starch/Stärke*, **74**, 2200034 (2022).

\* **First and co-first author.**

## Curriculum vitae

### *Personal data*

Family name: Alaneed  
First name: Razan  
Date of birth: 22.11.1987  
Place of birth: Damascus, Syria  
Nationality: Syrian

### *Education*

01/2017 - present      Doctoral studies  
                                 Martin-Luther Universität Halle-Wittenberg  
                                 Institute of Pharmacy  
                                 Supervisors: Prof. Dr. Jörg Kreßler  
   Prof. Dr. Markus Pietzsch

Nov/2016              Diploma in Pharmacy  
                                 Martin-Luther Universität Halle-Wittenberg  
                                 Institute of Pharmacy  
                                 Supervisors: Prof. Dr. Reinhard Neubert  
   Prof. Dr. Jörg Kreßler

09/2005 – 07/2010      Bachelor studies in Pharmacy  
                                 Arab International Private University, Damascus,  
                                 Syria

05/2005              Secondary school study  
                                 Dar alssalam school, Damascus, Syria